

A thesis entitled

Development of Plastic Materials for Nuclear Track Detection

Submitted to

Goa University
for the Degree of
Doctor of Philosophy
(in Chemistry)

by

547.84

MAS/Dev

T-376



Mr. Adlete A. A. Mascarenhas

M.Sc.

Department of Chemistry

Goa University

Taleigao Plateau

Goa 403 206

India

April 2007

T-376

DECLARATION

I hereby declare that the matter embodied in this thesis entitled 'Development of plastic Materials for Nuclear track Detection' is the result of investigations carried out by me, in the Department of Chemistry, Goa University, Goa, India under the supervision of Dr. V. S. Nadkarni, Senior Lecturer, Department of Chemistry, Goa University.


In keeping with the general practice of reporting scientific observations, due acknowledgement has been made wherever the work described is based on the findings of other investigators.

Goa University
April 2007

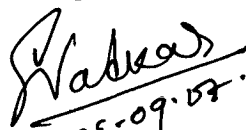



Mr. Adlete Mascarenhas

Examined by


08-09-2007

(Prof. M. A. Shrivastava)


08-09-07

CERTIFICATE

Certified that the work entitled 'Development of plastic Materials for Nuclear track Detection' presented in this thesis has been carried out by Mr. Adlete A A Mascarenhas under my supervision and the same has not been submitted elsewhere for the award of a degree.

Goa University

April 2007



A handwritten signature in black ink, appearing to read 'V. S. Nadkarni', written over a horizontal line.

Dr. V. S. Nadkarni

(Research Guide)

ACKNOWLEDGEMENT

During the course of this work, I have been assisted by a number of people. I wish to express my gratitude to them.

First and foremost I would like to thank my Guide Dr. V. S. Nadkarni, Senior lecturer, Department of Chemistry, Goa University, for being a source of inspiration to me. Working with him, has been a great learning experience for me. The values that have been imbibed in me, will be a treasure in my life. Thank you Sir, for all the help rendered.

My thanks to Prof. J. B. Fernandes (Head, Department of Chemistry, Goa University) and Prof. K. S. Rane (Former Head, Department of Chemistry, Goa University) in a special way, for providing necessary facilities for carrying out my research work.

To Dr. S. G. Tilve (Reader, Department of Chemistry, Goa University) for being closely associated with my research work, and for helping me through the completion of this thesis.

My sincere gratitude to Dr. A M Bhagwat, Former Head, RSSD, BARC; Dr. S B Monohar, Former Head, RCD, BARC; Mr. V B Joshi, ex. RSSD, BARC; Mr. R K Samant, ex. RSSD, BARC; Mr. R V Kolekar, RSSD, BARC for providing the necessary help in completion of this work. I also thank Dr. P C Kalsi, SO G, RCD, BARC for his kind help & useful discussions.

A special vote of thanks to Prof. S D Samant, UICT, Mumbai, for giving his valuable advice and help rendered for the library facili-

ties in UICT.

I am thankful to Dr. Parmeshwaram and Dr. C.G. Naik, for helping me to get the spectral data.

Thanks to all my teachers, from school to the post graduation level, for sowing the seeds of learning in me and for moulding me.

A special vote of thanks to all my research colleagues, for their unstinting support in the completion of this work.

I gratefully acknowledge the help rendered to me by the supporting staff of Department of Chemistry, USIC, Administrative Block and Library, Goa University.

I thank the Atomic Energy Regulatory Board (AERB) for providing a fellowship during the course of this investigation and also for funding this work.

I am indebted to my Parents and Brother for their encouragement, moral support, affection and selfless sacrifice.

I am greatly thankful to my wife Arlyn, for standing by me through the completion of my thesis. Her love and concern for my work, gave me the determination to achieve my goal.

Adlete Mascarenhas

CONTENTS

Page

Abbreviations

no.

General Remarks

Chapter 1: General Introduction and Literature status

1.1	Solid State Nuclear Track Detection.	01
1.1.1	Highlights of the research on Plastic Materials	03
1.1.2	Characteristic features of the charged particle latent tracks	06
1.1.3	Salient features of solid state nuclear track detectors.	06
1.1.4	Track Formation.	07
1.1.5	Track Development by chemical etching.	09
1.1.6	Criteria of track formation	15
1.1.7	The Environmental effects affecting track formation.	18
1.1.8	Track Visualization techniques.	19
1.1.9	Track Evaluation (counting) techniques.	23
1.1.10	Applications of Plastic SSNTDs.	24
1.1.11	Highlights of SSNTD research work In India.	26
1.1.12	Current status of SSNTD technique using plastic materials.	28
1.2	Allyl monomers and Polymers.	28
1.2.1	Classification of allylic compounds.	29
1.2.2	Radical polymerization of allyl compounds.	30
1.2.3	Polyfunctional allyl compounds.	31
1.3	Poly Allyl Diglycol Carbonate (PADC) as a particle track detector.	33
1.3.1	Preparation of Allyl Diglycol Carbonate (ADC)	36

monomer.		
1.3.2	Purification of the monomer.	40
1.3.3	ADC polymerization.	41
1.3.4	Kinetics of ADC polymerization.	43
1.3.5	Initiators for ADC Polymerization.	46
1.3.6	Mold Design and Materials for ADC polymerization.	48
1.3.7	Co-polymers of ADC monomer.	49
1.3.8	Structure and sensitivity effects in CR-39 and related polycarbonates.	50
1.3.9	Effect of additives on the sensitivity.	52
1.3.10	Etchants used for ADC polymer.	56
1.3.11	Etching mechanism and study of etchants in CR-39 polymer	57
1.4	Statement of objectives.	60
Chapter 2: Experimental		
2.1	Materials	64
2.1.1	Materials used.	64
2.1.2	Instrumentation.	64
2.2	Synthesis of monomers and initiators.	66
2.2.1	Synthesis of ADC monomer.	66
2.2.2	Synthesis of N-Allyloxycarbonyloxy diethanolaminebis- (allyl carbonate) (NADAC).	70
2.2.3	Synthesis of Allyl bis-(2-nitroxy-ethyl) carbamate (ABNEC).	71
2.2.4	Synthesis of Tris-(2,4-dioxa-3-oxohept-6-en-1-yl) nitromethane (TDONM).	73
2.2.5	Synthesis of Isopropyl peroxydicarbonates (IPP).	74
2.3	Kinetic Studies	75

2.4	Preparation of SSNTD films by cast polymerization.	77
2.5	Spectral Data of compounds.	82
Chapter 3: Results and Discussion		
3.1	Our Approach towards development of Plastic materials for SSNTD.	103
3.2	Cast polymerization of monomers.	106
3.2.1	Purification of the monomer.	108
3.2.2	Selection of initiator for polymerization.	109
3.2.3	Development of a constant rate polymerization cycle.	110
3.3.	Determination of Dials Constants.	112
3.3.1	Kinetic studies of ADC monomer using IPP initiator.	112
3.3.2	ADC polymerization using Benzoyl peroxide initiator.	124
3.3.3	Polymerization of NADAC and NADAC+ADC monomer with IPP initiator.	130
3.3.4	Polymerization of ABNEC monomer with IPP initiator.	137
3.3.5	Copolymerization of ABNEC-ADC (50:50 and 10:90 w/w) monomer with IPP initiator.	138
3.3.6	Polymerization of TDONM and TDONM+ADC monomer with IPP initiator.	145
3.4	Preparation of thin films by cast polymerization.	153
3.5	Studies on the optimum polymerization time cycle.	154
3.6	Testing of indigenously developed Plastic ma-	157

	terials for SSNTD.	
3.7	Optimization of etching conditions of the Plastic track detectors.	159
3.7.1	Etching of PNADAC and NADAC-DAC (50:50) track detectors.	160
3.7.2	Etching of ABNEC-ADC track detectors.	165
3.7.3	Etching of TDONM and TDONM-ADC track detectors.	167
3.8	Optimization of initiator concentration and sensitivity studies.	170
3.8.1	PADC Plastic Track Detectors.	170
3.8.2	PNADAC and NADAC-ADC (50:50) plastic track detectors.	175
3.8.3	ABNEC-ADC (10:90) Plastic Track Detector.	180
3.8.4	TDONM-ADC copolymer Plastic Track Detectors.	182
3.9	Uniformity of etching of the films.	188
3.9.1	PADC plastic Track detector	188
3.9.2	PNADAC and NADAC-ADC plastic Track Detectors.	190
3.9.3	ABNEC-ADC Nuclear Track detectors.	191
3.9.4	PTDONM and TDONM-ADC Nuclear Track Detectors.	193
3.10	Alpha track detection efficiency of newly developed plastic nuclear track detectors.	194
3.10.1	Studies on variation of alpha track density with etching time.	195
3.10.2	Determination of the background tracks.	196
3.10.3	Alpha track detection efficiency.	197
3.11	Correlation of sensitivities of plastic track detectors	200

3.12	Measurement of alpha to fission branching ratios by sequential chemical etching of alpha and fission tracks in homo and copolymer films.	201
4.0	Conclusions.	202
5.0	References.	206
6.0	Publications appended to the thesis.	216

General Remarks

All chemicals used for the synthesis were Grade AR and used without purification. Wherever required, drying of the chemicals was carried out, using suitable drying agents. ADC monomer (M/s Aldrich chemicals, USA) was used for comparison purpose.

For preparation of Mold for cast polymerization Glass plates manufactured by M/s Schott, Germany were used.

The polymerization was carried out in a specially designed bath for holding the molds. The heating was carried out by a programmable, microprocessor controlled liquid bath procured from M/s Julabo (F 25 HP) Germany.

IR spectra were recorded on Shimadzu FT-IR spectrophotometer. PMR and CMR spectra were recorded on Bruker 300 MHz spectrophotometer. Mass spectra were recorded on MS (TOF) system.

Thickness of the films was measured using a digital thickness gauge Alpha meter, Para Electronics, India, having a least count of 5 microns.

ABBREVIATIONS

1. AA - Allyl alcohol
2. ADC - Allyl diglycol carbonate
3. BAEP - 2,2-bis-(4-acryloyloxypolyethoxyphenyl)-propane
4. BuAc - Butanediol bisallyl carbonate
5. BzO₂ - Benzoyl peroxide
6. CE - Chemical etching
7. CHPC - Cyclohexyl peroxydicarbonate
8. CN - Nitocellulose (cellulose nitrate)
9. CR-39 - ADC polymer (Trademark of PPG Industries, UK)
10. CR-73 - Polymer of bisphenol-A bis allylcarbonate
11. DAA - Diallyl adipate
12. DACD - Diallyl chlorindate
13. DADDC - Diallyl di-diglycol carbonate
14. DAIP - Diallyl isophthalate
15. DAS - Diallyl succinate
16. DEAS - Diethylene glycol bisallyl sulphonate
17. DEG - Diethylene glycol
18. DNP - Dinonyl phthalate
19. DOP - Dioctyl phthalate
20. DOS - Dioctyl sebacate
21. DP - Degree of polymerization
22. ECE - Electrochemical etching
23. IPA - Isopropyl alcohol
24. LR 115 - (Trademark) CN SSNTD film manufactured by Kodak Pathe, France
25. MADC - Monoallyl diglycol carbonate

- 26. PAA - Polyallyl alcohol
- 27. PeAC - Pentanediol bisallyl carbonate
- 28. PM CR-39 - CR-39 SSNTD film manufactured by Pershore Mouldings, UK.
- 29. PrAc - Propanediol bisallyl carbonate
- 30. SC-79 - Copolymer of CR-39 and methyl methacrylate.
- 31. SR-86 - Copolymer of CR-39 and DEAS.
- 32. TBP - Tertbutyl peroxide.
- 33. TBHP - Tertbutyl peroxybenzoate
- 34. TEDM - Triethylene glycol dimethacrylate.

Physical Quantities:

- V_b - Bulk etch rate.
- V_t - Track etch rate.
- S - Sensitivity.
- θ_c - Critical angle of etching
- v - Velocity of charged particle
- c - Velocity of light
- m - Mass of a particle
- β - v/c
- V_R - Radial track etch rate
- L - Track length
- D_{crit} - Critical dose
- Z_{eff} - Effective atomic charge

Chapter 1

General Introduction & Literature

Status

1.1 Solid State Nuclear Track Detection.

Detection of nuclear radiations has been a subject of interest ever since the discovery of radioactivity by Becquerel in 1896. This led mankind towards the development of devices, for identification and quantification of these radiations.

Radiation detection methods are based on measurements of the change in the detector material/device on interaction with radiation. These changes can be either recorded in the form of an electronic output or as permanent physical change in the detector material itself. One of the earliest attempts in this direction was the Wilson's cloud chamber (1911), Nuclear emulsions (1929), Glaser's bubble chamber (1952) and Spark chamber (1957). This was followed by counting devices like, Geiger Muller (GM) counters, scintillation counters, surface barrier detectors and thermoluminescent detector (TLD) to name a few. Except nuclear emulsions (photographic plates) no other device mentioned above could record the nuclear tracks permanently.

D. A. Young¹ in his studies pertaining to the effect of fission fragments on crystal lattices observed that, LiF crystals exposed to fission fragments, from a uranium source held at a distance of 1 mm, could detect a number of shallow etch pits, on treatment with a chemical reagent ($\text{HF} + \text{CH}_3\text{COOH}$) saturated with FeF_3 .

These pits could be directly observed under an electron microscope, alternatively the pits could be observed under optical microscope after enlarging the size of the latent damage. This technique called track etching was later on elaborated by Silks and Barnes of Harwell². However, a team of R.L. Fleischer, P. B. Price and R.M. Walker working at General Electric Research Laboratory, New York, pioneered the extensive development of the track etching³⁻⁸ technique of Young, by studying a variety of other

materials such as glasses, plastics and mineral crystals.

The efforts in this direction of developing radiation detectors for permanently recording the information on radiation events led to the development of new method of radiation detection called Solid State Nuclear Track Detection (SSNTD). It is now well known that almost all naturally occurring, as well as man made insulating solid materials, like crystals, glasses and polymers, can record and store the trajectory of the fast moving charged particles through them.

Since the discovery of this event, a number of theories have been put forward to explain the phenomenon of track formation and the nature of tracks formed in dielectric materials. The process of track formation however, can be briefly explained as follows; heavily ionizing particles passing through insulating materials leave narrow ($\sim 5 - 100 \text{ \AA}$) trails of damage. In crystals and glasses this consists of atomic displacements surrounded by regions of considerable lattice strain. In plastics, the ionizing radiation produce ionized excited molecules and electrons. Both, ions and the excited molecules may acquire considerable vibrational energy and undergo bond rupture. These are called latent tracks, as they are too small, to be viewed under an optical microscope. However, more power imaging devices like Transmission electron microscope, X-ray scattering technique, Neutron scattering, Gas and liquid flow method, Scavenger technique have been used to study the formation of latent tracks in these materials⁹.

This technique of radiation measurement could attain a high level of popularity, only after the process of track development by chemical etching was used, in order to study the tracks, by simply enlarging the track diameter, and to view them using an optical

microscope. This method could be widely used in case of plastic materials, which has made them so popular in the field of SSNTD. The latent tracks formed in the materials are enlarged by treatment with certain chemical agents, so that they are visible under an optical microscope. The chemical agents like alkali metal hydroxides, degrade the damaged region at a much higher rate than the undamaged material, thereby enlarging the latent tracks in the form of 'etch pits'. Nowadays, even other methods are in use, such as short treatment of the alkali to the material, so that the tracks can be studied by the use of Atomic force microscopy¹⁰, Conductometric method¹¹ and Confocal microscopy¹².

1.1.1 Highlights of the research on Plastic Materials.

Out of more than 200 inorganic and plastics materials that have been tested so far, the more promising one has been the plastics. Some of the plastic materials that have been studied so far are shown in Table 1.1.(see next page). From the literature pertaining to SSNTDs, it can be seen that, since 1965 to 1976, the commercially available Cellulosics like cellulose-mono, di-, tri- acetates, cellulose acetate butyrate, were tested as SSNTDs. Thereafter, their use declined with the introduction of more sensitive plastic materials like Nitrocellulose (CN) and Bisphenol-A polycarbonate. While CN was used for environmental dosimetry of radon and thoron, Bisphenol-A polycarbonate was mainly used for fission fragment detection. After the discovery of CR-39 as a plastic SSNTD in the year 1978, it has remained a plastic of choice, mainly due to its high sensitivity to alpha particles and fission fragments coupled with its material characteristics like stability and excellent optical properties. Moreover, this material can be subjected to electrochemical etching. It has been a material of choice in the field of environmental dosimetry, neutron dosimetry, and other thrust areas in the field of nuclear research and technology.

Sr.No.	Chemical Name	Brand Name
1	Cellulose acetate(1) (mono R1 = -Ac, R2, R3 = -H) (di, R2, R3 = -Ac, R1 = -H) (tri, R1, R2, R3 = -Ac) (cellulose acetate butyrate, R1 = -H, R2 = -Ac, R3 = -COC3H7) (2)	Triafol TN Trianafol TN
2	Cellulose nitrate(di-tri) (3)	LR115, Daicell
3	Chitin (4)	
4	Bisphenol-A Polycarbonate (5)	Makrofol, Lexan.
5	Allyl diglycol carbonate(6)	CR-39,PM 355, Tastrack, MA-ND6
6	Methyl Methacrylate (7)	Perspex
7	Tetrafluroethylene (8)	Teflon
8	Vinyl chloride (9)	
9	Vinylidenfluoride (10)	
10	Diethylene terephthalate (11)	Levasan, mylar, Melinex, Chronar, Lumrior
11	Bisphenol-A-bis(allyl carbonate) (12)	CR-73
12	Allyl diglycol sulphonate (13)	SR-86, SR-90
13	Propanediol bis allylcarbonate, m=3 (14) Butanediol bis allylcarbonate, m=4 (15) Pentanediol bis allylcarbonate, m=5 (16) Diallyl succinate m=2 (17) Diallyl adipate, m=4 (18)	
14	Diallyl phthalate(R=2-COOR) (19) Diallyl isophthalate (R=3-COOR) (20)	
15	Diallyl terephthalate (R=4-COOR) (21) Triethylene glycol dimethacrylate (22)	
16	2,2-bis-(4-acryloyloxypolyethoxyphenyl) propane (23)	AW 15

Table 1.1 Monomers of some of the important polymers tested as SSNTDs (Please refer to Fig. 1.1 for structures)

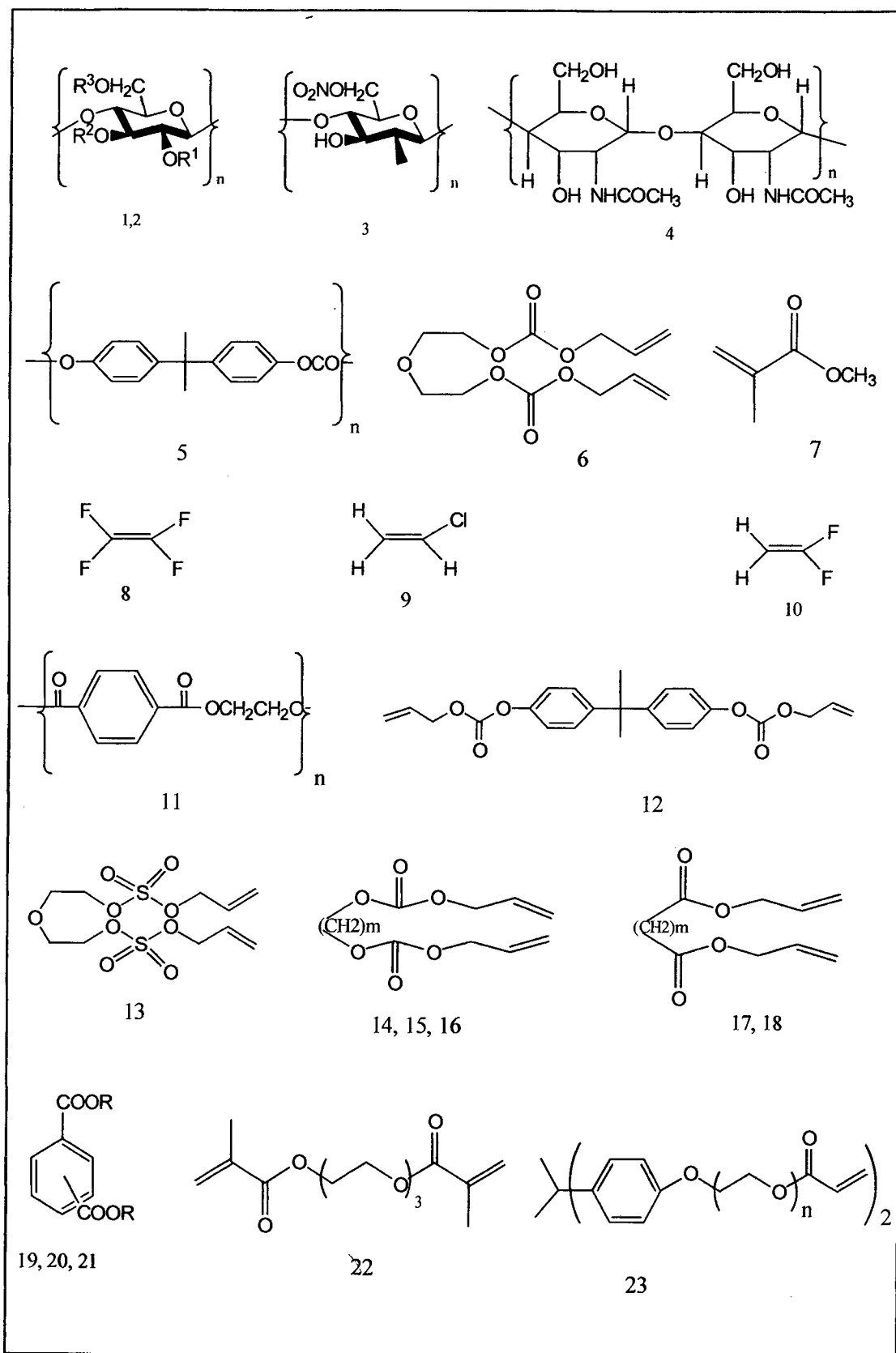


Fig. 1.1. Structures of important monomers.

After going through the available literature on SSNTD materials (plastics), it was observed that out of the available references, roughly 5 % of the references, deal with the preparation of SSNTD films (plastics). The remaining literature deals with the usage of these materials and various studies that have been carried out with them. The use of these materials in diverse fields of science and technology has been highlighted in the application of plastic SSNTDs.

1.1.2 Characteristic features of the charged particle latent tracks.

The available literature⁸ indicates following characteristic features of the latent tracks:-

- (1) They consist of damaged regions due to displaced atoms or broken molecular chains rather than electronic defects.
- (2) The region of damage is less than 10 nanometers in diameter and continuous. The length of the damaged trail is equal to the range of the charged particle in the material under study.
- (3) Metals and good semiconductors do not store tracks. Materials having electrical resistivity greater than 2000 ohm cm will store the tracks as can be seen in Table 1.2. (see next page)

However, the earlier view that metals do not store tracks appears to be a very crude idea, as recent reports indicate the formation of latent track in metals^{13,14}.

1.1.3. Salient features of solid state nuclear track detectors.

- 1) SSNTD materials are simple to use, durable and rugged. They are also cost effective compared to other methods of radiation detection as they could be used in very small or large size as per the requirements.
- 2) Useful as threshold detectors.
- 3) A permanent record of the process under study is obtained.
- 4) Possibility of rapid and automated analysis.

The technique, as such does not require any complicated electronic tools for analysis.

Materials	Resistivity (ohm.cm)
1 <i>Track forming</i>	
Alkali Halides	
Insulating glasses	$10^6 - 10^{20}$
Polymers	
Poor Insulators	3,000 - 25,000
Semiconductors	2,000 - 20,000
2. <i>Non track forming</i>	
Ge, Si	10 - 2000
Metals- Al, Cu, Au, Pt, W, Zn	$10^{-6} - 10^{-4}$

Table 1.2. Electrical resistivity values of some common materials.

1.1.4. Track Formation.

A) Mechanisms of track formation.

In order to explain the formation of tracks in materials the following mechanisms are put forward⁴:

- (1) Thermal spike model
- (2) Ion-explosion spike model
- (3) Radiochemical damage mechanism

(1) Thermal spike model

This model helps in explaining the track formation in inorganic materials. The energetic particles can produce considerable disruption of the crystal lattice producing intense heat in a localized region of the lattice. This region is therefore raised to a high temperature, from where it cools down rapidly via heat con-

duction. These heating processes induce various atomic processes, which damage the lattice region. This model helps in explaining the very fact that, insulators are capable of recording tracks whereas metals are not. In case of metals the energy is lost by delta rays primarily via electron-electron collisions down to low electron energies because the energy loss per collision is greater and the relaxation time is shorter. Thus, the excitation is spread throughout a large volume before any energy transfer occurs to the lattice. In insulators, the electrons can interact with the various modes of lattice vibration and the excitation is communicated to the lattice more conveniently.

(2)The Ion-explosion spike model.

This model again helps in explaining the track formation in inorganic materials. It takes into consideration the sudden burst in the ionization along the path of a charged particle to create an electrostatically unstable array of adjacent ions which eject one another from their normal sites into interstitial positions (see Fig. 1.2 a, page no. 10).

Following the primary ionization, an array of interstitial ions and vacant lattice sites is produced by the coulomb energy of the ions, after which elastic relaxation diminishes the acute local stresses by spreading the strain more widely thereby making it possible to observe the unetched tracks in crystals by transmission electron microscope. For this phenomenon to occur, the electrostatic stress produced by the penetrating particle must be greater than the internal mechanical strength or bonding strength. Thus materials of low mechanical strength, low dielectric constant and close interatomic spacing will act as more sensitive detectors. It is also essential that the damage done is atomi-

cally continuous and for this realization there should be at least one ionization per atomic plane traversed by the charged particle. It is also essential that the positive ions formed should have a life time greater than one lattice vibration time, *i.e.*, 10^{-13} sec.

(3)The Radiochemical damage mechanism

This model helps to explain the track formation in organic materials (polymers). The amount of energy required for track formation in polymers (~ 100 kilo Gray) is much lesser than that required for inorganic materials (~ 10 Giga Gray). The penetration of an energetic charged particle through the material breaks the covalent bonds it encounters, creating an array of radicals along its trajectory. The secondary electrons ejected during this process (delta rays) can also affect the covalent bonds (see Fig 1.2 b, next page). A bond breaking process follows due to which a permanent change of molecular structure is created in the volume along the ion's path by forming what is called a 'latent track'. Chemical agents like alkalis are able to degrade predominantly these regions of the latent track. Thus, after certain times of etching a tiny etch cone or pit is created which can be observed under an optical microscope (see Fig 1.3, page no. 11).

1.1.5. Track Development by Chemical Etching^{6,8}.

It is well known that all the particles that strike the detector cannot produce tracks, an understanding of these factors, which would govern the registration of tracks in detectors, is very essential. Many track registration criteria have been proposed, but before looking into these theories, it is necessary to understand the parameters which may influence track etching.

- (1) The material parameters like chemical composition, molecular weight, the extent of crystallinity, *etc.*
- (2) The particle parameters like charge Z , mass M , Velocity V .
- (3) The irradiation environment parameter like temperature, atmosphere *etc.*

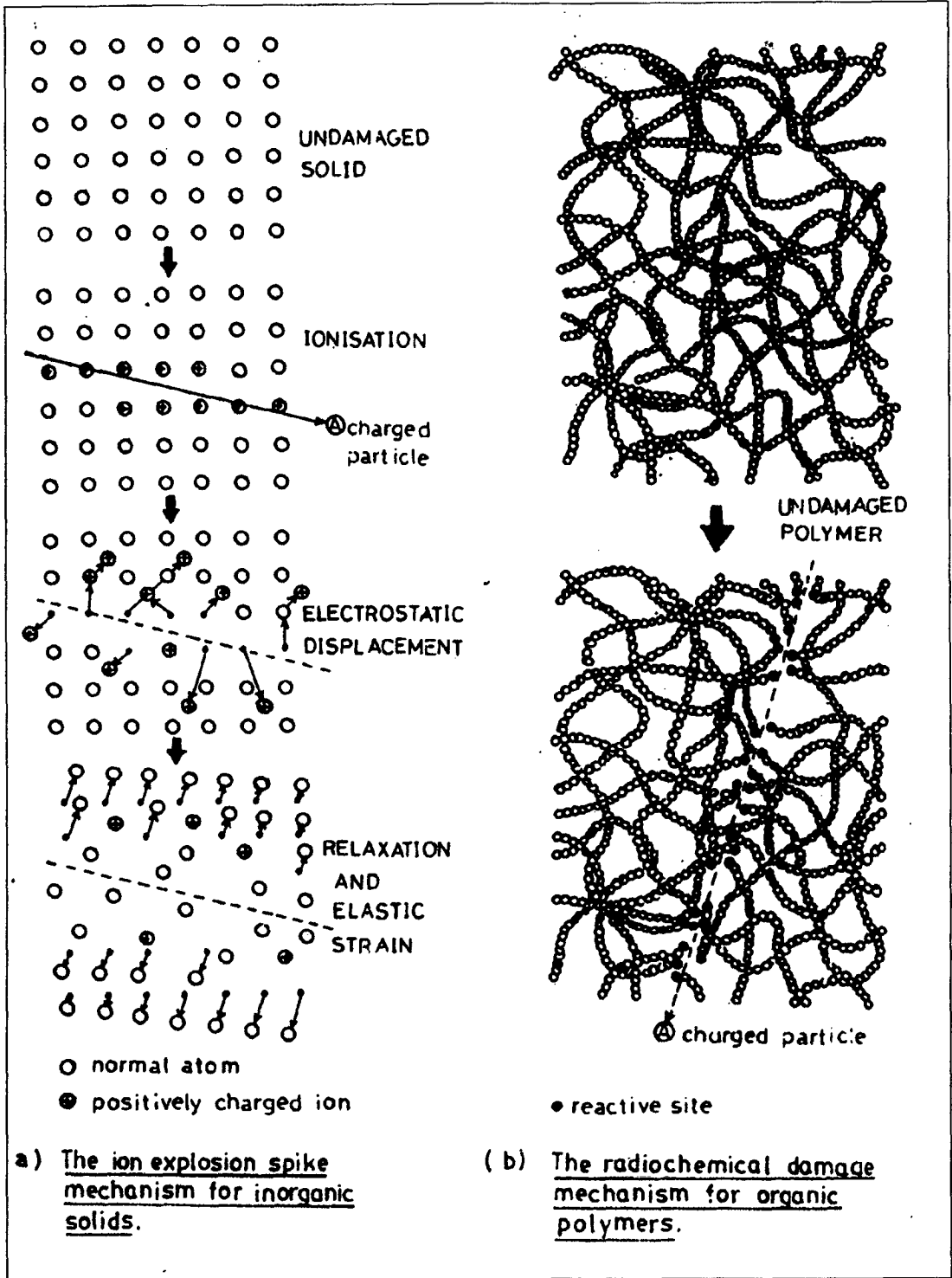


Fig 1.2 Models explaining the two mechanism involved in track formation.

(4) The pre-etch storing parameters like temperature, storage time and atmosphere.

(5) The etching parameters like etching solution, temperature, etc.

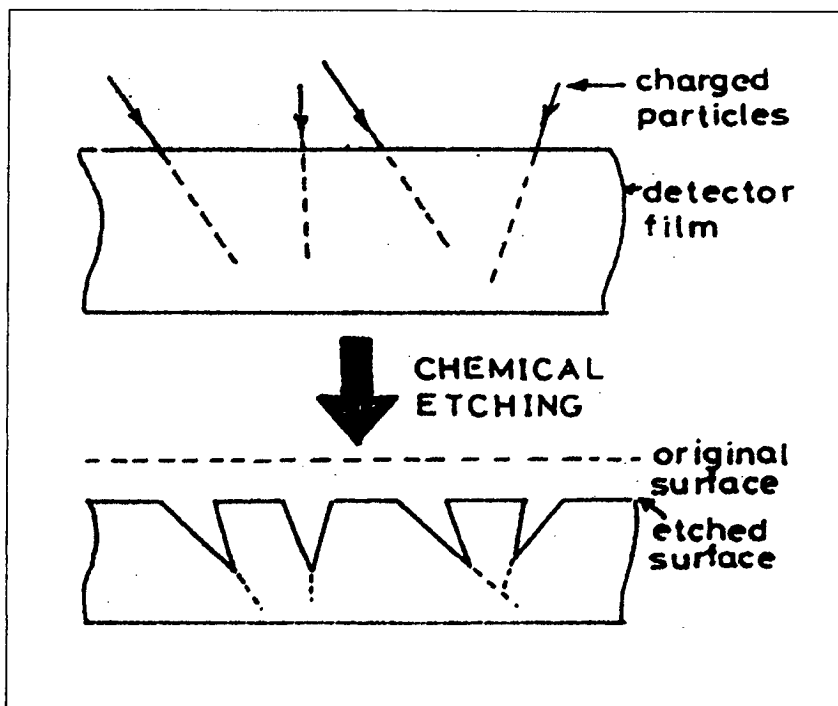


Fig. 1.3 The process of chemical etching

Certain factors, which affect this process of revelation of tracks, are given below⁹.

For tracks in the order of micrometer dimensions, two kinds of etch rates - the track and the bulk etch rate are used to describe etched tracks. The bulk etch rate (V_b) is the rate at which the undamaged material is removed from the surface. The Track etch rate (V_t) *i.e.*, the longitudinal track etch rate, is the rate at which the etchant penetrates along the ion's path into the track. The whole process is subdivided into a one-dimensional penetration of the etchant, along the ion's path and homogeneous bulk etching is outside the 'line' of the track. This bulk etching starts immediately after the etchant has reached its position along the

track. All physical processes like the transport of the etchant into the real track, which is of course not one-dimensional and removal of the etch products out of the track, are pressed into just one single parameter, *i.e.* the track etch rate. The two parameters V_b and V_t of the micrometer scale approximation have been sufficient to describe the etching process. The approximation however, has not addressed the question of why a latent track can be etched. For this, a \AA unit dimension scale approximation has been put forward. By studying the energy deposited per volume around the ion's path a new parameter, the radial track etch rate V_R , has been introduced. It is defined as the 'speed vertical to the ion's path with which the damaged matter is removed or with which the radius of the etch cylinder widens'. The radial track etch rate, depends on the energy deposited, which is high at the centre of the track and levels out into the regular bulk of the material.

The Track etch rate is dependent mainly on three conditions:-

- 1) The ion's energy loss properties *i.e.*, $d_E/d_x(Z, \alpha)$, where Z is the charge of the ion and α is the velocity of the ion.
- 2) The chemical constitution of the material.
- 3) The etching conditions like normality of the etchant, temperature, etc.

The bulk etch rate directly depends only on conditions 2 and 3 stated above. The essential condition to obtain an etch track has been that $V_t/V_b \geq 1$, which is described as the response function or the sensitivity (S) of the detector. In many cases ' S ' is found to be independent of the etching conditions and depends only on the energy loss and the type of the detector.

a. Critical angle of etching.

There exists a critical angle of etching (θ_c) for each detector material. Table 1.3 gives the values for some of the materials.

Material	θ_c (°)
1. Minerals	0-7
2. Glasses	
soda, borosilicate, flint, obsidian etc.	20 -70
Phosphate glass	1-5
Silica glass	13-19
3. Plastics	
Nitrocellulose	>2
Lexan	2.5
Makrofol	3

Table 1.3 θ_c values for full energy fission fragments.

From the θ_c values given above, it may be seen that plastics, are certainly going to be more efficient, owing to its lower value of θ_c . At any angle below θ_c , no etchable track will be observed after chemical etching. As a consequence of this, the directional efficiency (η) is always less than unity.

b. Detection threshold of commonly used track detectors.

The detection threshold of different track detectors varies considerably and depends upon the atomic charge (Z) and the energy (E) or more precisely on the velocity (v) of the charged particles. The parameter Z/β , where $\beta=v/c$ (c =velocity of light), is useful for the characterization of minimum detection limits of a

detector. The smaller the value of Z/β , the more sensitive is the detector. Some of the detection threshold values for the commonly used track detectors are given in Table 1.4.

Detector	Z/β	Detection threshold (MeV/mg.cm ²)
1. Inorganic	---	15
2. Organics		
Lexan, Makrofol	60	4
Cellulose acetate	40	—
Nitrocellulose	30	1
CR-39	6	< 0.05
SR-86		3 times more sensitive than CR-39

Table 1.4 Detection thresholds of some common detectors

c. Track geometry.

The nuclear particles incident on the detectors can be identified by their charge Z , Mass M , and energy E . Differences in these particle parameters are shown as changes in the track length L , and the track etching rate V_t . This characteristic helps in identification of the incident particles. As can be seen in the Fig.1.4 (see next page) the various parameters can be measured by solving the equations given below provided the V_t remains constant through out the etching time

$$L = (V_t - V_b) \times t \quad (1.1)$$

$$D = 2 \times V_b \times t \times (V_t - V_b / V_t + V_b)^{1/2} \quad (1.2)$$

$$f = \sin^{-1}(V_b / V_t) \quad (1.3)$$

Practically, the V_t may increase or decrease along the track length. This factor can also be used in the measurement of particle identification.

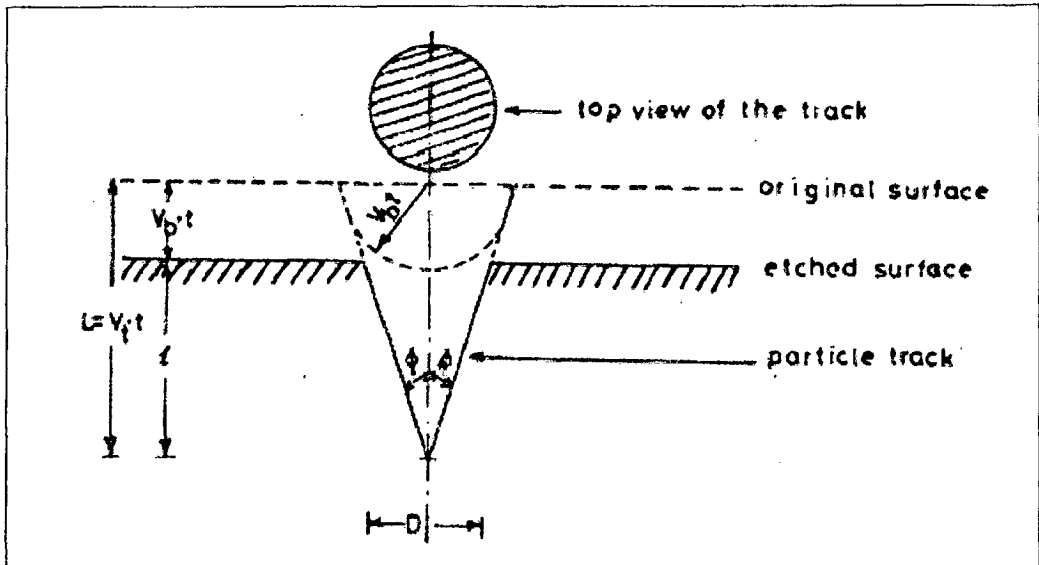


Fig. 1.4 The track geometry

1.1.6 Criteria of track formation.

A number of theories⁶ have been put forth to examine the validity of the condition $V_t/V_b \geq 1$. A simple and valid track formation criterion must use a parameter X , having a definite limit X_c below which a limit of non-etchability occurs.

1) Total energy loss rate criteria by Fleischer *et. al.*¹⁵.

This was the most natural explanation of track formation that it depended on the total amount of energy deposited per unit path length by the incident ion. Accordingly the total rate of energy loss per unit length d_E/d_x by the bombarding particle must exceed a critical value, $(d_E/d_x)_c$, which is a characteristic of the particular material. This proposition was found to work over a narrow region of particle velocities and failed for the high energy regions. The reason being the energetic delta (δ) rays produced tend to multiply and scatter away from the latent track region and deposit

their energy to the side of the path.

2) The primary ionization criterion (J) by Fleischer et. al.¹⁶.

This model takes into account the number of ions formed close to the path of the particle. A relationship for the primary ionization J, is defined as follows:-

$$J = C \left(Z_{\text{eff}}^2 / \beta^2 \right) \times [\ln(\beta^2/1-\beta^2) - \beta^2 - \delta + K] \quad (1.4)$$

Where Z_{eff} is the effective atomic charge of the particle

C and K are constants of the stopping media

β is the velocity of the charged particle.

δ is the relativistic correction term

The tracks are registered, only when 'J' exceeds a certain critical value. The shortcomings of this model have been that, it takes no account of the ionization produced by the low energy δ rays. Moreover in crystals the radial extent of unetched tracks is of the order of few \AA , so the primary process should predominate over the secondary ones, but it may not be the case in polymers. But in spite of this, the model has proved to be good for crystals as well as plastics and it has been found that the V_t is a continuous function of 'J'. Usually $V_t \propto J^a$ where a is of the order of ~ 2 for plastics.

3) The restricted energy loss (REL) criteria by Benton¹⁷.

It takes into account the secondary ionization and the excitation produced by the delta rays along the particle trajectory. It is based on the principle, that the total energy deposited in the core region by a charged particle decides the etchability of the latent track region. Thus a particle will produce a etchable track only if its REL is greater than $(\text{REL})_{\text{crit}}$ for the material. The calcu-

lations are made by considering only the delta rays having energy less than some cut-off value (W_0).

4) Radius restricted energy loss (RREL) criteria by Paretze¹⁸.

This criteria takes into account all the energy deposited by all the events occurring within a radius 'r' of the particle trajectory. Thus L_r criteria gives importance to the track region and tries to consider only that part of energy of delta rays, which actually gets deposited in the core region irrespective of the energy of the delta rays.

$$L_r = L_\infty a.Z_{\text{eff}}^2/\beta^2[\ln R/r-(1-r/R)] \quad (1.5)$$

Where

L = total rate of energy loss d_E/d_x

R = maximum track width

A = constant for a given medium

r = radial distance from the particle trajectory.

This model is an improvement over Benton's criterion.

5) The Delta-ray criterion by Katz and Kobetich¹⁹.

This approach is in contrast to that of the Total energy loss and the Primary ionization criterion; it suggests that the energy deposited by the delta rays, rather than the primary ionization is crucial in the formation of ethchable tracks. It is proposed that etchable track results when a critical dose (D_{crit}) of ionization energy is deposited by the secondary electrons at a critical distance from the ion path. This criterion can be fitted into the experimental data, but it appears unreasonable, that the contribution of primary ionization can be completely neglected.

6) The Delta-ray criterion by Monin²⁰.

This approach is similar to that of Katz and Kobetich. However no minimum critical radius is assumed initially. Dose calculations are made within cylinders of increasing radii. It is assumed that

etchability is created when the absorbed dose exceeds a specific value within a cylinder of certain radius.

1.1.7. The Environmental effects on track formation⁴.

The environmental effects are more related to the polymeric track detectors and can be classified into three distinct categories:

- (i) Prior to irradiation.
- (ii) During irradiation.
- (iii) After irradiation but prior to etching.

1) Environmental effects prior to irradiation²¹.

It has been reported that the chemical composition of the polymer material plays a very important role in deciding the V_b of a particular material. Excess of plasticizers and residual solvents tend to increase the rate of V_b . Pretreatment like UV or gamma rays irradiation also plays a crucial role as some materials may undergo cross linking, in such cases it may be better to irradiate the material.

2) Environmental effects during irradiation ^{22,23}.

The presence of free oxygen is important in the process of bond scission. Instead of recombining, ions and radicals combine with oxygen to produce permanent scission. Another important parameter is temperature; low temperature should inhibit the recombination of ions and free radicals and decrease the diffusion of these species away from the central core region.

3) Environmental factors after irradiation ^{23,24}.

At higher temperature more than 30 °C, significant loss of signals has been reported, whereas they are negligible under ambient conditions. Also, storage in the presence of oxygen results in increase in the bulk etch rates.

1.1.8 Track Visualization techniques.

The latent tracks formed in the detectors can be viewed directly with the help of a transmission electron microscope, X-ray scattering and neutron scattering. But the use of these techniques has some serious limitations like, very thin films of the order of few tens of nanometers are required, which are difficult to prepare. Further, the observation window is very small, so a high track density of about 100 million/cm² or more is required. Also some tracks may be annihilated in certain materials. Further, these systems are very expensive and hence their availability is restricted. The most widely used methods are the chemical and the electrochemical etching, which makes it possible to view the tracks under an ordinary optical microscope that it can be used in any ordinary laboratory conditions.

1) Selective chemical etching⁸.

The latent tracks in the detector material are centers of enhanced chemical activity compared to the undamaged material. They consist of disordered structures, which in turn are associated with large free energy. The damaged material is immersed in a suitable chemical solution called 'etchant' which degrades the damaged material in preference to the bulk of the material. When the dimensions of the tracks become comparable to that of the wavelength of visible light they act as strong scattering centers appearing black in normal bright field illumination and white in a dark field, under the optical microscope. This process of chemically enlarging the latent damages into visible tracks under the optical microscope is called chemical etching. The etching process is a heterogeneous process involving a solid liquid interface. The driving force for the reaction is the reduction in the free energy of the system. A typical chemical etching assembly is shown in Fig. 1.5.

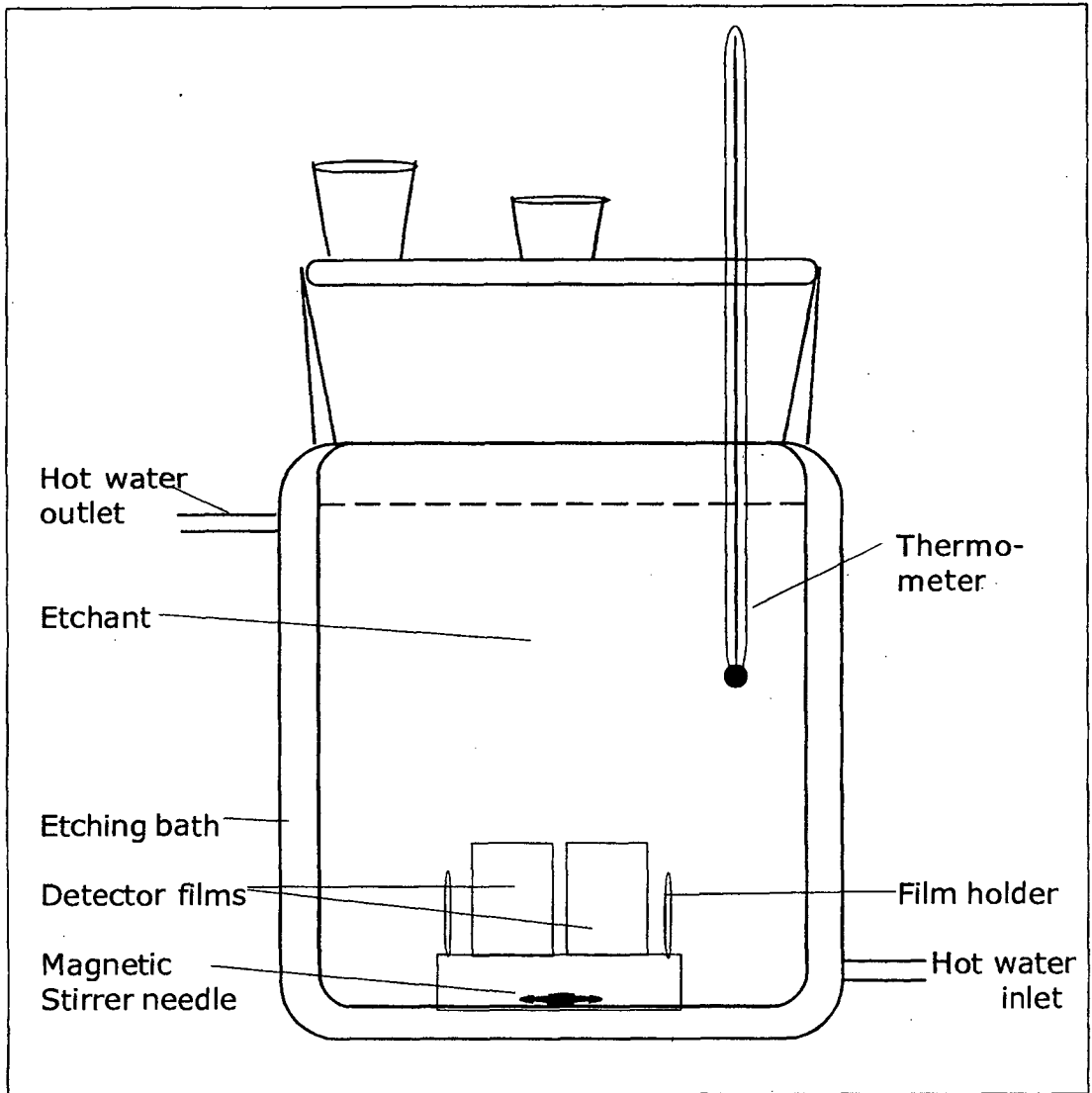


Fig.1.5. Chemical etching bath.

A suitable etchant must consist of the following properties:-

- 1) It must attack the latent track region in preference to the bulk of the material and the V_t should be independent of the angle between the latent track and the surface of the detector.
- 2) It should give a uniform V_b value across the material and should give little background etch pit formation.

A number of etching recipes have been tried for different glasses, minerals and plastic detectors. Some of the common ones are strong alkalies like NaOH and KOH, combination of alkali solution

and alcohols for plastics. Acids like H_2SO_4 , H_3PO_4 , HF, HI, glacial acetic acid, HCl have been used mainly for minerals and glasses. Some oxidizing agents like $\text{K}_2\text{Cr}_2\text{O}_7$, KMnO_4 , NaClO_4 have also been used in the case of plastics.

2) Electrochemical Etching²⁵.

The process of track revelation by chemical etching has been further enhanced by the speed at which the track revelation is obtained. This process is known as electrical breakdown or 'Treeing' process. During etching, the etchant rapidly diffuses in the pre-existing latent tracks preparing conductive paths which penetrate the dielectric material. If an alternating voltage is applied across the detector film, current is produced in these conducting paths. The energy given out as a result of this, dissipates in the track region leading to strong local heating of the etchant, thereby increasing the track etch rate. The amount of energy dissipated in these conducting paths is directly proportional to the frequency of the alternating voltage applied. The voltage applied concentrates at the tip of the conducting paths giving rise to a process called 'treeing'. Because of the high temperature at the tip of the conducting channels, the materials are thermally degraded leading to a continuous growth of the track and complete degradation causing the enlarged tracks to carbonize. Hence the ECE tracks are seen as black spots under a microscope. Because of the increase in the electric current the temperature of the entire dielectric foil increases both the bulk etch rate and the track etch rate. This technique is superior to the conventional chemical etching because it permits a large scale amplification of tracks so that they are easily seen by the naked eyes. A typical electrochemical etching assembly is shown in Fig. 1.6. The ECE technique has been mainly found to work with polymers with the following general properties⁸:

- 1) Good electrical properties, *i.e.*, high values of tensile strength,

dielectric strength and volume-resistivity.

2) Low water absorptivity.

3) Low value of dissipation factor or dielectric loss factor.

4) Polar nature of the material.

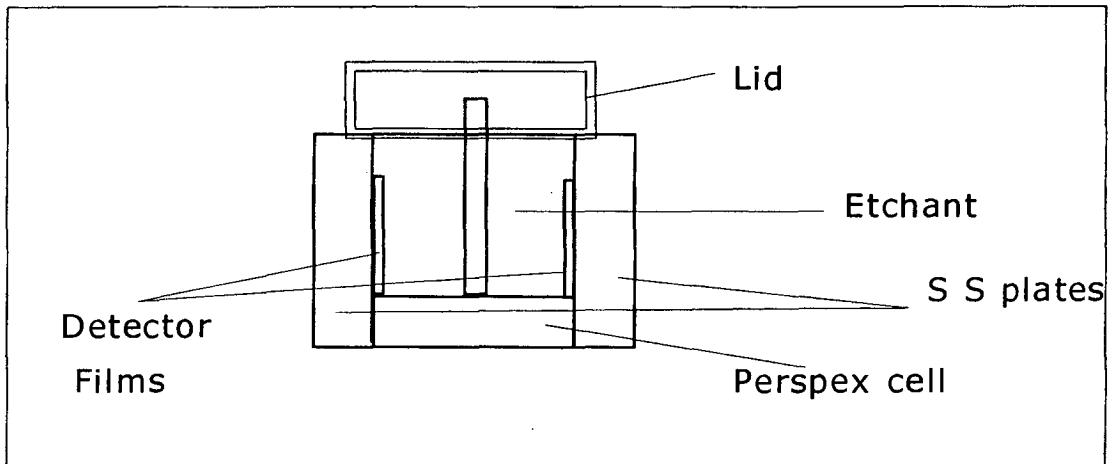


Fig. 1.6 Electrochemical etching bath

However, the ECE technique has been found to be of lower efficiency.

3) Graft and Dye Technique^{26,27}.

This is a non-etching process of track revelation in polymer materials. The Latent track region in a polymer is full of unstable or metastable species, like the free radicals, peroxy and hydroperoxy groups. If an appropriate unsaturated organic compound is allowed to react with these sites, the resulting chain polymerization yields a co-polymer. These polymeric sites are now grafted in the initially present latent tracks. The grafted chains extend sideways from a charged particle path and ensure the enlargement of the track diameter. If a dye which selectively fixes onto the grafted copolymer is added to this system, the tracks can be visualized under an optical microscope. A fluorescent dye may also be used under UV illumination.

1.1.9 Track Evaluation (counting) techniques.

They are classified as microscopic and macroscopic techniques.

A) Microscopic techniques.

1) Visual track counting under an optical microscope.

This is the simplest and widely used method of track counting for densities up to $10^5/\text{cm}^2$. The method is slow and tedious, but nowadays has been assisted by the image projection techniques and image analyzing systems.

2) Microdensitometry^{28,29}.

This technique measures the optical density of the films in determining the track densities up to 10^5 to $10^7/\text{cm}^2$

3) Measurement of the scattered light under darkfield illumination.

The etched tracks appear as bright spots in a dark background, so the integral amount of light scattered into a microscope objective by the individual tracks can be easily quantified by placing a photomultiplier near the eyepiece.

4) Confocal Microscope¹².

This has been used for a three dimensional reconstruction of track shapes. This technique has a strong potential for more accurate reconstruction of the original particle parameters such as charge, energy and mass number.

5) Atomic Force Microscope¹⁰.

Studies that have been not possible by an optical microscope, like the early stages of the etched track formation, surface roughness *etc.* can be easily performed by using this technique.

B) Macroscopic techniques.

1) Physical measurements.

Gas flow and ionic permeability through the tracks can be used to measure the number of holes in an etched detector foil. Electron penetration can be used to measure the number of holes in an

etched detector. These methods are useful only for low track densities.

2) Spark counting³⁰.

In this method of track counting the exposed and etched detector film is kept between two electrodes, one plain sheet of stainless steel or brass and other a thin layer of aluminium such as aluminized Mylar™. A spark passes through the track region when the electric field is applied and evaporates the aluminium from the Mylar™ thereby preventing a second spark in the same region. The sparks are simultaneously counted on a scalar. A visible track pattern is also recorded on the Mylar film. This method is suitable for track densities up to 5000 tracks/cm² only.

3) Using breakdown counter and the current pulse counter³¹.

The two counters consist of a capacitor made up of an insulator and a metal plate. The charged particles especially fission fragments are allowed to penetrate the insulator and the fluctuations in the capacitance or the current is measured.

4) Scintillator filled etch pit counting³².

In this method, the etch pits are filled with a suitable scintillating material and the excess is wiped out. An intense source of alpha particles is then placed close to the detector in a closed assembly and the scintillations produced are measured.

1.1.10 Applications of Plastic SSNTDs.

As SSNTDs are playing a dominant role in almost every field of science, it is difficult to remain updated very accurately about all the applications pertaining to SSNTD technique. However, some applications are cited below which would give a birds eye view, as to how wide the importance of this field has grown in almost all the areas of basic sciences. The reviews on technological applications of SSNTDs indicate more than 40 different areas of interest in this field⁸.

(1) Nuclear Physics and Technology.

- (a) Track detectors have been used extensively for studying the binary mode of fission. Ternary and quaternary fission of heavy elements like ^{235}U , induced by heavy ions have been studied.
- (b) Search for super heavy elements: SSNTDs have been useful in studying the possibility of finding heavy elements naturally occurring or artificially created.
- (c) Elemental content and its distribution: The emission of charged particles from any nuclear reaction, like (n,f) , (n,p) , (n,α) can be used to identify the elements like Li, B, Pb to name a few. The number and the characteristics of the tracks registered give information about the elemental content as well as its spatial distribution.

(2) Health physics.

- (a) Radon dosimetry in homes, workplaces *etc.*
- (b) Neutron dosimetry in and around nuclear installations.
- (c) Personal dosimetry of crew members of high altitude aircrafts.

(3) Biomedical sciences.

- (a) Microdistribution of alpha active aerosols in lungs.
- (b) Alpha activity content of blood can be monitored by immersing the detectors in frozen blood.
- (c) Lead content in the teeth and bone.
- (d) Cancer diagnostic and therapy: The use of heavy ions in cancer therapy requires prior knowledge of precise ion ranges, depth dose distribution *etc.*

(4) Technological Sciences.

- (a) Preparation of micro filters: By exposing the detector materials to a collimated beam of particles holes of controlled geometry can be obtained by varying the energy of the particles and the etching conditions. These filters can then be used as micro filters

in biological applications like separating cancerous cells from that of normal blood cells. Also these could be used as reaction vessels for chemical and biological reactions. In These type of materials the holes can be filled with subatances of different electrical and magnetic properties thus making them complex microelectronic devices.

5) Imaging techniques:

(a) To find the structure of crystalline solids.

(b) For neutron, proton and heavy ion radiography.

1.1.11 Highlights of SSNTD research work In India³³.

(A) Brief Overview.

The beginning of SSNTD in India dates back to 1965, with the visit of Prof. P.B. Price to the Tata Institute of Fundamental Research (TIFR) where cosmic ray pre-history was studied in meteorites. This work was then further extended to institutes like the Bhabha Atomic Research Centre (BARC), Kurukshetra University and at present is spread over 20 specialized centers all over the country. BARC played a important role in bringing all these groups under one roof, giving birth to 'Nuclear Track Society of India' (NTSI) which has been instrumental in conducting national symposia biennially since 1987. The Department of Atomic Energy (DAE) has been very much instrumental in this field and has supported many of the activities involving the applications of SSNTD like biomedical sciences, environmental sciences, material sciences, reactor physics, Uranium exploration *etc.*. Apart from its application point of view, efforts were also put towards the preparation of materials like, nitrocellulose in BARC³⁴ and UICT³⁵ Mumbai.

(B) Major Areas of SSNTD research in India.

(i) Cosmic rays and space science.

Some of the observations, made during the studies carried out in this area worth mentioning are, the anomalous cosmic ray components in near earth orbit and the first and direct unambiguous results on the ionization states of the anomalous cosmic ray components³⁶. Apart from these, various space mission programme studies have also been carried out.

(ii) Fusion-fission and particle evaporation³⁷.

A simple and unique method to study fusion-fission and particle evaporation in complete 4π geometry has been developed. The first visual detection of one and two evaporated particles from the highly excited compound nuclei before fission has been one of the important contribution in this field.

(iii) Nuclear track registration from solution media and its applications in nuclear science³⁸.

Nuclear track registration on detectors immersed in solution known as 'wet method' developed in BARC has opened up new areas of studies involving SSNTDs. This technique has been extensively used for neutron flux monitoring, microanalysis of Boron, Lithium, actinides etc. at ultra trace levels.

(iv) Absolute fission yield measurement in the neutron induced fission of actinides³⁹.

Development of a simple and elegant methodology known as 'track-etch cum gamma spectrometry' for the measurement of absolute fission yields in the thermal and fast neutron induced fission of a large number of actinide isotopes has been an important contribution. This is useful for evolving a proper reactor design, fuel handling, waste management etc.

1.1.12 Current status of SSNTD technique using plastic materials.

SSNTD is a very versatile tool of radiation detection which is being used in diverse branches of science and technology. Both inorganic and organic (polymer) materials contribute significantly in the applications of this tool. The organic materials have gained an edge over its inorganic counterpart, since these materials can be analyzed with simple and cost effective techniques of track development and evaluation. More than 50 plastic materials of different compositions have been tested as SSNTDs, and as can be seen CR-39 polymer is the most widely used material in this field. Our country is still dependent on foreign agencies for the procurement of these materials, though we have gained sufficient expertise in the applications of SSNTD. Over the past years *i.e.* since 1965 there have been very few serious attempts towards development of these materials in our country³⁴⁻³⁵. This leaves ample of scope in the direction of development of plastic materials for SSNTD.

1.2 Allyl monomers and Polymers.

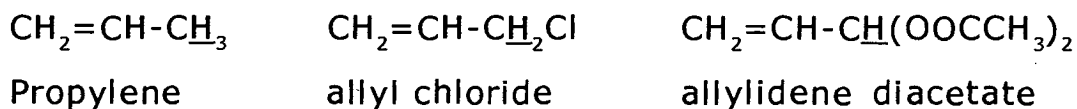
Allyl compounds are ethylenic compounds having lower reactivity towards polymerization, than the typical vinyl compounds⁴⁰. The word 'allyl' is derived from allyl sulfide compounds found in plants of allium or onion family. The name has been most frequently used for the allyl radical $\text{CH}_2=\text{CHCH}_2\cdot$. The mono allyl compounds do not yield homopolymers of high molecular weight by conventional free radical and ionic polymerization. This has been attributed principally to the high reactivity of allylic hydrogen or halogen atoms on the third carbon atom, in the termination of the growing polymer chain, by degradative chain transfer⁴¹. The monomer itself acts as an inhibitor in the formation of long chain polymer and only liquid low polymers result. However, some allylics

having, electron-displacing and/or resonance promoting groups attached to the ethylene nucleus activate the double bonds and thereby prevent the activity of hydrogen on the third carbon in degradative chain transfer⁴². Thus, methyl methacrylate $[\text{CH}_2=\text{C}(\text{COOCH}_3)\text{CH}_3]$ does not behave as an allyl compound although it possesses the allylic H-atom.

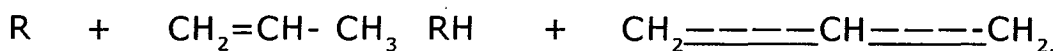
1.2.1 Classification of allylic compounds.

Allyl compounds can be classified based on the groups attached on the third carbon atom of the allyl radical. They can be classified as follows:

1) 1-olefins, $\text{CH}_2=\text{CHCH}_2\text{R}$, 2) allylidenes $\text{CH}_2=\text{CHCHR}_2$ 3) $\text{CH}_2=\text{CRCHR}_2$. In these compounds the ethylenic nucleus lacks strong activating groups, and allylic hydrogen atoms are present on the third carbon for chain transfer⁴². Allylic hydrogen atoms are shown in the following examples.



Removal of allyl hydrogen or chlorine atoms can terminate a growing chain radical and the resonance stabilized radical formed have low efficiency in propagating a new polymer chain.



Another way to classify allyl compounds is based on the fact that monoallyl compounds generally do not form homopolymers of high molecular weight by addition polymerization, using commercial catalytic systems. On the other hand, polyfunctional compounds can form very high molecular weight polymer materials. In the case of monoallyl compounds special catalysts systems such as Zeigler-Natta transition metal catalysts can yield homopolymers of controlled steric structure especially from 1-alkenes. Polyfunctional compounds however can form high molecular weight

homopolymers by suitable radical initiation, in spite of the macro radical wastage by degradative chain transfer and by also cyclization.

1.2.2 Radical polymerization of allyl compounds.

The monoallyl and monoalkylidene compounds do not form homopolymers, of high molecular weight, on heating with radical catalysts. Typically these monoallyl compounds, such as allyl acetate form oils or viscous liquid low polymers having low degree of polymerization. The explanation of Bartlett and co-workers has been generally accepted that reaction of radicals with allylic hydrogen atoms causes self-termination⁴³. The ability of allyl compounds to terminate chain reactions, can be used to control or retard radical type polymerization, oxidations and degradations e.g., allyl acetate is used as a stabilizer of diallyl phthalate prepolymer⁴⁴.

Under free radical conditions, most mono allyl compounds including propylene and higher olefins, copolymerize readily with sulphur dioxide, to give solid products of high molecular weight. Sulphur dioxide behaves as an acidic monomer wherein unshared electron pair of sulphur apparently acts like a pi electron pair of a monomer double bond. The sulfone polymer reaction was discovered by Solonina, who made SO₂ copolymers from allyl alcohol and allyl phenyl ether⁴⁵. Unsaturated compounds bearing electron attracting groups such as -COOH, -COOR, and halogens did not copolymerize with SO₂. Allyl compounds having two or more allyl groups often can be polymerized under free radical condition to form homopolymers, along with the waste of growing macroradicals by degradative chain transfer. These type of allyl monomers are the most widely used, for commercial purposes. The polyfunctional allyl compounds can be formed in partially polymerized state fol-

lowed by completion of polymers or curing to thermoset structure, by heating in the presence of peroxide initiators. Thus, Allyl Diglycol Carbonate (ADC) is used to cast optical plastics, and the Diallyl Phthalate (DAP) prepolymers are used in fiber- filler reinforced thermoset articles. The relatively low reactivity of allyl groups permits formation of fusible prepolymers.

Allyl monomers show slight reactivity for thermal polymerization without added initiators. If initiators are absent, some of them can be heated to very high temperature with a little reaction.

Air-drying polymerization of certain unsaturated hydrocarbons, long chain esters and ethers containing peroxydizable allylic hydrogen atoms, seem to involve radical processes quite different from homogenous conventional radical initiated polymerization. Oxidation at allylic H-atoms leads to hydroperoxide groups, which initiate formation of prepolymers, followed by cross-linking. For air oxidative polymerization to occur readily, a molecule seems to require at least two non conjugated double bonds associated with hydrocarbon or ether groups as in drying oils like sorbitol tetraallyl ether, polyallyl ethers of carbohydrates and certain diallylidene cyclic acetal esters. Most polyfunctional synthetic allyl monomers investigated have proved to slow down the rates of air-drying polymerization for large scale use in coatings.

Molecular oxygen retards polymerization of allyl esters, ADC, DAP, diallyl adipate, triallyl cyanurate, but the effect seems less in the case of typical acrylic and methacrylic compounds.

1.2.3 Polyfunctional allyl compounds.

It is quiet clear from the theoretical considerations that the polyfunctional allyl compounds are the most important monomers to get high molecular weight polymers by free radical polymeriza-

tion. In this section, a brief overview of the different allylic monomers is presented along with their applications.

Divinyl benzene isomers were the first readily available crosslinking monomers but were unstable under storage. They generally give brittle copolymers. Monomers such as dimethyl acrylate, of tri or tetramethyl glycol and diallyl monomers show better stability as monomers and in their copolymers. In general, polyfunctional allyl and allyl vinyl monomers are useful because of better latitude in controlling cross linking *e.g.*, allyl methacrylate, diallyl maleate, diallyl fumarate, diallyl phthalate, triallyl cyanurate and triallyl isocyanurate, in 1-5 % concentration can be employed to cross-link not only co-monomers and partial polymers but also substantially saturated polymers. Applications involved are dental plastics, finished synthetic rubbers, electrical insulators, optical plastics and crosslinked fibres. Allyl monomers such as DAP, ADC, triallyl isocyanurate and diallyl adipate can be brought to formable, partial polymer stage before being cured into finished product. It is also known that one polyfunctional allyl monomer, allyl cinnamate, had been polymerized thermally and photochemically in 1912. The finished crosslinked polymers were brittle but were considered as amber substitutes⁴².

Recent development in polyfunctional monomers that have been polymerized includes use of radiation like X-rays, high energy electrons, gamma radiation and UV radiation. However high temperature radical initiators, are also being used for accomplishing similar curing without radiation.

One of the important polyfunctional allylic monomer has been the allyl diglycol carbonate (ADC) which was synthesized in 1940. Due to highly superior optical properties of its homopolymer (PADC) or CR-39™, this monomer has gained a tremendous commercial

potential. CR-39™ finds application in optical products like contact lenses and as a substitute for glass e.g. windshield for airplanes, apart from being used as a SSNTD.

1.3. Poly Allyl Diglycol Carbonate (PADC) as a particle track detector.

The PADC plastic material is the leading detector material used in the field of SSNTD. Commercially it is available under various trade names like CR-39, PM, Trastrack etc.. It is a highly cross-linked thermoset plastic prepared from a liquid monomer called Allyl diglycol carbonate (ADC). The structure of ADC is shown in Fig. 1.7

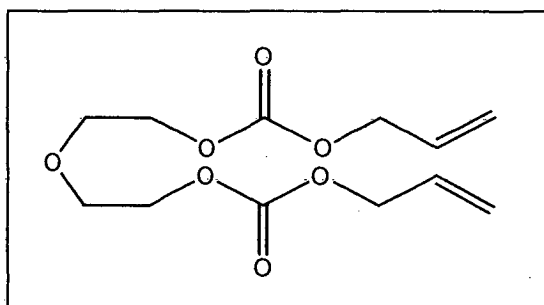


Fig 1.7. Structure of ADC

Carbonic acid allyl ester 2-(2-allyloxycarbonyloxy-ethoxy)-ethyl ester,
OR Allyl Diglycol Carbonate (ADC) OR Diallyl Diglycol Carbonate

Some of the important IUPAC and common names mentioned in the chemical abstracts for the ADC monomer are listed in Table 1.5 (see next page).

IUPAC Names.	
CAS Reg. No. 142-22-7	
1)	Oxydi-2,1-ethane-diyl di-2-propenyl ester
2)	Diethylene glycol bis (allyl carbonate)
3)	9-Oxo-2-propenyl ester of 2,5,8,10 tetraoxatridec-12-enoic acid
4)	Diethylene glycol diallyl dicarbonate
Trade Names.	
1)	CR 39™
2)	Nouryset 200™
3)	NSC 5246™
4)	RAV 7AT™
5)	RAV 7N™
6)	Transallyl CR 39™
7)	TS 16™
8)	3D CONCORD™

Table. 1.5 IUPAC and Trade names for ADC monomer

ADC was first prepared by Muskat, Strain and co-workers⁴⁶ of Pittsburg Plate Glass (PPG) industries, USA in the year 1940 under the brand name CR- 39™; CR indicates the name of the project, Columbia Resins, under which it was synthesized and 39 indicates the successful batch number. The compound was trademarked by the PPG industries for its future use. The polymer PADC from the ADC monomer was prepared by Dial and Gould⁴⁷ in 1945. This material was in use for its several optical and other applications over many years. Cartwright (1978) successfully tested this material for SSNTD applications for the first time⁴⁸. Other SSNTD workers soon established its importance as a unique, highly sensitive track detector material.

1) Typical properties of commercial ADC monomer⁴⁹

Solubility: Miscible in acetic acid, acetone, ethyl acetate, ethyl alcohol, ethyl ether, chloroform, methyl methacrylate, styrene and vinyl acetate. Partly soluble in amyl alcohol, carbon disulphide, gasoline and ligroin. Insoluble in ethylene glycol, glycerol and water.

Appearance	: clear, colorless liquid
Color	: APHA <10
Odor	: none to slight
Specific gravity 20°C	: 1.15 g/cm ³
Boiling point at 2mm Hg	: 166 °C
Refractive index, n_D at 20°C	: 1.452
Melting point (supercooled)	: -4 to 0 °C
Viscosity at 25°C, mm ² /s (= cSt)	: 15
Flash point	
Seta closed cup, °C	: 173
Cleveland open cup, °C	: 186
Water content, slightly hygroscopic, %	: 0.1

2) Properties of Polyallyl diglycol carbonate made from Allyl diglycol carbonate CR-39™ monomer⁴⁹.

Physical and mechanical properties:

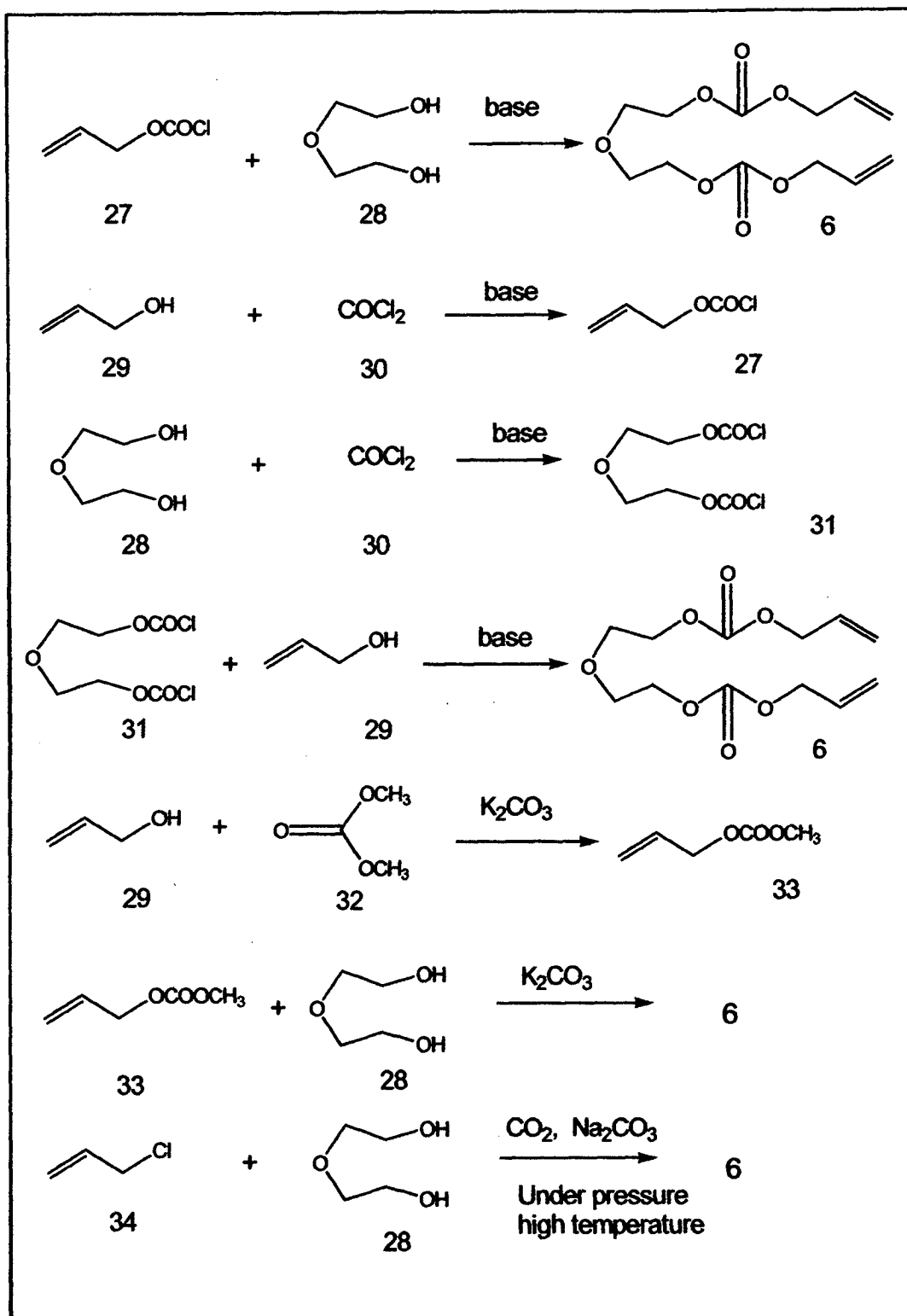
Density (g/cm ²)	: 1.31
Hardness, Rockwell	: M95-M100
Tensile strength, psi	: 5,000-6,000
Compressive strength, Ult, psi	: 22,500
Impact strength, 25°C,(ft lb./in.)	
Izod, notched	: 0.2-0.4
Izod, unnotched	: 2-3
Mold shrinkage (% volume)	: 12-13

Thermal properties:

Conductivity (Btu in./hr ft ² °F)	:	1.45
Specific heat(Btu /lb. °F)	:	0.55
Glass transition temperature (°C)	:	85
Resistance to chemical reagents		
(% gain in weight after 7 days immersion, 25°C)		
Distilled Water	:	0.7
30% H ₂ SO ₄	:	0.5
1% HNO ₃	:	0.7
Conc. HCl	:	0.1(discoloration)
10% HCl	:	0.4
10% NH ₄ OH	:	0.8
95% Ethanol	:	0.1
Acetone	:	0.5
CCl ₄	:	0.6
Benzene, Toluene	:	0.6
Characteristics useful for SSNTD application:		
Z/β	:	6
Detection threshold	:	< 0.05 MeV/mg. cm ²

1.3.1 Preparation of Allyl Diglycol Carbonate (ADC) monomer.

From the literature survey carried out for preparation of ADC monomer, it has been found that the monomer has been prepared by three different methodologies *viz.*, Phosgenation, Transesterification and high pressure synthesis using CO₂ (Scheme 1.1 see next page). All the literature available with respect to the preparation of ADC monomer has been briefly described below.



Scheme 1.1. Various methods for ADC preparation.

1) Use of phosgene.

Allyl diglycol carbonate (ADC) was first prepared by Muskat and Strain⁴⁶ by reacting allyl chloroformate and diethylene glycol in the presence of a basic catalyst like pyridine. Allyl chloroformate in turn was prepared by the reaction of phosgene with allyl alcohol. This was the most conventional method of synthesizing the monomer. A few other researchers have also reported ADC synthesis by this route⁵⁰⁻⁵².

ADC is also prepared by the reaction of diethylene glycol with phosgene i.e. preparation of diethylene glycol chloroformate which on reaction with allyl alcohol would give ADC. A number of authors have reported the synthesis of ADC by this route, using various basic catalysts like pyridine, sodium hydroxide, sodium carbonate etc. Table 1.6 gives the references for the preparation of ADC by this route using various catalysts.

Sr.No.	Catalyst	Reference
1	Sodium Hydroxide	53,54,55-57, 60,
2	Quaternary ammonium salts	58
3	Pyridine	50-52

Table 1.6 Various catalysts used for ADC synthesis.

2) Transesterification.

Transesterification is environmentally benign process for preparation of ADC. Aliphatic carbonates like Me_2CO_3 , Et_2CO_3 obtained by high pressure reactions of CO , CH_3OH and EtOH can be used. In this process dimethyl carbonate, allyl alcohol, and diethylene glycol are reacted in presence of a transesterification catalyst

which are usually alkali or alkaline earth metal derivatives⁶¹. Alternatively, diallyl carbonate can be reacted with diethylene glycol in the presence of a transesterification catalyst^{62,63}. The monomer is found to have the following impurities Mono allyl diglycol Carbonate (MADC) (24), Mono allyl diglycol dicarbonate (MADDC) (25), Di allyl diglycol dicarbonate (DADDC) (26) which depend on the type of process used for the preparation of ADC monomer. These impurities are known to result in poor quality of the films and hence purification of the monomer prior to polymerization is essential⁶⁴. Fig. 1.8. gives the structures of compounds which are impurities formed during the manufacture of ADC.

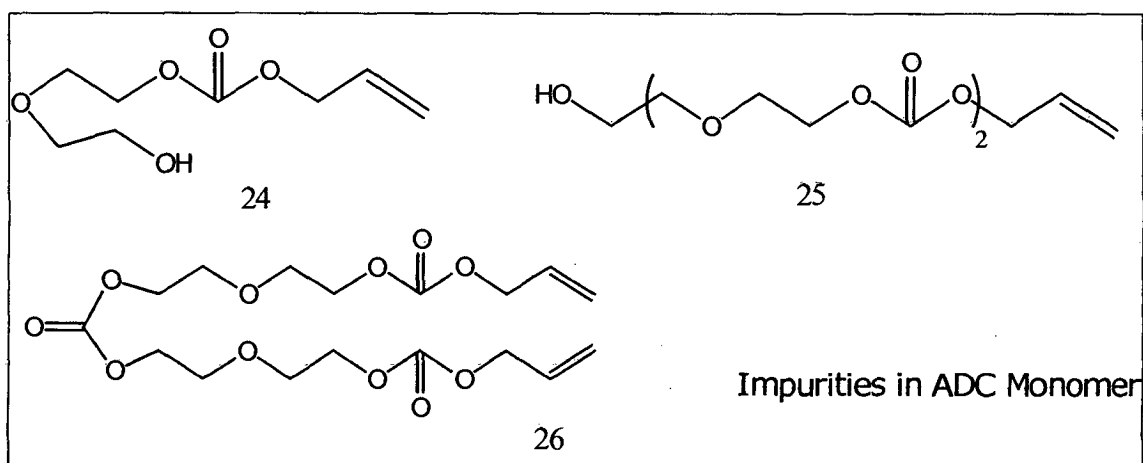


Fig. 1.8 Impurities formed during the manufacture of ADC

3) Synthesis under high pressure and temperature, using carbon dioxide.

ADC can also be prepared by using autoclaves in which an alkali halide is reacted with diethylene glycol and carbon dioxide in the presence of a suitable catalyst⁶⁵⁻⁷¹ at high pressure $\sim 100 \text{ kg/cm}^2$ and temperature of $100\text{-}200^\circ\text{C}$.

1.3.2. Purification of the monomer.

The purification of the monomer is an important step in the manufacture of ADC. It has been found that, impurities present in ADC monomer alter the track recording properties and etching behavior of the PADC films. Tarle (1982) studied the commercially available CR-39 monomer using mass spectroscopy. He found that apart from the molecular ion at $m/z=274$ small peaks at m/z 190, 332, 406 were also recorded. He studied the manufacture process of ADC and assigned the peaks to MADC (24), MADDC (25), and DADDC (26), formed during the course of the reaction⁷². The separation of MADC from ADC is hampered by azeotrope formation and hence can only be removed by cold water washings. The presence of -OH groups due to MADC, gives a bad post etched surface and the reduction in this certainly improves the surface characteristics, of the etched films. The recommended ratio of concentrations of MADC/ADC is as low as 0.002. MADDC is present in small amounts and hence, is harmless. Huang (1982) has proposed that washings with dilute Hydrochloric acid followed by column chromatographic purification⁷³ can remove the MADC impurity.

Portwood (1984) studied the ADC monomer samples by Gas chromatography. To purify, the monomer was dried over 5 A molecular sieves, for several days and later distilled using a short vigreux column at ~ 1 torr. The main fraction was collected at 160 °C. Gas chromatography showed that the distilled compound was free from the impurities present in the untreated compound⁷⁴.

Lembo used the SE (30) chromatographic column to analyze the CR-39 monomer and found the presence of DADDC and MADC. He suggested the use of Flash chromatography to separate MADC and DADDC present in the monomer. Water, if present, could be effectively removed by adsorbents like activated carbon or alu-

mina⁷⁵.

Yang (1986) used FT-IR, GC and GPC to analyze the impurities in ADC samples. He found that FT-IR is not much effective, but GC and GPC show the presence of impurities. He suggested the use of vacuum distillation of ADC, followed by GC or GPC analysis to find the effectiveness of the distillation process⁷⁶.

Ahmad (1991) proposed that in order to reduce the depth dependence of the bulk etch rate, ADC with uniformly high density of crosslink's should be used. Hence, he suggested that the monoallyl derivative (MADC) should be completely removed before polymerization in order to ensure the uniform etching of the plastic⁷⁷.

ADC has also been purified by treating with acids like Hydrochloric acid, Formic acid and Oxalic acid followed by oxidizing agents like H_2O_2 ⁷⁸. The process of crystallization has also been used, wherein ADC was purified from methanol or ethanol⁷⁹.

1.3.3 ADC polymerization.

Generally, mono allyl monomers and specially those containing electron donating groups like -OH, -SH, -C=NH- are difficult to polymerize using radical catalysts, but the di, tri or poly allyl monomers would undergo polymerization readily^{80,81}. This is due to the fact that although the allylics are known for degradative chain transfer reaction, compounds having two or more double bonds are capable of initiating the chemical reaction at more than one centre, thereby yielding a three-dimensional network. As the polymerization of ADC proceeds, the state of the sample changes from a liquid at the beginning to a rubber like gel and finally into a glassy plastic at the end of polymerization. The transition from the liquid into the rubber-like gel is determined by the formation

of an infinite three-dimensional network in the system which up to this point contained finite size clusters. As the gel consists of one large macromolecule it cannot flow without breaking the chemical bonds. However, the chain segments in such a loose network are sufficiently elastic to sustain large rubber-like deformations. With increasing conversion the density of the network increases and the mobility of the segments decreases. At the point when there are no reorganizing or recognizable segments, the polymer reaches a glassy state. The commercially important polycarbonates and polyesters mainly include diallyl carbonates and diallyl phthalates respectively. Out of these, the carbonates have gained tremendous importance due to their excellent optical clarity, resistance to chemical reagents, their mechanical strengths and other properties. The most important diallyl monomer that has been found useful, is of the type $\text{ACO}_3\text{-CH}_2\text{-CH}_2\text{-O-CH}_2\text{-CH}_2\text{-CO}_3$ ⁸¹ (A=Allyl) and not A_2CO_3 . A few other important allylic monomers having similar structural features⁸² have been shown in Fig. 1.9.

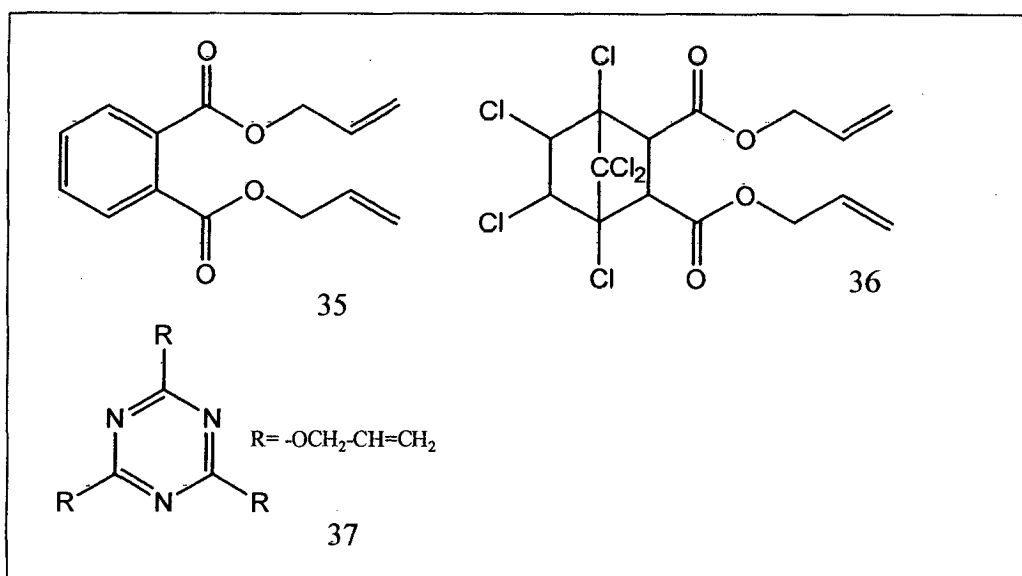


Fig. 1.9. Some other important allyl monomers.

1.3.4 Kinetics of ADC polymerization.

Allylic polymerizations are well known for their exothermic nature which leads to cracking of the films and also bad surface properties. A number of researchers have studied the kinetics of polymerization in order to circumvent these problems. In the study towards, these kinetic parameters, various methods have been used, like DSC, IR and titrimetric methods.

The first systematic study towards the polymerization kinetics of this monomer was done by Dial *et.al.*, Dial proposed the use of some low temperature decomposition initiators so that the polymerization could be initiated at lower temperatures thus avoiding the problems like cracking of the films due to the strong exotherm developed, specially when initiators like benzoyl peroxide were used⁴⁵. Hence, initiators which facilitate the use of lower initial temperatures for the polymerization are favored e.g. Peroxydicarbonates⁷⁹. Dial and co-workers prepared a kinetic model for polymerization of ADC using isopropyl peroxy dicarbonate (IPP) initiator. They proposed that polymerizing ADC as per a calculated profile of temperature with respect to time, would involve a constant rate of polymer formation, thus resulting in a slow and constant rate of heat evolution⁸³.

Later Fowler and Co-workers⁸⁴, studied the process of polymerization, by recording the internal temperature of the films, with the help of embedded thermistors and pointed out that a slight change in temperature (order of 1 °C) of the curing bath, would lead to a thermal runaway. Henshaw and Co-workers⁸⁵, have shown that the temperature gradients, also affect the depth dependent sensitivity of the films. Continued studies in this area, have shown that these factors can be reduced, by curing the plastic at a temperature, such that the internal temperature rise,

within the plastic, during the cure is negligible. For this, the curves of temperature with respect to time, that best fit to allow heat flow by making use of the differential equations by Dial et.al., has to be followed. Henshaw and co-workers⁸⁶, have also shown that different initiator concentrations lead to films of varying sensitivity values, for different initiators used. They studied the effects of various initiator concentrations by measuring the sensitivity (S), which is a ratio of bulk etch rate (V_b) and the track etch rate (V_t). Portwood (1984), modified the cycle for polymerization, using the equations for one dimensional heat transfer⁸⁷⁻⁸⁹. He, also constructed an empirical cycle, where over the total time of cure, the temperature variations would not exceed 0.1 °C. Using a FT-IR, he studied the polymerization, as per the new cycle and found that an exactly defined nuclear track detector could be designed. He also proposed, that the concentrations of the initiators, are not an important factor, in deciding the initial curing cycle, but the thickness of the films would play a major role. Portwood, further studied the kinetics of CR-39 polymerization, using an FT-IR and confirmed that the allylic abstraction and degradative chain transfer processes, were occurring during the polymerization of CR-39, which is most common in allylic monomers⁹⁰.

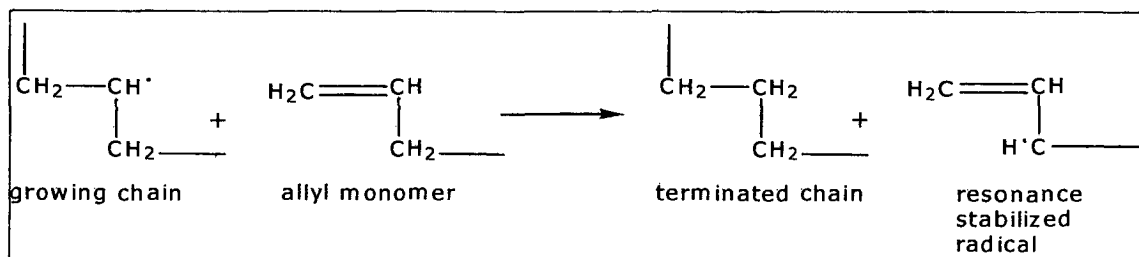


Fig. 1.10 Process of allylic H-abstraction in degradative chain transfer

Thus, the ratio of propagation to that of the chain transfer would decide the chain length, which would define the structure of the

material and also the etching behavior. He found that with increasing temperature there would be a reduction in the chain transfer phenomenon⁵⁴. As the allylic radical, is more stable than the saturated counterpart, it cannot initiate another chain, but recombines with other radicals. Thus, the hydrogen abstraction, followed by recombination occurs, which is called the degradative chain transfer, and this explains the need for higher initiator concentrations during the polymerization. But it has also been found that with increasing initiator concentration the chain length would decrease⁹¹.

Portwood also studied the polymerization process by computer simulation, which would predict the gel point and the average chain length correctly, and proved using his experimental results⁹².

Nikiforenko *et.al.*⁹³, studied the rate constants of initiation, chain propagation, chain transfer, re-initiation and chain termination, for the radical polymerization of ADC using BP initiator.

Schnarr *et.al.*,⁹⁴ studied the initial stages of the free radical polymerization of ADC at 35 - 65 °C. The kinetic order with respect to the initiator, di-sec-Bu peroxydicarbonate was determined. It has been observed, that the order increases slightly with peroxydicarbonate concentration, over the range 0.018 - 0.22 mole. Schnarr⁹⁴ also observed, that the bulk polymerization, as in free radical polymerization of other allyl and diallyl monomers, is degradative chain transfer, in which the growing polymer radical, abstracts a Hydrogen atom from a monomer unit, to give a relatively unreactive allylic radical.

The kinetics of photopolymerization of ADC, in the presence of dimethoxydeoxybenzoin, as catalyst has been described by Bellobono *et. al.*⁹⁵. The rate of polymerization, when the catalyst

cleaves to two radicals, of equal chain propagation ability, was found to obey first order reaction. Apart from these studies, a number of researchers have also studied the kinetics by radiation and microwave induced polymerizations⁹⁶⁻⁹⁷.

1.3.5 Initiators for ADC Polymerization.

Various initiators have been used for the polymerization of CR-39. Ahmad, has studied the effect of various initiators, on track detection characteristics of polymers and found that the initiators, having higher decomposition temperatures, led to materials with higher glass transition temperature⁹⁸, which in turn, is a measure of density of crosslink's in the material. The table 1.7 below gives the temperature range which is followed for the curing for the specific initiator used. Fig 1.11 gives the structures for the initiators (see next page).

Initiator	Curing Temp. Range (°C)	T _g (°C)
Isopropyl peroxy dicarbonate (IPP) (38)	45-90	77
Tert-Butyl Peroxide (TBP) (39)	120-180	109
Tert-butyl peroxybenzoate (TBPB) (40)	100-150	105
Cyclohexyl Peroxy dicarbonate (CHPC) (41)	65 - 90	NA
Benzoyl Peroxide (BP) (42)	70-115	90

Table 1.7. Glass transition values of PADC synthesized using different initiators

Portwood tried to use α, α' -azobisisobutyronitrile (AIBN) (43) as initiator for ADC. However, a rubbery plastic having bubble like features was obtained due to the evolution of nitrogen gas⁹⁹.

There are few reports on the use of benzoyl peroxide as initiator for casting sheets of CR-39 for SSNTD^{98,100,75}. Other catalysts like IPP and CHPC^{84,85,101} have been extensively used.

J. Stejny (2000), has explored a new class of U.V. photoinitiators for CR-39 polymerization. The use of UV photoinitiators for the cast polymerization of CR-39 offers the possibility to control the concentration of the initiating free radicals independent of the temperature by changing the UV dose rate at each stage of the curing process. The UV photoinitiators used, in this case were, 2-ethoxy-2-phenylacetophenone also known as benzoin ethyl ether (BEE) (44) and 2, 2-dimethoxy-2-phenyl-acetophenone (DMPA)¹⁰² (45).

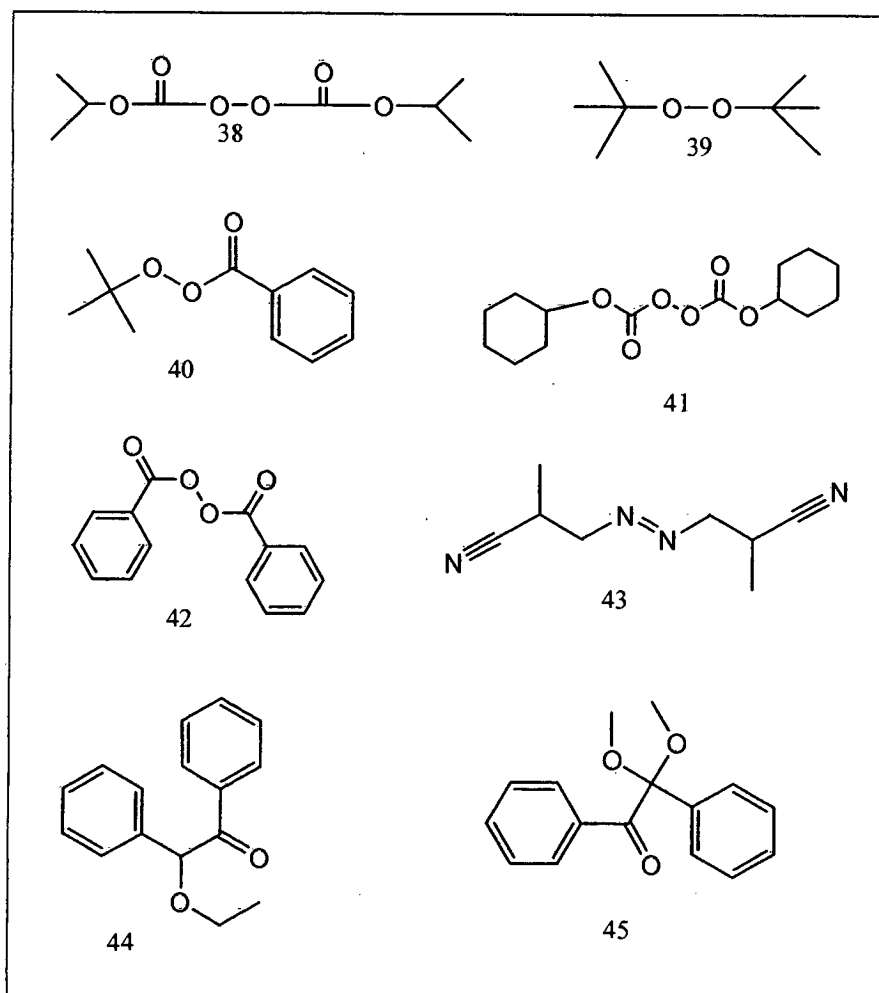


Fig. 1.11. Different initiators used for ADC polymerization.

1.3.6 Mold Design and Materials for ADC polymerization.

The materials used for the mold design in polymerization of ADC have been mostly glass and steel. Generally, for a small scale preparation of PADC films, glass has been the material of choice^{84-88,101,103}. Kinoshita, has suggested the use of plate glass, lantern slide glass or a float glass sheet of about 3 mm thickness and of the required size¹⁰³.

Tarle (1982), observed that float glass contains embedded tin, on one side of the sheet, which can be easily marked with the help of UV light (254 nm). He suggested that the side containing Tin should be kept as the outer side of the mold which helps in eliminating numerous flaws that occur after etching¹⁰⁴. Kinoshita also suggested that an inert material like silicone, plasticized polyvinyl or Teflon™ may be used for preparing the gaskets for the mold. The thickness of the film prepared, would largely depend on the thickness of the gasket used for the film preparation. The glass plates, may be cleaned with soap and a solvent, like ethanol or isopropyl alcohol. One of the glass plates is leveled and the gasket is fixed on the other. The required amount of monomer is then poured on the plate and the second plate is pressed onto the liquid, until just enough of the monomer flows out of the edge of the gasket. The assembly is then held together using clamps⁸⁴. Alternatively, the monomer may be injected into a previously prepared mold, having a small inlet, for the purpose of injection¹⁰³. This method, has an advantage over the previously described, as it avoids spillage of the monomer and the air bubbles are not trapped in the liquid monomer film. The mold is then placed in a suitable heating assembly like air oven, vacuum oven, or water bath and the curing is carried out for the required time.

The ADC monomer, can also be cast directly in a glass cell with flexible separating gaskets. Dial and Gould, described the preparation of CR-39 films, by the cast polymerization using 3% benzoyl peroxide⁷³. They, poured a pre-polymerized thickened viscous ADC monomer in a mold, clamped the glass plates and heated the mold in predetermined temperature steps with increasing pressure on the mold periodically. This avoided breaking of the film due to the shrinkage of the monomer volume as it gets converted into a solid polymer. The pressure was released only at about 90 % conversion of the monomer and the molds were allowed to cool overnight.

1.3.7 Co-polymers of PADC.

ADC monomer has been co-polymerized, with many other allylic monomers, in various proportions and in many cases, it has been found to be more sensitive towards the charged particles than the homopolymer.

ADC has been co-polymerized with Methyl methacrylate (MMA), in the ratio of 70:30 using benzoyl peroxide (1% w/w) as initiator. It has been noted that when the MMA concentration exceeds 10 %, the polymerization reaction should be started below 70 °C in order to prevent the premature rapid polymerization accompanied by boiling and bubble formation in the polymer film⁷⁶. It is well known that allyl compounds polymerize well with sulphur dioxide (SO₂) to give solid products of relatively higher molecular weights. Taking this advantage, ADC can be conveniently co-polymerized with liquid sulphur dioxide, by the U.V. catalyzed polymerization. The polysulphones, are chemically unstable towards heat and aqueous alkalies^{80,105}. Another monomer called DEAS was copolymerized with ADC monomer in 10 and 20 % concentration of the former in weight proportions using IPP as initia-

tor. These materials were found to be three times more sensitive than the homopolymer of ADC. These material were trade marked as SR-86 (10) and SR-86(20)^{106,107}.

Co-polymers of ADC with maleic anhydride⁷⁵ and methyl acrylamido glycolate methyl ether⁹¹, have been prepared. Apart from these, co-polymers with other alkylacrylates^{108,109} have also been reported. Most of these co-polymers, have an advantage over the homopolymers of ADC as they show lower etching time for alpha or fission fragments but some of them were found to have lower track registration efficiency than CR-39.

Ogura *et.al.*, carried out co-polymerization of CR-39 with twelve different monomers and found that a co-polymer with N-isopropylacrylamide (NIPAAm) showed the highest sensitivity to low LET particles. This polymer contained upto 3 % of NIPAAm^{110,111}. The post etched surface of this material however was not good. This was further refined by adding an antioxidant like Naugard 445 and a new co-polymer having the following constitution was prepared, CR-39/NIPAAm/Naugard 445 in weight ratio of 99/1/0.01 trade named as TNF-1⁷⁰. This was found to have very good sensitivity towards the low LET particles and also good post etch surface.

Tsuruta, has prepared co-polymer with diallyl phthalate (DAP). The results obtained by varying the concentration of the mixtures, showed intermediate characteristics of the co-polymers prepared, compared to the homopolymers of CR-39 and diallyl phthalate (DAP)^{112,113}.

1.3.8 Structure and sensitivity effects in CR-39 and related polycarbonates.

Although, various materials *viz.*, cellulose nitrates, CR-39

polycarbonates, bisphenol-A-polycarbonate are well known in the field of SSNTD, the structure and sensitivity relationship, has not been studied in details. Although, CR-39 has a unique position in this field, there has been no much systematic study, carried out to establish the relation between structure of the polymer and its sensitivity. Stejny¹⁰⁵, prepared a polymer by introducing $-\text{SO}_2-$ linkages in the CR-39 polymer matrix, which proved that it is possible to incorporate such weaker linkages. A study by Fujii *et.al.*,^{106,107} showed that it is possible to prepare materials of higher sensitivity by incorporating some very weak linkages like that of the $-\text{SO}_3-$ in the polymer matrix. Although, the material is susceptible to etching by aqueous sodium carbonate, the $-\text{SO}_2-$ linkage has been found to be radiation sensitive. Fujii *et.al.*, prepared a series of materials which were relatively similar to that of ADC and tried to study their response towards charged particles by measuring their sensitivity. From the results obtained some generalizations have been made^{106,107}.

(1) All polymers containing aromatic rings [BAEP (23), DAIP (20), CR-73 (12)] have lower sensitivity as compared to CR-39.

(2) The chain bridging the carbonate moieties is crucial for sensitivity. Compounds with ethylene bridge ($-\text{CH}_2-\text{CH}_2-$) were found to show optimum sensitivity. Thus DAS (17) has higher sensitivity than DAA (18).

(3) An additional ether linkage was found to be beneficial. Thus a co-polymer of DAS (17) and TEDM (22), has higher sensitivity than the homopolymer of pure DAS. Further, CR-39 polymer is four times more sensitive than PeAc (16). Both have almost the same distance between the two $-\text{CO}_3-$ groups which suggest that the ether linkage in CR-39 plays a vital role in imparting sensitivity to the polymer.

(4) The $-\text{CO}_3-$ linkage, is crucial for the sensitivity, and a polymer containing $-\text{CO}_3-$ linkage is more sensitive as compared to the one having $-\text{CO}-\text{O}-$ linkage. It was observed that the alpha sensitivity decreased in the order:-

CR-39 > PrAC > BuAC > PeAC > DAS > DAA

(5) It has been found that $-\text{SO}_2-$ linkage is radiation sensitive, though it is, weak and susceptible, to etching by aqueous sodium carbonate. Also, the $-\text{SO}_3-$ linkage has been found to be very radiation sensitive.

1.3.9 Effect of additives on the sensitivity.

In order to improve the response of the materials, like CR-39, towards the charged particles for the dosimetric applications, effects of many additives like plasticizers, antioxidants, some chlorinated compounds were studied.

1) Effects of plasticizers.

One problem associated with use of PADC as track detectors, is the surface opaqueness, exhibited by some samples after etching. Therefore, the need for additives like plasticizers was felt, so that, these additives could reduce or eliminate any surface related problems. In this direction, phthalate esters are well known.

Tarle (1981), proposed that a heavy phthalic acid ester like DBP (46) or DOP (47), acts as a plasticizer, gives a more homogeneous plastic and also improves the post-etched surface of the plastic¹¹⁴. However, it was pointed out that CR-39 with addition of DOP, showed lesser sensitivity than that of pure CR-39, probably due to the presence of aromatic rings in DOP. Hence, a new plasticizer dioctyl sebacate (DOS) (48) was used by Portwood and Stenjoy¹¹⁵. DOS is free from any aromatic rings and it was observed

that upto 0.3 % DOS concentration, would give better post etched surfaces and the sensitivity values for CR-39 (DOP) were lower compared to that of CR-39 (DOS).

Price and O'Sullivan extended the study of additives and tested dioctyl terephthalate (DOTP) (49), di-isodecyl phthalate (DIDP)¹¹⁶ (50). This study which was mainly carried out to find the effect of additives on the reduced etch rates Z/β . It was found that for the materials with and without additives, the depth dependence was different and that it would be possible to choose, a suitable additive to optimize the response of the track detector for a particular application in nuclear particle identification. Following this, O'Sullivan *et.al.*, (1984) introduced a new dopant called dinonyl phthalate (DNP) (51), with this dopant a very uniform response over the entire area of the film was achieved¹¹⁷.

De-Ling Pang *et.al.*, studied the effects of Diallyl phthalate (DAP) (19), Dibutyl Phthalate (DBP), Di-(2- ethyl hexyl)phthalate (DIOP) (52) and methyl methacrylate (MMA) (7). This study showed that the relative sensitivity of PADC material with DOP as additive, will increase and that a concentration of 1 % of DAP would be the optimum concentration¹¹⁸. This study also proved that DIOP and DBP should not be used in detectors as the relative sensitivity decreased significantly; the addition of MMA does not affect the relative sensitivity of the detectors.

2) Effect of chlorinated compounds.

In order to improve the sensitivity of the detector films, the following compounds were used. Diallyl chlorindate (DADC) (36) and hexachlorobutadiene (HCB) (53), were two such compounds that were tried in case of CR-39¹¹⁹. It was observed that CR-39 with 2 % DADC, showed a higher sensitivity value compared to pure CR-39, whereas that with HCB did not show any alteration in

the sensitivity values. However, the post etched surface characteristics in both the cases were better compared to pure CR-39.

3) Ageing effects and the use of antioxidants.

The observed response of PADC detectors, to radiation, are greatly influenced by the environment, in which the material is stored, between the time of manufacture and radiation exposure. It has been observed, that PADC plastic stored in air ages faster. High temperature and relative humidity, in the environment, are some of the other reasons, which lead to the aging of the material. The oxidative degradation of the polymer, can be avoided by either using an antioxidant or modifying the structure itself. The sensitivity values are known to fall rapidly within three weeks of manufacture and then at a slower rate. At $-20\text{ }^{\circ}\text{C}$ the fading rate is much reduced. To avoid the phenomenon of fading, Portwood, used an antioxidant Naugard 445 (54) in 0.01 % concentrations¹²⁰. However, the use of this compound was found to be unsuitable as it underwent several other unwanted reactions during the process of polymerization and the films showed lower sensitivity as compared to pure CR-39. Ogura¹²¹ used Naugard 445 (0.01%) along with the two chlorinated compounds HCB and DADC and found that these films were suitable, for a particular application like the search for magnetic monopoles as it helped in reducing the unwanted background in the films. However, it has been pointed out that CR-39 containing Naugard 445 tend to show lower depth dependent sensitivity as compared to pure CR-39. Another antioxidant Cyanox 1790 (55), was also tried, but it is found that, Naugard 445 gave a higher sensitivity value in comparison to this. This observation is also supported by Patrizi¹²². The chemical structures of various additives used during PADC preparation are given in Fig. 1.12 (see next page).

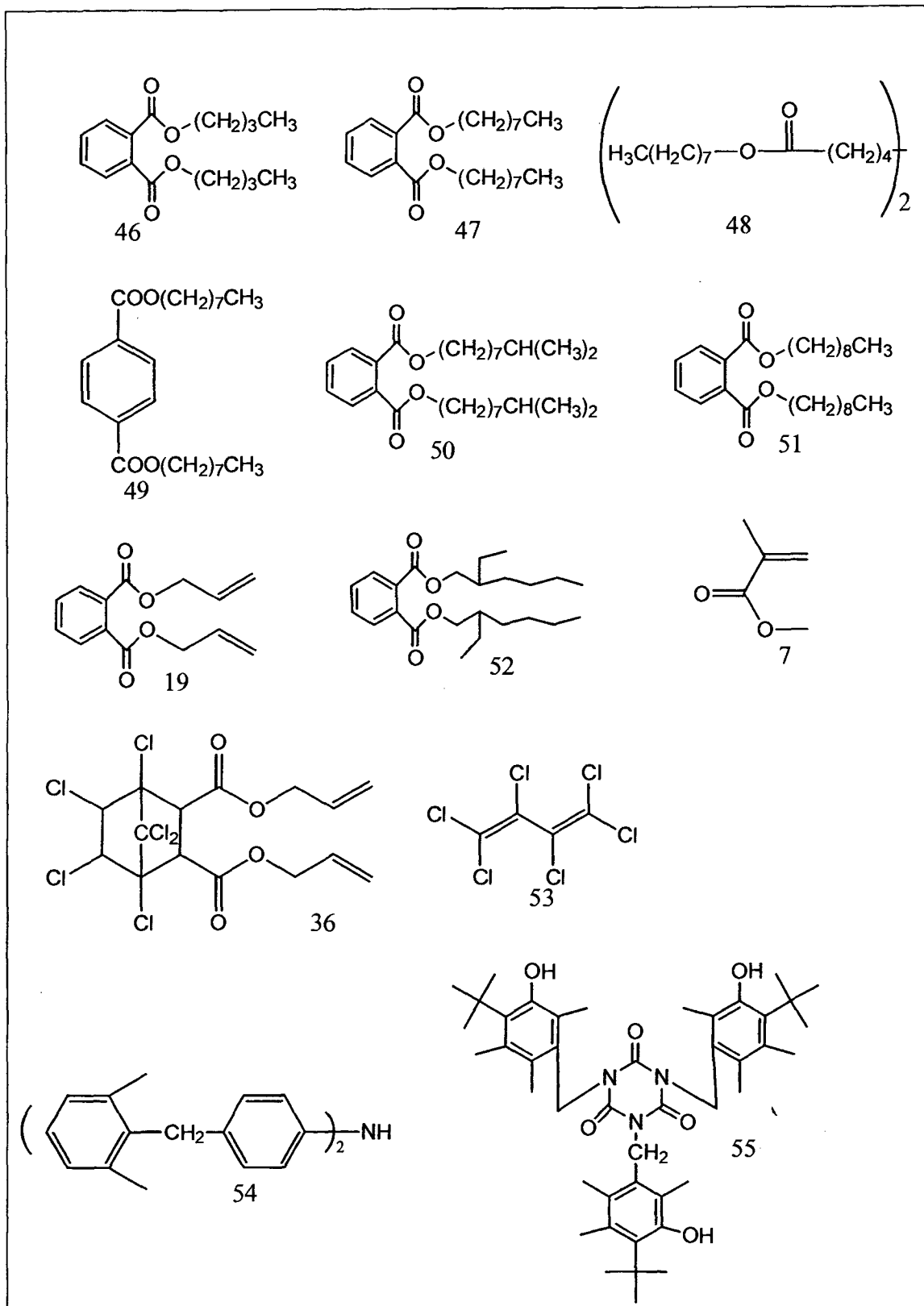


Fig. 1.12 Structures of different additives used for ADC

Portwood, gave a more mechanistic insight into the polymer degradation process at room temperature. He explained that the CR-39 polymer is susceptible to oxidative degradation due to the tertiary H atom in the polymer.

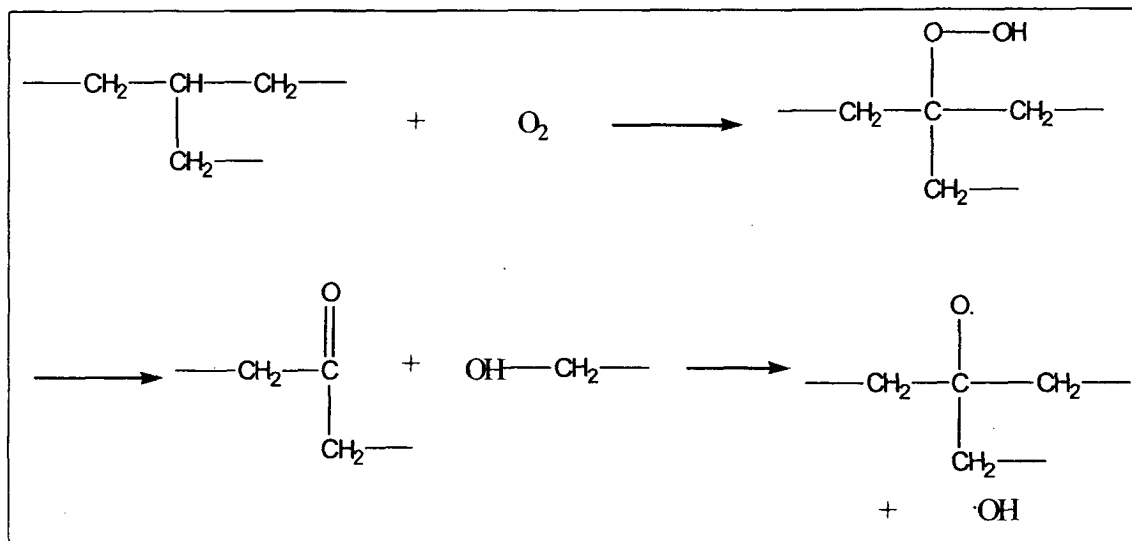


Fig 1.13 Oxidative degradation of ADC polymer

This can be avoided, if the tertiary atom in the system is absent and for this, the use of diethylene glycol bis (methallyl carbonate) has been proposed, which would result in an polymer devoid of any tertiary H-atom.

1.3.10 Etchants used for ADC polymer.

The most commonly used etchants for CR-39 polymer etching has been the alkaline chemical reagents like LiOH, NaOH and KOH. It is well known that the ideal condition for etching CR-39 polymer, has been 6N NaOH at 70 °C. Additions of solvents, like alcohols have been tried, but have been found to be unsatisfactory, due to decrease in the sensitivity values. The search for new etchants, has been a challenge in this field, with the main thrust, being on reducing the etching time for the development of tracks. Tahiri *et.al.*, apart from studying the Group IA metal hydroxides, also investigated the Group II-A metal hydroxides $\text{Mg}(\text{OH})_2$ and $\text{Ca}(\text{OH})_2$, which are relatively less soluble

in water and therefore do not provide sufficient OH^- ions to attack the plastic material, hence are unable to act as etchants even after long etching time¹²³. $\text{Ba}(\text{OH})_2 \cdot 8\text{H}_2\text{O}$, which belongs to the same group, has a much better solubility in water compared to calcium and magnesium hydroxides. Thus different concentration of $\text{Ba}(\text{OH})_2 \cdot 8\text{H}_2\text{O}$ of range 0.5 to 2.75 M, were prepared and studied at different temperatures. As the solubility of $\text{Ba}(\text{OH})_2 \cdot 8\text{H}_2\text{O}$ is found to be maximum at 78 °C the study of etching of the films was primarily carried out at this temperature. It was found that a concentration of 2.75 M and temperature 78 °C were optimum conditions for etching of CR-39 films¹²⁴.

Molten $\text{Ba}(\text{OH})_2 \cdot 8\text{H}_2\text{O}$ was also tested for etching of the films and has been found to be a very efficient etchant for the CR-39 films which reduced the time of track revelation below 30 min for both alpha particles and fission fragments¹²⁴.

1.3.11 Etching mechanism and study of etchants in CR-39 polymer.

Gruhn *et.al.*, studied the mode of degradation of CR-39 (Fig.1.14 outlines the reaction involved), by hydroxides and its etching behavior was compared to Lexan. It was observed that the attack of the OH^- results in the hydrolysis of the carbonate ester bonds in the polymer¹²⁵. The etch products that were obtained were Poly allyl alcohol (PAA) and 2,2'-oxydiethanol. While 2,2'-oxydiethanol is extensively soluble in the etchant, PAA has a limited solubility. It can be separated from the etching solution as a sticky brownish oil and at high concentrations of etchant (NaOH , ~ 18 M) can be easily seen as a layer on the surface of the plastic being etched. Table 1.8 gives the different quantities of etch products obtained (see next page). The identification of this compound was established by Infra-Red Spectrum. Additional etch products can arise from incomplete conversion of the double bonds in the monomer and from the catalyst that

has been used for polymerization. The presence of unsaturation would lead to the formation of allyl alcohol and use of initiators like IPP would give rise to isopropyl alcohol and carbonate ions as etch products¹²⁵.

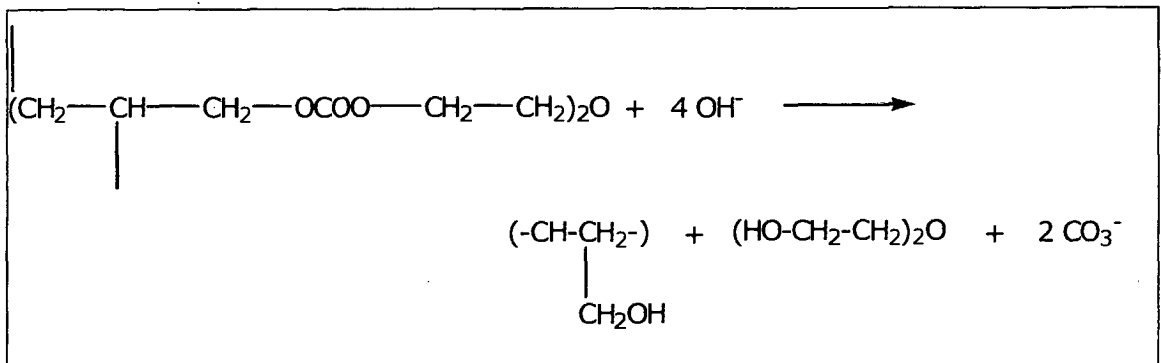


Fig 1.14 Hydrolysis of ADC polymer

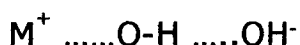
CO ₃ ⁻ ion	DEG	PAA	AA	IPA
44 g	38 g	33 g	8 g	2 g

Table 1.8 Quantities of etch products per 100 g of ADC polymer.

By studying the polymeric etch product PAA, for its characteristics, like its average molecular weight and molecular weight distribution the behavior of the plastic material can be studied as it will largely reflect, the extent and uniformity of polymerization and cross-linking for a given plastic. Such a study was undertaken by Stenjy, by hydrolyzing the CR-39 polymer in 6.25 N NaOH, at 80 °C for 36 h in a sealed tube⁹⁰. After the hydrolysis, the reaction mixture was neutralized with HCl, and extracted with ethanol. These dry etch products, were found to be free from the carbonate groups. The etch products were further treated with acetic anhydride and analyzed by GPC. The molecular weight distribution of PAA was determined and it was observed that the PAA chain length decreased continuously with increasing initiator concen-

tration (3 - 17 %). A recent report, has identified the carbonate ions formed in the etching process, as Thermonatrite mineral ($\text{Na}_2\text{CO}_3 \cdot \text{H}_2\text{O}$) apart from the formation of Na_2CO_3 . This mineral is available in nature as arid lake evaporates, soil efflorescence and fumeroles. However, this is the only synthetic method reported to obtain the mineral of highest grade¹²⁶. This study, was also used to attribute the sensitivity of CR-39 polymer to the presence of carbonate groups. It was proposed by Huang (1982), that the scission of the polyallyl chain at the tertiary carbons also imparts sensitivity to the CR-39¹²⁷. Gruhn¹²⁵, observed that the bulk etch rate of CR-39 decreased at a high etchant ($> 20 \text{ M}$) concentration. This is attributed to the built up of the thick PPA layer on the surface of the plastic material.

It was shown by Charvat (1988), that NaOH and KOH did not show a significant difference in their etching ability¹²⁸. However, it is well known that the reactivity of a Hydroxide ion increases rapidly, as the hydration of these ions decreases *i.e.*, the concentration of the solution increases. Kinetically, an unhydrated ion is supposed to be more active than the hydrated one. The order of hydration is as follows: $\text{KOH} < \text{NaOH} < \text{LiOH}$. Thus, the reactivity decreases in order of $\text{KOH} > \text{NaOH} > \text{LiOH}$ ¹²⁹. Another factor which affects the reactivity in concentrated solutions is solvent bridged-ion pairs *i.e.*,



These species, tend to reduce the reactivity of hydroxide solutions, with the effect expected to be maximum when M^+ is smaller, which also proves the reactivity for the alkali hydroxides as shown above. The addition of organic solvents to aqueous solutions can greatly increase the reactivity of hydroxide ions, if they effectively reduce the solvation of the ions. Organic solvent like alcohol can suppress the formation of ion pairs, however addition of alcohol, has been found to reduce the sensitivity of CR-39¹³⁰. This was also confirmed by Amin

(1981), who also showed that either in KOH or NaOH etchant, maximum sensitivity occurs when the concentration is at around 20 %¹³¹.

It has been shown that, during etching of CR-39, the concentration of the etchant increases by 8 % after 15 h of etching. This increase in the concentration has been attributed to the increase in the etch products over a period of time. The change in concentration of the etchant has also been followed by the electrical conductivity and density measurements, and a standard calibration for maintaining the concentration of the etchant has been derived⁸⁹.

1.4 Statement of objectives.

From the foregoing introductory remarks it can be observed that Solid State Nuclear Track Detection is nearly a five decade old technique and is used for permanently recording the radiation induced damage in dielectric materials. This technique is being used popularly in various branches of science and technology where there is a need for qualitative as well as quantitative measurement of radiation. It has gained lot of popularity due to the simplicity of the experimental procedures involved *i.e.*, chemical etching, counting under optical microscope, and possibility of automated analysis of the tracks. Among the various types of materials tested as SSNTD *e.g.* mineral crystals, glasses and plastics, the plastics dominate the field of SSNTD due to the simplicity in handling/ track evaluation. As seen from the literature, there is ample scope for reforming these materials with respect to their polymer matrix and designing newer materials. The composition of the materials can be altered, by selecting suitable monomers and also the polymerization conditions. Although, more than 50 plastic materials have been tested as SSNTDs, Nitrocellulose and polycarbonates like CR-39 and Bisphenol-A polycarbonate dominate the scene owing to their relatively higher sensitivity to charged particles. CR-39 has been

the material of choice since its inception as SSNTD in 1978. CR-39 is an allylic thermoset material which has a three dimensional network. Considering these aspects, the present work is aimed at studies relating to design and synthesis of new allylic monomers and corresponding thermoset plastic materials.

It is important to note at this juncture that, India is still dependant on foreign agencies for the supply of the above mentioned materials for various SSNTD applications. Although, there are many research groups in India working on SSNTD, their focus is mainly on the applications of such detectors in various fields. In the present work therefore, emphasis will be given on designing and developing newer materials indigenously, keeping in mind the earlier efforts taken, during the period 1992-1995. *i.e.* mainly preparation of Nitrocellulose films³⁵. Some efforts towards the development of PADC films were carried out during the same period but were mainly restricted to preliminary investigations. In the present work therefore, efforts will be directed towards the development of PADC detector films that is comparable to the commercially available CR-39 detector films by polymerization of the ADC monomer prepared indigenously by us, using an environmentally benign process of transesterification¹³².

Thus, the aims and objectives of the present investigation can be briefly described as follows:-

I) Design and Development of new monomers and polymer materials thereof: The present investigation will focus on designing some allylic monomers (other than ADC/PADC) and polymer materials, either as homo or co-polymers. While designing the monomers emphasis would be on the following facts:

1) It is well known that a polymer matrix having higher density of crosslinks would be more sensitive, so compounds that would yield higher crosslinks on polymerization may be expected to perform better.

2) It has been shown that presence of certain functional groups/linkages contribute significantly towards the radiation sensitivity of a polymer. Hence, it would be rewarding to synthesize such monomers that would have more than one functional group in its structure *e.g.* nitrate ester, carbonate, amide, sulphonate *etc.*. Nitrocellulose ($-\text{ONO}_2$) and PADC ($-\text{CO}_3^-$) are the most popular track detectors at present. It would be worthwhile to prepare polymers which contain both nitrate as well as carbonate ester groups and also other functional groups like carbamates ($-\text{CONH}$). Effect of replacement of etheral oxygen in diethylene glycol moiety ($-\text{CH}_2-\text{CH}_2-\text{O}-\text{CH}_2-\text{CH}_2-$) by nitrogen ($-\text{CH}_2-\text{CH}_2-\text{N}-\text{CH}_2-\text{CH}_2-$) would be interesting to observe. Moreover, nitrocellulose which contains $-\text{ONO}_2$ group is a thermoplastic. It would be thus interesting to synthesize allylic monomers containing both, $-\text{C}-\text{NO}_2$ and $-\text{ONO}_2$ links, that would result in a thermoset polymer and study their track detection characteristics.

Also the focus would be to prepare the co-polymers of the new monomers prepared with that of the ADC monomer, as it is well known in literature that co-polymers tend to be more sensitive than the homopolymers. The most important initiators used in ADC polymerization are the peroxydicarbonates and are commercially not available due to their unstable nature and hence need to be synthesized. Such initiators will be synthesized in our laboratory and used them for polymerization. The plastic materials prepared will be evaluated based on following aspects of track detection.

- 1) Uniformity of etching.
- 2) Variation in the track density with etching time.
- 3) Track detection efficiency as compared to PM PADC.
- 4) Measurement of alpha/fission branching ratio.
- 5) Sensitivity of the films to alpha particles.
- 6) Optimization of etching conditions.

II) Development of PADC plastic material: Apart from designing new materials, the process for refining PADC film, preparation has also been planned and all the studies mentioned above with respect to the SSNTD characteristics would be studied in correlation with that of PM PADC.

III) Materials and design for the mold and polymerization bath: The preparation of mold and design for carrying out the polymerization is an important aspect in the preparation of thin films. The surface characteristics and thickness of the films obtained would depend on these aspects.

IV) To study the kinetics of the polymerization process: Wherever possible, kinetic studies of all the allylic monomers synthesized would be carried out in order to develop a constant rate polymerization cycle by extending the kinetic model proposed by Dial *et.al.*

Chapter 2

Experimental

2.1. Materials and methods.

2.1.1 Materials used.

1) Monomers: All the monomers *viz.*, ADC, NADAC, ABNEC and TDONM used were indigenously prepared. The chemicals used for the synthesis of monomers and initiators were procured from M/s Loba Chemie, India; M/s Merck, India and M/s Qualigens Fine Chemicals, India; and were used as such. Wherever required, drying of the chemicals was carried out, using proper drying agents. ADC monomer (M/s Aldrich chemicals, USA) was used for comparison purpose. Some of the monomers were purified before use, by charcoal treatment, followed by vacuum distillation. The monomers were characterized by suitable spectroscopic techniques.

2) Plasticizers: Commercially available Dioctyl phthalate (DOP) was used without further purification.

3) Initiators: i) Benzoyl peroxide (moistened) was recrystallized from mixture of methanol and chloroform in 3:1 v/v proportions.

ii) Isopropyl peroxydicarbonate was prepared in the laboratory and used without further purification.

4) Mold preparation: Glass plates (Schott, Germany), thin Teflon™ sheets, aluminium plates were used for the polymerization molds. A typical mold assembly is shown in Fig 2.1.

(see next page)

2.1.2 Instrumentation.

1) Polymerization bath: The polymerization was carried out in a specially designed bath (Fig 2.2, see next page) for holding the molds. The heating was carried out by a programmable, micro-processor controlled water bath (Julabo, F 25 HP, Germany), having a temperature controller with an accuracy of $\pm 0.01^\circ\text{C}$.

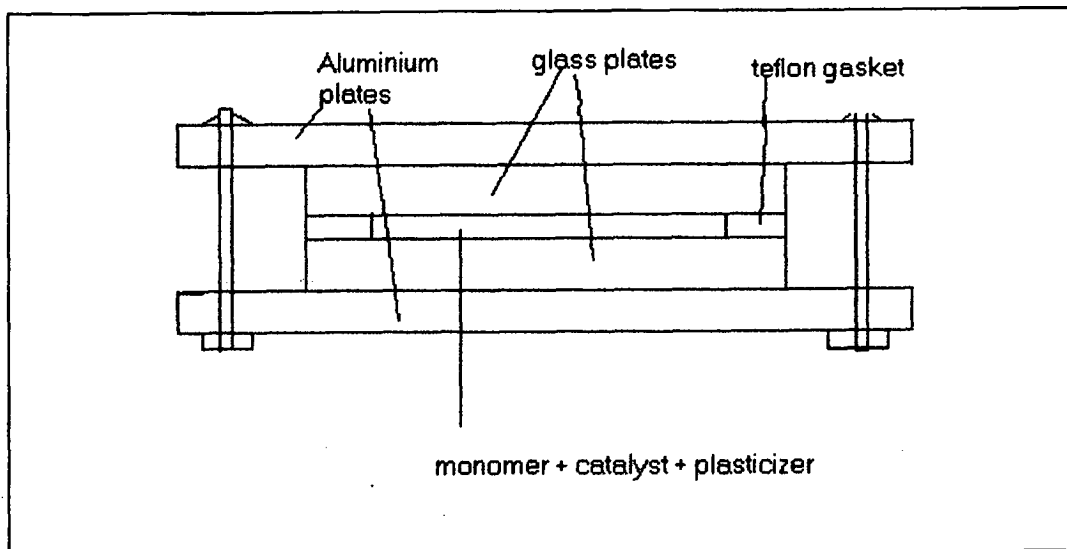


Fig. 2.1 Mold assembly for cast polymerization

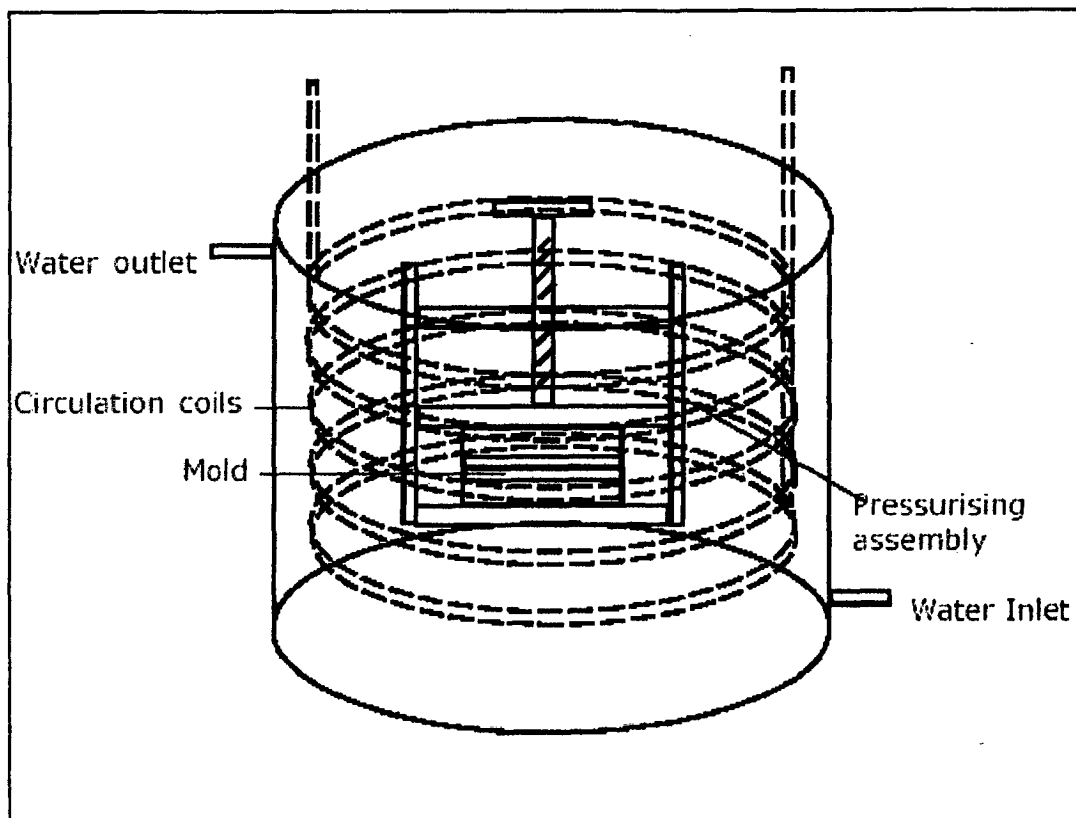


Fig. 2.2 Polymerization bath holding the mold assembly.

2) Optical microscope for track counting: Nuclear tracks in the detector materials were viewed with the help of a trinocular optical microscope (Axiostar, Carl Zeiss, Germany)

3) Thickness measurement: For the thickness measurement of the detector films, a digital thickness gauge (Alpha meter, Para Electronics, India), with a least count of 5 μm was used. It could be used over four ranges, *viz.*, 0-50, 0-100, 0-200, 200-999 μm depending upon the thickness of the sample under study.

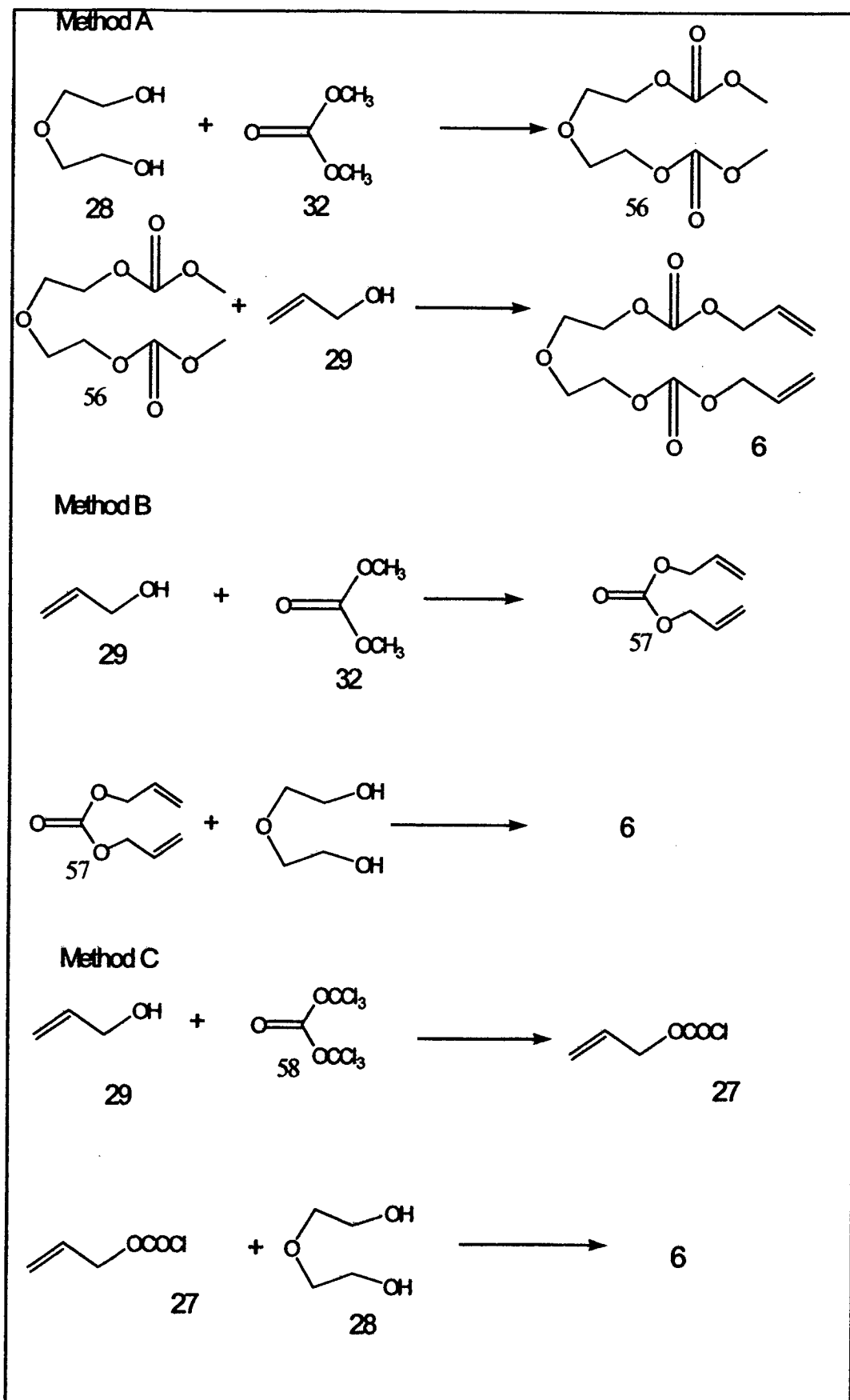
2.2 Synthesis of monomers and initiators.

The chemicals used in the synthesis were dried using 3 A grade molecular sieves, anhydrous potassium carbonate and potassium hydroxide pellets as per the requirement. The products were distilled for obtaining pure compounds.

IR spectra were recorded on Shimadzu FT-IR spectrophotometer. H^1 and C^{13} spectra were recorded on Bruker 300 MHz spectrophotometer. Mass spectra were recorded on MS (TOF) system. The spectral data for all compounds are discussed in Sec. 2.5.

2.2.1 Synthesis of ADC monomer.

As seen from the literature cited in sec 1.3.1, various processes are known for the preparation of allyl carbonate esters of glycols or polyglycols^{61,62,63}. ADC monomer was thus synthesized by using the following methods *viz.*, phosgenation using triphosgene and transesterification. Both the processes are described in Scheme 2.1.(see next page)



Scheme 2.1 Synthetic strategies for ADC preparation.

1) Synthesis of ADC by the transesterification route^{61,62}.

Method A: Dimethyl carbonate (28.0 g, 0.315 mole) and K_2CO_3 (0.5 % by wt. of dimethyl carbonate) catalyst were placed in a three neck flask, equipped with an overhead stirring arrangement, thermometer and a dropping funnel. At the top of the dropping funnel was attached a bulb containing nitrogen gas. Through the addition funnel Diethylene glycol (2.22 g, 0.021 mole) was added drop wise over a period of 90 min at 70 °C. The temperature of the reaction mixture was slowly raised from 70 to 84 °C, when methanol distills out. After almost quantitative recovery of dimethyl carbonate (at 90 °C) the contents of the flask which mainly contained diethylene glycol bis (methyl carbonate) was taken in ether and washed with cold water to remove soluble impurities. Diethylene glycol bis (methyl carbonate) (10.0 g, 0.0515 mole) was then reacted with allyl alcohol (94.30 g, 0.77 mole) in the presence of K_2CO_3 (1 % by weight of carbonate) in a similar manner described above. The temperature was slowly raised from 70 to 90 °C and methanol was collected. After completion of the reaction the excess of the allyl alcohol was recovered by vacuum distillation. The product (ADC) was distilled at 156 °C at 2 mm of Hg, the yield of the product obtained was 70 % (7.0 g) w.r.t. Diethylene glycol bis (methyl carbonate) used. The intermediate and the product were further characterized by IR and H^1NMR , and compared with the imported monomer, which confirms the formation of the ADC monomer.

Method B⁶²: Allyl alcohol (115.0 g, 1.98 mole), Cyclohexane (50 ml) and KOH (0.9 g, 1.5 % by weight of allyl alcohol) were taken in a three neck flask aided with an addition funnel and

thermometer at the side arms. The center neck was fitted with a vertical fractionating column so that the azeotropic mixture of methanol and cyclohexane formed during the course of reaction could be efficiently removed overhead. Dimethyl carbonate (60.0 g, 0.666 mole) was slowly added over a period of 2 h and the azeotropic mixture of methanol and cyclohexane was removed continuously over period of 6 h. The Diallyl carbonate formed was later recovered (b.p. 166 °C). The yield was 90% (182.0 g) based on the dimethyl carbonate feed. The recovered (unreacted) dimethyl carbonate and allyl alcohol could be recycled in the next batch.

Diallyl carbonate (146.0 g, 0.9056 mole) prepared by the above method and Diethylene glycol (12.0 g, 0.113 mole) were placed in a three neck flask aided with a gas passing tube and a thermometer. The mixture was stirred for about 15 min at 70 °C. KOH in catalytic amount was then added to the reaction mixture and the mixture was stirred for about 3 h at 90 °C with continuous removal of allyl alcohol. The product obtained was colorless and the yield obtained was 90 % (27.1 g) based on the glycol feed. The excess of Diallyl carbonate was then recovered. This method proved to be an improvement to method A in terms of the percentage yield as well as the time taken for the reaction.

2) Synthesis of ADC using Triphosgene (Bis Trichloromethyl Carbonate) (BTC).

a) Synthesis of allyl chloroformate: BTC (9.34 g, 0.03156 mole) and methylene chloride (70 ml) were placed in a two neck round bottom flask. Both the ends of the flasks were sealed with silicone stoppers. The contents of the reaction flask were cooled

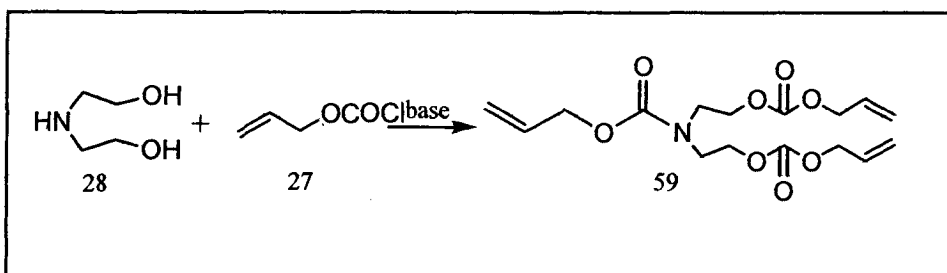
to 0 °C by means of external cooling. With the help of two syringes, pyridine (6.79 g, 0.0860 mole) and Allyl alcohol (5.0 g, 0.0860 mole) were added through the two necks of the flask, over a period of 30 min. Care was taken to see that the phosgene released in the flask was always in excess to the allyl alcohol added. After the addition was over, the mixture was stirred for 1 h at 0 °c. The reaction mixture was then washed with cold water (2 x 20 ml) and dried over anhydrous sodium sulphate. The excess of methylene chloride was then carefully removed by fractional distillation using a 150 mm Dufton glass column. It was observed that in spite of taking all the care to remove the solvent, some azeotrope formation between allyl chloroformate and methylene chloride occurred, that resulted in loss of some allyl chloroformate along with methylene chloride. Attempts to change the solvent resulted in byproducts like diallyl carbonate. The product allyl chloroformate was then characterized by its IR spectrum.

b) Synthesis of ADC from allyl chloroformate and diethylene glycol: In a round bottom flask diethylene glycol (5.0 g, 0.0476 mole) and pyridine (7.42 g, 0.0952 mole) were dissolved in acetone. Allyl chloroformate was then added through a pressure equalizing funnel at a temperature of 0 - 5 °C. After the addition was over the solvent was removed using vacuum and the product (10.2 g, 82 % yield) obtained was distilled .

2.2.2 Synthesis of N-Allyloxycarbonyloxydiethanolaminebis-(allyl carbonate) (NADAC).(see scheme 2.2 next page)

Dry diethanolamine (6.0g, 0.0578 mole), acetone (100 ml) (dry) were taken in a three necked round bottom flask, equipped

with a thermometer, drying tube (CaCl_2) and an addition funnel. The outer surface of the flask was cooled by circulating cold methanol ($-5\text{ }^\circ\text{C}$) the internal temperature of the reaction mixture was maintained between $0 - 5\text{ }^\circ\text{C}$. Allyl chloroformate (21.61 g, 0.1771 mole) and pyridine (13.8 g, 0.1771 mole) were then added simultaneously with stirring. The reaction mixture was then stirred for about 1 h and contents of the flask were allowed to attain room temperature. The solvent was then removed under reduced pressure at room temperature. The reaction mixture was then suspended in ether (50 ml) and washed with water (4 x 20 ml) and dried over anhydrous sodium sulphate. The solvent was removed under reduced pressure at room temperature. The crude product weighing 17.5 g was then distilled over vacuum at $180\text{ }^\circ\text{C}$ at 0.1 mbar pressure. The distilled product weighed 16.5 g (80 % based on diethanolamine).



Scheme 2.2. Synthesis of NADAC monomer.

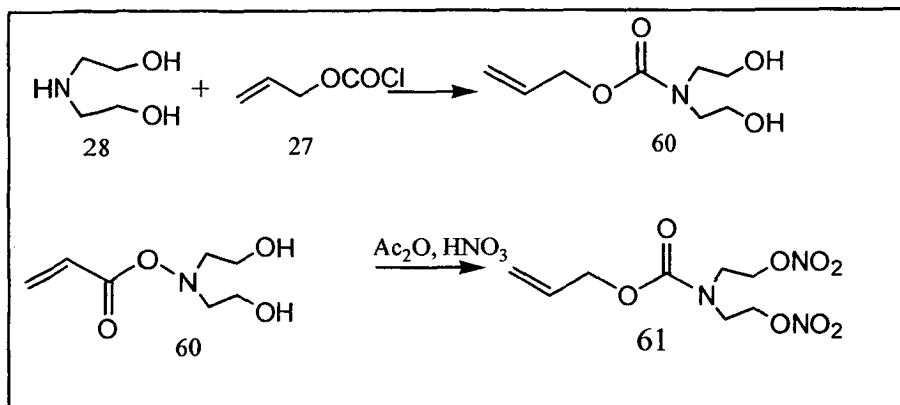
2.2.3 Synthesis of Allyl bis-(2-nitroxy-ethyl) carbamate (ABNEC).

The synthesis of this monomer was carried out through a two step process. The first step involved the selective formation of the allyl carbamate linkage followed by the nitration of the two hydroxyl groups from the diethanolamine moiety in the second step.

Step 1: Synthesis of Allyl bis-(2-hydroxyethyl) carbamate:

Diethanolamine (5.0 g, 0.0475 mole) was taken in acetone (100 ml) in a three neck round bottom flask equipped with a thermometer, addition funnel and a drying tube (Calcium chloride). Allyl chloroformate (5.79 g, 0.0475 mole) was added in a drop wise manner such that the temperature remained below -5 °C. After the additions of chloroformate was over the solvent was removed over vacuum and the reaction mixture was suspended in ether. The reaction mixture was shaken with ether (4 x 40 ml). The product (6.2 g, 65 % yield) was then recovered by drying over sodium sulphate and distillation of ether.

Step 2: The above product was then nitrated by the known method¹³³. Allyl bis-(2-hydroxyethyl) carbamate (2.5 g, 0.013 mole) was added dropwise to a mixture of acetic anhydride (10 ml) and nitric acid (0.5 ml, 70 % v/v) taking care that, the temperature of the reaction mixture never exceeded 5 °C. After completion of the reaction (as monitored on TLC) the reaction mixture was then neutralized by addition of aqueous sodium carbonate till the solution was neutral to litmus. The product was then extracted from the aqueous phase in methylene chloride (3 x 20 ml). The product (3.0 g 65 % Yield) was dried over anhydrous sodium sulphate and molecular sieves 3A for two days. The product was characterized by IR, H¹ & C¹³ NMR. Scheme 2.3 gives the chemical reactions involved.(see next page)



Scheme 2.3. Synthesis of ABNEC monomer.

2.2.4 Synthesis of Tris-(2,4-dioxa-3-oxohept-6-en-1-yl) nitromethane (TDONM).

The monomer was synthesized by a two step process. Tris hydroxy methyl nitromethane was first prepared by formylation of nitromethane, which was then treated with allyl chloroformate to yield TDONM.

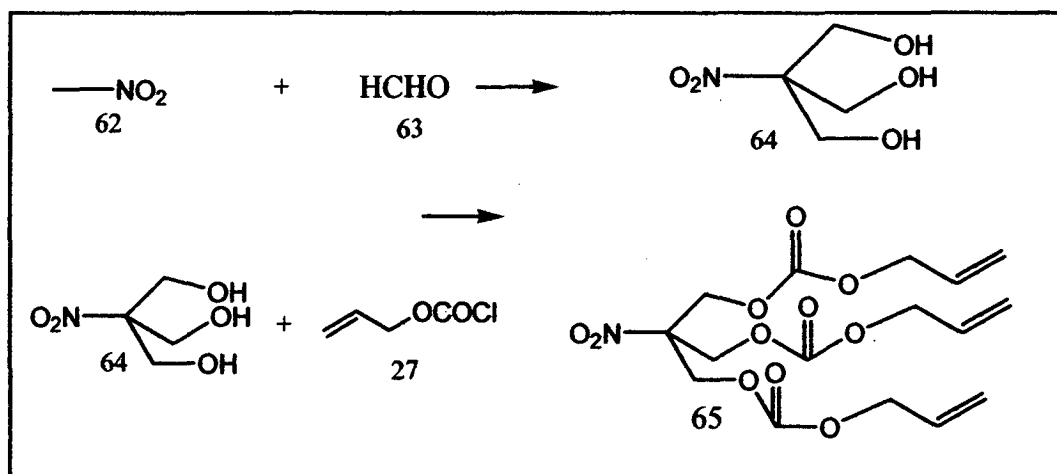
Step1:

Synthesis of Tris (Hydroxymethyl) nitro methane¹³⁴: Nitromethane (40 g, 0.65 mole), Methanol (75 ml) and methylene chloride (2 ml) were placed in a two neck round bottom flask (250 ml) capacity and NaOH (0.4 g) was added. The mixture was stirred for 0.5 h. Paraformaldehyde (58.5 g, 1.95 mole) was then added in portions, taking care that the temperature of the reaction mixture would remain between 45 – 55 °C. The solvent was then removed under vacuum. The product obtained was recrystallised from hot 1:1 Ethyl acetate-Benzene mixture.

Step 2:

Synthesis of Tris-(2,4-dioxa-3-oxohept-6-en-1-yl) nitromethane: Tris (Hydroxymethyl) nitro methane (5.0 g, 0.034 mole) was stirred

with Allyl chloroformate (12.4 g, 0.102 mole) and Pyridine (7.9 g, 0.102 mole) . After completion of the reaction, which can be monitored on TLC, the reaction mixture was washed with dil. Hydrochloric acid followed by water. The product was obtained on removal of solvent under vacuum, the product weighed 12.0 g (87 % yield w.r.t. Tris (hydroxymethyl) nitro methane. The product was characterized by IR, H¹ & C¹³ NMR, Mass spectroscopy.

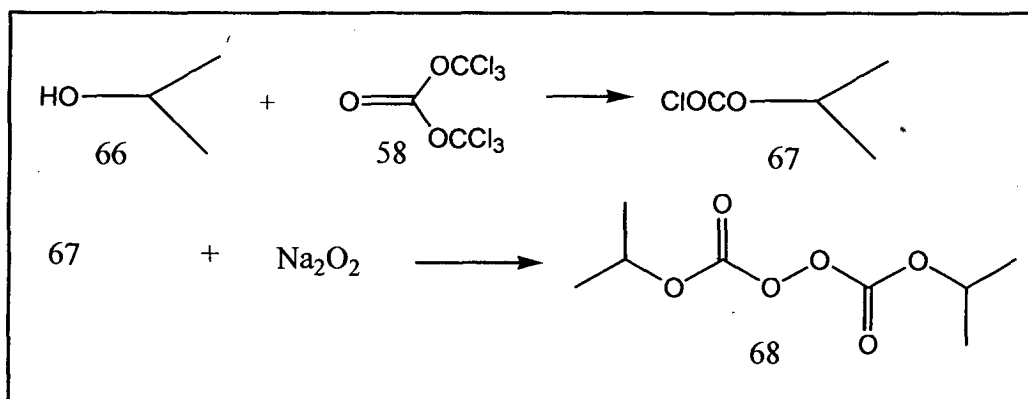


Scheme 2.4 Synthesis of TDONM monomer

2.2.5 Synthesis of Isopropyl peroxydicarbonates (IPP).

IPP can be prepared by the condensation of Isopropyl chloroformate (IPCI) with sodium peroxide. The methodology followed for the synthesis of IPCI was very much similar to that of allyl chloroformate (Sec. 2.2.1) except that isopropyl alcohol was used in place of allyl alcohol to get the desired chloroformate. Isopropyl alcohol (9.0 g, 0.15 mole) and Pyridine (7.5 g, 0.096 mole) were added with the aid of syringes to BTC (5.0 g, 0.016 mole) in methylene chloride (70 ml) over a period of 30 min to get isopropyl chloroformate. The isopropyl chloroformate obtained was used as

such in the next step towards preparation of IPP. A previously known procedure¹³⁵ was followed for the preparation of IPP. Isopropyl chloroformate (2.0 g, 0.014 mole) was added dropwise to Sodium peroxide (0.546 g, 0.007 mole), the mixture was stirred vigorously for 30 min, the mixture was then taken up in methylene chloride. The organic layer was passed through anhydrous sodium sulphate. The solvent was then removed by using vacuum. The product obtained weighed 3.4 g (% yield, 72 w.r.t. isopropyl chloroformate). The product was characterized by using IR spectroscopy. IPP was then stored safely under refrigerator conditions. The product was, however, prepared only in small quantities whenever required as large quantities (3.0 g) was vulnerable for degradation. The product was analyzed iodimetry by the known literature method¹³⁶ just before use.



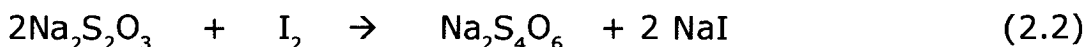
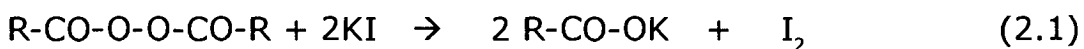
Scheme 2.5. Synthesis of IPP initiator

2.3 Kinetic Studies.

The Wij's solution, 10% KI solution, 0.01 and 0.1 N Na₂S₂O₃, 0.1 N KIO₃ solutions were prepared as per the standard methods available in literature¹³⁷.

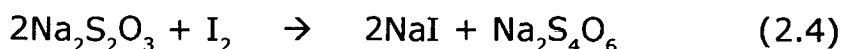
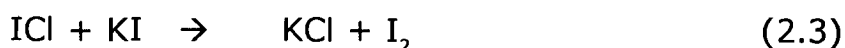
1) Peroxide determination^{135,136}: This involves, treatment of a known

amount of the initiator with KI in acetic anhydride, followed by titrimetric determination of iodine liberated using standard sodium thiosulphate solution. The chemical processes involved are as follows:



i.e., 2000 ml of 1 N $\text{Na}_2\text{S}_2\text{O}_3$ equals molecular weight of the peroxydicarbonate initiator used. Using this relationship the amount of active peroxide linkage present in the sample can be determined. 1.0 g of the monomer sample containing known percentage of initiator was dissolved in acetic anhydride and treated with solid KI. The mixture was left undisturbed for 20 min. Chloroform (10 ml) was then added and the flask was stoppered, shaken well and titrated against 0.01 N $\text{Na}_2\text{S}_2\text{O}_3$ (previously standardized against 0.01 N KIO_3). The titration is carried out using a starch indicator towards the end point, till the color changed from blue to colorless.

2) Determination of unsaturation: Known amount of monomer is dissolved in an inert solvent like chloroform, which is treated with an excess of Iodine monochloride (ICI) (Wij's solution). The unreacted ICI was back titrated with standard $\text{Na}_2\text{S}_2\text{O}_3$ solution after adding 10 % aqueous KI solution. The chemical processes involved are as follows:



2000ml of 1N $\text{Na}_2\text{S}_2\text{O}_3 = 1\text{I}_2 = n \times \text{C}=\text{C}$ *i.e.* molecular weight of the monomer, n stands for the number of double bonds. Thus, by knowing the amount of ICI required for the reaction, the amount of the

monomer can be calculated. Known weight of the monomer containing the initiator was taken in a stoppered conical flask and 10 ml of Wij's solution was added. The flask was stoppered tightly and kept in the dark for about 1 h with periodic swirling. 10 ml of 10 % KI solution was then added to it and the flask was stoppered immediately and shaken well. The contents of the flask were then titrated against 0.1 N $\text{Na}_2\text{S}_2\text{O}_3$ using a starch solution as an indicator towards the end point, till the color changed from blue to colorless.

3) Determination of the peroxide content and unsaturation during the polymerization process: 1.5 g of monomer was taken in a stoppered test tube and flushed with nitrogen gas for 30 min followed by addition of initiator. The test tubes were stoppered immediately and made air tight with rubber stoppers and silicone film. The test tubes were then kept in a constant temperature water bath at varying temperatures. The test tubes were periodically removed and the contents were analyzed for the unreacted initiator and unsaturation. This data was then used for constructing the temperature vs time heating cycle.

2.4 Preparation of SSNTD films by cast polymerization.

The monomer was filtered through a sintered G4 glass crucible, to remove any solid impurities. The monomer was then stirred under nitrogen atmosphere, for several hours to remove the dissolved air and oxygen, which hinder the process of polymerization; this was followed by addition of the initiator. The purified monomer, containing the initiator and plasticizer, was carefully injected into the mold, by using a syringe, through a previously prepared tiny hole in the Teflon™ gasket. Special care was taken to avoid any air bubble formation, in the liquid monomer film, during the injection into the mold. The entire assembly was tightened, by sandwiching between

two flat aluminum plates of size 12.5 cm x 12.5 cm using special assembly designed for pressurizing the molds (Fig 2.3). The molds were then placed into the polymerization bath. The molds were gradually heated, according to the previously determined polymerization cycle, over a period of time, with periodic tightening of the molds. The molds were allowed to cool slowly, and opened. A clear transparent film was obtained which was carefully detached from the glass plates.

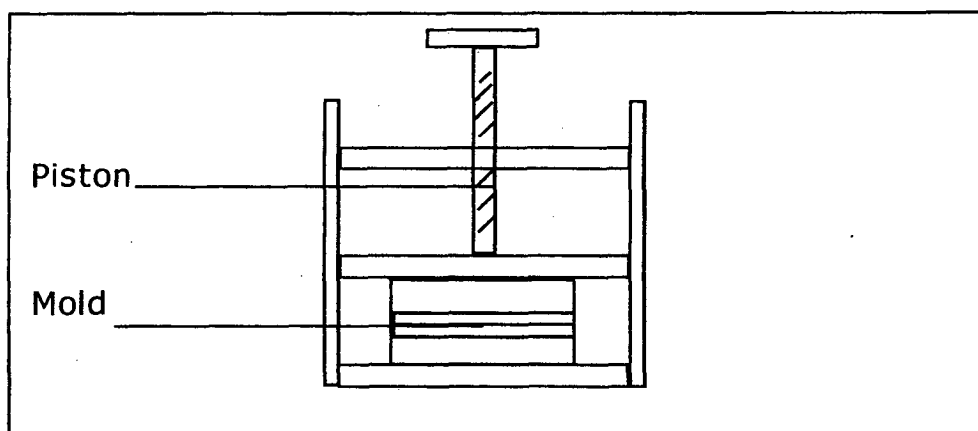


Fig. 2.3. Assembly for pressurizing the mold

2) Thickness measurement: The thickness of the films prepared was measured, over the entire surface of the films, randomly at 50 different points, for a film of size 8 cm x 8 cm, using a digital thickness gauge (Alpha meter, Para Electronics, India).

3) Exposure of SSNTD films to charged particles: The side of the film that was to be exposed was first marked. Small pieces of size 2 cm x 2 cm were exposed to an electrodeposited source by using the arrangement shown in Fig. 2.4. (see next page) It can be seen that only a circular portion of area 1 cm x 1 cm is exposed to the radiations. The distance between the films and the source can be adjusted as per the requirement. A distance of 2 cm was used to ensure normal incidence of the alpha particles.

4) Exposure of SSNTD films to charged particles for sensitivity studies: To irradiate the films with alpha particles and fission fragments, the films were exposed to ^{252}Cf source of 300 dpm strength. The same exposure arrangement as shown in Fig. 2.4. was used except that the films were mounted in a radial manner on an arc shaped stand with arc radius of 5 cm. The stand was 3 cm in width and had a narrow band of 2 cm width grooved over it. Thus, approximately 6 pieces of films of size 1 cm x 1 cm at a distance of 5 cm from the source could be simultaneously exposed to charged particles. This

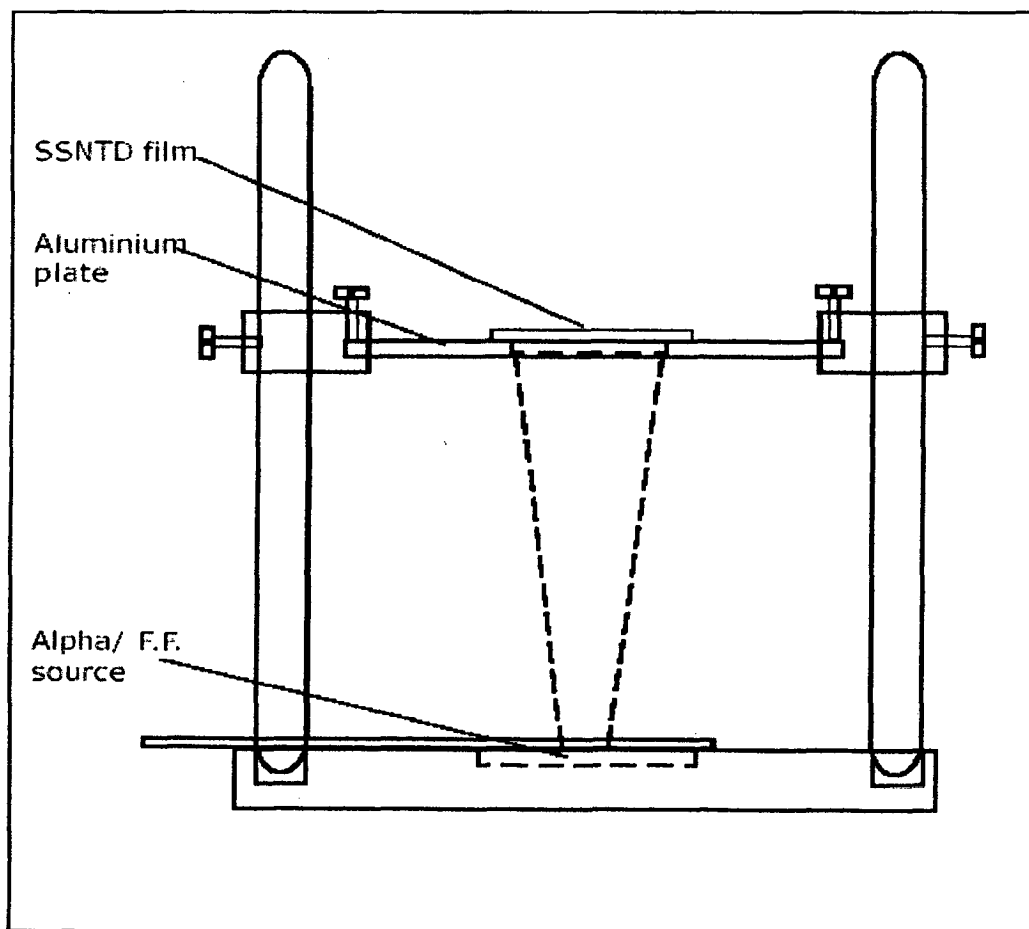


Fig. 2.4. SSNTD exposure Arrangement.

exposure assembly was kept in a vacuum desiccator and the films were exposed for about 3 to 5 h, after applying a vacuum of 0.1 torr. Sensitivity was calculated as given by equation 2.5.

$$\text{Sensitivity} = \frac{1 + (D_a/D_f)^2}{1 - (D_a/D_f)^2} \quad (2.5)$$

Where D_a is the diameter of alpha track.

D_f is the diameter of fission fragment.

See Annexure I for Photomicrographs of the films.

5) Chemical etching: For the purpose of chemical etching of the films, the assembly shown in Fig. 1.5 was used. The temperature of the etchant was maintained, as required by using a constant temperature circulating water bath. The films were held vertically in a stainless steel wire gauze holder which could carry a maximum of 6 films of size 2 cm x 2 cm. The etchant was stirred during the process of chemical etching. After etching the films for the required time interval, the films were washed several times with cold distilled water and dried by pressing between the folds of a tissue paper, followed by drying under a lamp.

6) Microscopic counting of the tracks: The dry, chemically etched films were kept on a glass slide and focused properly under the required magnification. The tracks in each view were then counted. The views were selected using an X-Y stage attached to the microscope. About 100 views were counted for a film of size 1 cm x 1 cm. The area of each view under given magnification was determined using the stage micrometer. The track density was determined using the following relationship.

$$\text{Track density (tracks/cm}^2\text{)} = \frac{\text{Total number of tracks counted}}{\text{Total number of views} \times \text{area of the view}} \quad (2.6)$$

7) Bulk etch rate determination: Bulk etch rate can be determined by following any of the three methods *i.e.*, 1) Change in thickness of the films upon etching. 2) Weight loss method. 3) Fission fragment diameter method. The thickness measurement method involves measurement of thickness of the films over its entire surface, so it can be used, only if films of uniform thickness are obtained. In the present studies the weight loss method and fission fragment diameter method were used for determination of the bulk etch rates. The bulk etch rates can be determined by using the following equations available from the literature⁶.

Weight loss method:

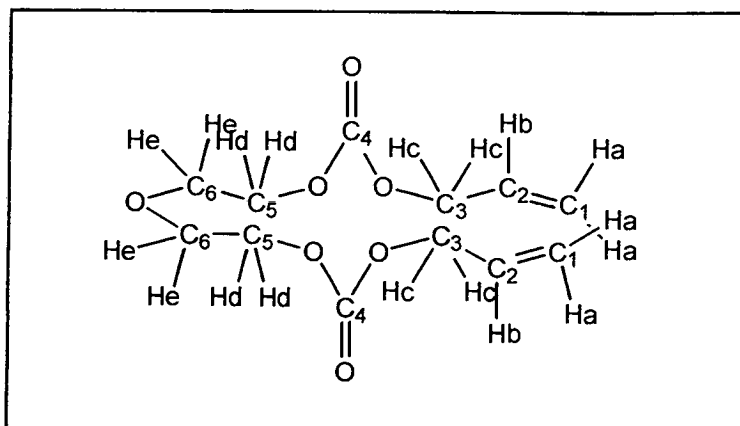
$$V_b (\mu\text{m/h}) = \frac{\text{Initial thickness} \times \text{Change in weight of the films}}{2 \times \text{time of etching} \times \text{initial weight of films}} \quad (2.7)$$

Fission fragment method:

$$V_b (\mu\text{m/h}) = \frac{\text{Diameter of fission fragment}}{2 \times \text{time of etching}} \quad (2.8)$$

2.5 Spectral Data of compounds.

Spectral data of ADC:

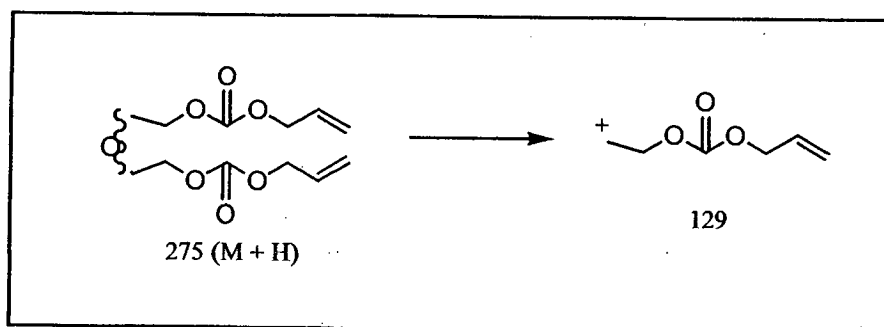


IR (neat) (cm⁻¹): 1758, 1655, 1250.

¹H NMR (CDCl₃, 300 MHz): δ (ppm) 5.20 - 5.40, t (H_a); 5.80 - 6.00, m, (H_b); 4.72 - 4.80, d, (H_c); 4.20 - 4.30, t, (H_d); 3.70 - 3.80, t, (H_e).

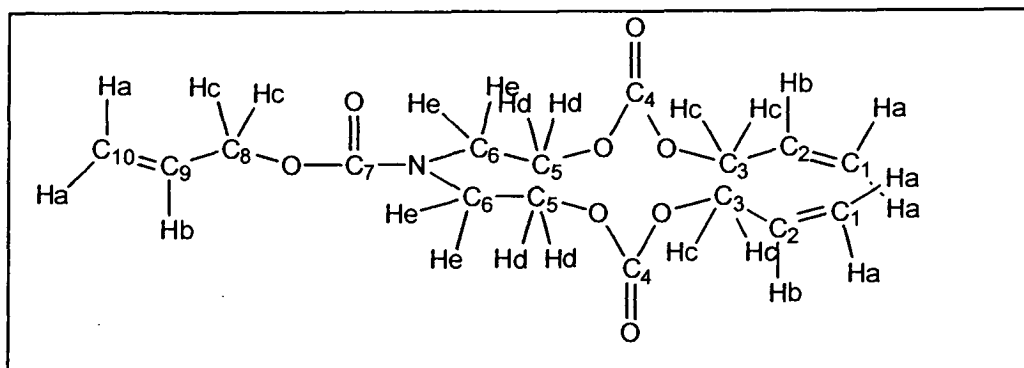
¹³C NMR (CDCl₃, 75 MHz): 118.828 (C₁), 131.518 (C₂), 68.865 (C₃), 154.890 (C₄), 66.838 (C₅), 68.461 (C₆).

Mass Spectrum: TOF MS-CI : m/z (amu) 275 (M + H), 129.



Mass fragmentation pattern for ADC

Spectral data of NADAC:



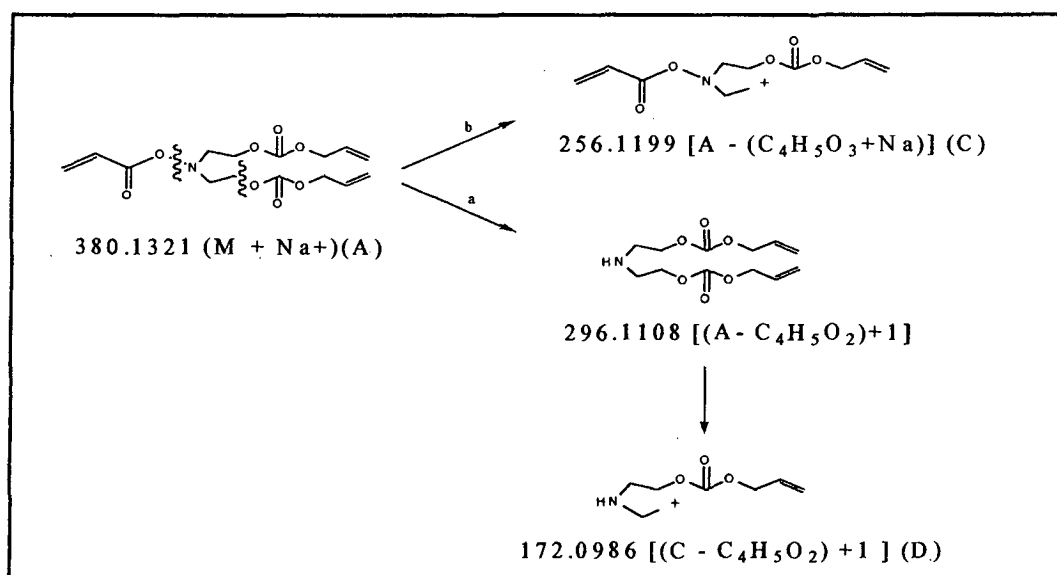
IR (neat) (cm^{-1}): 1758, 1710, 1655, 1250.

^1H NMR (CDCl_3 , 300 MHz): δ (ppm) 5.11 - 5.31, t (H_a); 5.78 - 5.89, m, (H_b); 4.51 - 4.55, d, (H_c); 4.18 - 4.21, t, (H_d); 3.51 - 3.55, t, (H_e).

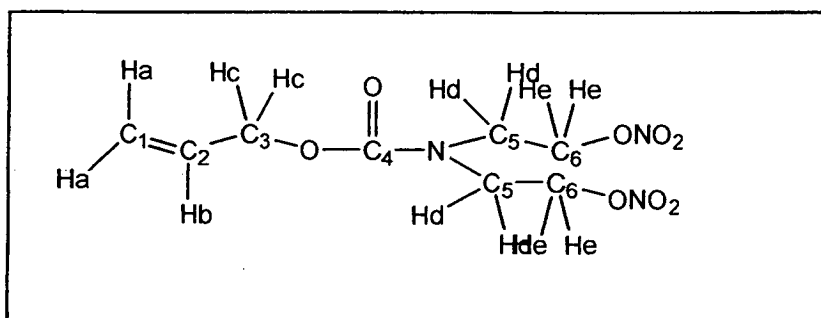
^{13}C NMR (CDCl_3 , 75 MHz): 117.613 (C_1), 131.356 (C_2), 68.453 (C_3), 154.671 (C_4), 65.851 (C_5), 46.995 (C_6), 155.585 (C_7), 132.508 (C_9), 118.45 (C_{10})

Mass Spectrum:

TOF MS-ESI : m/z (amu) 380.1321 ($\text{M} + \text{Na}^+$)(A), 296.1108 [$(\text{A}^- - \text{C}_4\text{H}_5\text{O}_2) + 1$] (B), 256.1199 [$\text{A} - (\text{C}_4\text{H}_5\text{O}_3 + \text{Na})$] (C), 172.0986 [$(\text{C} - \text{C}_4\text{H}_5\text{O}_2) + 1$]



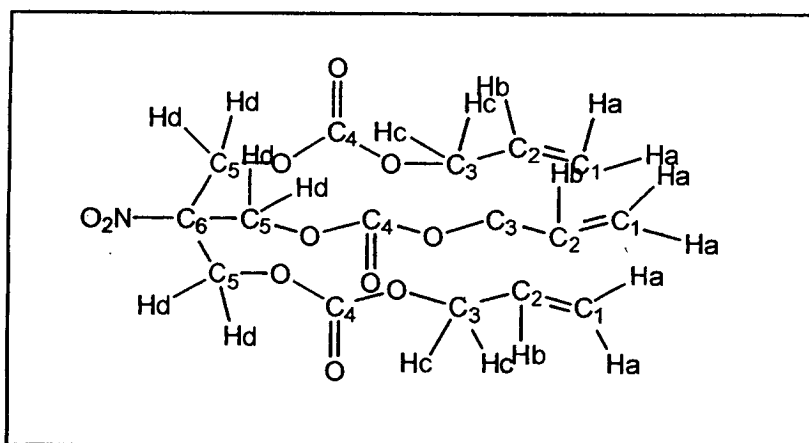
Mass fragmentation pattern for NADAC monomer.

Spectral data for ABNEC:

IR (cm⁻¹) : 1710, 1650, 1250.1454.

¹H NMR (CDCl₃, 300 MHz): δ (ppm) 5.12 – 5.23, t (H_a); 5.75 – 5.88, m, (H_b); 4.49 – 4.53, d, (H_c); 3.41 – 3.56, t, (H_d); 4.20 – 4.28, t, (H_e).

¹³C NMR (CDCl₃, 75 MHz): δ (ppm) 118.224 (C₁), 132.047 (C₂), 70.848 (C₃), 155.444 (C₄), 41.749 (C₅), 45.828 (C₆).

Spectral data for TDONM:

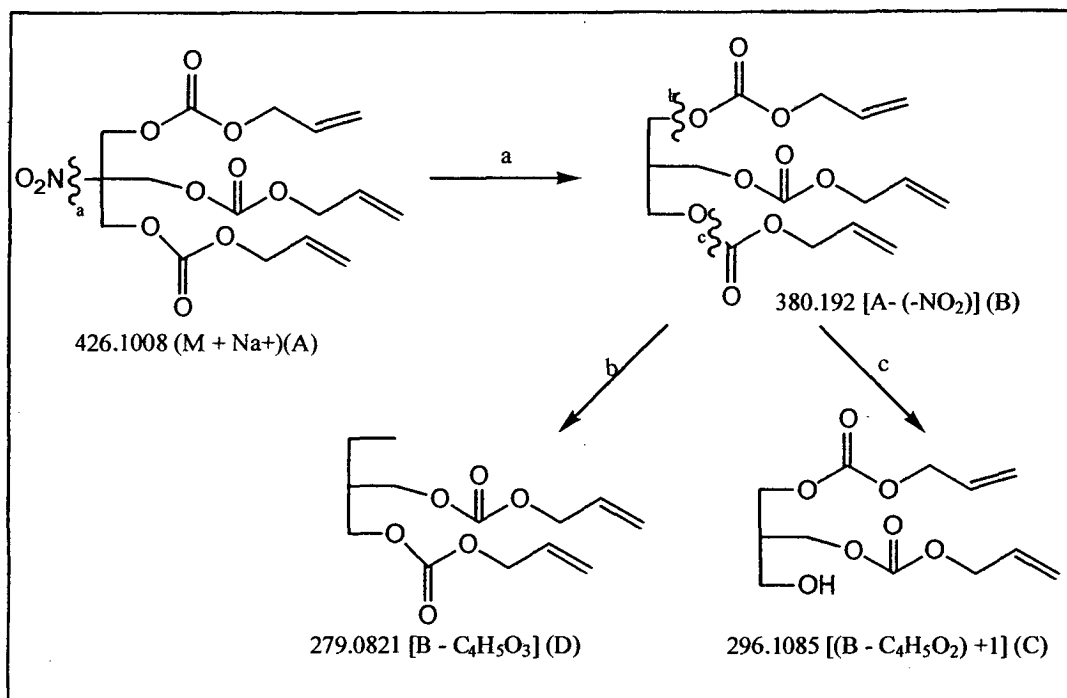
IR (neat) (cm⁻¹): 1655, 1758, 1454, 1560.

¹H NMR (CDCl₃, 300 MHz): δ (ppm) 5.280, t (H_a); 5.830, m, (H_b); 4.591, d, (H_c); 4.234, s, (H_d); 4.234, t, (H_e).

¹³C NMR (CDCl₃, 75 MHz): δ (ppm) 121.034 (C₁), 132.204 (C₂), 70.715 (C₃), 155.013 (C₄), 65.070 (C₅), 89.086 (C₆).

Mass Spectrum:

TOF MS-ESI : m/z (amu) 426.1008 ($M + Na^+$)(A), 380.192 [$A - (-NO_2)$] (B), 296.1085 [$(B - C_4H_5O_2) + 1$] (C), 279.0821 [$B - C_4H_5O_3$] (D)



Mass fragmentation pattern for TDONM

All the spectra (IR, PMR, CMR, MS) are reproduced in Fig no. 2.5 - 2.21 (pg. no. 86 - 102)

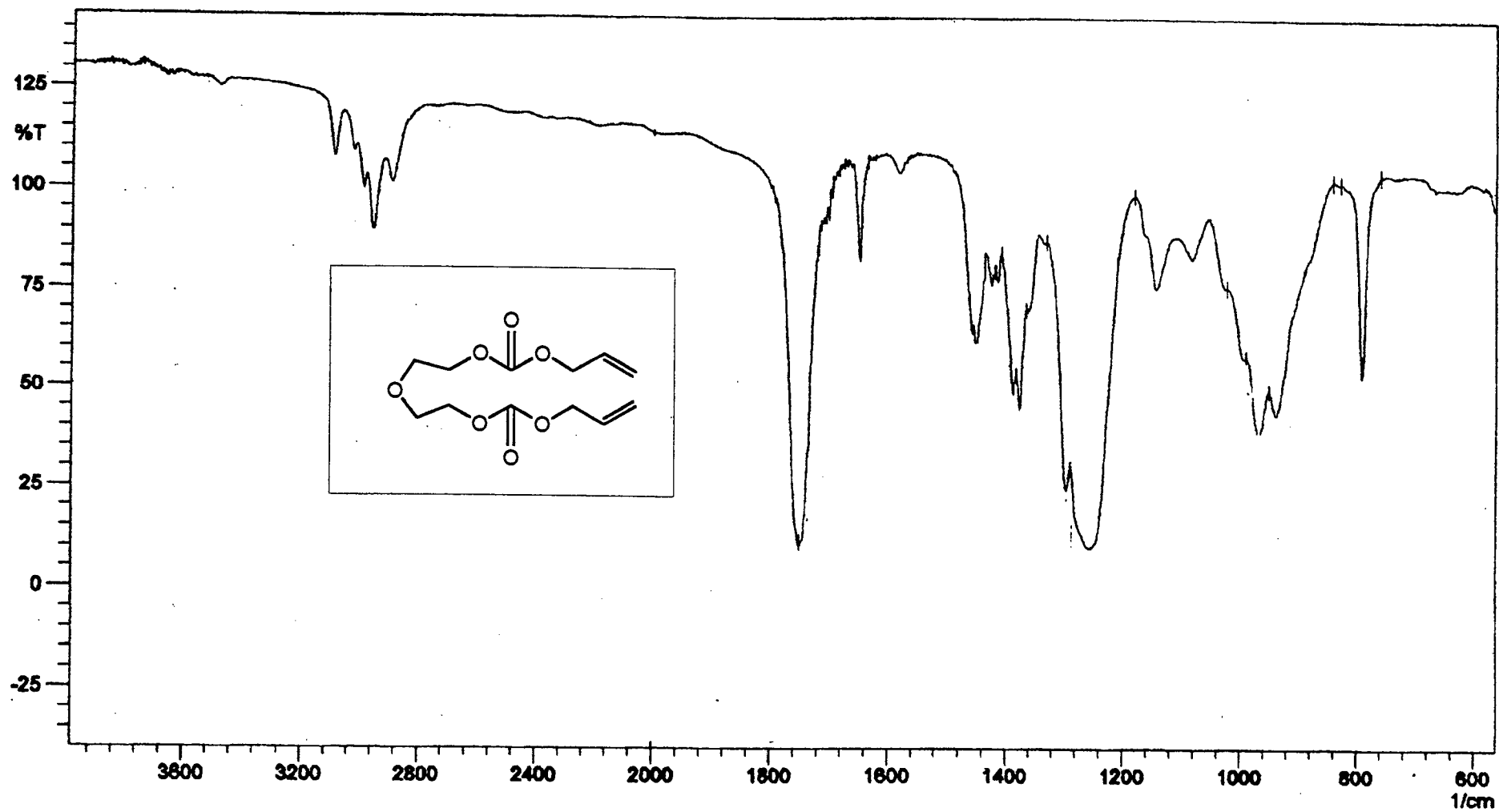


Fig. 2.5 IR spectrum of ADC monomer

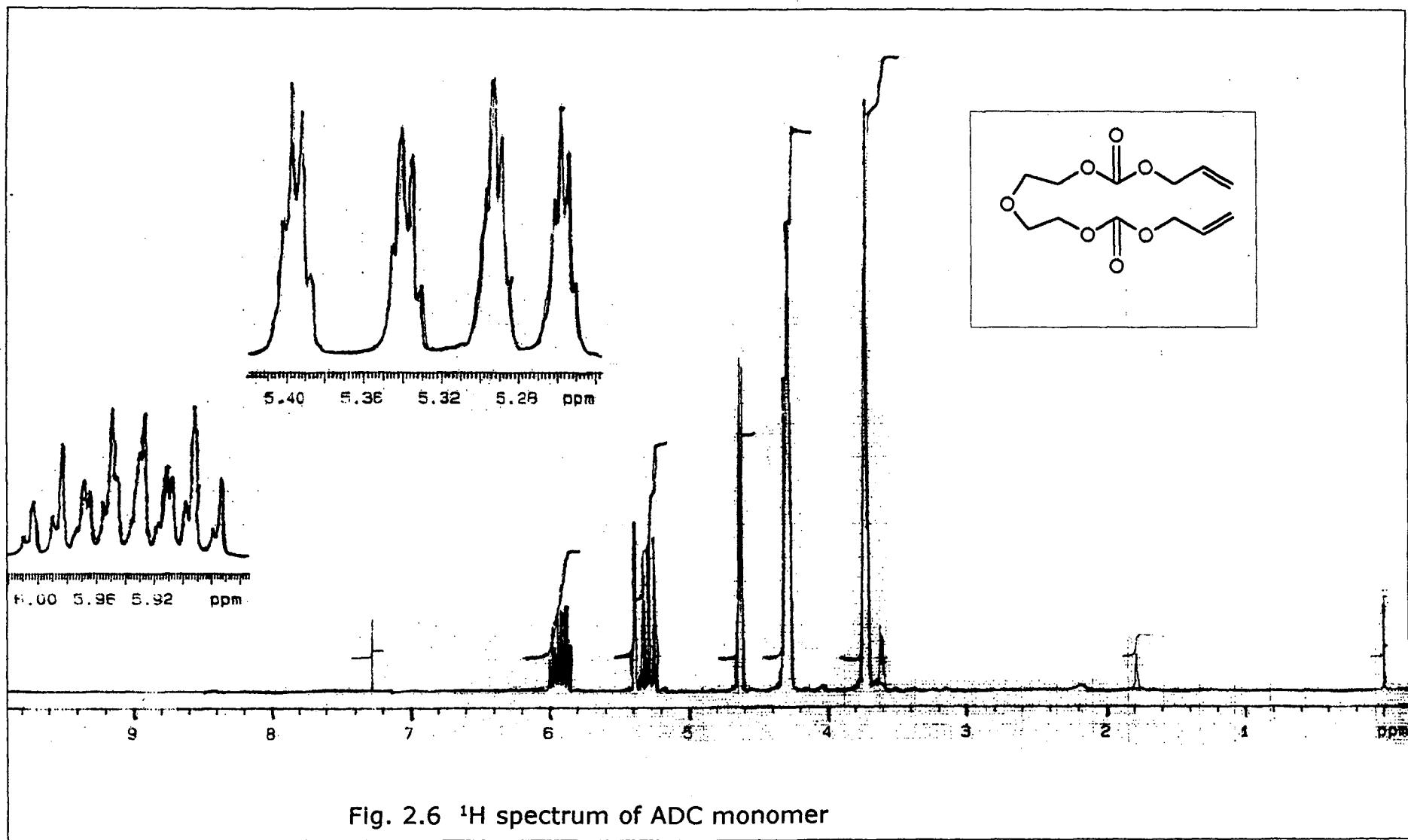


Fig. 2.6 ^1H spectrum of ADC monomer

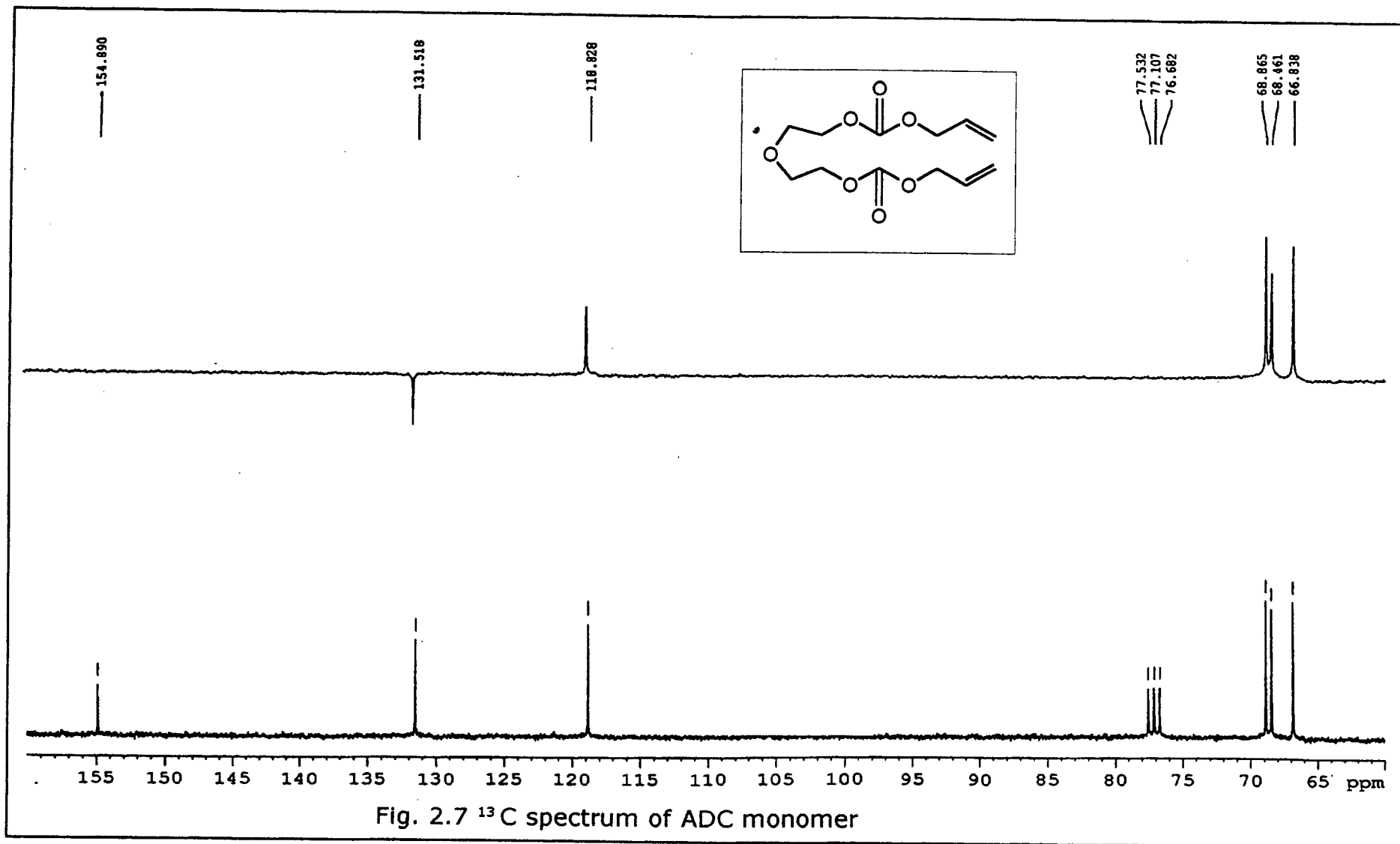


Fig. 2.7 ^{13}C spectrum of ADC monomer

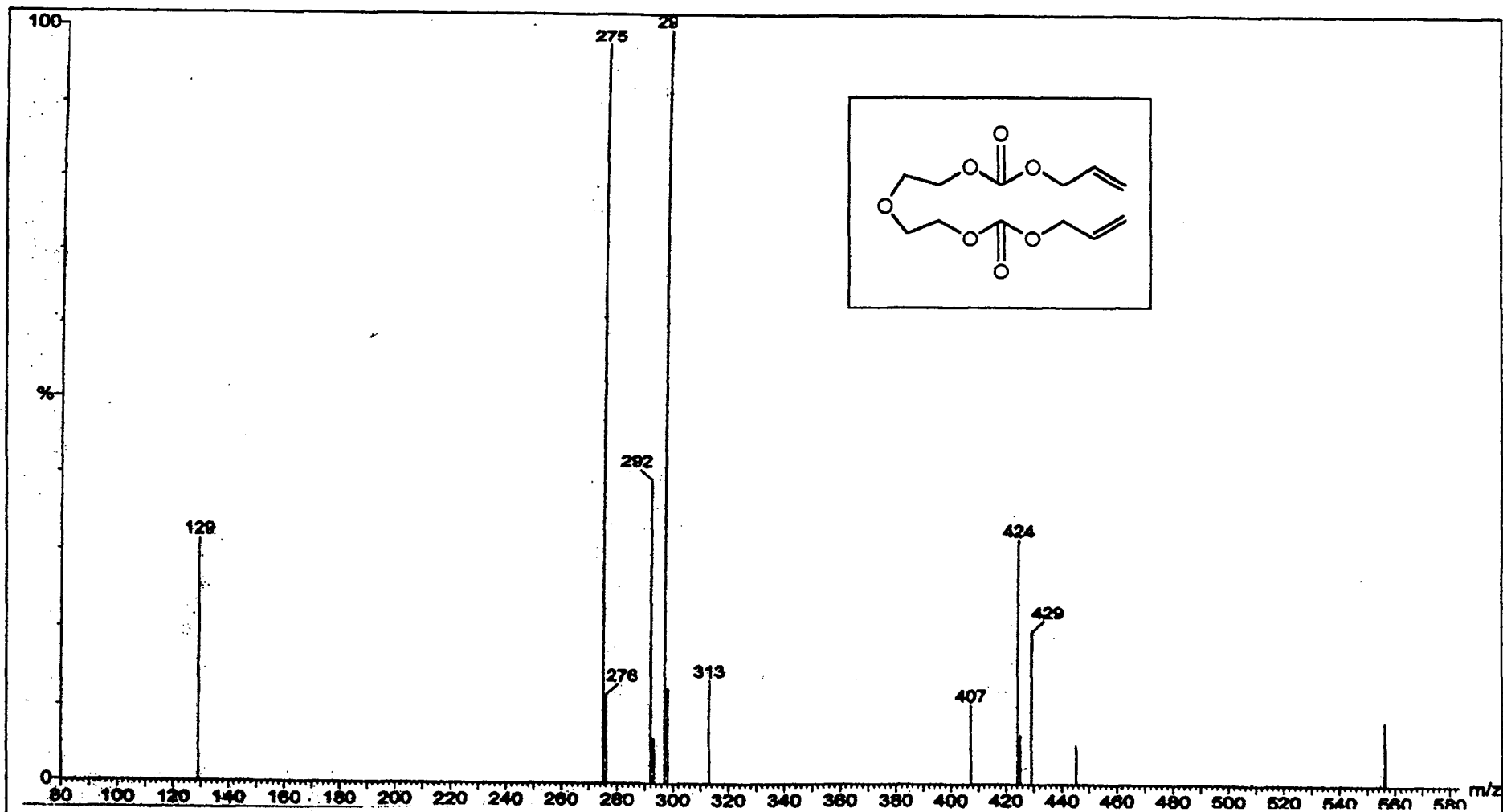


Fig. 2.8 Mass spectrum of ADC monomer

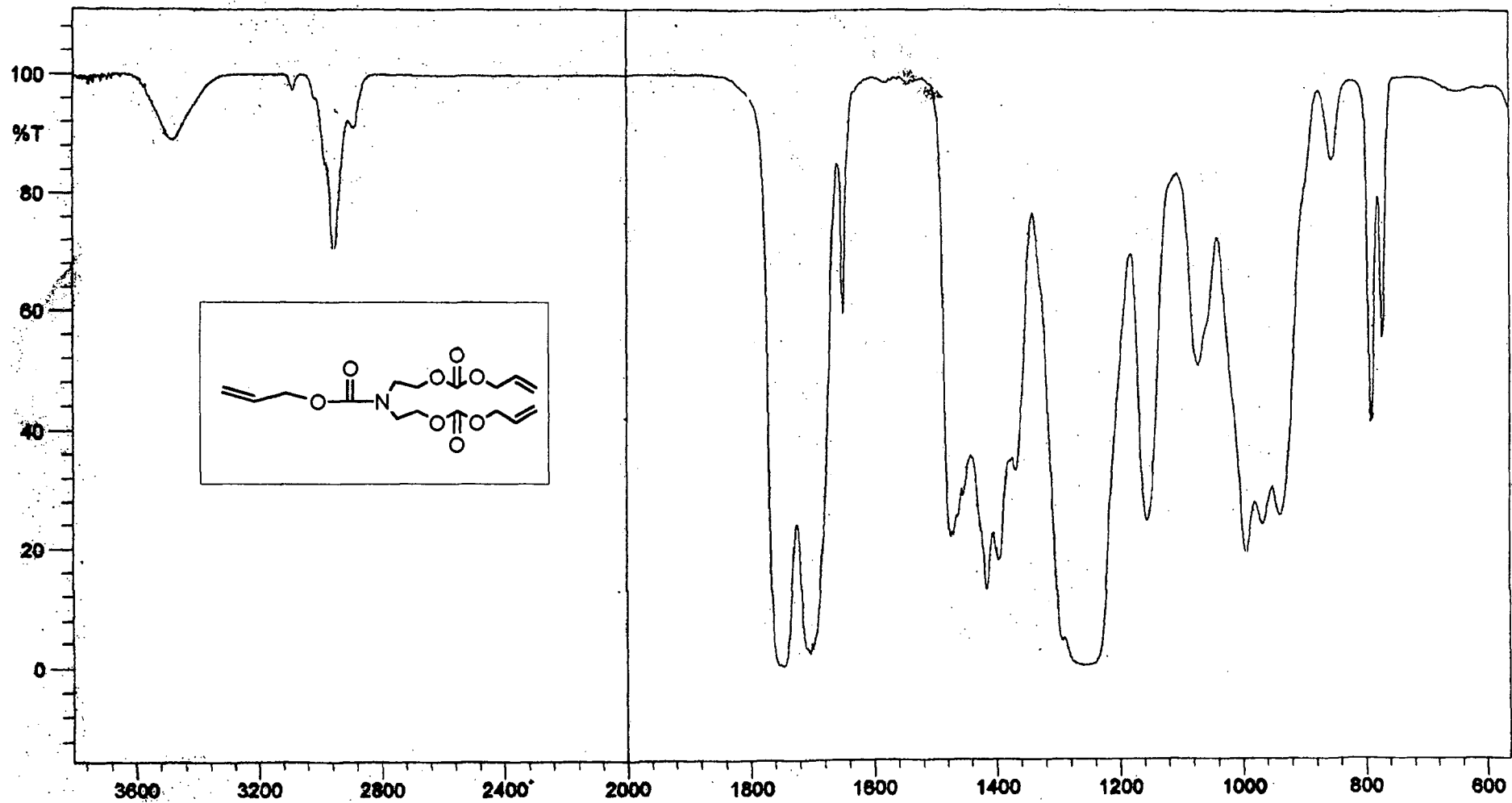
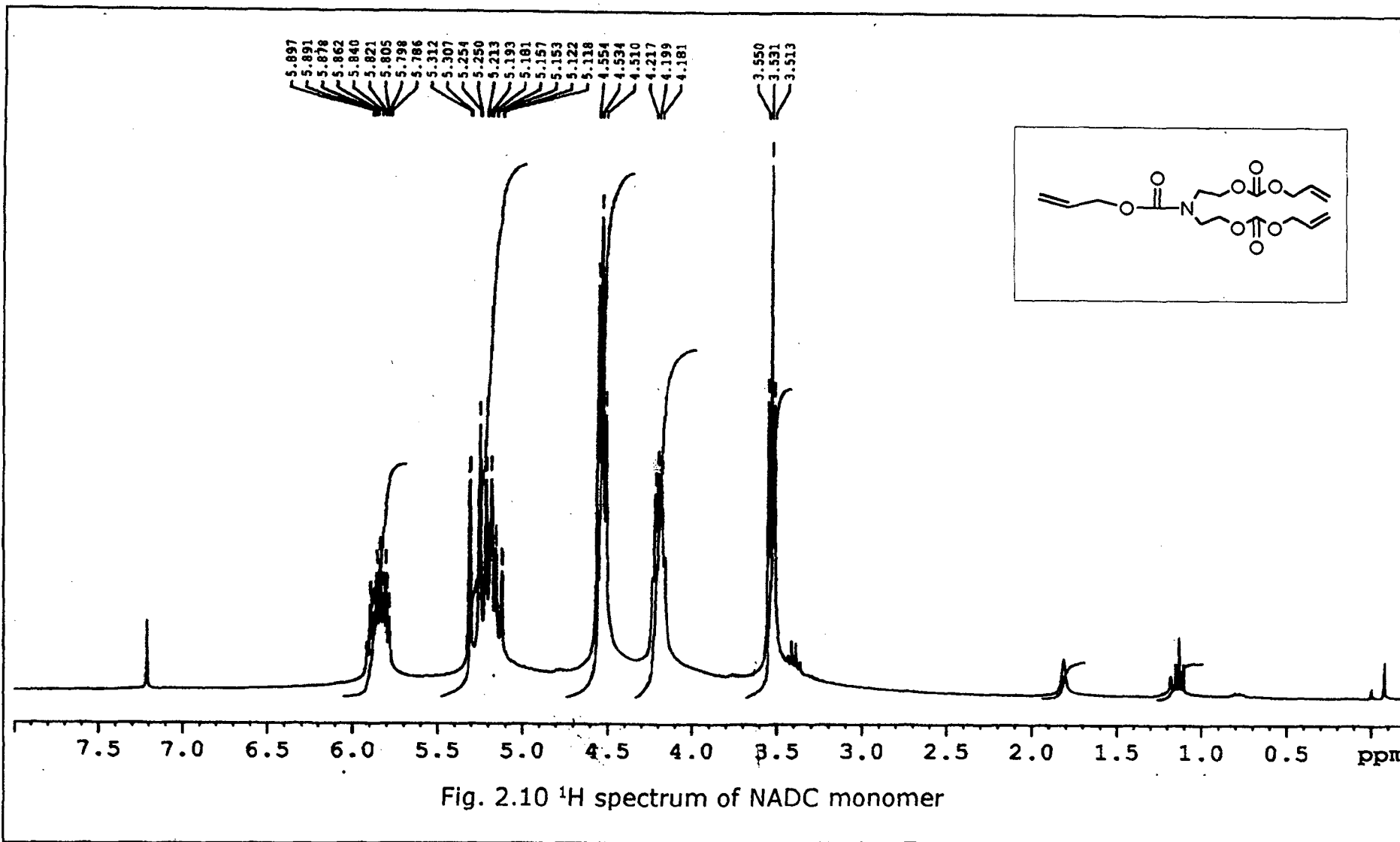
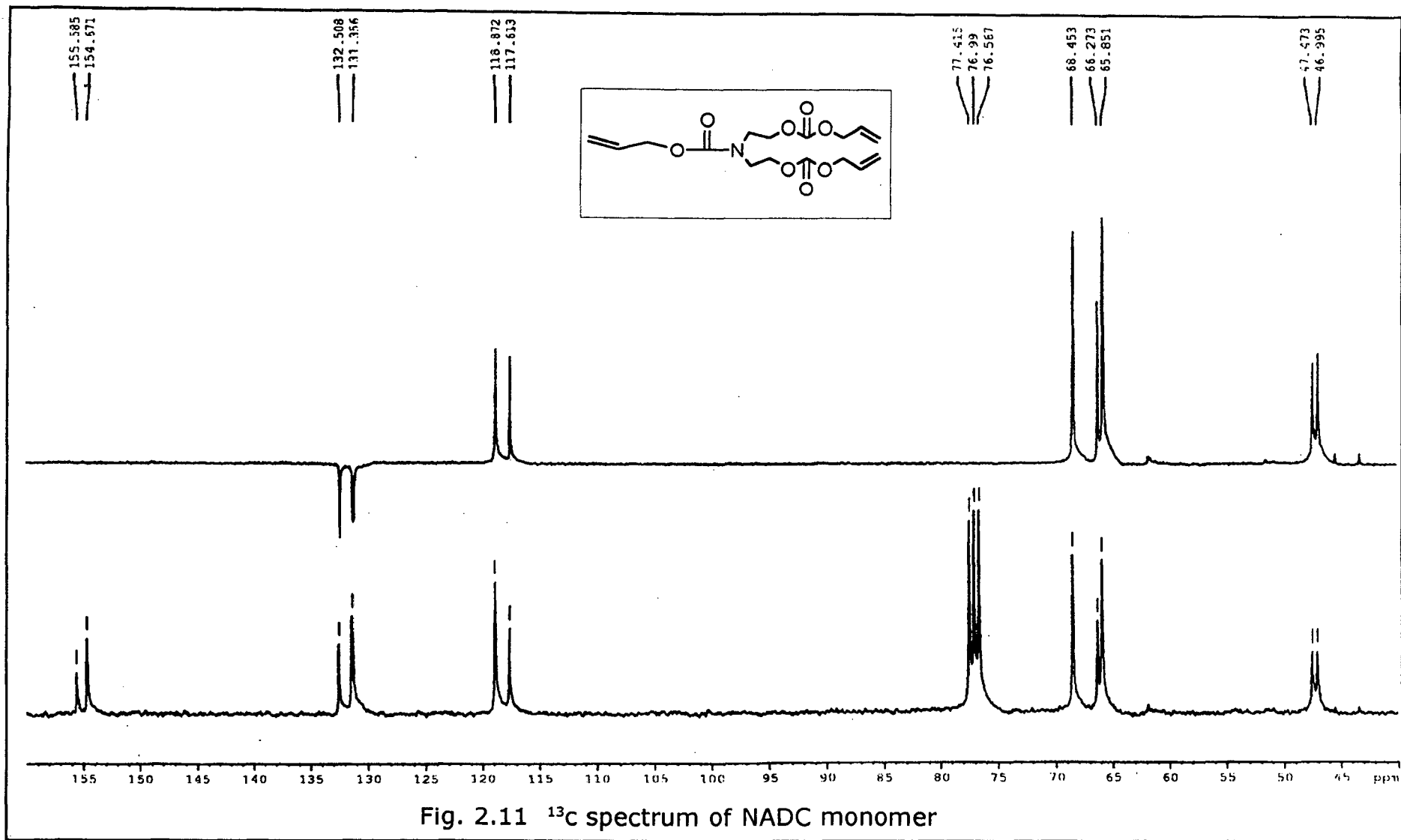


Fig. 2.9 IR spectrum of NADC monomer





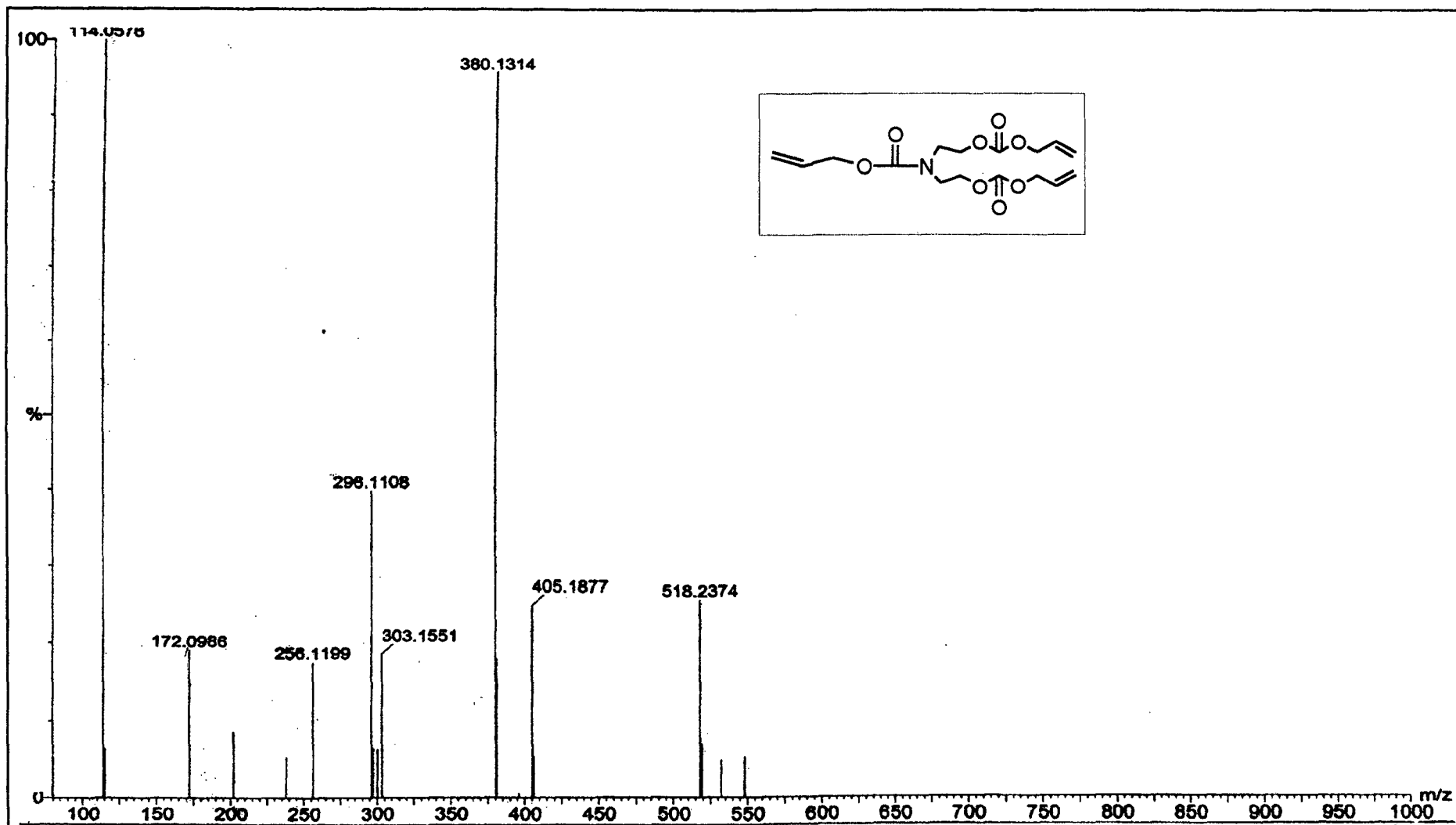


Fig. 2.12 Mass spectrum of NADC monomer

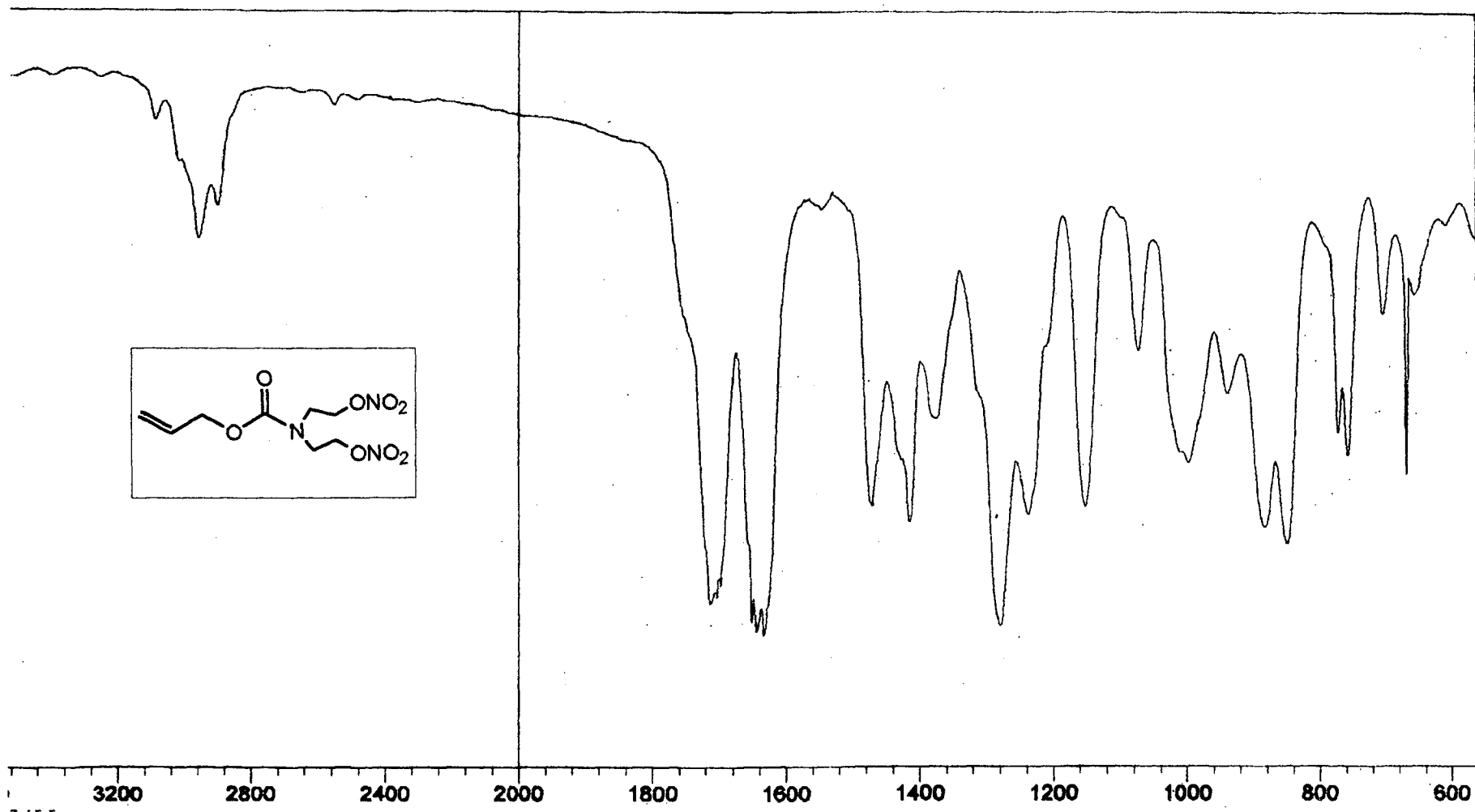
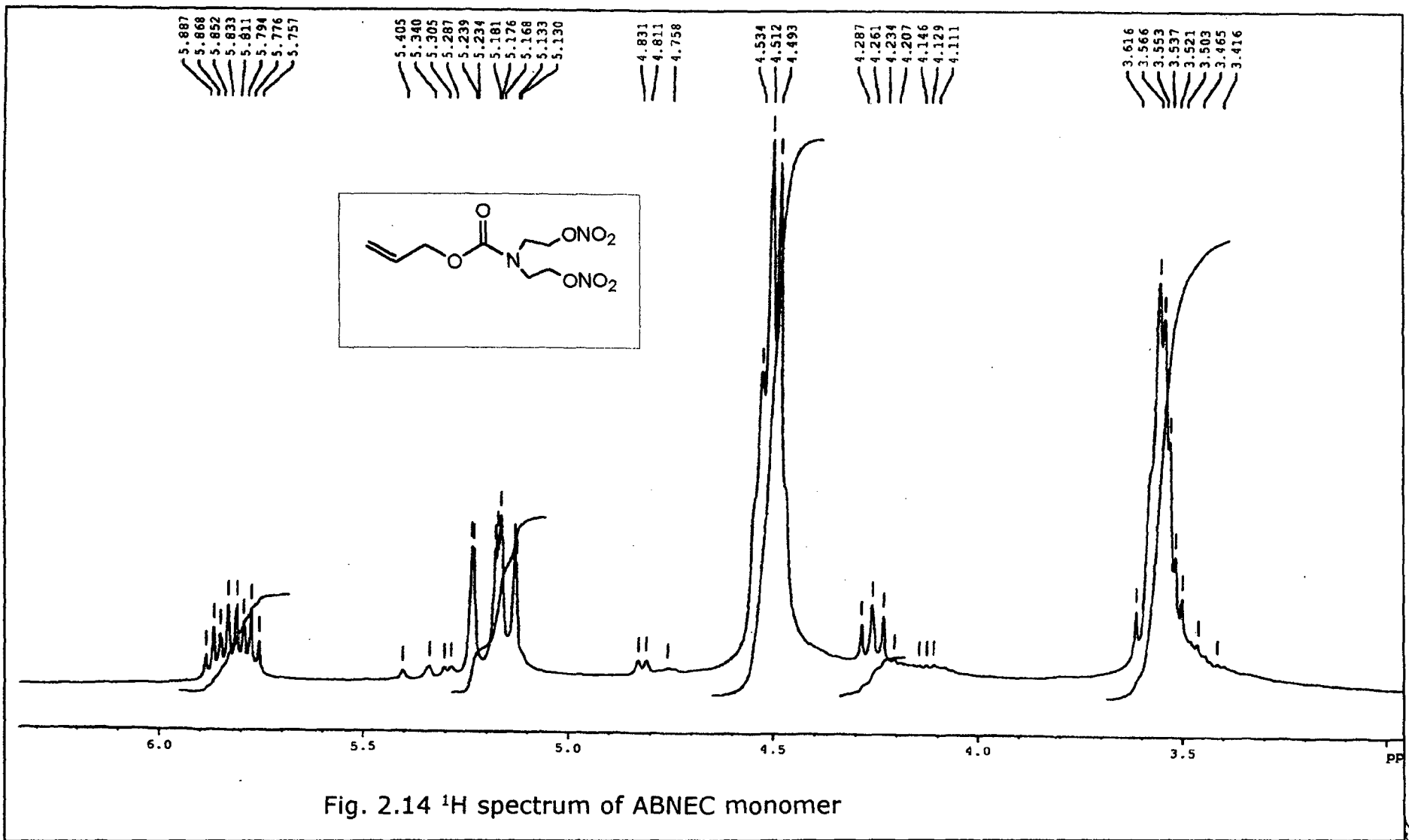


Fig. 2.13 IR spectrum of ABNEC monomer



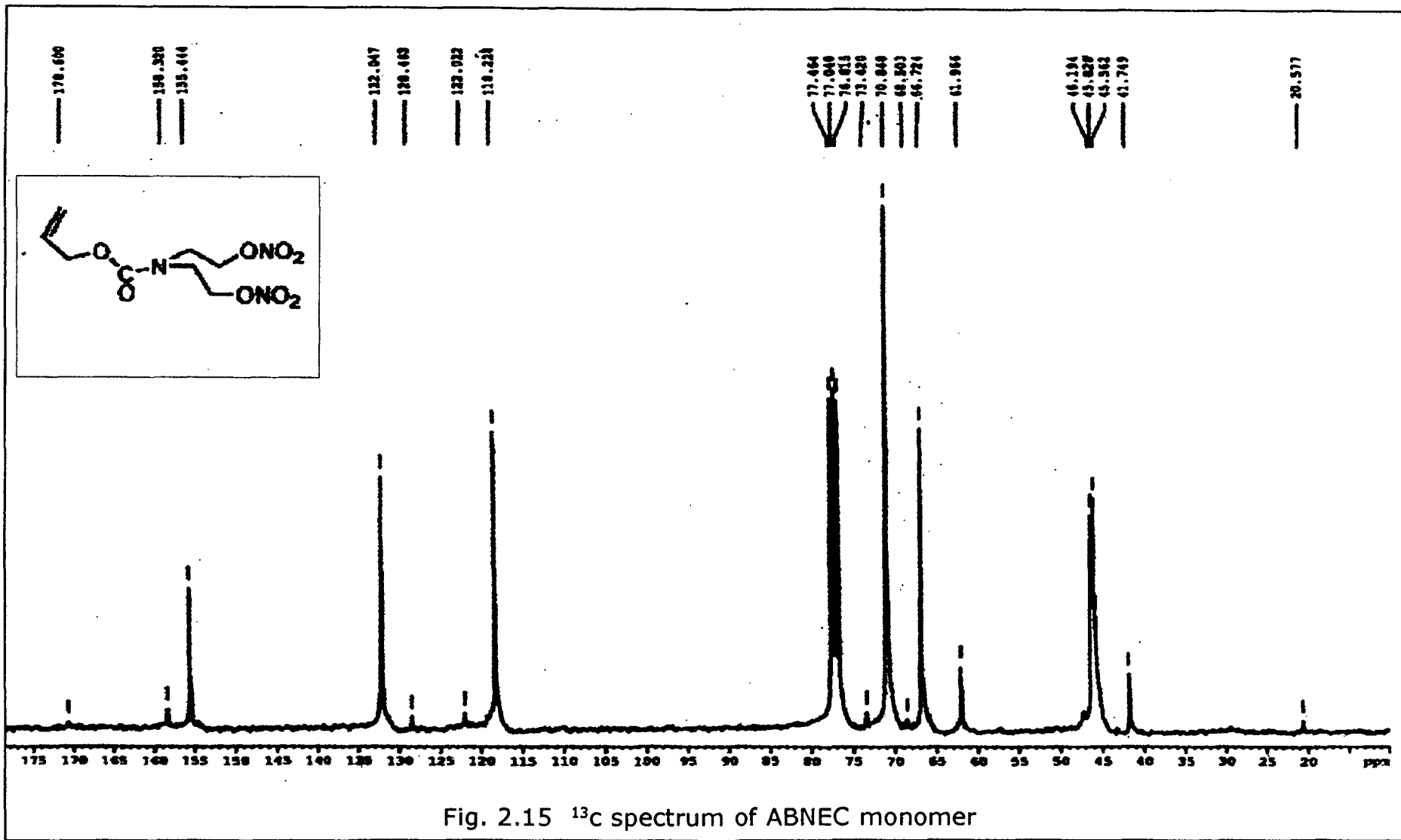


Fig. 2.15 ¹³C spectrum of ABNEC monomer

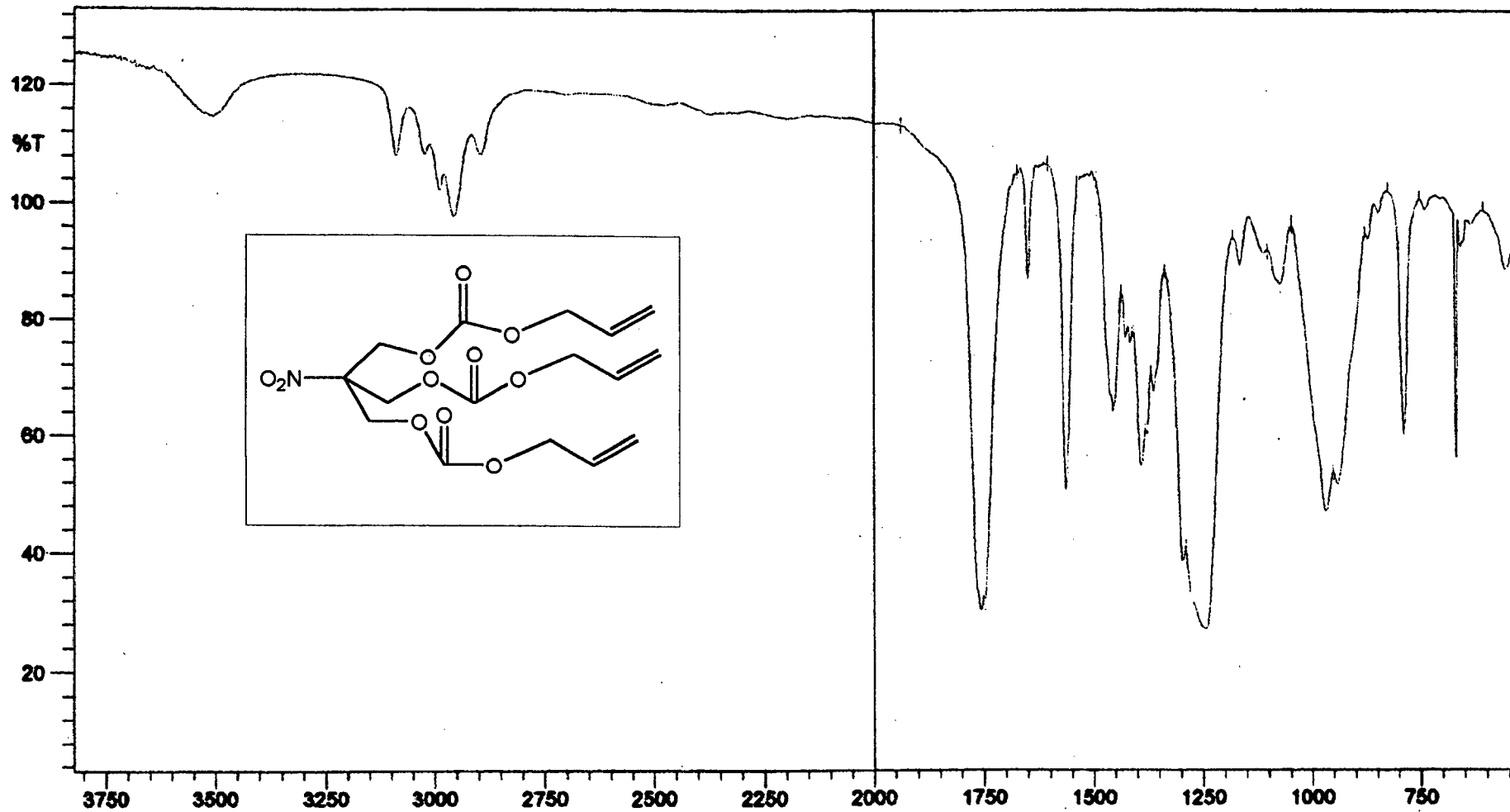


Fig. 2.16 IR spectrum of TDONM monomer

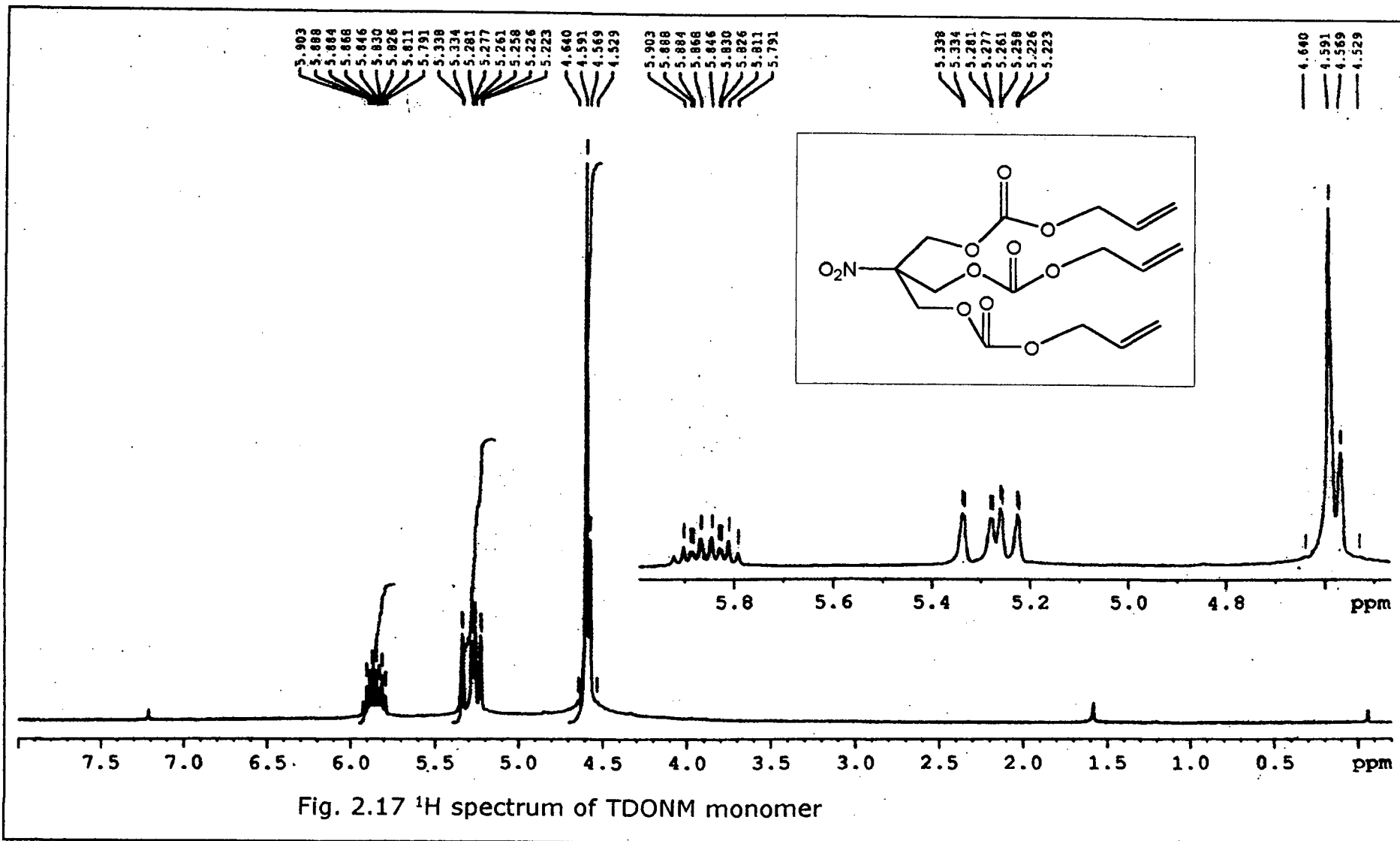


Fig. 2.17 ^1H spectrum of TDONM monomer

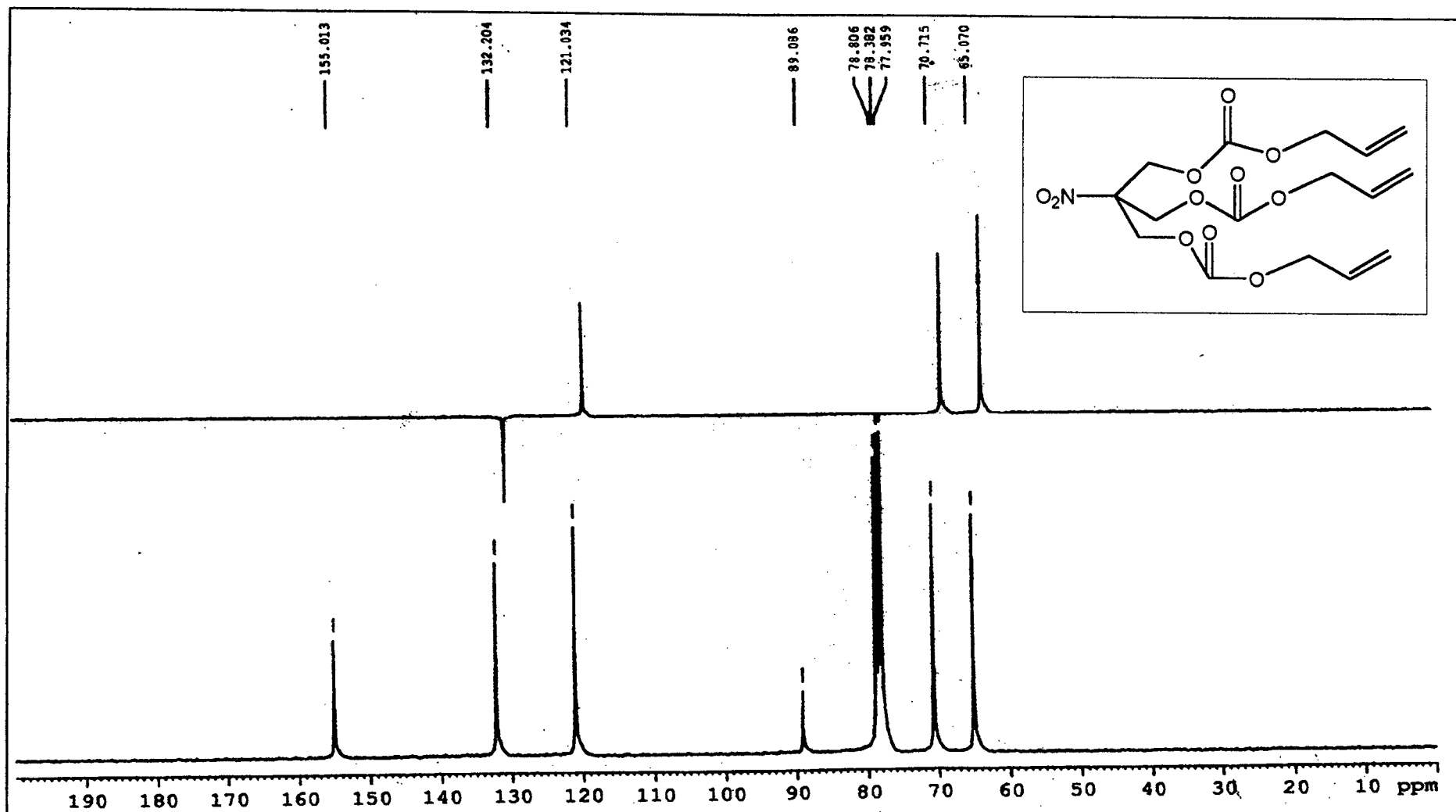


Fig. 2.18 ^{13}C spectrum of TDONM monomer

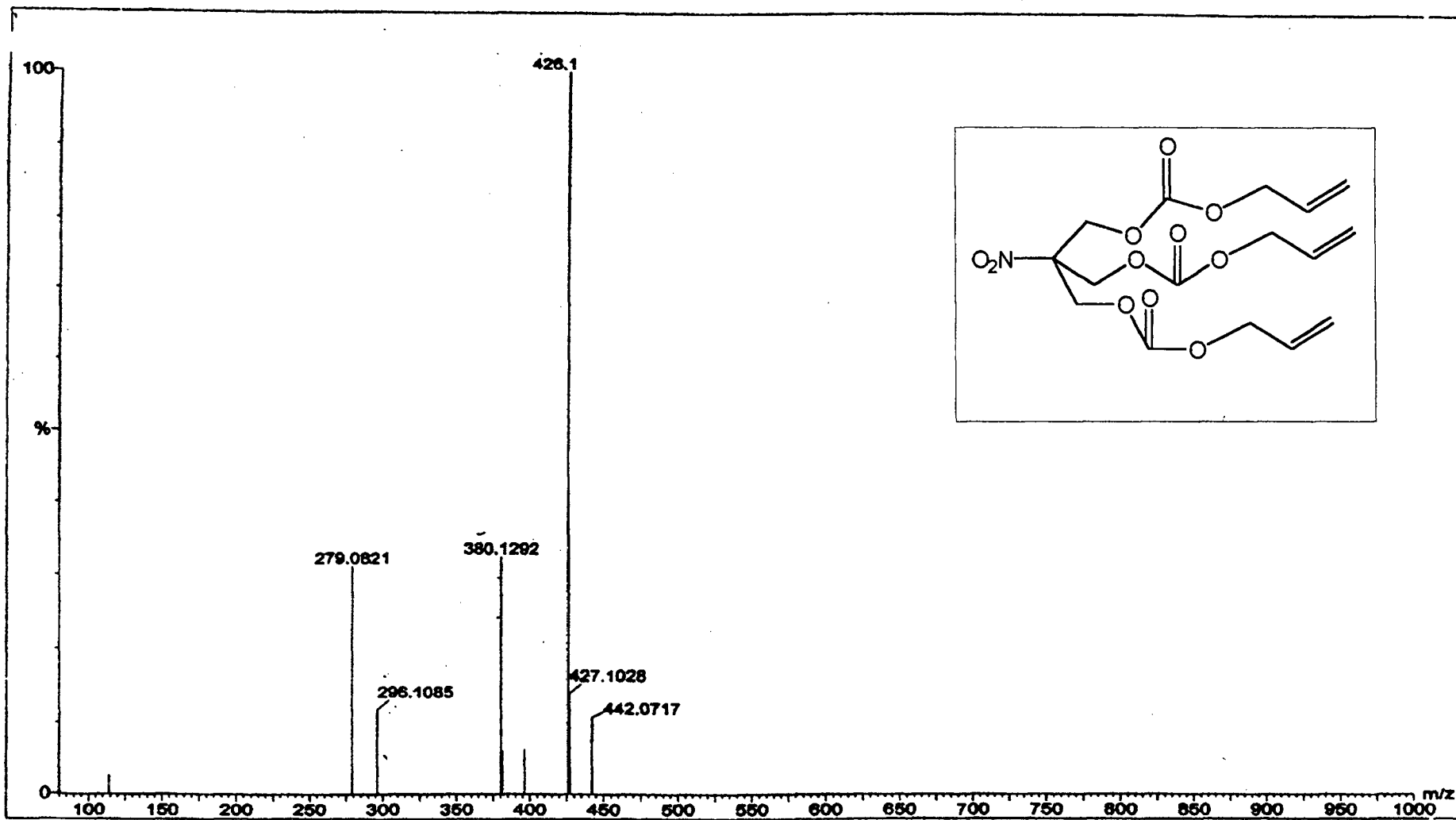


Fig. 2.19 Mass spectrum of TDONM monomer

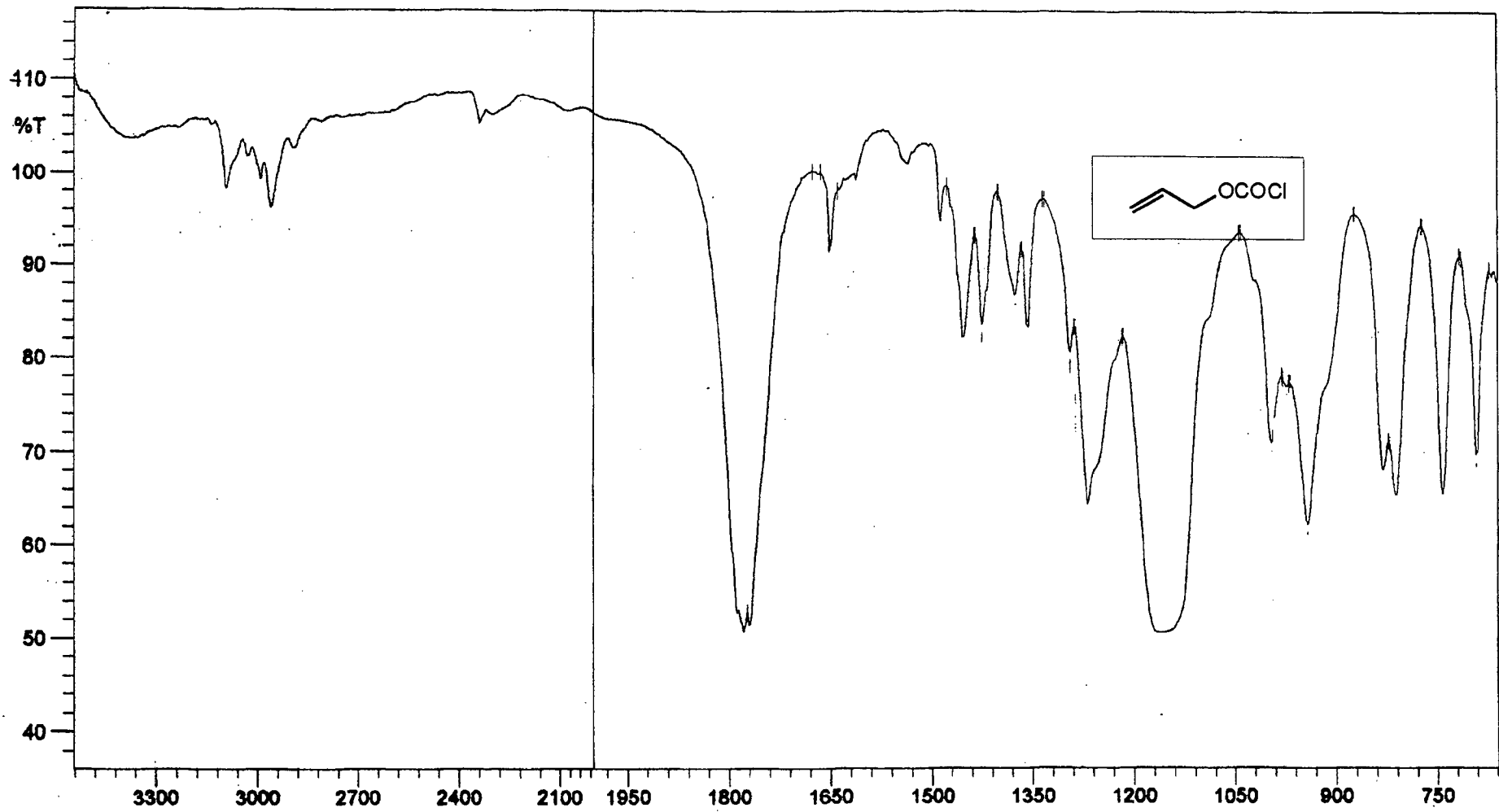


Fig. 2.20 IR spectrum of Allyl chloroformate

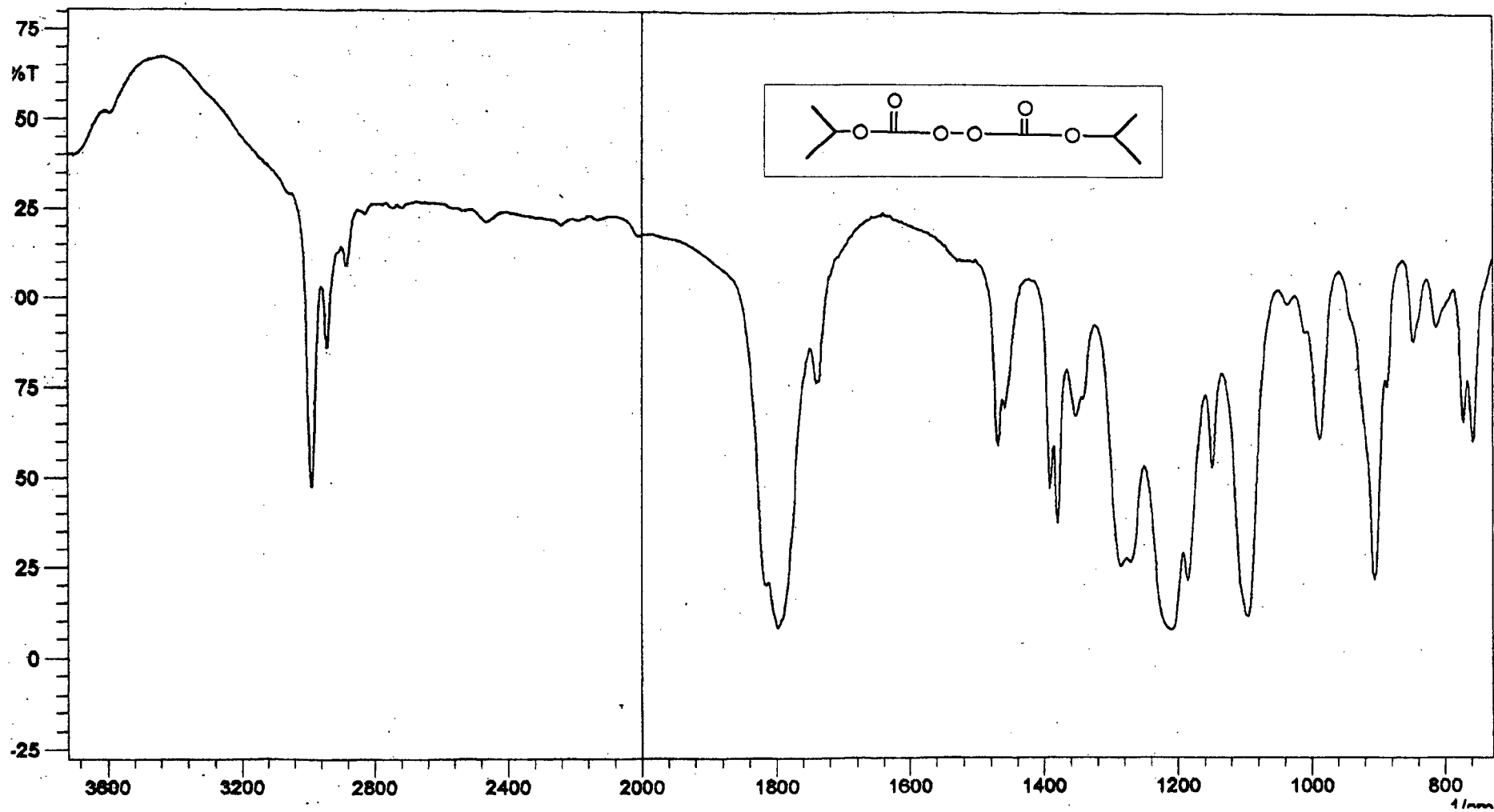


Fig. 2.21 IR spectrum of isopropyl peroxydicarbonate

Chapter 3

Results and Discussion

3.1 Our Approach towards development of Plastic materials for SSNTD.

In our endeavor towards developing materials for SSNTD, we defined a strategy, which would be followed uniformly for all the materials we desired to prepare and is outlined as follows.

1) Design and synthesis of monomers.

Since our approach was to have thermoset materials with different radiation sensitive groups, we first defined the type of monomers that we wanted to prepare. All the monomers prepared had to be allylic monomers, since a free radical cast polymerization process was to be followed. After defining the monomer, synthetic strategies were developed to prepare the monomers. The first monomer that we planned to study was ADC, for which the synthesis process was indigenously developed¹³². After studying the PADC material successfully, we decided to design some new monomers and the chronological development is as follows:

a) N-Allyloxycarbonyloxydiethanolaminebis- (allyl carbonate) (NADAC): This monomer was designed for two reasons 1) To have two different types of radiation sensitive groups *i.e.* carbonate and carbamate. 2) To have more crosslinking in the polymer matrix, since this is a hexafunctional monomer. The monomer was synthesized from diethanolamine and allyl chloroformate in a one step process as described in Sec. 2.2.2.

b) Allyl bis-(2-nitroxy-ethyl) carbamate (ABNEC): This monomer was designed in order to have thermoset materials containing the nitrate ester group. Nitrocellulose, a thermoplastic material containing nitrate ester groups was the first material used for SSNTD, so we decided to have nitrate ester linkages in a thermoset polymer and study its track detection properties. The mono-

mer was synthesized by a two step process from diethanolamine, as described in Sec. 2.2.3. This is the first thermoset poly(nitro-carbamate) material which is evaluated as a track detector.

c) Tris-(2,4-dioxa-3-oxohept-6-en-1-yl)nitromethane (TDONM):

After studying ABNEC polymer we observed that, nitrate ester (-ONO₂) linkages were susceptible for degradation. ABNEC being a bifunctional monomer it was not possible to prepare a homopolymer using the free radical polymerization process. So we decided to study the nitro group (-C-NO₂) and hence prepared a hexafunctional monomer containing a nitro group. The monomer was synthesized from nitro methane as described in Sec. 2.2.4. This also happens to be a novel thermoset poly(nitro-carbonate) material which is evaluated as a track detector.

2) Cast Polymerization of Monomers.

Since most of the polymers were allylic monomers like ADC, the constant rate polymerization cycle was developed using Dial *et.al.* kinetic model to prepare polymers. In the case of copolymers kinetic studies were performed for a mixture containing 50:50 wt. proportions of the monomers. The monomers were then cast polymerized by using indigenously prepared mold.

3) Testing of polymers for SSNTD.

The materials prepared were then tested for nuclear track detection. Small pieces of films were cut and exposed to ²³⁹Pu and ²⁵⁶Cf sources. The materials were then etched using the optimum etching conditions used for PADC. i.e. 6 N NaOH, 70 °C, to decide whether newly developed polymers develop the tracks or not.

4) Kinetic Studies for monomer polymerization.

Kinetic studies for polymerization were then carried out for monomers whose homo or copolymers were able to detect both alpha

and fission fragments.

5) Optimization of Etching conditions.

Etching conditions for the materials (detecting both alpha and fission fragment particles) were optimized by following the bulk etch rates, the time required for development of tracks and the post-etch surface properties.

6) Study of various track detection related parameters like Sensitivity, Alpha track detection efficiency etc.

Various parameters that would define important properties of the track detectors were studied. The most successful allylic thermoset material that has been tested as SSNTD has been prepared from ADC monomer. The literature pertaining to polymerization of ADC monomer indicates certain facts which were taken as guidelines in our efforts towards indigenous preparation of allylic polymers. The intricacies involved in the polymerization of ADC monomer, in particular, can be highlighted as follows:

- 1) It is well known that the quality/purity of the monomer plays a very crucial role in ensuring better quality films and would also affect the etching process.
- 2) The polymerization of ADC monomer is accompanied by 13-14% shrinkage of the monomer volume, as it turns into a solid polymer. If there is no uniform pressure applied to the mold used, it leads to the cracking of the films and unevenness in the thickness of the films, which would seriously affect the etching parameters like its bulk etch rate (V_b) and post etch surface which ultimately decides the track development properties of the material.
- 3) The process of allylic polymerization is exothermic in nature and failure in the proper dissipation of heat, during polymerization would further enhance the cracking in the films and also lead to

bad surface characteristics.

- 4) The presence of air/oxygen would result in poor optical clarity, as well as yellowing of the films. Also the material used in mold preparation would play a very crucial role in the quality of the films.

Considering the above facts, it was decided to study the monomers which we synthesized with respect to the following aspects.

- 1) Purity of the monomer.
- 2) Designing the mold, the choice for the material to be used and the polymerization bath.
- 3) Use of initiators like peroxydicarbonates that allows polymerization at low temperatures, apart from commercially available benzoyl peroxide.
- 4) Development of constant rate polymerization cycle for the respective monomer and initiator system to control the dissipation of heat evolved as suggested by Dial *et.al.*⁸³.

3.2. Cast polymerization of monomers.

1) Design and Materials for Mold preparation.

The choice of the materials and the design of the mold used in the polymerization would particularly decide the surface characteristics and in general the quality of the films obtained. The most important prerequisite for the materials to be used is that, it has to be inert towards the monomer and initiator, and also be thermally stable at which the polymerization bath is to be operated. Also, the polymer film should not adhere strongly to the mold surface. In the literature it has been found that highly polished glass has been used¹⁰⁴. Commercially available float glass pieces of the size 7.5 cm x 7.5 cm were taken. The thickness across their surface was found to have a variation of 1.35 %. Teflon was chosen as a material for

gasket due to its well known thermal properties and inertness. Thus a gasket, of outer sides 7.5 cm x 7.5 cm and width 1.25 cm, coated with thin layer of commercially available pressure sensitive adhesive on both the sides was sandwiched between two float glass plates. The mold assembly was then covered on the sides with paraffin film followed by a masking tape so that the glass plates would remain steady.

2) Cast polymerization.

The mold assembly described above, was then sandwiched between two flat aluminium plates of thickness about 3 - 4 mm and the mold was tightened on all four corners with the help of wing-nuts and bolts. In order to avoid cracking of the glass plates, thick neoprene rubber strips were kept in between the aluminium plates on all the sides of the glass mold taking into consideration the thickness of the glass mold assembly. The monomer was injected into the vertically held mold, with the aid of a syringe, through previously prepared tiny window into the Teflon gasket. This helped in avoiding trapping of air bubbles in the monomer film. The molds were then placed in a specially designed polymerization bath and heated as per predetermined heating profile. After cooling for a sufficiently long time, the mold assembly was removed from the polymerization bath. The following observations were made:-

- 1) The films were found to be uneven in nature and cracks were observed.
- 2) The films had some contour like impressions on its surface.

This is attributed mainly to the uneven surface of commercially available float glass. Taking into consideration the above observations, highly polished optical glass plates having a thickness variation of 0.5 % were used, instead of the ordinary float glass plates.

It was observed that the films obtained were more or less uniform with a thickness variation of 0.7 %. Since the inner surface of each glass plate used in the mold was highly polished, it helped to improve the surface of polymer films as contours like features were not observed. Hence a similar polymerization experiment was carried out using Schott brand optical glass plates, wherein a polymer film of size 6.5 cm x 6.5 cm could be obtained. The following observations were made i) The thickness of these glass plates were found to be perfectly uniform across its surface with a variation of 0.5 %. Thus, in all further experiments of polymerization the Schott brand optical glass plates were used. ii) The problem of cracking of the films could be completely solved by designing a proper assembly to hold the glass plate that would evenly pressurize the surface of the mold. Thus, uniform mechanical pressure could be applied with help of this assembly, resulting in crack free films. The glass mold was directly kept between two flat aluminium plates, of uniform thickness. With these modifications in the design of the molds and the assembly for holding we could achieve films, crack free and of uniform thickness. When the mold was prepared using the above mentioned materials *i.e.*, Schott glass plates, Teflon gasket, pressure sensitive adhesive, it was observed that thickness of the film prepared, varied as the thickness of the Teflon gasket and thickness (amount) of the pressure sensitive adhesive applied to it. It was observed that the amount of the pressure sensitive adhesive applied, causes an increase in the film thickness by 100-150 microns.

3.2.1 Purification of the monomer.

As seen in the literature, the monomer used in the casting of films, needs to be pure so that the surface properties of the films are

not affected by these impurities. Thus, the monomer was first degassed by keeping under vacuum (0.05 mbar) and subsequently dried over molecular sieves and finally distilled using vacuum. The monomer was then passed through a sintered column (in order to remove suspended matter and dust etc.,) and later on kept under nitrogen atmosphere to remove any air present in the monomer. The monomer, was also checked for its purity by Gas Chromatography and were found to be 96 % pure.

3.2.2 Selection of initiator for polymerization.

The commercially used initiators for the polymerization of ADC monomer are the peroxydicarbonates e.g. isopropyl peroxydicarbonate or cyclohexylperoxydicarbonate and peroxides like benzoyl peroxide. The peroxydicarbonates are preferred, owing to their lower decomposition temperature, which allows the initiation of polymerization at lower temperature. But at the same time, these initiators cannot be purified before use due to their unstable nature. Benzoyl peroxide on the other hand can be purified very easily. Commercial benzoyl peroxide is available in the moistened form which can be conveniently crystallized from methanol-chloroform mixture (3:1 parts v/v). It is also known that films prepared with benzoyl peroxide as initiator, will have higher crosslink's in the polymer matrix, whereas those cured with isopropyl peroxydicarbonate does not lead to maximum crosslinking as the polymerization stops due to the vitrification of the network⁸⁰. The degree of polymerization as expressed by the glass transition temperature (T_g) increases with the temperature of the polymerization bath and the decomposition temperature of the initiator⁹⁸. In this regard benzoyl peroxide is advantageous over peroxydicarbonate type initiators. Hence, it was worth investigating the process of polymerization of ADC monomer using both IPP and BP initiators.

3.2.3 Development of a constant rate polymerization cycle.

It is well known that PADC shows a depth dependant bulk etch rate and also a stronger angular dependence of the response. These defects have been attributed to the non-uniform polymerization that takes place during the polymerization process. Allylic polymerization is exothermic in nature and is known for shrinkage of the monomer volume by about 14 %. These two factors synergistically lead to the cracking of the film. In order to circumvent this problem, Dial *et.al.*,⁸³ studied the polymerization of ADC using IPP initiator and found that the rate of the monomer conversion to that of the initiator decomposition is of first order. Dial *et.al.*, derived a kinetic model with the help of which, special heating temperature - time cycles can be constructed. These time cycles would lead to constant rate of polymerization, giving rise to controlled heat evolution, thus preventing the sudden rise in temperature, due to exothermic nature of allylic polymerizations. The kinetic model derived by Dial *et al.*, involves the following set of equations (see next page).

Where Z_1, Z_3 are the Arrhenius constants; E_1 and E_3 are the corresponding activation energies; C_0 and M_0 are the initial concentrations of initiator and monomer respectively; K_1 is the slope, K_3 is the rate of reaction and K_4 is the rate of polymerization. Dial *et.al.*, have successfully calculated these constants (hence forth referred as Dial's constants) for ADC using IPP initiator and assuming that the constants would hold good, a number of authors have used these values for constructing the heating cycles for the CHPC initiator^{85,86}.

$$K_4 = Z_3 e^{-E_3/RT} (M_0 - K_4 t) \sqrt{C_0 - \frac{K_4 t}{Z_1 e^{-E_3/RT}}} \quad (3.1)$$

$$E_1 = \frac{T_1 T_2}{T_1 - T_2} \text{Log}_e \frac{K_1}{K'_1} \quad (3.2)$$

$$K_1 = Z_1 e^{-E_1/RT} \quad (3.3)$$

$$K_3 = -\frac{1}{t} \left[\frac{1}{\sqrt{C_0 - \frac{M_0}{K_1}}} \log_e \frac{\sqrt{C_0 - \frac{M_0}{K_1} + \frac{M}{K_1}} - \sqrt{C_0 - \frac{M_0}{K_1}}}{\sqrt{C_0 - \frac{M_0}{K_1} + \frac{M}{K_1}} + \sqrt{C_0 - \frac{M_0}{K_1}}} - \frac{1}{\sqrt{C_0 - \frac{M_0}{K_1}}} \log_e \frac{\sqrt{C_0} - \sqrt{C_0 - \frac{M_0}{K_1}}}{\sqrt{C_0} + \sqrt{C_0 - \frac{M_0}{K_1}}} \right] \quad (3.4)$$

$$E_3 = \frac{T_1 T_2}{T_1 - T_2} \text{Log}_e \frac{K_3}{K'_3} \quad (3.5)$$

$$K_3 = Z_3 e^{-E_3/RT} \quad (3.6)$$

The decomposition temperatures of CHPC and IPP are 65 and 45 °C respectively and thus the values of K_1 and K_3 must change even if T_1 and T_2 are constant. Hence using the same constants for CHPC may not lead to proper solutions. Dial *et.al.*, have made a cursory reference to the application of this kinetic model to benzoyl peroxide initiated polymerization, but the necessary constants have not been mentioned. Hence, it was decided to study the rate of polymerization using such different initiators for the ADC monomer and also extend this kinetic model to other newly developed monomers. This mainly involves determination of the concentrations of monomer and initiator at different temperature and time intervals. Dial *et.al.*, employed the iodimetric method, the determination of initiator concentration and density measurement for the monomer concentration. FT-IR and refractometry methods have also been used in the kinetic studies for polymerization of ADC monomer.

In the present study the following methods were used:

- 1) Determination of unsaturation by the Wij's method.
- 2) Determination of initiator concentration by iodimetry.

Before the actual study of kinetics of the polymerization reaction, the gelation time of the monomers with the known initiator concentration was studied at three different sets of temperature.

3.3. Determination of Dials Constants.

In our first efforts in solving the Dial *et. al.*, kinetic model, we decided to use the indigenously prepared ADC monomer and the IPP initiator for our studies and compare it with the available literature

3.3.1 Kinetic studies of ADC monomer using IPP initiator.

Dial *et.al.*, carried out the kinetic studies of ADC monomer with IPP initiator (3.3 %) at three different sets of temperatures *viz.* 40, 50 & 60 °C and derived a constant rate polymerization cycle. We decided to use the same set of conditions for our indigenously prepared ADC monomer and verify these constants as it would also prove the suitability of methodology used for determination of unsaturation and initiator concentration at different time intervals.

ADC monomer containing 3.3 % IPP concentration was taken in test tubes and was heated at different temperatures; the time required for the immobile gel formation from the monomer was recorded. The results are given in Table 3.1. It was observed that the immobile gel formation corresponds to approximately 75 % unsaturation.

Sr. No.	Temperature (°C)	Time (h)	Observation
1	40	8	Mobile gel
2	50	2	Immobile gel
3	60	1	Immobile gel

Table 3.1 Time required for the gelation of ADC monomer at different temperatures using IPP initiator.

Thus, the percentage unsaturation and initiator concentration with respect to time and temperature were followed for the ADC monomer with 3.3 % initiator concentration, as per the procedure outlined in section 2.3. ADC monomer containing 3.3 % of the initiator was taken in different test tubes, which were sealed with silicone film (parafilm). The monomer was flushed with nitrogen gas for about half an hour, prior to addition of initiator. The set of test tubes containing the monomer and initiator were then immersed in a thermostat. Test tubes were removed from the thermostat one after another at different time intervals and the contents were analyzed. The results of this study at three different temperatures are given in Table 3.2 - 3.4.(see page no. 114 & 115) The results are also depicted in Fig.3.1.(page no. 115)

Sr. No.	Time (h)	Peroxide (%)	Unsaturation (%)
1	0.00	3.30	100.00
2	1.00	3.18	96.23
3	2.00	3.11	93.52
4	3.00	3.06	89.56
5	4.00	3.01	86.51
6	5.00	2.95	83.56
7	6.00	2.90	80.15
8	7.00	2.84	77.56
9	8.00	2.80	74.65

Table 3.2 Peroxide and unsaturation contents at different time intervals at 40 °C

Sr. No.	Time (h)	Peroxide (%)	Unsaturation (%)
1	0.00	3.30	100.00
2	0.45	3.15	92.45
3	1.50	2.93	85.46
4	2.25	2.72	76.52
5	3.00	2.57	69.42
6	3.45	2.40	63.05
7	4.30	2.25	55.15
8	5.15	2.12	50.19
9	6.00	2.00	45.10

Table 3.3 Peroxide and unsaturation contents at different time intervals at 50 °C.

Sr. No.	Time (h)	Peroxide (%)	Unsaturation (%)
1	0.00	3.30	100.00
2	0.20	2.80	71.56
3	0.40	2.45	53.48
4	1.00	2.15	47.65
5	1.20	1.85	41.56
6	1.40	1.60	37.12
7	2.00	1.37	32.45
8	2.20	1.20	28.54
9	2.40	1.05	25.50

Table 3.4 Peroxide and unsaturation contents at different time Intervals at 60 °C.

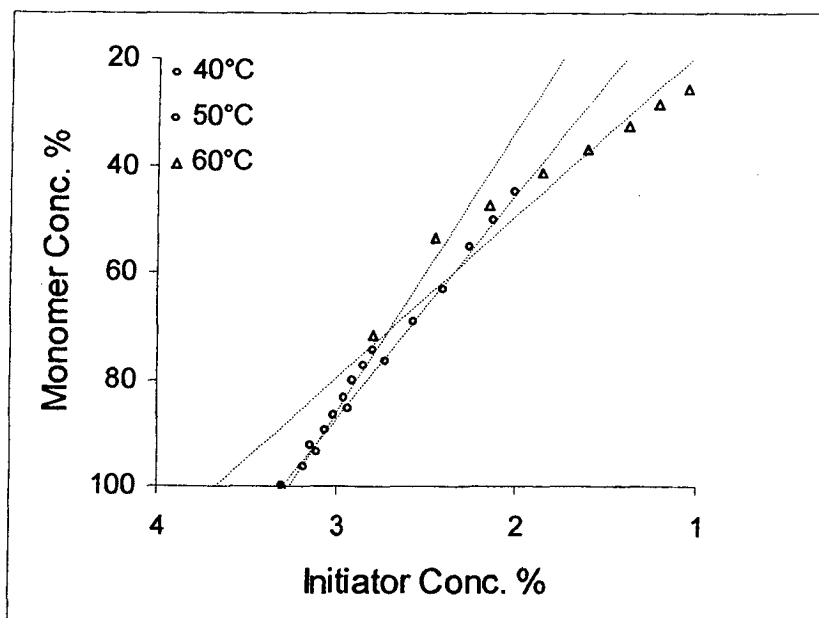


Fig. 3.1 Decomposition of IPP initiator in ADC at 40, 50 & 60 °C.

The slopes (K_1) were found, the values are given below:

K_1	=	52.79	at	40 °C
	=	41.29	at	50 °C
	=	29.85	at	60 °C

The values for Z_1 and E_1 were obtained by solving equation no. 3.3 & 3.2. The values of K_1 were then substituted in equation no. 3.4. It was found that due to some reason error occurred in the calculations, the value of K_3 could not be obtained. After a careful study of the equation it was observed that there exists a limiting value for the slopes of the graphs and this limiting value is constant for a particular initiator concentration used for polymerization. In the equation no. 3.4 proposed by Dial *et.al.*, it was found that the term $vC_0 - m_0 / K_1$ was negative in the case of temperature set 60 °C . Hence, the kinetic study at 60 °C was repeated in order to see if any error occurred during the estimation of the monomer and catalyst concentration. It was found that the same slope value was obtained. This could be attributed to the reason also pointed out by Dial *et al.*, that the catalyst utilization at higher temperature is less efficient and a deviation is observed. So it was decided to study the kinetics of the polymerization reaction at lower temperature in order to avoid this type of a problem. The temperature sets chosen were 35, 45 & 55 °C. Once again the gel formation time studies were carried out. The observations are given in Table 3.5 (see next page). The limiting slope value for this initiator concentration was calculated. The data obtained is given in Table 3.6 - 3.8 (see page no.117 & 118) The results are also depicted in Fig. 3.2 (see page no. 119).

Sr. No.	Temperature (°C)	Time (h)	Observation
1	35	8.0	Mobile gel
2	45	2.5	Immobile gel
3	55	1.5	Immobile gel

Table 3.5 Time required for the gelation of ADC monomer at different temperatures using IPP initiator.

Sr. No.	Time (h)	Peroxide (%)	Unsaturation (%)
1	0.0	3.30	100.00
2	1.0	3.25	97.25
3	2.0	3.21	94.15
4	3.0	3.16	90.78
5	4.0	3.12	86.63
6	5.0	3.07	83.84
7	6.0	3.03	81.02
8	7.0	2.97	80.10
9	8.0	2.95	78.65

Table 3.6. Peroxide and unsaturation contents at different time intervals at 35 °C.

Sr. No.	Time (h)	Peroxide (%)	Unsaturation (%)
1	0.0	3.30	100.00
2	1.0	3.15	93.25
3	2.0	2.93	86.85
4	3.0	2.72	78.14
5	4.0	2.57	70.15
6	5.0	2.42	64.64
7	6.0	2.30	55.15
8	6.5	2.24	50.19
9	7.0	2.20	47.10

Table 3.7 Peroxide and unsaturation contents at different time intervals at 45 °C.

Sr. No.	Time (h)	Peroxide (%)	Unsaturation (%)
1	0.00	3.30	100.00
2	0.45	2.88	73.44
3	1.05	2.60	55.74
4	1.25	2.34	49.25
5	1.45	2.03	43.48
6	2.05	1.90	37.15
7	2.25	1.80	33.28
8	2.45	1.73	28.02
9	3.05	1.70	26.10

Table 3.8 Peroxide and unsaturation contents at different time intervals at 55 °C

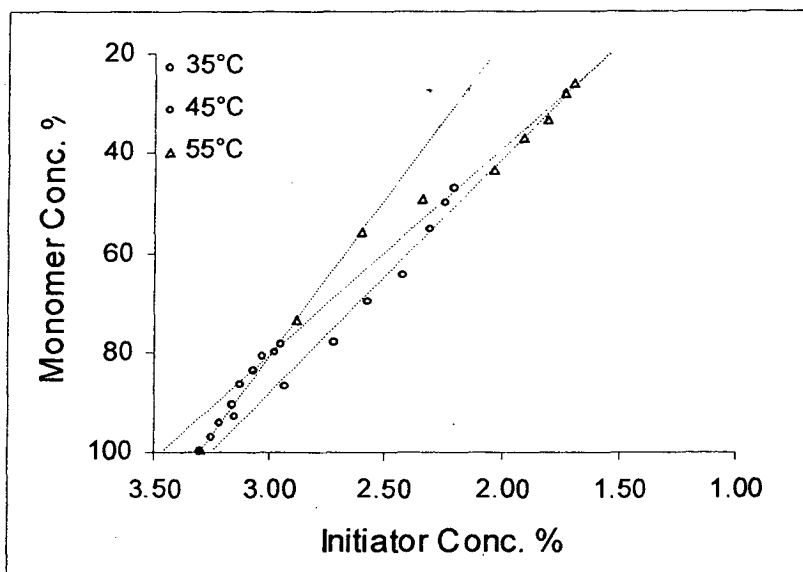


Fig. 3.2. Decomposition of IPP initiator in ADC at 35, 45 & 55 °C

The slopes (K_1) were found, the values are given below:

K_1	= 63.15 at 35 °C
	= 46.85 at 45 °C
	= 41.63 at 55 °C

It can be seen that at these temperatures, the K_1 values are well above the limiting values for the slope. These values were then used to find the constants E_1 , Z_1 , E_3 , and Z_3 , which are given in Table 3.9 (see next page). In order to solve the Dial *et.al.* equations, a Fortran program was used¹³⁸ and a temperature v/s time polymerization cycle was calculated. As pointed out by Dial himself, it was seen at the end of the cycle that the roots of Dials equation became imaginary and thus the program failed to

calculate the values towards the end of the cycle.

Constants Obtained		Constants by Dial <i>et.al.</i>	
E_1	-4202 cal	E_1	-4410 cal
Z_1	0.064	Z_1	0.043
E_3	28147 cal	E_3	29050 cal
Z_3	1.4×10^{18}	Z_3	3.51×10^{18}

Table 3.9. Constants involved in the Dial's equations for ADC polymerization using IPP initiator.

This can be attributed to the fact that at higher temperature the rate of monomer conversion to that of initiator decomposition is no longer a first order phenomenon. In order to complete the time period of the cycle a smooth extrapolation of the graph was done to 90 °C, which is the final decomposition temperature for IPP initiator. The temperature v/s time polymerization profile is shown in Fig. 3.3.

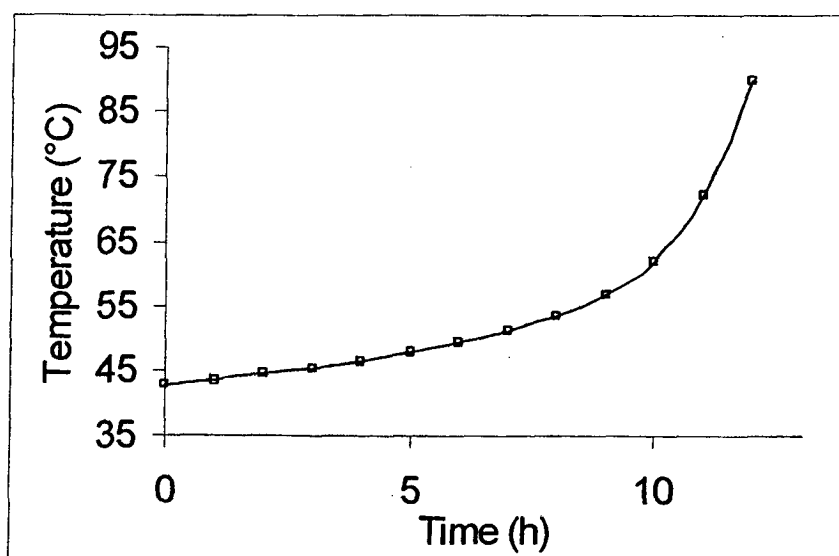


Fig. 3.3. 12 h constant rate polymerization cycle for ADC.

In order to check the effectiveness of the heating time cycle obtained as shown in Fig.3.3, a series of test tubes containing the monomer and initiator were placed in the polymerization bath and the unsaturation content was checked over a period of twelve hours by following the heating profile. The data is represented in Fig.3.4. Since Dial *et al.*, have proposed polymerization at constant rate, a linear correlation is expected between yields of polymer as a function of time. This is supported well by the linear correlation coefficient (R^2) of 0.9978 obtained from calculated yields at a given time interval. The calculated and observed sets of data show a slight variation; this is reflected by the average deviation from expected value of - 0.68. These deviations could be attributed in general, to experimental errors in estimating monomer/initiator concentrations titrimetrically and also the efficiency of the electronic temperature controller used for heating purpose.

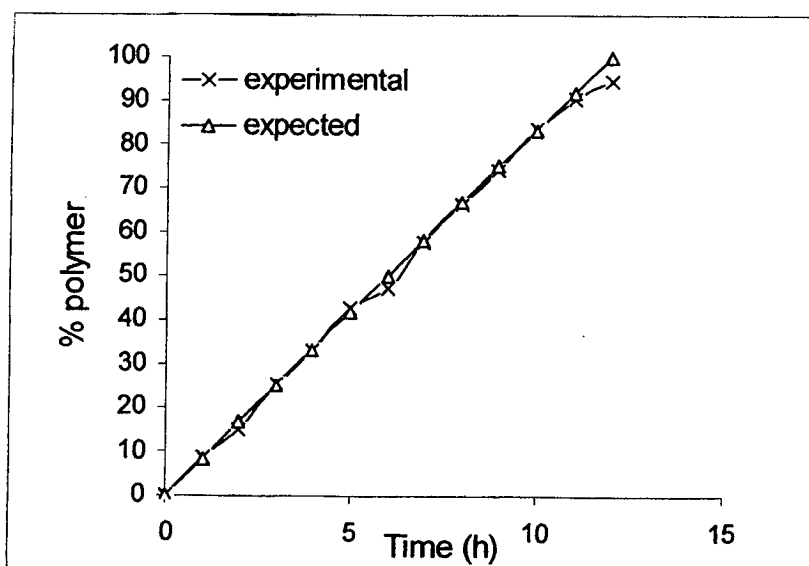


Fig. 3.4 Polymerization of ADC in 12 h time cycle (initiator concentration 3.3 %)

Looking at the success achieved with respect to kinetic studies of ADC, we decided to undertake the kinetic studies pertaining to three novel monomers mentioned previously *i.e.*, NADAC, ABNEC & TDONM by extending the kinetic model proposed by Dial *et.al.*. IPP (and Benzoyl Peroxide in some cases) was chosen as initiator for this purpose. The various combinations of monomer and initiator are as follows:

- 1) ADC with IPP initiator.
- 2) ADC with BP initiator.
- 3) NADAC with IPP initiator.
- 4) NADAC + ADC with IPP initiator.
- 5) ABNEC + ADC with IPP initiator.
- 6) TDONM with IPP initiator.
- 7) TDONM + ADC with IPP initiator.

Kinetic studies were used to decide the suitable temperature v/s polymerization time cycle; these studies were carried out only for such monomers wherein both alpha and fission fragments were obtained. ABNEC monomer did not undergo gelation which appears to be a characteristic of mono allylic compound⁸¹. Hence its kinetic studies could not be carried out. The combination of monomers was studied in varying proportions by its weight ratios.

The gel formation behavior of the different combinations of monomer as mentioned above is presented in Table 3.10. (see next page) The monomer gel formation studies were carried out by using ADC monomer as a reference monomer, since most of the monomers prepared were allylic monomers they were expected to show a similar behavior.

Sr. No.	Monomer/ Monomers	W/W ratio	Initiator Ratio	Temp. °C	Time (h)	Observation			
1	ADC		IPP (3.30%)	35	8.0	Mobile gel			
				45	2.5	Immobile gel			
				55	1.5	Immobile gel			
						BP (3.00%)	55	16.0	Mobile gel
							60	10.0	Mobile gel
							65	6.0	Mobile gel
							70	3.0	Immobile gel
							75	1.5	Immobile gel
80	0.5	Immobile gel							
2	NADAC		IPP (3.00%)	35	8.0	Mobile gel			
				45	2.0	Immobile gel			
				55	1.0	Immobile gel			
3	NADAC+ ADC	50:50	IPP (3.00%)	35	8.0	Mobile gel			
				45	2.0	Immobile gel			
				55	1.0	Immobile gel			
4	ABNEC+ ADC	10:90	IPP (5.0%)	40	9.0	Mobile gel			
				50	3.0	Immobile gel			
				60	1.5	Immobile gel			
5	ABNEC+ ADC	50:50	IPP (8.00 %)	40	8.0	Mobile gel			
				50	2.0	Immobile gel			
				60	1.0	Immobile gel			
6	TDONM		IPP (8.00 %)	35	8.0	Mobile gel			
				45	2.0	Immobile gel			
				55	1.5	Immobile gel			
7	TDONM+ ADC	50:50	IPP (6.0%)	35	8.0	Mobile gel			
				45	2.0	Immobile gel			
				55	1.0	Immobile gel			
			20:80	IPP (6.0%)	35	8.0	Mobile gel		
					45	2.0	Immobile gel		
					55	1.0	Immobile gel		
		10:90 (5.0%)	IPP	35	8.0	Mobile gel			
				45	2.0	Immobile gel			
				55	1.0	Immobile gel			

Table 3.10 Gel formation studies for the monomers.

Using these observations the initiator concentration for the kinetic studies were fixed. The criteria fixed for this purpose was obtaining an immobile gel after about 1h at the minimum possible temperature *i.e.* around 45 – 55 °C.

3.3.2 ADC polymerization using Benzoyl peroxide initiator.

Benzoyl peroxide is known to decompose at around 65 °C. It was observed that the gelation time was relatively higher at 55 °C whereas it was very short at 80 °C. The kinetic studies were decided to be carried out at 60, 70 & 80 °C and with 3.0 % initiator concentration. As in the case of ADC polymerization with IPP initiator the monomer concentration and initiator concentration were monitored using the Wij's method of unsaturation analysis and the iodimetric method of peroxide determination. ADC monomer, containing 3.0 % by wt. of benzoyl peroxide initiator was taken in different test tubes, which were heated at constant temperature and analyzed at three different sets of temperature. Residual unsaturation and initiator concentration were determined at different time intervals. The data is given in Table 3.11 – 3.13 (page no. 125 &126) The results are also depicted in Fig 3. 5. (page no. 126)

Sr. No.	Time (h)	Peroxide (%)	Unsaturation (%)
1	0.00	3.00	100.00
2	0.45	2.94	99.06
3	1.30	2.88	97.12
4	2.15	2.82	94.65
5	3.00	2.76	91.50
6	3.45	2.71	87.05
7	4.30	2.66	84.26
8	5.25	2.61	81.48
9	6.00	2.59	78.57

Table 3.11 Peroxide and unsaturation contents at different time intervals at 60 °C.

Sr. No.	Time (h)	Peroxide (%)	Unsaturation (%)
1	0.00	3.00	100.00
2	0.45	2.89	92.16
3	1.30	2.81	87.12
4	2.15	2.73	82.13
5	3.00	2.62	78.65
6	3.45	2.54	76.42
7	4.30	2.47	73.76
8	5.25	2.36	67.58
9	6.00	2.30	64.54

Table 3.12 Peroxide and unsaturation contents at different time intervals at 70 °C.

Sr. No.	Time (h)	Peroxide (%)	Unsaturation (%)
1	0.00	3.00	100
2	0.30	2.86	87.43
3	1.00	2.19	75.36
4	1.30	2.02	66.31
5	2.00	1.77	59.52
6	2.30	1.50	55.01
7	3.00	1.45	48.02
8	3.30	1.36	42.82
9	4.00	1.29	40.05

Table 3.13 Peroxide and unsaturation contents at different time intervals at 80 °C.

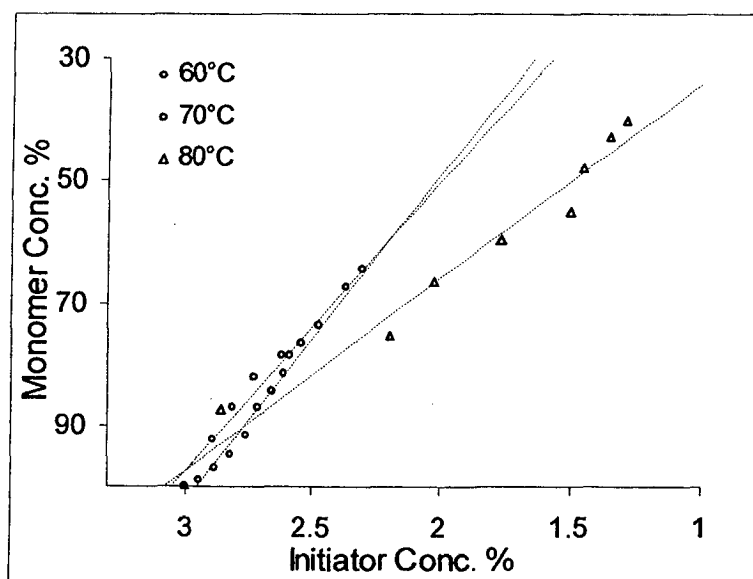


Fig. 3.5. Decomposition of BP initiator in ADC at 60, 70 & 80 °C.

As per the Dial's equations the slopes were found. The values are given below:

K_1	=	53.74 at 60 °C
	=	47.23 at 70 °C
	=	31.63 at 80 °C

It can be seen that K_1 is much above its limiting value of 33.33 at temperature of 60 and 70 °C. However, it is less (31.63) than 33.33 at 80 °C. Hence a new set of kinetic data must be obtained. Since benzoyl peroxide decomposes very slowly at 55 °C, longer time is required for polymerization and it would be futile carrying out the kinetic studies at this temperature. Hence, it was decided that a new set of data should be obtained at 75 °C. This is given in Table 3.14. The kinetic data for the temperature sets 60, 70 & 75 °C are depicted in Fig. 3.6.(see next page)

Sr. No.	Time (h)	Peroxide (%)	Unsaturation (%)
1	0.00	3.00	100.00
2	0.45	2.80	86.96
3	1.30	2.62	80.13
4	2.15	2.48	73.52
5	3.00	2.20	66.03
6	3.45	1.95	58.84
7	4.30	1.84	55.31
8	5.25	1.67	48.49
9	6.00	1.56	45.14

Table 3.14 Peroxide and unsaturation contents at different time intervals at 75 °C.

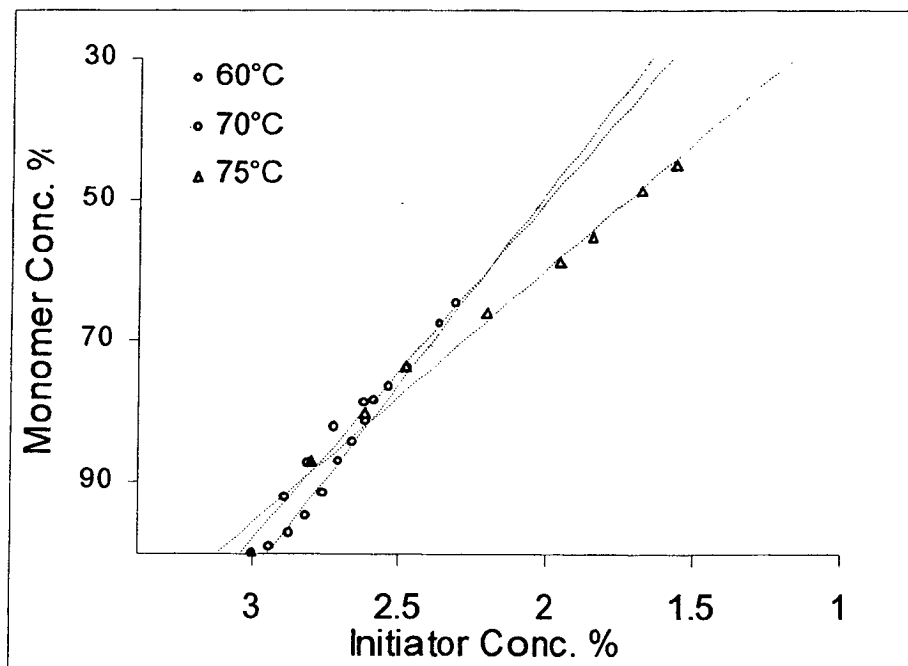


Fig. 3.6 Decomposition of BP initiator in ADC at 60, 70 & 75 °C.

As per the Dial's equations the slopes were found and the values are given below:

K1	=	53.74 at 60 °C
	=	47.23 at 70 °C
	=	35.45 at 75 °C

These values were then used to find the constants E_1 , Z_1 , E_3 , and Z_3 , which are given in Table 3.15.

Constants	
E_1	= - 5565 cal
Z_1	= 0.0098
E_3	= 29594 cal
Z_3	= 5.1×10^{17}

Table 3.15 Constants for deriving polymerization cycle for ADC monomer using BP initiator.

A constant rate of polymerization cycle was obtained for a period of 12 h. Similarly different time cycles can be obtained by changing the value of K_4 which is time dependant. Fig. 3.7 gives one such typical cycle.

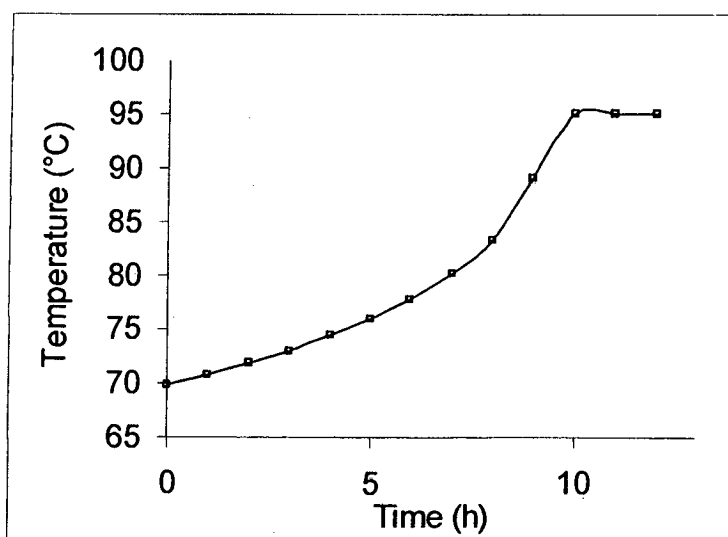


Fig 3.7 A 12 h, constant rate polymerisation cycle for ADC polymerisation using BP initiator.

The effectiveness of the heating time cycle obtained as shown in Fig. 3.7 was tested, by placing a series of test tubes containing

the monomer and initiator, were placed in the polymerization bath and the polymer formed was checked over a period of twelve hours. The data is represented in Fig. 3.8. The linear correlation coefficient (R^2) for the yield of polymer as a function of time for ADC monomer with BP initiator are also close to one *i.e.* 0.9876, it can be said that they obey the same kinetic model as proposed by Dial *et. al.* The calculated and observed sets of data show a slight variation, which is reflected by the average deviation from expected value of 0.33.

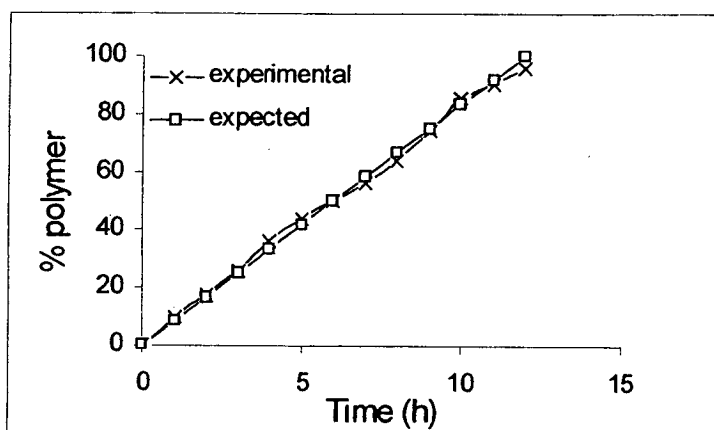


Fig. 3.8 Polymerization of ADC in 12h time cycle (initiator concentration 3.0 %)

3.3.3 Polymerization of NADAC and NADAC+ADC monomer with IPP initiator.

Since the time required for the gelation of the monomer using 3.0 % IPP was same as that observed for ADC monomer, it was decided to study the kinetics of polymerization at 35, 45 & 55 °C. The data obtained for this study at three different set of temperatures are given in Table 3.16-3.18 (see page no. 131 &132).The results are also depicted in Fig. 3.9 & Fig. 3.10 (see page no. 132 & 133).

Sr.No.	Time (h)	Peroxide (%)		Unsaturation (%)	
		I	II	I	II
1	0	3.00	2.80	100.00	100.00
2	1	2.80	2.65	95.25	96.12
3	2	2.74	2.58	90.25	92.15
4	3	2.68	2.50	87.05	88.15
5	4	2.62	2.44	83.25	84.50
6	5	2.56	2.38	81.35	82.15
7	6	2.51	2.32	79.35	80.17
8	7	2.47	2.27	78.02	78.15
9	8	2.41	2.22	77.52	75.19

Table 3.16 Peroxide and unsaturation contents at different time intervals at 35 °C. I & II indicate NADAC and NADAC-ADC.

Sr.No.	Time (h)	Peroxide (%)		Unsaturation (%)	
		I	II	I	II
1	0	3.00	2.80	100.00	100.00
2	1	2.61	2.64	91.92	92.67
3	2	2.41	2.50	85.21	89.52
4	3	2.20	2.35	80.12	85.34
5	4	2.05	2.22	74.95	81.67
6	5	1.91	2.15	69.87	79.05
7	6	1.85	2.05	63.12	75.35
8	7	1.79	1.96	58.14	69.52
9	8	1.74	1.93	51.02	60.05

Table 3.17 Peroxide and unsaturation contents at different time intervals at 45 °C. I & II indicate NADAC and NADAC ADC.

Sr. No.	Time (h)		Peroxide (%)		Unsaturation (%)	
	I	II	I	II	I	II
1	0.00	0.00	3.00	2.80	100.00	100.00
2	1.00	0.50	2.60	2.60	85.15	87.95
3	2.00	1.00	2.20	2.25	73.25	80.44
4	3.00	1.50	1.83	2.05	65.02	74.11
5	4.00	1.75	1.70	1.89	57.50	69.15
6	5.00	2.00	1.54	1.75	51.32	64.18
7	6.00	2.25	1.40	1.67	47.25	59.24
8	7.00	2.50	1.28	1.63	42.10	55.42
9	8.00	2.75	1.24	1.60	35.96	50.15

Table 3.18 Peroxide and unsaturation contents at different time intervals at 55 °C. I & II indicate NADAC and NADAC-ADC.

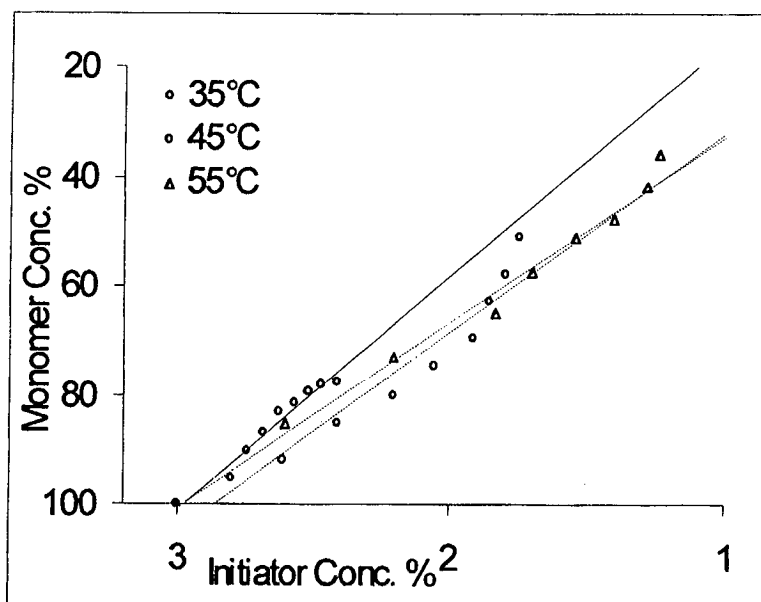


Fig 3.9 Decomposition of IPP initiator in NADAC at 35, 45 & 55°C

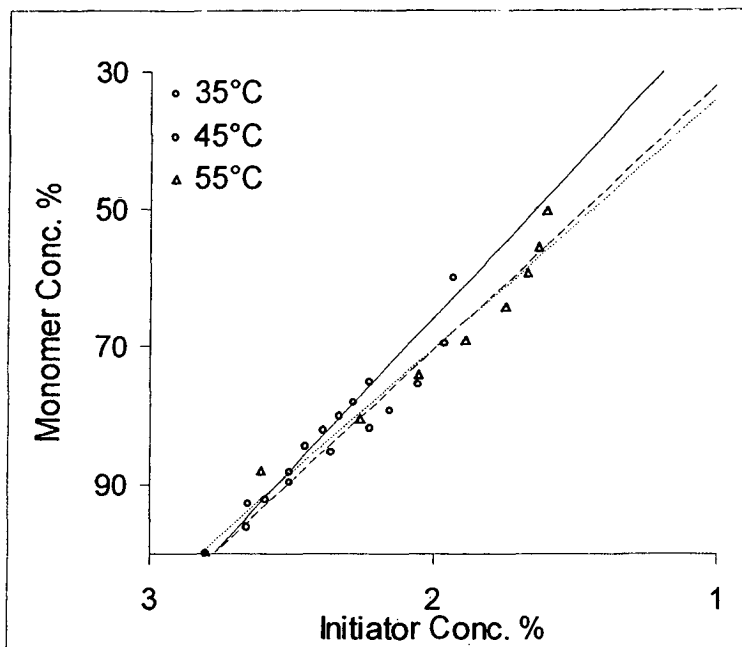


Fig. 3.10 Decomposition of IPP initiator in NADAC-ADC at 35, 45 & 55°C

As per the Dial's equations the slopes (K_1) were found the values are given in Table 3.19

Temperature	K_1	
	NADAC	NADAC-ADC
35°C	42.59	44.28
45°C	36.19	38.28
55°C	34.00	36.22

Table 3.19 Slopes obtained for polymerization of NADAC and NADAC-ADC (50:50) monomers.

It can be seen that, at these temperatures the K_1 values are well above the limiting values *i.e.* 33.33 for the slope. These values were then used to find the constants E_1 , Z_1 , E_3 , and Z_3 , which are given in Table 3.20.

Constants	NADAC	NADAC-ADC
E_1	-2254 cal	-2011.1 cal
Z_1	1.01	1.00
E_3	18711 cal	16896 cal
Z_3	5.2×10^{11}	2.3×10^{10}

Table 3.20 Constants for deriving polymerization cycle for NADAC and NADAC-ADC (50:50) monomer using IPP initiator.

The constants obtained were then substituted in the equation (3.1) to get the desired heating time cycle for polymerization. It is to be noted that the equation could give the solution upto 8 h, a smooth extrapolation of the graph was done upto 90 °C. Fig. 3.11 (see next page) gives the polymerization time cycle for NADAC and NADAC+ADC mixture. In order to check the effectiveness of the heating time cycle obtained as shown in Fig. 3.11, a series of test tubes containing the monomer and initiator were placed in the polymerization bath and the unsaturation content was checked over a period of twelve hours. The data obtained is shown in Fig. 3.12. (see next page)

From the data given in Fig. 3.12, it can be seen that there are some deviations in the values of the polymer formed with respect to time, in relation to that of the theoretically calculated ones. These deviations can be attributed to the experimental errors in estimating the monomer and initiator concentration by titrimetric method of analysis. There is also a limitation upon the electronic temperature controller which has been used in heating the polymerization bath. The linear correlation coefficient (R^2) for the given in Fig. 3.12 & 3.13 the unsaturation removed with respect to

time was found, the values for homopolymer was found to be 0.9899 which is well within the acceptable limits (see Fig. 3.13 next page). This indicates that the scheme proposed by Dial *et.al.*, for the ADC monomer can be extended to hexafunctional allylic monomers.

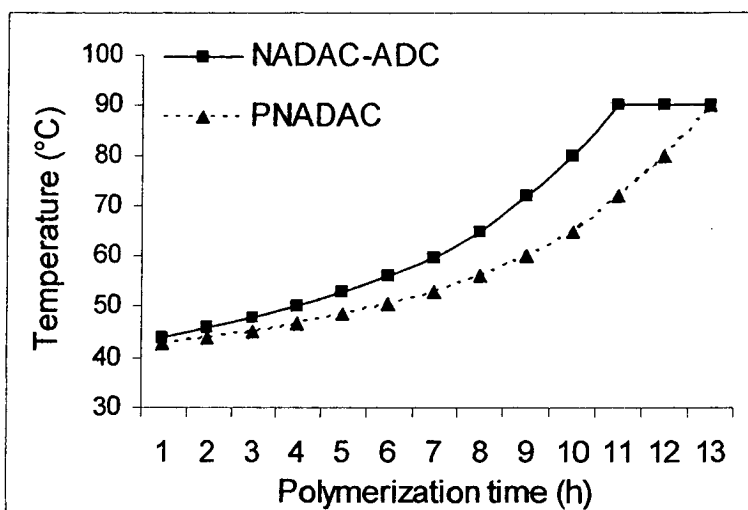


Fig. 3.11 12 h time constant rate polymerization cycle for NADAC and NADAC-ADC (50:50) using IPP initiator.

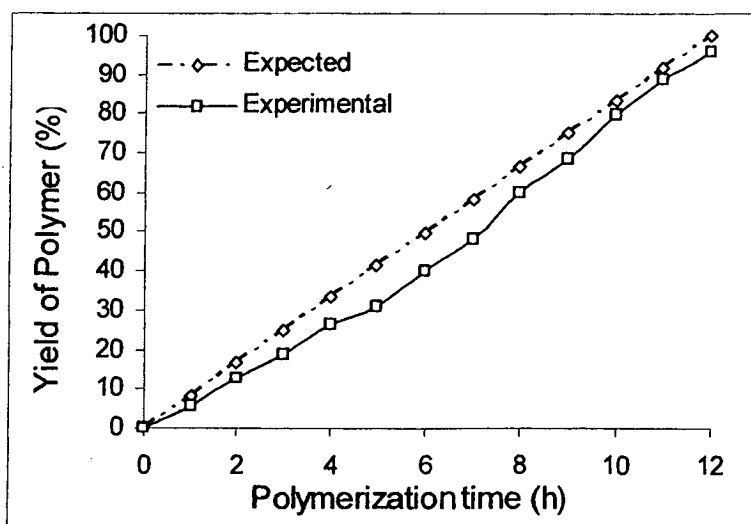


Fig. 3.12 Polymerization of NADAC in 12h time cycle (initiator concentration 3.0 %)

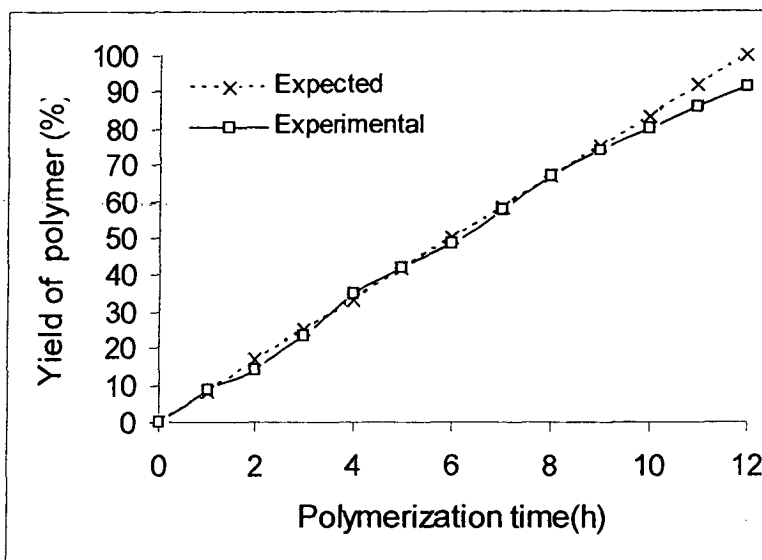


Fig. 3.13 Polymerization of NADAC-ADC in 12h time cycle (initiator concentration 2.8 %)

Since the linear correlation coefficient (R^2) for the yield of polymer as a function of time is close to one (0.9953), it can be said that it obeys the same kinetic model as proposed by Dial *et al.* The calculated and observed sets of data show a slight variation however, which is reflected by the average deviation from expected value -5.71. These deviations could be attributed in general, as mentioned previously to experimental errors in estimating monomer / initiator concentration titrimetrically and also the electronic temperature controller used for heating purpose. The higher deviation in case of copolymerization compared to homopolymer may be due to the fact in this case the kinetic model by Dial *et al.* is applied to a mixture of two different monomers. Thus it shows that the Dial's kinetic model can also be applied in principle, to a mixture of tetra and hexa functional monomers.

3.3.4 Polymerization of ABNEC monomer with IPP initiator.

ABNEC monomer, unlike other allylic monomers discussed so far, is mono allylic and hence is bifunctional. It is well known that it is very difficult to get solid polymer compositions from mono allyl compounds by the process of cast polymerization. Hence we expected a very different polymerization behavior in case of ABNEC monomer, compared with allylic monomers of higher functionality. We studied the gel formation times with varying initiator concentration, at a constant temperature of 60 °C. It is clear from our studies with ADC and NADAC monomer that the gelation time at 60 °C with IPP initiator (~3.0 % w/w) should be around 1-2 h. The observations of gel formation time studies for ABNEC monomer at 60 °C are given in Table 3.21.

Sr. No.	Initiator Conc. (%)	Time	Observation
1	3.0	8h	No gelation
2	5.0	8h	No gelation
3	8.0	8h	No gelation
4	15.0	8h	No gelation

Table 3.21 Gel formation studies of ABNEC monomer at different initiator (IPP) concentrations.

From these studies it is quiet clear that, it would be difficult to get solid homopolymer from ABNEC by heating with IPP (3.0 – 15.0 %) initiator. It was then decided to study the effect of benzoyl peroxide initiator (3.0 - 15.0 %) at varying temperature (60 – 80 °C) and initiator concentration. It was observed that there was no formation

of solid polymer. At higher temperature *i.e.* 70 and 80 °C, there was a change of coloration of the monomer, which indicated some decomposition of the monomer. The Thermal gravimetric studies were also carried out for ABNEC monomer, for which the monomer was heated in static air, from ambient to 150 °C, it was observed that after reaching a temperature of 60 °C there was a gradual loss in mass of the sample. Since the above studies showed that, it would not be possible to prepare solid polymers of ABNEC monomer by heating with IPP and BP initiators, it was decided to study the copolymerization of ABNEC with ADC monomer.

3.3.5 Copolymerization of ABNEC-ADC (50:50 and 10:90 w/w) monomer with IPP initiator.

ABNEC-ADC (50:50 and 10:90 w/w) monomer mixture was heated at various initiator concentrations at 60 °C to test the gel formation time. The observations are given in Table 3.22.

Sr. No.	Initiator conc. (%)		Time (h)		Observation
	I	II	I	II	
1	3.0	3.0	4.0	2.5	Mobile gel
2	5.0	4.0	2.0	1.5	Immobile gel
3	8.0	5.0	1.0	1.0	Immobile gel

Table 3.22 Time required for the gelation of mixture of ABNEC-ADC at different initiator (IPP) concentrations and constant temperature 60 °C. I & II indicate 50:50 and 10 :90 composition.

As can be seen from the observations in Table 3.22, an initiator concentration of 8.0 & 5.0 % would give satisfactory results in studying the kinetics of the ABNEC-ADC monomer mixtures. In order to ascertain whether the same sets of temperature as used for ADC could also be used the mixture of monomers were heated at 35, 45 and 55°C. The results are given in Table 3.23.

Sr. No.	Temp. (°C)	Time (h)	Observation
1	35	12	Mobile gel
2	45	4	Immobile gel
3	55	2	Immobile gel

Table 3.23. Time required for the gelation of mixture of ABNEC-ADC Monomers (50:50 and 10:90 composition) at different temperatures and constant initiator concentration of 8.0% (50:50) and 5.0 % (90:10).

It may be observed from the data given in Table 3.23, the time required for gelation was higher, hence it was decided to study the kinetics at 40, 50 & 60 °C, and the observations are given in Table 3.24-3.26 (see page no. 140 & 141) the results are also depicted in Fig. 3.14 & Fig 3.15 (page no. 141 & 142).

Sr. No.	Time (h)		Peroxide (%)		Unsaturation (%)	
	I	II	I	II	I	II
1	0.00	0.00	8.00	5.00	100.00	100.00
2	1.25	1.00	7.82	4.94	96.54	95.23
3	2.50	2.00	7.65	4.88	92.15	91.45
4	3.45	3.00	7.51	4.81	87.46	87.54
5	5.00	4.00	7.32	4.75	83.15	83.59
6	6.25	5.00	7.18	4.68	80.14	79.52
7	7.50	6.00	7.09	4.61	77.65	76.52
8	8.45	7.00	6.95	4.57	73.95	73.14
9	10.00	8.00	6.80	4.50	70.20	70.50

Table 3.24 Peroxide and unsaturation contents at different time intervals at 40 °C. I & II indicate ABNEC-ADC (50:50) and ABNEC-ADC (10:90)

Sr. No.	Time (h)	Peroxide (%)		Unsaturation (%)	
		I	II	I	II
1	0.00	8.00	5.00	100.00	100.00
2	1.00	7.82	4.83	92.15	92.54
3	2.00	6.82	4.65	85.16	84.56
4	3.00	6.59	4.50	77.35	76.24
5	4.00	5.96	4.33	68.59	67.15
6	5.00	5.59	4.16	64.51	60.35
7	6.00	5.40	4.01	60.30	55.63
8	7.00	5.31	3.87	56.25	49.86
9	8.00	5.20	3.75	53.20	44.56

Table 3.25 Peroxide and unsaturation contents at different time intervals at 50 °C. I & II indicate ABNEC-ADC(50:50) and ABNEC-ADC (10:90).

Sr. No.	Time (h)	Peroxide (%)		Unsaturation (%)	
		I	II	I	II
1	0.00	8.00	5.00	100.00	100.00
2	0.50	6.72	4.75	74.25	81.56
3	1.00	5.73	4.52	64.74	72.56
4	1.50	5.20	4.29	59.21	61.25
5	2.00	4.40	4.08	51.12	52.96
6	2.50	3.90	3.83	45.65	40.25
7	3.00	3.45	3.61	40.25	30.98
8	3.50	3.20	3.37	35.45	24.58
9	4.00	3.10	3.15	29.60	19.90

Table 3.26. Peroxide and unsaturation contents at different time intervals at 60 °C. I & II indicate ABNEC-ADC (50:50) and ABNEC-ADC (10:90)

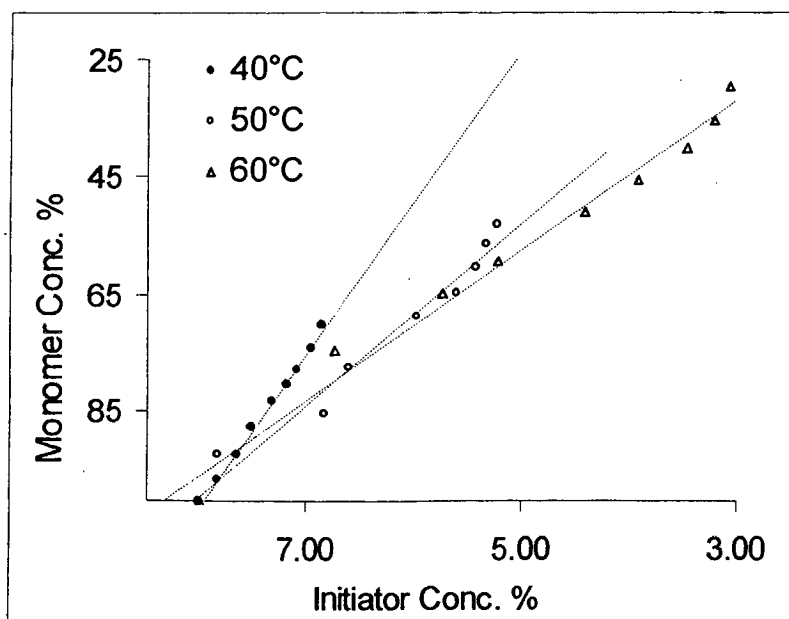


Fig 3.14. Decomposition of IPP catalyst in ABNEC-ADC (50:50) at 40, 50 & 60 °C.

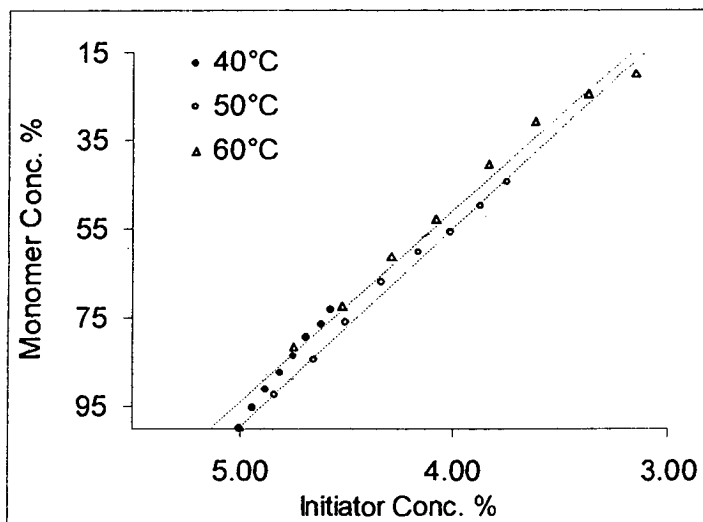


Fig 3.15 Decomposition of IPP catalyst in ABNEC-ADC (10:90) at 40, 50 & 60 °C

K_1 was then calculated for ABNEC:ADC (50:50) & (10:90) and is given below.

Temperature	K_1	
	ABNEC- ADC (50:50)	ABNEC -ADC (10:90)
40°C	25.63	59.98
50°C	15.26	44.66
60°C	12.73	43.13

The above mentioned values of K_1 were then used to find the constants E_1 , Z_1 , E_3 , and Z_3 , which are given in Table 3.27.

Constants	ABNEC- ADC (50:50)	ABNEC -ADC (10:90)
E_1	- 7226 cal	- 3416 cal
Z_1	0.0002	0.23
E_3	20686 cal	15498 cal
Z_3	4.4×10^{12}	1.6×10^9

Table 3.27. Constants for deriving polymerization cycle for ABNEC-ADC (50:50) and ABNEC -ADC (10:90) monomer using IPP initiator.

These constants were then substituted in the equation (3.1) to get the desired heating time cycle for polymerization. It is to be noted that the equation could give the temperature values only up to 8 h. A smooth extrapolation of the graph was done to the final temperature of 90 °C, which is the final decomposition temperature of IPP initiator. (see Fig. 3.16)

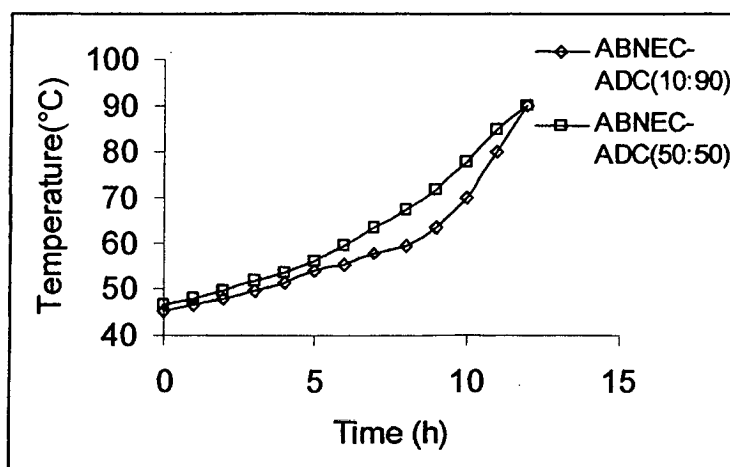


Fig. 3.16 12 h constant rate polymerization cycle for ABNEC-ADC monomer mixture.

In order to check the effectiveness of the heating time cycle obtained as shown in Fig. 3.16 a series of test tubes containing the catalyzed monomer were placed in the polymerization bath and the unsaturation content was checked over a period of twelve hours. The data obtained is shown in Fig. 3.17

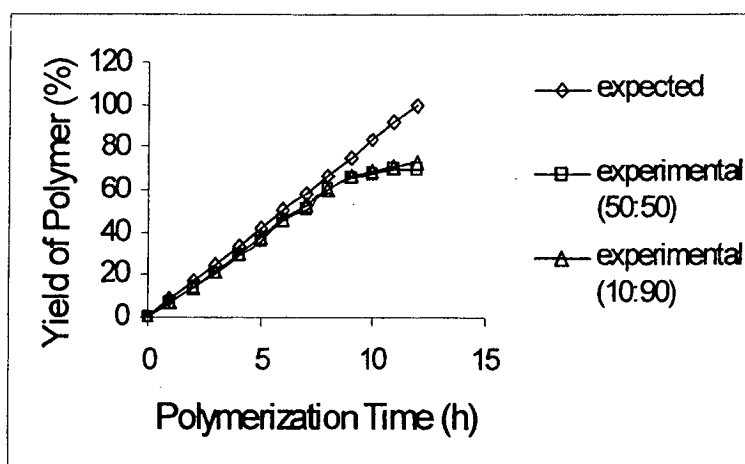


Fig. 3.17 Polymerization of ABNEC-ADC using 12h time cycle

The linear correlation coefficient (R^2) for the yield of polymer as a function of time was found to be 0.9689 and 0.9705 for ABNEC-ADC (50:50) and ABNEC-ADC (10:90) respectively, which is much less than unity. The calculated and observed sets of data show a large degree of variation, which is reflected by the average deviation from expected value - 9.01. These deviations could be attributed in general, to the reasons stated previously in connection with ADC, NADAC etc. The higher deviation in case of ABNEC-ADC mixture of monomers could be due to the interaction between free radicals generated with $-\text{ONO}_2$ groups. It is also possible that $-\text{NO}_2$ group acts as a scavenger for peroxide radicals hence the polymerization slows down. Another reason could be the fact that ABNEC monomer

starts decomposing above 70°C. The kinetic model by Dial *et. al.*, does not properly fit in this case of ABNEC-ADC monomer mixture, especially above 60 °C. However, the polymerization time cycle derived using Dial's kinetic model could be used upto 7 h of polymerization time, since at this time the temperature of the polymerization bath reaches around 65 °C. The polymerization was then continued at a constant temperature of 65 °C over extended period of time. The unsaturation levels were checked and it was found that after about 24 h of heating the process was complete. The modified polymerization temperature -time cycle is shown in Fig. 3.18.

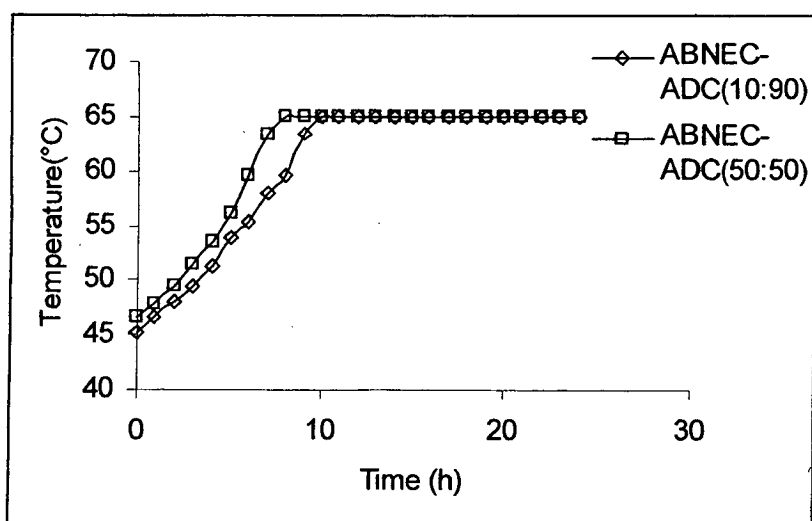


Fig. 3.18 Modified 24 h time constant rate polymerization cycle for ABNEC-ADC monomer mixture.

3.3.6 Polymerization of TDONM and TDONM+ADC monomer with IPP initiator.

The polymerization studies were carried in case of TDONM and TDONM - ADC copolymer (50:50, 10:90 & 20:80 copolymers). The temperature sets chosen in this case were same as in the case of ADC polymerization Kinetic studies, *i.e.* 35, 45, 55 °C. The initiator

concentration chosen for this purpose was 8.0, 5.0 & 6.0 % for TDONM and TDONM - ADC copolymer (50:50, 10:90 & 20:80 copolymer) respectively. The observations are given in Table. 3.10. Since the time required for the gelation of the monomer was same as that observed for ADC monomer, it was decided to study the kinetics of polymerization at 35, 45 & 55 °C. The data obtained for this study at three different temperatures is given in Table 3.28-3.30 (see next page). The data is also shown in Fig. 3.19-3.22 (see Page no. 148 & 149).

Sr. No.	Time (h)	Peroxide (%)				Unsaturation (%)			
		I	II	III	IV	I	II	III	IV
1	0	8.00	6.00	5.00	6.00	100	100	100	100
2	1	7.75	5.80	4.95	5.90	97.25	97.50	96.50	96.20
3	2	7.55	5.65	4.89	5.81	93.50	92.85	93.50	92.50
4	3	7.45	5.50	4.85	5.72	86.23	87.45	90.55	89.50
5	4	7.34	5.40	4.80	5.65	80.25	80.25	87.60	86.45
6	5	7.25	5.32	4.76	5.58	75.26	74.58	83.50	81.45
7	6	7.14	5.22	4.73	5.50	70.23	69.87	80.30	78.45
8	7	7.05	5.14	4.68	5.42	66.25	65.48	78.50	74.65
9	8	7.10	5.10	4.60	5.30	63.30	62.50	75.12	72.56

Table 3.28 Peroxide and unsaturation contents at different time intervals at 35 °C. I, II, III & IV indicate TDONM, TDONM-ADC(50:50), TDONM-ADC(10:90) & TDONM-ADC(20:80).

Sr. No.	Time (h)	Peroxide (%)				Unsaturation (%)			
		I	II	III	IV	I	II	III	IV
1	0.0	8.00	6.00	5.00	6.00	100	100	100	100
2	1.0	7.70	5.75	4.90	5.78	91.25	91.50	95.85	91.56
3	2.0	6.75	5.60	4.85	5.58	84.26	82.56	90.15	86.45
4	3.0	6.60	5.45	4.78	5.40	74.12	73.54	86.95	78.45
5	4.0	6.40	5.25	4.70	5.28	63.25	64.58	81.45	69.85
6	5.0	6.15	5.05	4.62	5.09	54.26	55.23	76.52	62.45
7	6.0	5.98	4.80	4.56	4.90	45.36	48.97	70.24	54.12
8	7.0	5.85	4.55	4.50	4.72	38.25	41.23	65.48	48.45
9	8.0	5.70	4.20	4.20	4.50	31.30	37.30	60.25	42.15

Table 3.29 Peroxide and unsaturation contents at different time intervals at 45 °C. I,II,III &IV indicate TDONM, TDONM-ADC(50:50), TDONM-ADC(10:90) & TDONM-ADC(20:80)

Sr. No.	Time (h)	Peroxide (%)				Unsaturation (%)			
		I	II	III	IV	I	II	III	IV
1	0.0	8.00	6.00	5.00	6.00	100	100	100	100
2	1.0	6.65	5.60	4.80	4.78	80.25	87.50	75.55	75.90
3	2.0	6.10	5.25	4.55	4.51	67.25	78.56	59.90	60.50
4	3.0	5.50	4.90	4.30	4.27	54.98	67.90	48.60	48.55
5	4.0	4.80	4.55	4.12	4.00	45.56	56.45	41.30	40.20
6	5.0	3.90	4.22	3.95	3.74	38.56	47.89	36.30	34.60
7	6.0	3.50	3.98	3.75	3.50	31.25	39.85	33.52	30.54
8	7.0	3.10	3.65	3.60	3.28	25.58	32.56	27.50	26.50
9	8.0	2.95	3.50	3.50	3.10	20.30	24.60	23.65	23.55

Table 3.30 Peroxide and unsaturation contents at different time intervals at 55 °C. I,II,III &IV indicate TDONM, TDONM-ADC(50:50), TDONM-ADC(10:90) & TDONM-ADC(20:80)

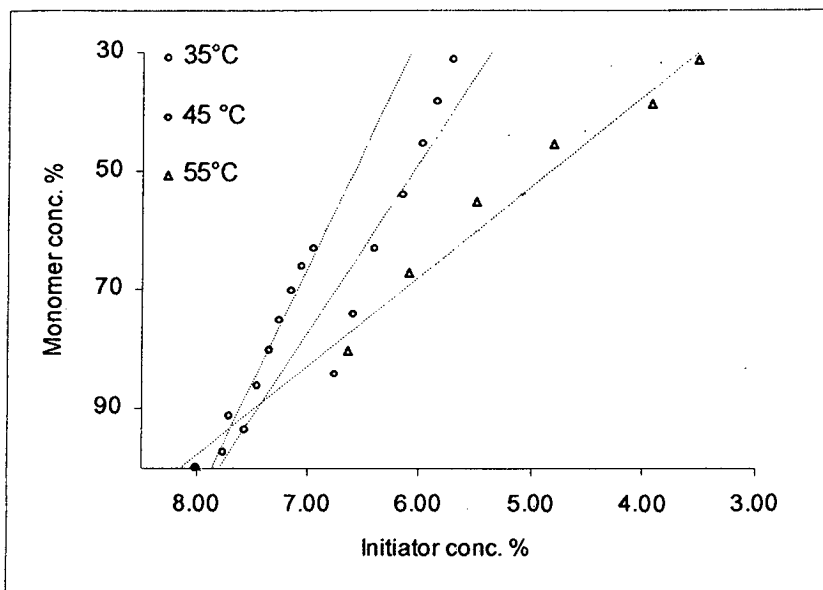


Fig 3.19 Decomposition of IPP initiator in TDONM at 35, 45 & 55 °C

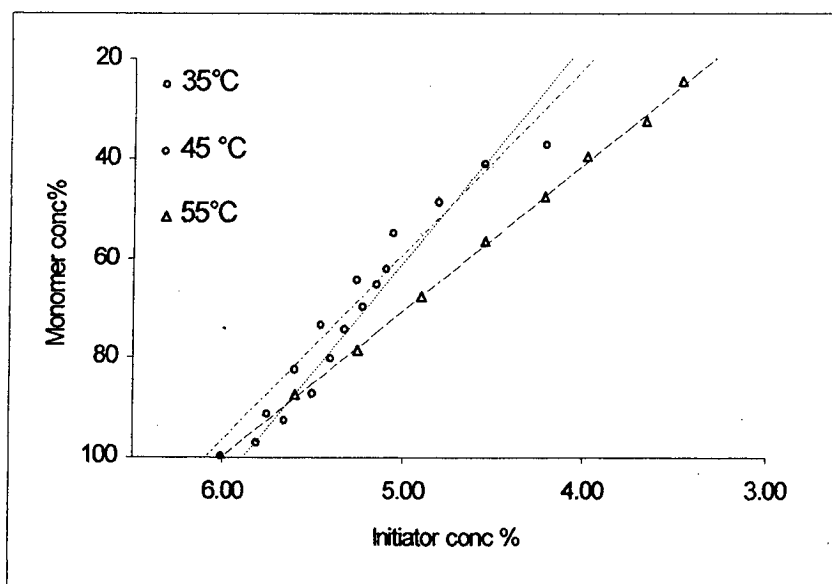


Fig. 3.20. Decomposition of IPP initiator in TDONM-ADC (50:50) at 35, 45 & 55 °C.

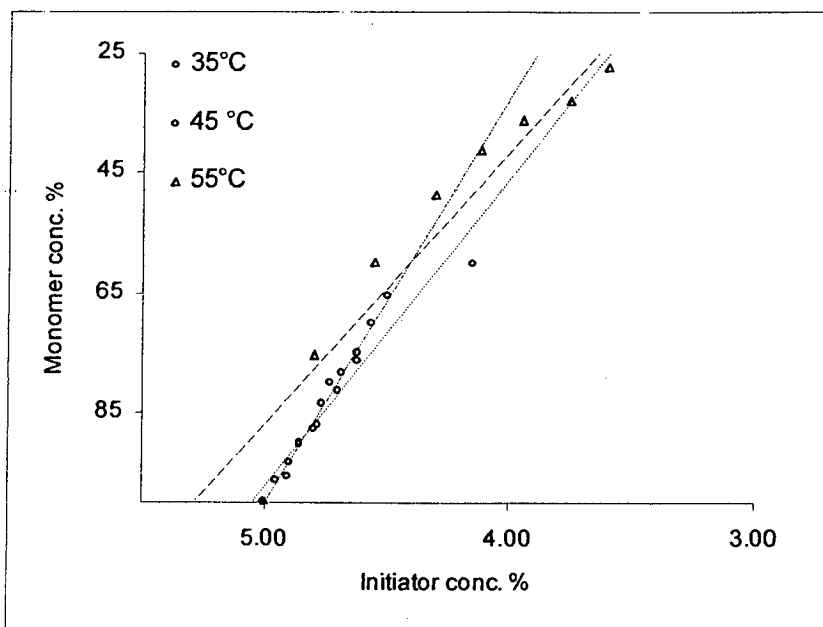


Fig. 3.21 Decomposition of IPP initiator in TDONM-ADC (10:90) at 35, 45 & 55 °C.

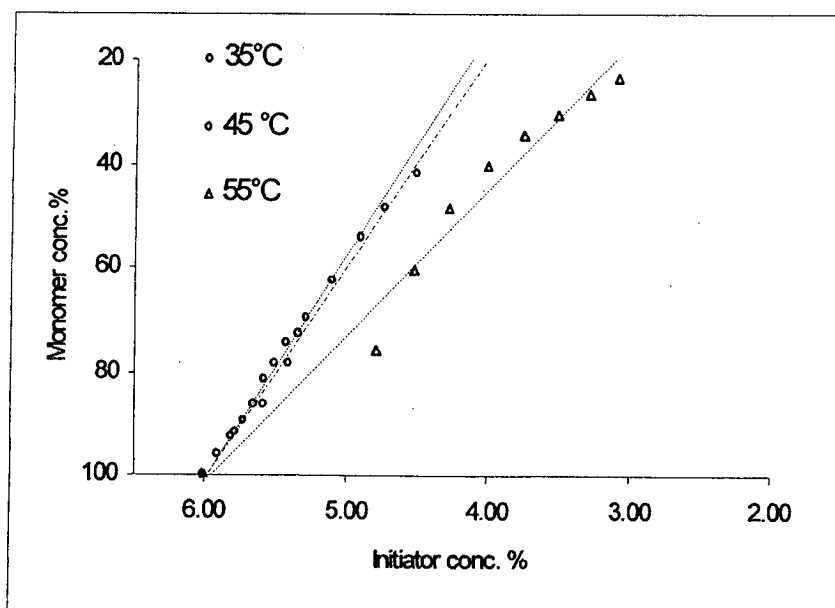


Fig. 3.22 Decomposition of IPP initiator in TDONM-ADC (20:80) at 35, 45 & 55 °C.

As per the Dial's equations the slopes (K_1) were found. The corresponding values are given below:

Temp. °C	TDONM	TDONM-ADC (50:50)	TDONM-ADC (10:90)	TDONM-ADC (20:80)
35	39.24	44.22	67.85	43.02
45	28.64	37.57	51.52	40.51
55	15.04	29.26	45.48	28.04

It can be seen that at these temperatures the K_1 values are well above the limiting values of slope for the respective monomers. These values were then used to find the constants E_1 , Z_1 , E_3 , and Z_3 , which are given in Table 3.31.

Constants	TDONM	TDONM-ADC (50:50)	TDONM-ADC (10:90)	TDONM-ADC (20:80)
E_1	-9513 cal	-4105 cal	-3998.5 cal	-4228 cal
Z_1	0.006	0.0052	0.009	0.0042
E_3	20765 cal	19128 cal	22818 cal	21642 cal
Z_3	4.9×10^{12}	4.1×10^{11}	9.9×10^{13}	2.0×10^{13}

Table 3.31 Constants for deriving polymerization cycle for TDONM, TDONM-ADC (50:50), TDONM-ADC (10:90) & TDONM-ADC (20:80) monomer using IPP initiator.

These constants were then substituted in the equation (3.1) to get the desired heating time cycle for polymerization. It is to be noted that the equation could give the temperature values only upto 8 h, a smooth extrapolation of the graph was done to the final tempera-

ture of 90 °C, which is the final decomposition temperature of IPP.

Likewise, different time cycles can be obtained by changing the value of K_4 i.e. the rate of polymerization which is time dependant. Fig. 3.23 gives one such typical cycle.

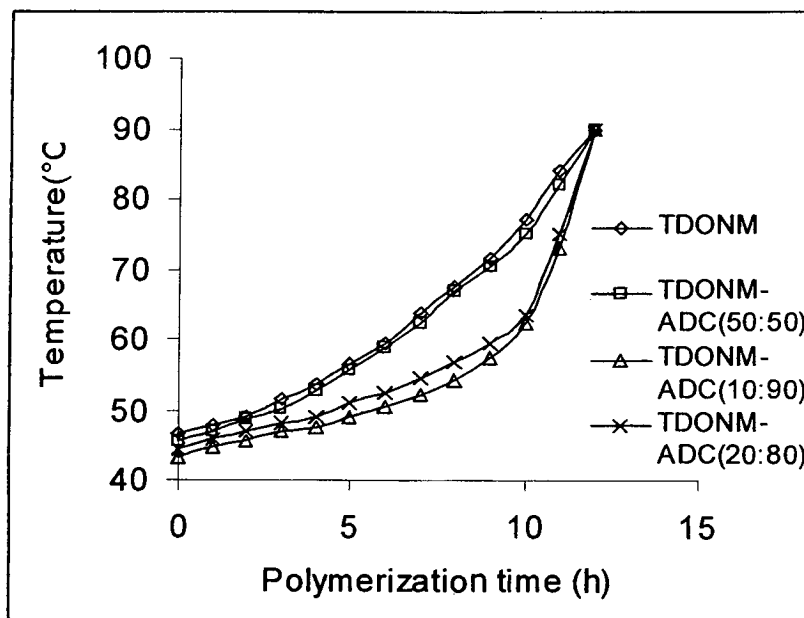


Fig. 3.23 12 h constant rate polymerization cycle for TDONM, TDONM-ADC (50:50), TDONM-ADC (10:90) & TDONM-ADC (20:80)

In order to check the effectiveness of the heating time cycle obtained as shown in Fig. 3.23, a series of test tubes containing the monomer and initiator were placed in the polymerization bath and the unsaturation content was checked over a period of twelve hours. The data obtained is shown in Fig. 3.24 (see next page)

From the data given viz. Fig. 3.24 it can be seen that there are sharp deviations in the expected values of the polymer formed with respect to time, in relation to that of the theoretically calculated ones. These deviations were also observed in case of ABNEC monomer.

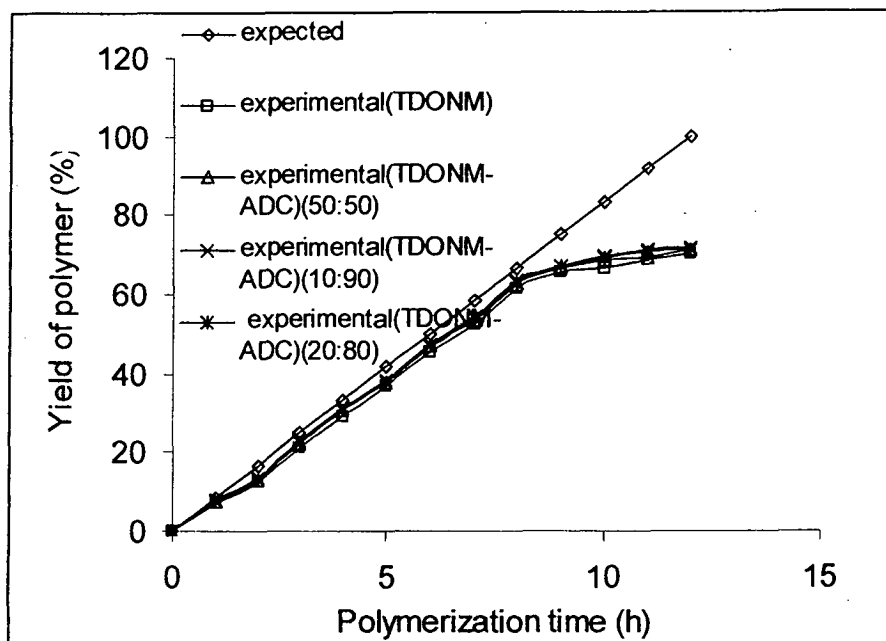


Fig. 3.24 Polymerization of TDONM, TDONM-ADC (50:50), TDONM - ADC (10:90) & TDONM-ADC (20:80) in 12 h time cycle.

The similarity between both the monomers is the presence of nitro groups, so we can say that the process of polymerization is not of first order in case of these monomers due to the possible interaction of the free radicals with the nitro groups and hence the Dial's model cannot be used as such. The linear correlation coefficient (R^2) for the above data *viz.* the unsaturation removed with respect to time was found, the values for homopolymer was found to be 0.9586, for the copolymers TDONM-ADC (50:50), TDONM-ADC (10:90) & TDONM-ADC (20:80) it was 0.9605, 0.9684 & 0.9715 respectively. The calculated and observed sets of data show a large degree of variation, which is reflected by the average deviation from expected value *i.e.* PTDONM, - 10.5; TDONM-ADC (50:50), - 9.8; TDONM-ADC (10:90), - 9.5; TDONM-ADC (20:80), - 9.3; The

polymerization was then continued at a constant temperature of 65 °C over extended period of time. The unsaturation levels were checked and it was found that after around 24 h of polymerization the process was complete. The modified polymerization temperature–time cycle is shown in Fig. 3.25.

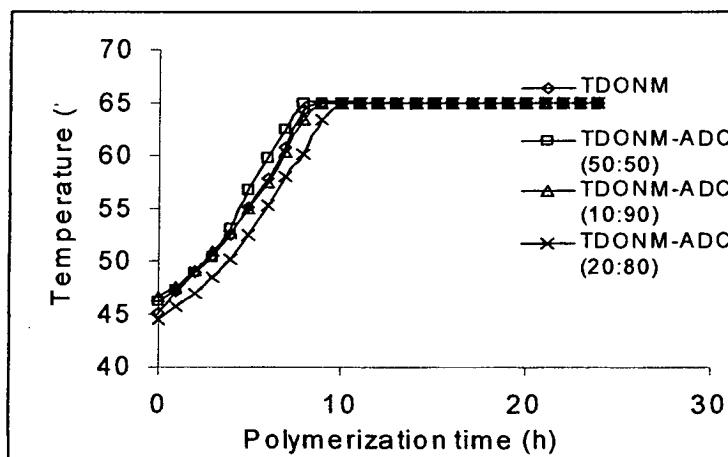


Fig. 3.25 Modified 24 h time constant rate polymerization cycle for TDONM homo and copolymers.

3.4. Preparation of thin films by cast polymerization.

After the development of the constant rate of polymerization cycle, it was decided to prepare thin films, with thickness of about 500 microns. Initially, a 12 h polymerization cycle was chosen. The monomer containing the initiator (% concentration) and DOP (1.0 %, w/w) as plasticizer, were then filled in the glass mold with the help of syringe, taking care that no air bubbles are trapped in the liquid film formed. The polymerization was then carried out as discussed in section 2.1.3. The polymerization cycles that were used in the preparation of homo and copolymers are shown in Fig. 3.26 (see next page)

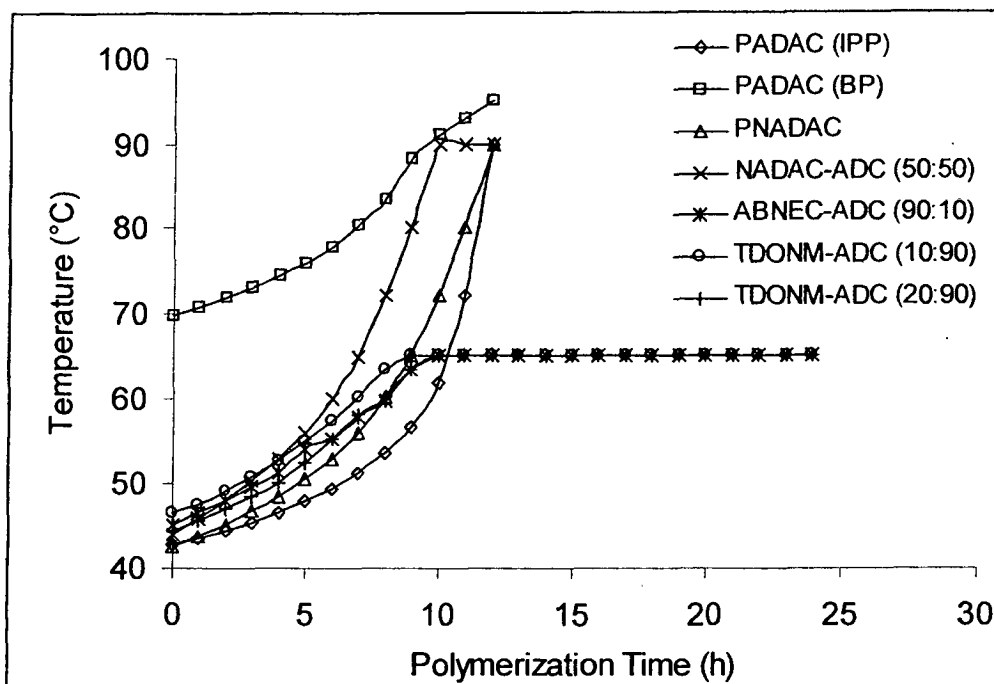


Fig. 3.26 Polymerization time cycles for different monomers

3.5. Studies on the optimum polymerization time cycle.

The polymerization time cycle, definitely has an important role in deciding the extent of cross-linking that would take place. Hence, it is important to study the effect of polymerization time, on the response of the plastic material towards nuclear track detection. The literature available for the preparation of thin films for SSNTD shows the use of 12 h polymerization time cycle in most of the cases. As in the case of ADC polymerization it is very difficult to obtain 100 % polymerized network, because the polymer matrix gets vitrified due to the three dimensional network formation and further conversion of all the double bonds becomes difficult. Hence, it was decided to optimize the polymerization time cycle, by observing the sensitivity of the films as a function of different curing times, but with same initiator concentration. The time cycles used are shown in Fig. 3.27.

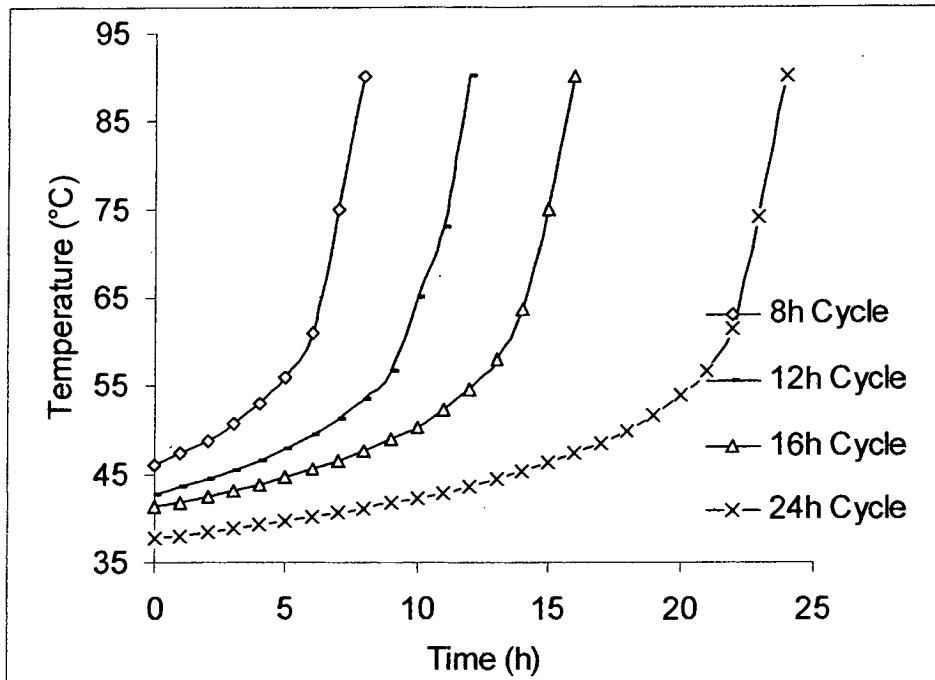


Fig. 3.27. Polymerization time cycles for ADC Polymerization.

The percentage unsaturation present in the films were determined, the results are given in Table 3.32 (see next page). The sensitivity studies were also carried out as outlined in section 2.1.3, the results are shown in Fig. 3.28 (see next page). It can be seen that the sensitivity values for the films cured by 8 h time cycle had very low value. Whereas the sensitivity values increased for films prepared by following the 12 to 24 h cycles. In view of practical limitations, a time of 12 h was chosen, as it would complete the polymerization upto ~ 92 - 95 % and would also result in films with better sensitivity to charge particles.

Polymerization Time (h)	Unsaturation (%)
8	15.0
12	8.5
16	7.5
24	5.5

Table 3.32 Unsaturation data for films cured with different polymerization time cycles.

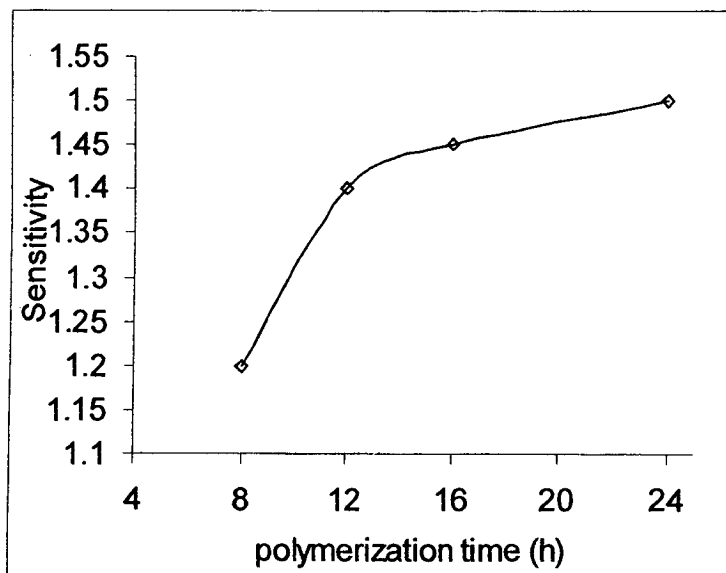


Fig. 3.28 Sensitivity of films cured using different polymerization cycles.

It can also be seen that 8 h polymerization led to a film with more unsaturation in the polymer matrix which is undesirable.

3.6. Testing of indigenously developed Plastic materials for SSNTD.

The newly developed polymer materials were cut into small pieces of 1 cm x 1 cm size and exposed to alpha and fission fragments using ^{252}Cf and ^{239}Pu electrodeposited source. In the case of ^{252}Cf source, the exposure was made in close contact whereas for ^{239}Pu the films were kept in close contact as well as at a distance of 0.5, 1.0, 2.0 & 2.5 cm. The films were then etched at optimum etching conditions reported for PADC track detectors *i.e.*, 70 °C, 6 N NaOH. The films were periodically removed from the etching bath and tested for the development of tracks. The observations are given in Table 3.33.

Material	Track development time (h)	
	F.F	Alphas
PM PADC(500 μ)	1.0	3.0
PM PADC(250 μ)	0.5	3.0
PADC (IPP)	1.0	3.5
PADC (BP)	1.0	3.5
PNADAC	1.0	10.0
NADAC-ADC (50:50)	1.0	8.0
ABNEC-ADC (10:90)	0.5	7.0
ABNEC-ADC (20:80)	0.5	---
ABNEC-ADC (30:70)	0.5	---
ABNEC-ADC (40:60)	0.5	---
ABNEC-ADC (50:50)	0.5	---
PTDONM	1.0	4.0
TDONM-ADC (10:90)	1.0	4.0
TDONM-ADC (20:80)	1.0	4.0
TDONM-ADC (30:70)	1.0	---
TDONM-ADC (40:80)	1.0	---
TDONM-ADC (50:50)	1.0	---

Table 3.33 Track development times in different polymer films

The track development times *i.e.* the time required to develop a given charged particle track that is well distinguished from similarly looking background features in the polymer, were compared with PM PADC films. The following observations were made:

- 1) In case of PM PADC films the alpha particle track development time, was shorter by 30 minutes than that, for the indigenous PADC material. It can also be seen that the fission fragment tracks in case of PM PADC (250 μ) films appear at almost half the time interval than observed in PM PADC (500 μ) and indigenously developed PADC films.
- 2) On etching the films under the optimum conditions known for PADC films, the PNADAC and NADAC-ADC films were also found to detect alpha and fission fragment tracks. However, the time required for the development of the charge particle tracks by chemical etching, were relatively higher compared to PM PADC track detector. Well developed fission fragments were seen in the homo and copolymer films after, 1.5 and 1.0 h of etching time respectively. The alpha particles could be revealed in the homo and copolymer films only after 15 and 10 h of etching time respectively. The bulk etch rates ($\mu\text{m/hr}$) were also found to be less compared to that of PM PADC films. Hence the optimization of etching conditions was necessary for these films.
- 3) All the compositions of the ABNEC-ADC copolymer *i.e.*, 50:50 to 10:90 were studied for charged particle determination and it was found that the copolymer ABNEC-ADC with composition 10:90 was found to detect both alpha particles and fission fragments, whereas the rest could detect only fission fragments. The bulk etch rates were determined under the standard etching conditions of PADC *i.e.*, 70 °C, 6 N NaOH and found to be of the same order as that of PADC (1.87 $\mu\text{m/h}$). The standardization of the etching conditions were

necessary in order to investigate whether the track development time could be reduced further.

4) The PTDONM and TDONM-ADC copolymers were also tested and it was observed that PTDONM was able to detect, low energy alpha particles (approx. 4 Mev and less) whereas in the copolymers, TDONM-ADC, only two compositions viz., 10:20 and 20:80, could develop an autoradiograph of the ^{239}Pu alpha source after exposure in contact. Also the films were able to detect fission fragments. The bulk etch rates determined were found to be much higher (about 3-3.5 $\mu\text{m}/\text{h}$) and the films appeared hazy upon etching. Thus optimization of etching conditions was necessary in order to find milder etching conditions that would give better post etching surface properties.

3.7 Optimization of etching conditions of the Plastic track detectors.

It is well known that the conditions under which the plastic detectors are etched, profoundly affects the response of the plastic materials to the charged particles. The following factors are found to play an important role in the response of the plastic materials⁸:

- 1) The track development in a material is achieved by the realization of the condition $V_t/V_b > 1$, so it is necessary to follow the bulk etch rates as well as the track etch rates.
- 2) The track revelation times are also very important, since one of the practical requirement is the need for rapid analysis of the films.
- 3) One important characteristic of the SSNTD films, which is directly affected by the etching conditions is the sensitivity, which is expressed by the equation 2.5. (see page no. 80)
- 4) The surface characteristics of the films, since the films should be transparent upon etching in order to carry out the analysis under optical microscope.

Though several etchants have been tested for the etching of CR-39 polymer, KOH and NaOH are the most common. Recently, there has been a report on the use of $\text{Ba}(\text{OH})_2 \cdot 8\text{H}_2\text{O}$ ¹²⁴ as an etchant which significantly reduces the time for development of tracks. It has also been established that NaOH and KOH do not show much difference in the etching of PADC¹²⁸. The indigenously prepared PADC films were etched under standard etching conditions of 6 N NaOH, 70 °C. The indigenously prepared PADC track detectors were found to have comparable bulk etch rates and track development times, to that of imported PADC detectors.

In order to optimize the etching conditions for the newly developed polymers, the track development time and the clarity of the films were taken as the main criteria for deciding the optimum etching conditions. The bulk etch rates were also noted. Three pieces, each of size 10 mm x 10 mm, from each of the two batches of all the films were etched, at four different concentrations of the etchant, at different temperature, and the track development time and bulk etch rates were compared with that for PM PADC films under identical etching conditions.

3.7.1 Etching of PNADAC and NADAC-ADC (50:50) track detectors.

In order to optimize the etching conditions, the PNADAC and NADAC-ADC films were etched at different sets of temperature and using different etchant concentrations. The results are represented in table 3.34 & Fig. 3.29 (see next page).

It may be seen from Fig. 3.29 the bulk etch rates of PNADAC and NADAC-ADC differ considerably with that of PM PADC. It is to be noted that a concentration above 6 N does not profoundly affect the bulk etch rate of the materials, this has been pointed out in literature¹³¹.

Sr. No.	Conc. of etchant (N)	PNADAC		NADAC-ADC		PM PADC
		V_b (I) $\mu\text{m/h}$	V_b (II) $\mu\text{m/h}$	V_b (I) $\mu\text{m/h}$	V_b (II) $\mu\text{m/h}$	V_b $\mu\text{m/h}$
1	5	0.28	0.31	0.69	0.69	1.25
2	6	0.51	0.54	1.61	1.68	1.87
3	7	0.58	0.63	1.66	0.75	1.98
4	8	0.56	0.59	1.97	2.05	2.20

Table 3.34 Bulk etch rates of PNADAC and NADAC-ADC (50:50) films at 70 °C. I & II indicate two different batches

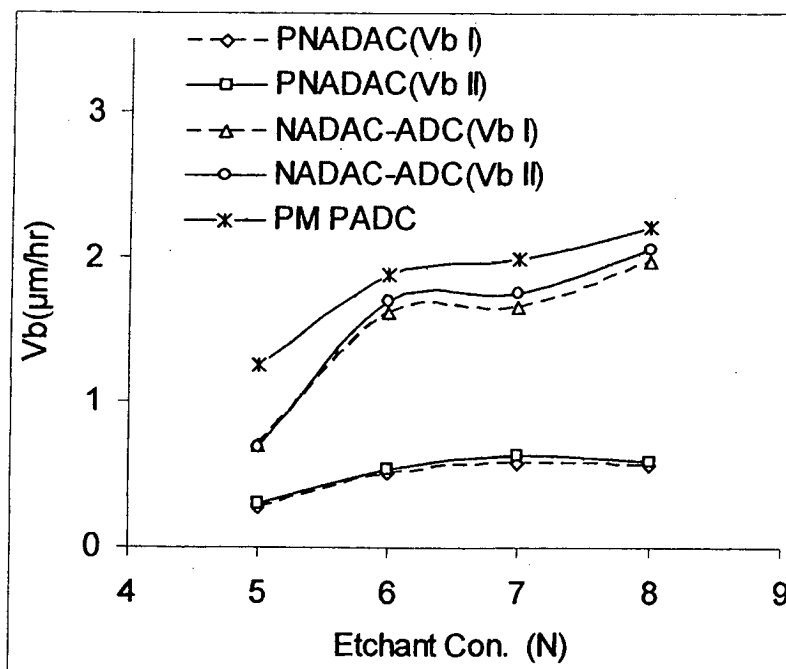


Fig. 3.29. Variation of the bulk etch rate of PNADAC, NADAC-ADC and PM PADC films with 5 – 8 N NaOH at 70 °C. I & II indicate two different batches

In fact, a too high concentration of etchant decreases bulk etch rate because of layer formation of the hydroxide on the surface of the material. So in order to attain a higher bulk etch rate the films were etched at a higher temperature *i.e.* 75 °C. The results are shown in Table 3.35 and Fig. 3.30 (see next page).

Sr. No.	Conc. of Etchant (N)	PNADAC		NADAC-ADC		PM PADC
		V _b (I) µm/h	V _b (II) µm/h	V _b (I) µm/h	V _b (II) µm/h	V _b µm/h
1	5	0.41	0.48	0.81	0.83	1.74
2	6	0.83	0.89	2.00	2.10	2.35
3	7	1.00	1.05	2.37	2.48	2.45
4	8	1.02	1.09	3.00	3.10	2.52

Table 3.35 Bulk etch rates at varying concentration of etchant at constant temperature of 75 °C. I & II indicate two different batches.

It can be seen that the bulk etch rates for NADAC-ADC copolymer films are almost comparable to PM PADC. Also there is an improvement in the bulk etch rate of PNADAC but not comparable with that obtained for standard conditions for PM PADC material. The next set of experiment was conducted at a temperature of 80 °C using the same concentrations of NaOH. The results are shown in Table 3.36 (see page no. 164) and Fig. 3.31(see next page).

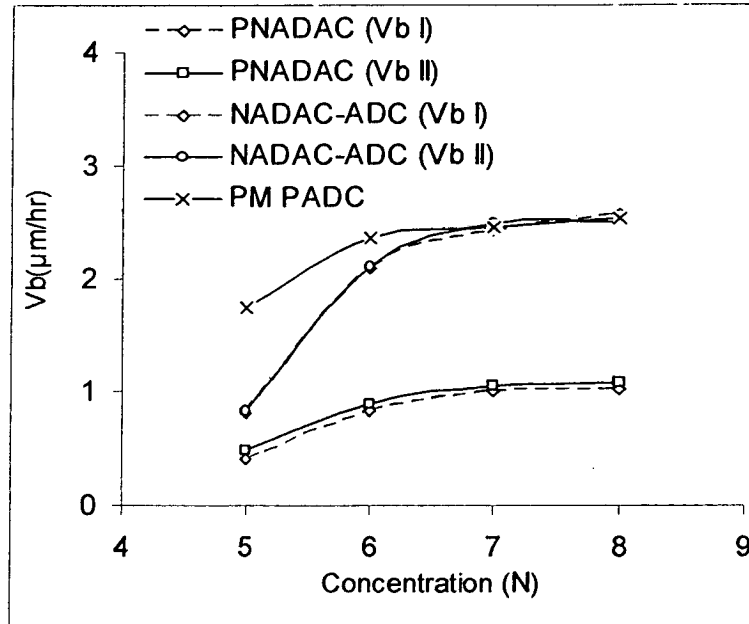


Fig. 3.30 Variation of the bulk etch rate of PNADAC, NADAC-ADC and PM PADC films with 5 – 8 N NaOH at 75 °C. I & II indicate two different batches.

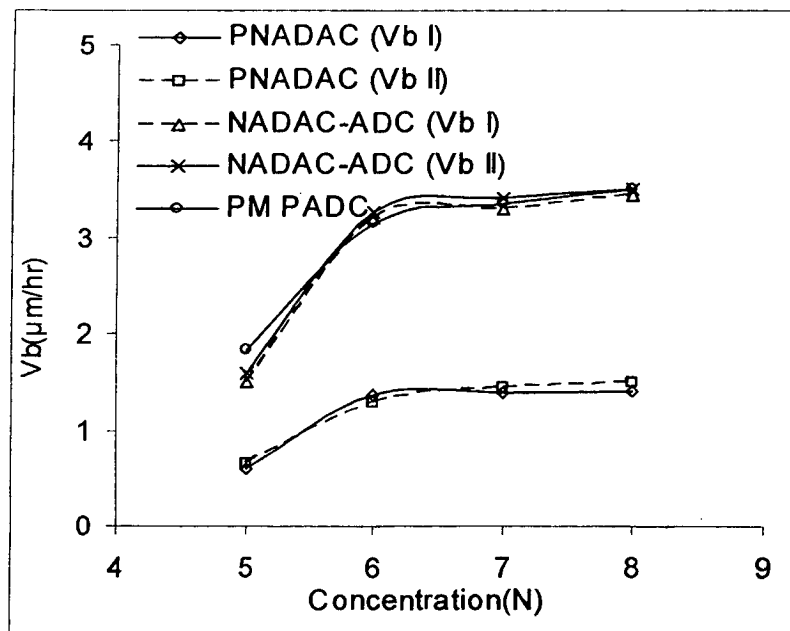


Fig. 3.31. Variation of the bulk etch rate of PNADAC, NADAC-ADC and PM PADC films with 5 – 8 N NaOH at 80 °C. I & II indicate two different batches

Sr. No.	Conc. of etchant (N)	PNADAC		NADAC-ADC		PM PADC
		V_b (I) $\mu\text{m/h}$	V_b (II) $\mu\text{m/h}$	V_b (I) $\mu\text{m/h}$	V_b (II) $\mu\text{m/h}$	V_b $\mu\text{m/h}$
1	5	0.59	0.62	1.50	1.60	1.84
2	6	1.36	1.34	3.12	3.25	3.15
3	7	1.38	1.36	3.30	3.48	3.20
4	8	1.40	1.42	3.80	3.90	3.22

Table 3.36 Bulk etch rates at varying concentration of etchant at constant temperature of 80 °C. I & II indicate two different batches

In case of etching of the PNADAC homopolymer and NADAC-ADC copolymer films (50:50), the bulk etch rates of the PNADAC homopolymer differs considerably, whereas that of copolymer shows a similar trend as compared to PM PADC. The homopolymer films (PNADAC) showed a maximum V_b of 1.4 $\mu\text{m/h}$ at 80 °C, even at the highest temperature used. As pointed out by Amin & Henshaw¹³¹, it was observed that NaOH concentration above a certain value (6.25 N) had no effect on V_b of PNADAC, NADAC-ADC and ADC. The alpha track revelation time studies for the different films were also carried out simultaneously and the results are shown in Table 3.37 (see next page).

The track revelation time indicates that there is not much difference in the time for etching temperature of 75 & 80 °C in the case of NADAC-ADC copolymer films. The NADAC-ADC copolymer films appeared hazy when etched at 80 °C. For PNADAC homopolymer

films a higher temperature was desired i.e. 80 °C.

Thus, the optimum etching conditions for the PNADAC and NADAC-ADC (50:50) materials were chosen as 6 N NaOH, at 80 and 75 °C, respectively.

Conc. of Etchant (N)	Temp. (°C)	Track revelation time (h)		
		PNADAC	NADAC-ADC	PM PADC
5	70	---	14.0	6.0
6		15.0	10.0	3.0
7		15.0	10.0	3.0
8		15.0	10.0	3.0
5	75	17.0	10.0	5.0
6		10.0	6.0	2.5
7		10.0	6.0	2.5
8		10.0	6.0	2.5
5	80	12.0	9.0	5.0
6		8.0	5.5	2.0
7		8.0	5.5	2.0
8		8.0	5.5	2.0

Table 3.37 Track revelation by chemical etching for varying concentration of etchant and temperature for PNADAC, NADAC-ADC and PM PADC.

3.7.2 Etching of ABNEC-ADC track detectors.

The films were etched at 70 °C at different concentrations of NaOH solution and V_b was calculated. The results are shown in Table 3.38 (See next page).

It can be seen that the bulk etch rates compare well with that of PM PADC. The track revelation time (see Table 3.39, next page) was also noted for all the compositions. With 6 N NaOH at 70°C, the track revelation time for the alpha and fission fragments in case of ABNEC-ADC (10:90) copolymer were 7 & 1 h respectively, whereas in all the other polymer compositions the fission fragments time development was within 30 min. In order to minimize the alpha track revelation time, it was decided to etch the films at 75 °C using 6 N NaOH solution. Upon etching at 75 °C it was observed that there was a marked increase in coloration of the films within 4 h of etching time, with no development of alpha tracks. The surface of the films, as observed under the microscope was bad. This may be due to the decomposition of the $-ONO_2$ functional group present in the polymer matrix. So it was decided to use 6 N NaOH, 70 °C as the etching conditions for the ABNEC-ADC copolymer films.

NaOH Conc. (N)	ABNEC-ADC copolymer										PM PADC
	$(V_b) \mu\text{m/h}$										
	(50:50)		(40:60)		(30:70)		(20:80)		(10:90)		
	(I)	(II)	(I)	(II)	(I)	(II)	(I)	(II)	(I)	(II)	
5	1.1	1.1	1.0	1.0	1.0	1.0	0.9	0.9	0.9	0.8	1.2
6	1.6	1.6	1.6	1.6	1.5	1.5	1.4	1.4	1.3	1.4	1.8
7	1.7	1.6	1.6	1.6	1.5	1.6	1.5	1.5	1.4	1.4	1.9
8	1.7	1.7	1.6	1.6	1.6	1.5	1.5	1.5	1.5	1.4	2.2

Table 3.38 Bulk etch rates for different ABNEC-ADC polymer compositions at 70 °C with different concentrations of etchant. I and II indicate batch numbers.

NaOH Conc. (N)	Track revelation time (min)						PM PADC (α)
	ABNEC:ADC						
	(50:50) (f.f)	(40:60) (f.f)	(30:70) (f.f)	(20:80) (f.f)	(10:90) (f.f) (α)	(α)	
5	60	90	90	90	90	720	360
6	20	30	30	45	60	420	180
7	20	30	30	45	60	420	180
8	20	30	30	45	60	420	180

Table 3.39 Alpha and fission fragment track revelation time for different ABNEC-ADC polymer compositions at 70 °C different concentrations of etchant.

3.7.3 Etching of TDONM and TDONM-ADC track detectors.

In the case of TDONM homo and copolymers it can be seen from Table 3.40 (see page no. 169) that the bulk etch rates are much higher compared to that of PM PADC films. Also the films appeared hazy at the optimum etching conditions used for PM PADC films. So it was decided to use mild etching conditions in order to have better post etch surface properties. The films were thus etched at lower temperatures of 60 and 65 °C and using 3-6 N NaOH solution. It can be observed from the data obtained, that the copolymer films had higher bulk etch rates compared to that of PM PADC, but at higher temperature the films turned opaque, so moderate-etching conditions *i.e.*, 4 N NaOH at 60 °C can be considered as the optimum etching conditions for these polymers. The data is shown in Fig. 3.32 -3.34 (see page no. 168 &169).

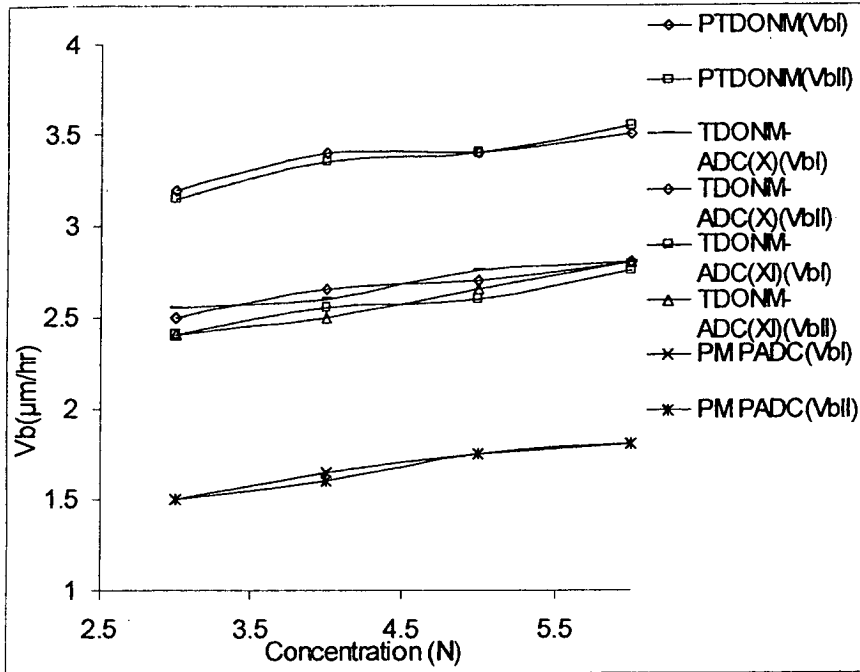


Fig. 3.32 Variation of the bulk etch rates of PTDONM, TDONM-ADC and PM PADC films with 3-6 N NaOH at 70 °C

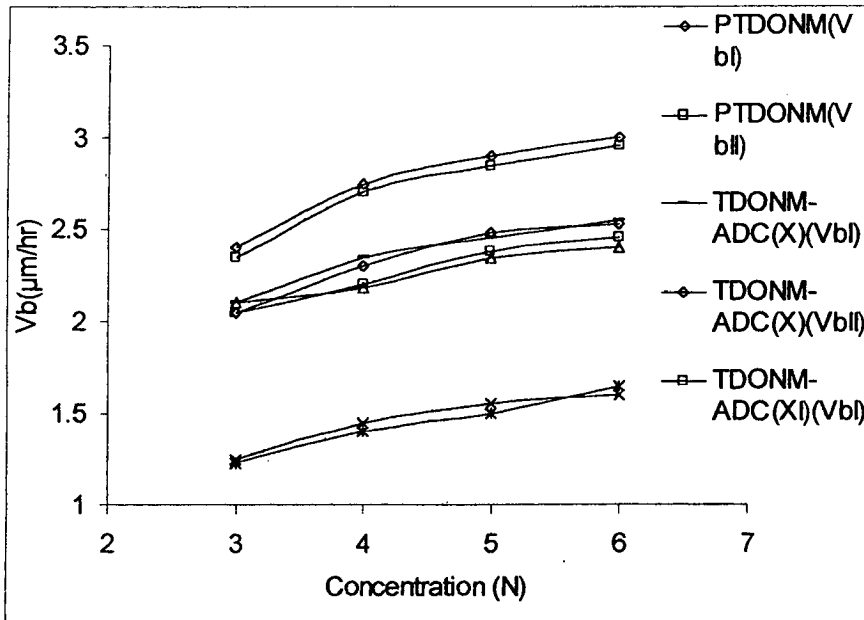


Fig. 3.33 Variation of the bulk etch rates of PTDONM, TDONM-ADC and PM PADC films with 3-6 N NaOH at 65 °C

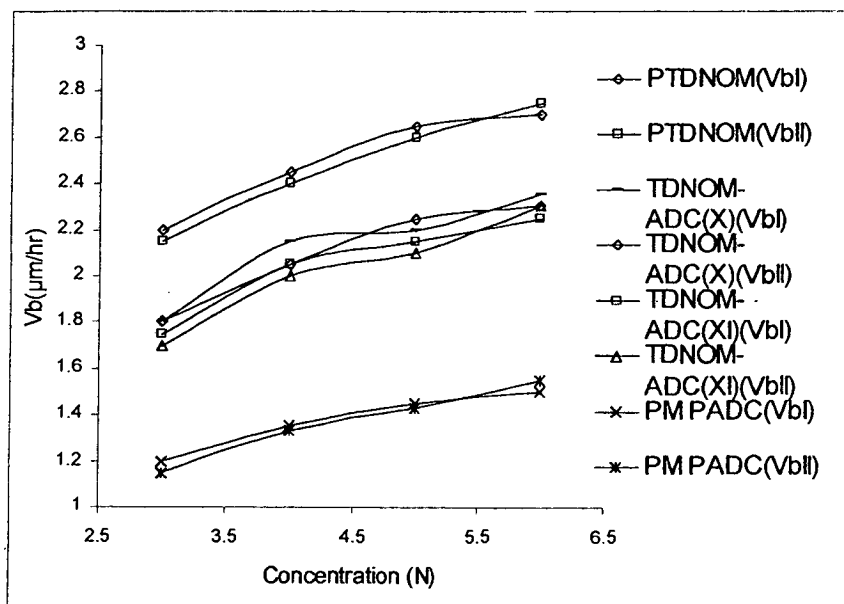


Fig. 3.34 Variation of the bulk etch rates of PTDONM, TDONM-ADC and PM PADC films with 3-6 N NaOH at 60 °C.

Conc. of etchant (N)	Temp. (°C)	Track revelation time (h)				
		PTDONM	PTDONM-ADC		PM PADC	
			(I)	(II)		
3	60	5.0	5.0	5.0	8.0	
4		4.0	4.0	4.0	4.5	
5		4.0	4.0	4.0	4.5	
6		4.0	4.0	4.0	4.5	
3		65	5.0	5.0	5.0	7.0
4			4.0	4.0	4.0	4.0
5	4.0		4.0	4.0	4.0	
6	4.0		4.0	4.0	4.0	
3	70		4.0	4.0	4.0	6.0
4			3.0	3.0	3.0	3.0
5		3.0	3.0	3.0	3.0	
6		3.0	3.0	3.0	3.0	

Table 3.40 Track revelation time by chemical etching for varying concentration of etchant and temperature for PTDONM, PTDONM-ADC and PM PADC films. I and II indicate 10:90 and 20:80 weight proportions of monomers.

3.8. Optimization of initiator concentration and sensitivity studies.

It is well known that the performance of PADC resin as the nuclear track detector depends strongly upon the curing conditions *i.e.*, temperature, concentration of initiator which controls the structure of the matrix *etc.*. Sensitivity depends upon factors, like the uniformity of the polymerization, extent of cross linking, etching conditions, etc. So the optimum initiator concentration can be found as a function of sensitivity of a particular material. Portwood and Stejny determined the concentration of unpolymerized allyl groups by IR spectroscopy of CR-39 which was cured with different concentrations of initiator and related it to the sensitivity of the resin⁹⁰. It was found that the dependence of the bulk etch rate exhibits a minimum, located at the same initiator concentration as the minimum in the amount of unpolymerized allyl groups left in the resin. It was decided to study the sensitivity of the films, with respect to the various concentrations of the initiator used, by etching the plastic materials under its standard etching conditions. In order to find the sensitivity the films were exposed to charged particles as described in Sec 2.1.3.

3.8.1 PADC Plastic Track Detectors.

Two pieces each, of size 1.5 cm x 1.5 cm, cured with IPP and BP initiators were exposed to charged particles in vacuum (0.1 mbar at a distance of 5 cm from ²⁵²Cf source). The films were then chemically etched under its optimum etching conditions *i.e.*, 70 °C, 6 N NaOH. The diameters of fission fragments and alpha tracks were measured at regular intervals and the sensitivity values were calculated using equation no. 2.5. It was observed that upto 2 h of etching time only fission fragments were developed, the average track diameter was found

to be 5 μm . The alpha tracks were seen only after three hours of etching time. The results are given in Table 3.41-3.45.

Sr. No.	Initiator Conc. (% by Wt.)	Etch pit diameter (μm)				Sensitivity (S)	
		D_f		D_α		PADC (IPP)	PADC (BP)
		PADC (IPP)	PADC (BP)	PADC (IPP)	PADC (BP)		
1	1.0	9.0	10.0	1.0	1.0	1.02	1.02
2	2.0	8.0	5.0	1.0	1.0	1.03	1.08
3	3.0	7.0	7.5	1.0	1.0	1.04	1.03
4	4.0	9.0	7.5	1.0	1.0	1.02	1.03
5	5.0	10.0	8.0	1.0	1.0	1.02	1.15
	PM PADC (250 μ)	13.0	---	4.0	---	1.18	----

Table 3.41 Track etch parameters after 3h of chemical etching.

Sr. No.	Initiator Conc. (% by Wt.)	Etch pit diameter (μm)				Sensitivity (S)	
		D_f		D_α		PADC (IPP)	PADC (BP)
		PADC (IPP)	PADC (BP)	PADC (IPP)	PADC (BP)		
1	1.0	12.0	12.5	2.0	2.5	1.05	1.08
2	2.0	11.0	7.5	3.0	2.0	1.16	1.15
3	3.0	10.0	10.0	3.0	2.5	1.19	1.13
4	4.0	12.0	10.0	3.0	2.5	1.13	1.10
5	5.0	13.0	11.0	3.0	2.5	1.11	1.10
	PM PADC (250 μ)	---	16.0	---	5.0	---	1.16

Table 3.42 Track etch parameters after 4h of chemical etching.

Sr. No.	Initiator Conc. (% by Wt.)	Etch pit diameter (μm)				Sensitivity (S)	
		D_f		D_α		PADC (IPP)	PADC (BP)
		PADC (IPP)	PADC (BP)	PADC (IPP)	PADC (BP)		
1	1.0	15.0	15.0	3.0	3.0	1.08	1.08
2	2.0	13.0	10.0	4.0	3.0	1.20	1.19
3	3.0	12.5	12.5	5.0	3.0	1.38	1.12
4	4.0	14.0	12.5	5.0	3.0	1.29	1.12
5	5.0	15.0	14.0	5.0	3.0	1.25	1.09
	PM PADC (250 μ)	18.0	---	6.0	----	1.25	---

Table 3.43 Track etch parameters after 5h of chemical etching

Sr. No.	Initiator Conc. (% by Wt.)	Etch pit diameter (μm)				Sensitivity (S)	
		D_f		D_α		PADC (IPP)	PADC (BP)
		PADC (IPP)	PADC (BP)	PADC (IPP)	PADC (BP)		
1	1.0	18.0	17.5	3.0	4.0	1.05	1.10
2	2.0	15.0	12.5	4.0	3.0	1.08	1.12
3	3.0	15.0	15.0	5.0	4.0	1.25	1.15
4	4.0	17.0	15.0	5.0	3.0	1.18	1.08
5	5.0	17.5	16.0	5.0	3.0	1.17	1.07
	PM PADC (250 μ)	21.0	----	6.0	----	1.17	---

Table 3.44 Track etch parameters after 6h of chemical etching

Sr. No.	Initiator Conc. (% by Wt.)	Etch pit diameter (μm)				Sensitivity (S)	
		D_f		D_α			
		PADC (IPP)	PADC (BP)	PADC (IPP)	PADC (BP)	PADC (IPP)	PADC (BP)
1	1.0	21.0	21.0	4.0	5.0	1.07	1.12
2	2.0	19.0	15.0	5.0	4.0	1.14	1.15
3	3.0	19.0	18.0	6.0	5.0	1.22	1.16
4	4.0	21.0	19.0	6.0	4.0	1.17	1.09
5	5.0	22.0	20.0	6.0	4.0	1.16	1.08
	PM PADC (250 μ)	24.0	---	7.0	---	1.17	---

Table 3.45 Track etch parameters after 7h of chemical etching

From Tables 3.41 - 3.45 it can be seen that the sensitivity as determined using 6 N NaOH at 70 °C increased from 3 to 5 h, after which a drop in the sensitivity was observed. This is mainly due to the increase in the bulk etch rates which in turn is calculated from the diameter of fission fragments. Thus, the optimum time of etching to get the maximum sensitivity under these etching conditions was found to be 5 h. It can be seen that both V_t and V_b and hence the sensitivity (S) depend upon the initiator used. In the case of benzoyl peroxide it can be seen that films prepared with an initiator concentration of 2 % was found to be more sensitive, whereas for IPP it was found to be 3 %. Table 3.46 gives the unsaturation present in the films cured with different initiator concentration. The curing cycles

were calculated using equation 3.1 for the different initiator concentrations.

Sr. No.	Initiator conc.(%)	Unsaturation (%)	
		IPP	BP
1	1.0	10.11	8.56
2	2.0	8.44	7.25
3	3.0	5.11	4.52
4	4.0	4.75	3.85
5	5.0	3.25	2.78

Table 3.46 Percentage unsaturation in PADC films prepared with different initiator concentrations.

The dependence of the sensitivity (S) on the amount of initiator used, was confirmed for a few more batches of PADC and are given in Table 3.47 and shown graphically in Fig. 3.35(see next page).

Sr. No.	Initiator (%)	Sensitivity (S)			
		Batch I		Batch II	
		PADC(IPP)	PADC(BP)	PADC(IPP)	PADC(BP)
1	1	1.08	1.08	1.1	1.12
2	2	1.2	1.19	1.25	1.22
3	3	1.38	1.12	1.35	1.1
4	4	1.29	1.12	1.25	1.13
5	5	1.25	1.09	1.2	1.11

Table 3.47 Sensitivity of PADC films prepared with different initiator concentrations.

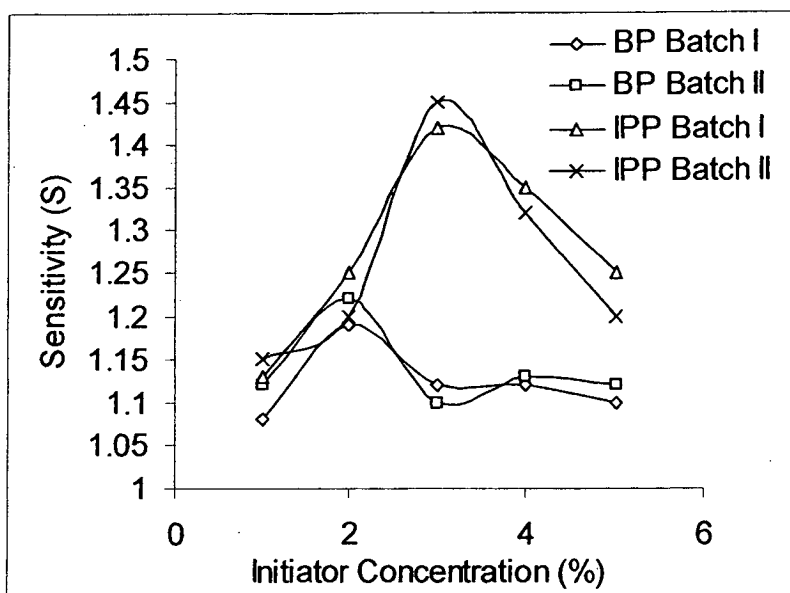


Fig. 3.35 Dependence of sensitivity on Initiator concentration in PADAC films.

3.8.2 PNADAC and NADAC-ADC (50:50) plastic track detectors.

Two pieces each of PNADAC and poly-[(NADAC)-co-(ADC)] cured with IPP were exposed to charged particles in vacuum. The films were then chemically etched under its optimum etching conditions *i.e.*, 80 °C, 6 N NaOH and 75 °C, 6 N NaOH. The diameters of fission fragments and alpha tracks were measured at regular intervals and the sensitivity values were calculated using equation no. 2.1. It was observed that the alpha particle tracks appeared after 4 and 8 h in case of PNADAC and NADAC-ADC copolymer films respectively. The results are given in Table 3.48 - 3.53.

Sr. No.	Initiator Conc. (% by Wt.)	Etch pit diameter (μm)				Sensitivity (S)	
		D_f		D_a			
		I	II	I	II	I	II
1	1.0	9.0	12.0	—	2.5	—	1.09
2	2.0	8.0	11.5	2.5	4.0	1.22	1.28
3	3.0	7.5	10.0	2.5	4.0	1.25	1.38
4	4.0	7.5	11.0	2.5	4.0	1.25	1.30
5	5.0	8.0	11.5	2.5	4.0	1.22	1.28

Table 3.48 Track etch parameters of NADAC-ADC after 4 h (I) & 5 h (II) of chemical etching

Sr. No.	Initiator Conc. (% by Wt.)	Etch pit diameter (μm)				Sensitivity (S)	
		D_f		D_a			
		I	II	I	II	I	II
1	1.0	15.0	17.5	3.0	4.0	1.08	1.11
2	2.0	14.0	17.0	5.0	6.0	1.29	1.28
3	3.0	12.5	15.0	5.0	7.5	1.38	1.67
4	4.0	13.5	16.0	5.0	7.0	1.32	1.47
5	5.0	14.0	17.0	5.0	7.0	1.29	1.41

Table 3.49 Track etch parameters of NADAC-ADC after 6h (I) & 7 h (II) of chemical etching.

Sr. No.	Initiator Conc. (% by Wt.)	Etch pit diameter (μm)				Sensitivity (S)	
		D_f		D_a			
		I	II	I	II	I	II
1	1.0	20.0	23.0	5.0	6.0	1.13	1.15
2	2.0	19.0	22.0	7.0	8.0	1.31	1.30
3	3.0	17.5	20.0	8.0	9.0	1.53	1.51
4	4.0	18.0	21.0	7.5	8.0	1.42	1.34
5	5.0	19.0	22.0	7.5	8.0	1.37	1.30

Table 3.50 Track etch parameters of NADAC-ADC after 8hs (I) & 9 h (II) of chemical etching.

Sr. No.	Initiator Conc. (% by Wt.)	Etch pit diameter (μm)				Sensitivity (S)	
		D_f		D_α		I	II
		I	II	I	II		
1	1.0	15.0	17.0	---	2.0	---	1.02
2	2.0	13.0	15.0	2.0	3.0	1.02	1.08
3	3.0	10.0	11.0	2.5	4.0	1.06	1.26
4	4.0	12.5	15.0	2.5	4.0	1.08	1.13
5	5.0	15.0	17.5	2.5	4.0	1.05	1.09

Table 3.51 Track etch parameters of PNADAC after 8h (I) & 9 h (II) of chemical etching.

Sr. No.	Initiator Conc. (% by Wt.)	Etch pit diameter (μm)				Sensitivity (S)	
		D_f		D_α		I	II
		I	II	I	II		
1	1.0	20.0	23.0	3.0	4.0	1.06	1.06
2	2.0	17.5	20.0	4.0	5.0	1.11	1.13
3	3.0	12.5	17.5	5.0	5.0	1.38	1.18
4	4.0	17.5	20.0	5.0	5.0	1.17	1.18
5	5.0	21.0	25.0	5.0	5.0	1.12	1.08

Table 3.52 Track etch parameters of PNADAC after 10h (I) & 11 h (II) of chemical etching

Sr. No.	Initiator Conc. (% by Wt.)	Etch pit diameter (μm)				Sensitivity (S)	
		D_f		D_α		I	II
		I	II	I	II		
1	1.0	27.0	28.0	4.0	4.0	1.04	1.03
2	2.0	23.0	24.0	5.0	5.0	1.09	1.07
3	3.0	22.0	23.0	5.0	5.0	1.16	1.10
4	4.0	24.0	25.0	5.0	5.0	1.13	1.10
5	5.0	28.0	29.0	5.0	6.0	1.09	1.07

Table 3.53 Track etch parameters of PNADAC after 12h (I) & 13 h (II) of chemical etching.

From Table 3.48 to 3.53 it can be seen that the sensitivity for the homo polymer increased from 8 to 10 h, where as for the copolymer it was from 4 to 6 h, after which a drop in the sensitivity was observed (refer Fig.3.36, next page). Thus, the optimum time of etching to get the maximum sensitivity under these etching conditions was found to be 10 and 6 h for the homo and copolymer respectively. It can be seen that both V_t and V_b and hence the sensitivity (S) depend upon the initiator used. The sensitivity values were found to be maximum for films prepared with 3.0 % initiator concentration (refer Fig. 3.37, next page) for the homo and copolymers and this observation is in accordance with many other literature references. Table 3.54 gives the unsaturation present in the films cured with different initiator concentration.

Sr. No.	Initiator conc. (%)	Unsaturation (%)	
		PNADAC	NADAC-ADC
1	1	7.98	8.5
2	2	6.52	6.23
3	3	4.15	4.35
4	4	3.58	2.67
5	5	3.25	3.14

Table 3.54 Percentage unsaturation in PNADAC & NADAC-ADC films prepared with different initiator concentrations.

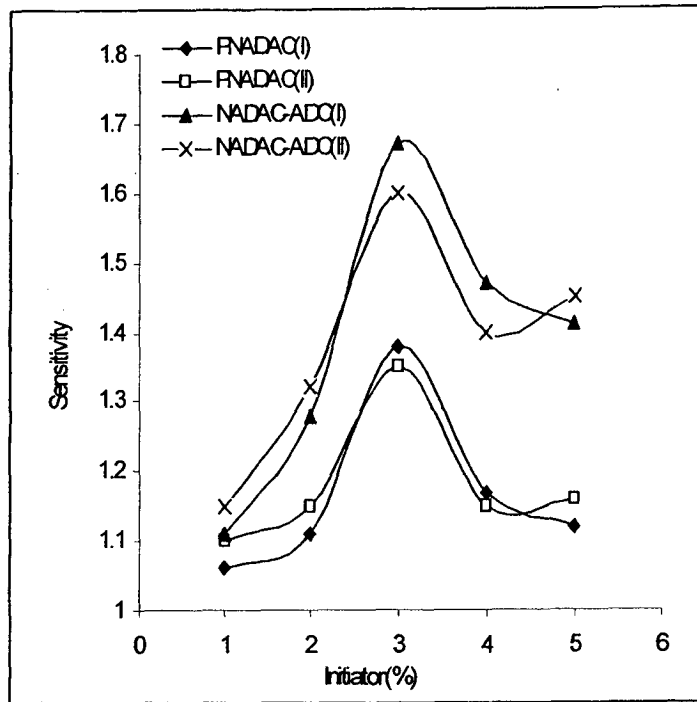


Fig. 3.36 Variation of the sensitivity of PNADAC and NADAC-ADC films with different amount of initiator.(I & II indicate batch no.)

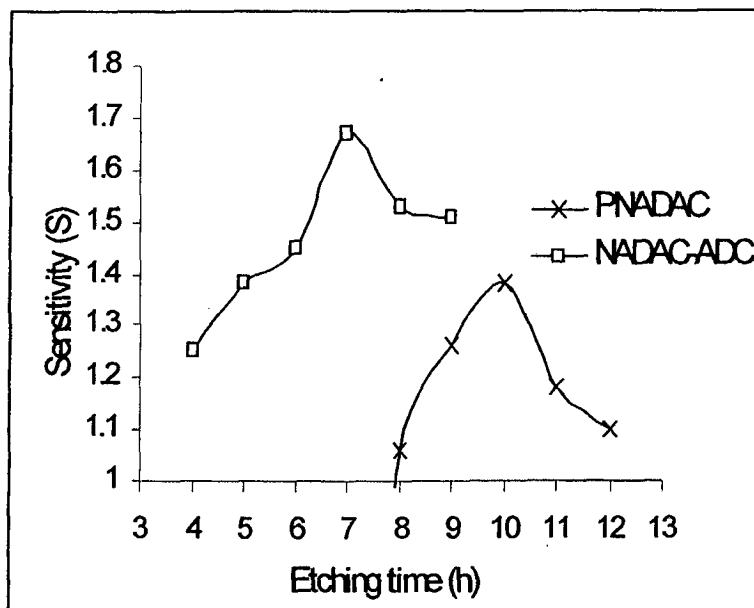


Fig. 3.37 Variation of sensitivity as a function of etching time.

3.8.3 ABNEC-ADC (10:90) Plastic Track Detectors.

Since, among all the copolymers of ABNEC-ADC the one with composition ABNEC-ADC (10:90) could detect both alpha and fission fragments the initiator concentration optimization studies were carried out only for this particular copolymer constitution. In order to find the optimum initiator concentration, films with varying initiator concentration 2 - 6 % were prepared using the constant rate of polymerization cycle developed. The results are given in Table 3.55 - 3.57.

Sr. No.	Initiator Conc. (% by Wt.)	Etch pit diameter (μm)				Sensitivity (S)	
		D_f		D_α		I	II
		I	II	I	II		
1	2.0	27.0	29.0	---	---	---	---
2	3.0	26.0	28.0	---	2.5	---	1.02
3	4.0	22.5	25.0	2.5	4.0	1.02	1.05
4	5.0	22.0	24.0	2.5	4.0	1.03	1.06
5	6.0	23.0	25.0	2.5	4.0	1.02	1.05

Table 3.55 Track etch parameters of ABNEC-ADC (10:90) after 7 h(I) & 8 h (II) of chemical etching.

Sr. No.	Initiator Conc. (% by Wt.)	Etch pit diameter (μm)				Sensitivity (S)	
		D_f		D_α		I	II
		I	II	I	II		
1	2.0	29.0	32.0	---	---	---	---
2	3.0	28.0	30.0	2.5	3.0	1.02	1.05
3	4.0	27.0	29.0	5.0	6.0	1.07	1.15
4	5.0	25.0	29.0	5.0	6.0	1.08	1.15
5	6.0	26.0	30.0	5.0	6.0	1.03	1.10

Table 3.56 Track etch parameters of ABNEC-ADC (10:90) after 9h (I) & 10 h (II) of chemical etching.

Sr. No.	Initiator Conc. (% by Wt.)	Etch pit diameter (μm)				Sensitivity (S)	
		D_f		D_a		I	II
		I	II	I	II		
1	2.0	35.0	38.0	---	---	---	---
2	3.0	32.0	34.0	3.0	3.5	1.02	1.05
3	4.0	32.0	34.0	6.0	6.5	1.10	1.08
4	5.0	32.0	34.0	6.0	6.5	1.10	1.08
5	6.0	33.0	34.0	6.0	6.5	1.08	1.06

Table 3.57 Track etch parameters of ABNEC-ADC (10:90) after 11h (I) & 12 h (II) of chemical etching.

From table 3.55-3.57 given above & Fig . 3.38 , it can be seen that the sensitivity as determined using the standard etching conditions for ABNEC-ADC (10:90) copolymer increased from 8 to 10 h, after which the values were observed to be the same. Thus the optimum time of etching to get the maximum sensitivity under these etching conditions was found to be 9 h. It can be seen that both V_t and V_b and hence the sensitivity (S) depend upon the initiator used. The sensitivity values were found to be maximum for films prepared with 5.0 % initiator concentration. (refer Fig. 3.39, next page)

Sr. No.	Initiator Conc. (%)	Unsaturation (%) ABNEC-ADC(10:90)
1	2	9.56
2	3	8.54
3	4	5.45
4	5	4.65
5	6	4.25

Table 3.58 Percentage unsaturation in ABNEC-ADC (10:90) films prepared with different initiator concentrations.

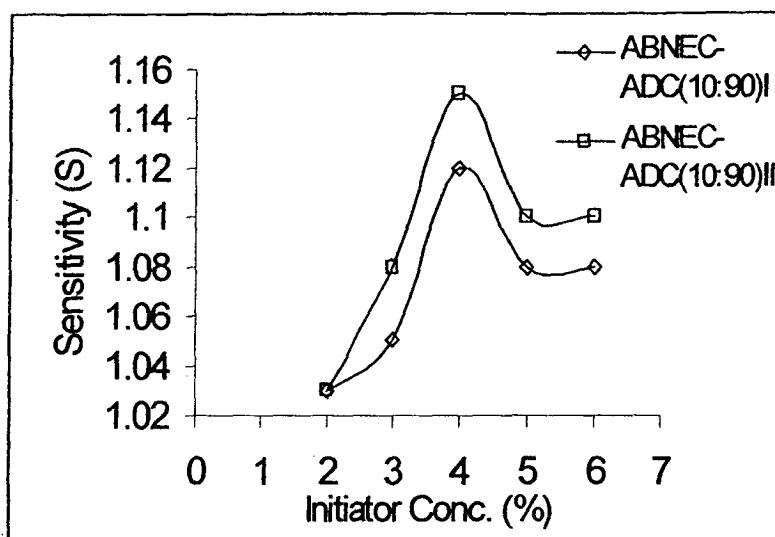


Fig. 3.38 Variation of the sensitivity of ABNEC-ADC (10:90) films with different amount of initiator. (I & II indicate batch no.)

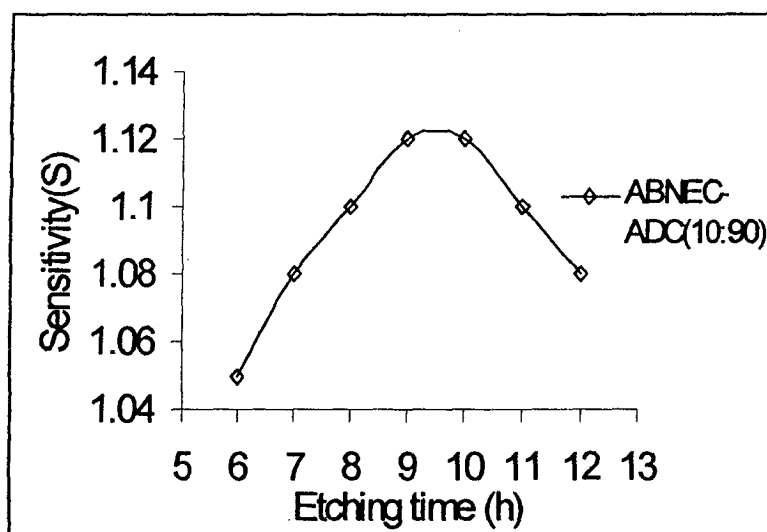


Fig. 3.39 Variation of sensitivity as a function of etching time

3.8.4 TDONM-ADC copolymer Plastic Track Detectors.

Among the TDONM-ADC copolymers only two compositions were able to detect alpha and fission fragments *i.e.* TDONM-ADC (10:90)

& TDONM-ADC (20:80), the homopolymer was able to detect only low energy alpha particles hence its sensitivity studies could not be carried out. The films were exposed to californium source, and etched under its optimum etching conditions. The track diameters and sensitivity values were found after interval of 1 h. The data is given in Table 3.59-3.66.

Sr. No.	Initiator Conc. (% by Wt.)		Etch pit diameter (μm)				Sensitivity (S)	
			D_f		D_α			
	I	II	I	II	I	II	I	II
1	3.0	5.0	5.5	7.0	--	--	--	--
2	4.0	6.0	5.0	7.0	1.0	1.0	1.04	1.02
3	5.0	7.0	5.0	7.0	1.0	1.0	1.08	1.04
4	6.0	8.0	5.5	7.0	1.0	1.0	1.07	1.04
5	7.0	9.0	5.5	7.0	1.0	1.0	1.07	1.04

Table 3.59 Track etch parameters after 3 h of chemical etching. I & II indicate TDONM-ADC (10:90) & TDONM-ADC (20:80) respectively.

Sr. No.	Initiator Conc. (% by Wt.)		Etch pit diameter (μm)				Sensitivity (S)	
			D_f		D_α			
	I	II	I	II	I	II	I	II
1	3.0	5.0	7.0	9.0	1.0	1.0	1.15	1.05
2	4.0	6.0	6.0	9.0	2.0	2.0	1.25	1.10
3	5.0	7.0	6.0	9.0	2.0	2.0	1.25	1.10
4	6.0	8.0	6.0	9.0	2.0	2.0	1.25	1.10
5	7.0	9.0	7.0	9.0	2.0	2.0	1.25	1.10

Table 3.60 Track etch parameters after 4 h of chemical etching. I & II indicate TDONM-ADC (10:90) & TDONM-ADC (20:80) respectively.

Sr. No.	Initiator Conc. (% by Wt.)		Etch pit diameter (μm)				Sensitivity (S)	
			D_f		D_a			
	I	II	I	II	I	II	I	II
1	3.0	5.0	9.0	11.0	2.0	2.0	1.25	1.15
2	4.0	6.0	8.0	10.0	3.0	3.0	1.33	1.20
3	5.0	7.0	8.0	10.0	3.0	3.0	1.33	1.20
4	6.0	8.0	9.0	10.0	3.0	3.0	1.33	1.20
5	7.0	9.0	9.0	10.0	3.0	3.0	1.33	1.20

Table 3.61 Track etch parameters after 5 h of chemical etching. I & II indicate TDONM-ADC (10:90) & TDONM-ADC (20:80) respectively.

Sr. No.	Initiator Conc. (% by Wt.)		Etch pit diameter (μm)				Sensitivity (S)	
			D_f		D_a			
	I	II	I	II	I	II	I	II
1	3.0	5.0	11.0	13.0	3.0	3.0	1.30	1.20
2	4.0	6.0	10.0	12.0	4.0	4.0	1.38	1.25
3	5.0	7.0	10.0	12.0	4.0	4.0	1.38	1.25
4	6.0	8.0	11.0	12.0	4.0	4.5	1.38	1.25
5	7.0	9.0	11.0	12.0	4.0	4.5	1.38	1.25

Table 3.62 Track etch parameters after 6 h of chemical etching. I & II indicate TDONM-ADC (10:90) & TDONM-ADC (20:80) respectively.

Sr. No.	Initiator Conc. (% by Wt.)		Etch pit diameter (μm)				Sensitivity (S)	
			D_f		D_a			
	I	II	I	II	I	II	I	II
1	3.0	5.0	14.0	15.0	4.0	4.0	1.35	1.15
2	4.0	6.0	13.0	14.0	5.0	5.0	1.42	1.23
3	5.0	7.0	12.0	14.0	5.0	5.0	1.42	1.23
4	6.0	8.0	12.0	14.0	5.0	5.0	1.42	1.23
5	7.0	9.0	13.0	15.0	5.0	5.0	1.42	1.23

Table 3.63 Track etch parameters after 7 h of chemical etching. I & II indicate TDONM-ADC (10:90) & TDONM-ADC (20:80) respectively.

Sr. No.	Initiator Conc. (% by Wt.)		Etch pit diameter (μm)				Sensitivity (S)	
			D_f		D_a			
	I	II	I	II	I	II	I	II
1	3.0	5.0	16.0	18.0	5.0	5.0	1.38	1.15
2	4.0	6.0	14.0	16.0	6.0	6.0	1.45	1.22
3	5.0	7.0	14.0	16.0	6.0	6.0	1.45	1.22
4	6.0	8.0	14.0	16.0	6.0	6.0	1.45	1.22
5	7.0	9.0	15.0	17.0	6.0	6.0	1.45	1.22

Table 3.64 Track etch parameters after 8 h of chemical etching. I & II indicate TDONM-ADC (10:90) & TDONM-ADC (20:80) respectively.

Sr. No.	Initiator Conc. (% by Wt.)		Etch pit diameter (μm)				Sensitivity (S)	
			D_f		D_a			
	I	II	I	II	I	II	I	II
1	3.0	5.0	18.0	20.0	6.0	5.0	1.30	1.10
2	4.0	6.0	18.0	19.0	6.5	6.5	1.32	1.22
3	5.0	7.0	17.5	19.0	6.5	6.0	1.32	1.22
4	6.0	8.0	17.0	19.0	6.5	6.0	1.32	1.22
5	7.0	9.0	18.0	20.0	6.5	6.5	1.32	1.22

Table 3.65 Track etch parameters after 9 h of chemical etching. I & II indicate TDONM-ADC (10:90) & TDONM-ADC (20:80) respectively.

Sr. No.	Initiator Conc. (% by Wt.)		Etch pit diameter (μm)				Sensitivity (S)	
			D_f		D_a			
	I	II	I	II	I	II	I	II
1	3.0	5.0	21.0	23.0	6.5	7.0	1.25	1.10
2	4.0	6.0	19.0	22.0	7.0	7.0	1.25	1.20
3	5.0	7.0	19.0	22.0	7.0	7.0	1.25	1.20
4	6.0	8.0	19.0	22.0	7.0	7.0	1.25	1.20
5	7.0	9.0	20.0	22.0	7.0	7.0	1.25	1.20

Table 3.66 Track etch parameters after 10 h of chemical etching. I & II indicate TDONM-ADC (10:90) & TDONM-ADC (20:80) respectively.

From Tables 3.59 to 3.66 it can be seen that the sensitivity as determined using the standard etching conditions for the copolymers *i.e.*, 60 °C, 4 N NaOH, the sensitivity for the TDONM-ADC (10:90) copolymer increased from 3 to 8 h, where as for the TDONM-ADC (20:80) copolymer it was from 3 to 6 h, after which a drop in the sensitivity was observed. Thus, the optimum time of etching to get the maximum sensitivity under these etching conditions was found to be 7 and 5 h for the TDONM-ADC (10:90) and TDONM-ADC (20:80) respectively (refer Fig. 3.40). It can be seen that both V_t and V_b and hence the sensitivity (S) depend upon the initiator used. The sensitivity values were found to be maximum for films prepared with 5.0 and 6.0 % initiator concentration for the TDONM-ADC (10:90) and TDONM-ADC (20:80) respectively (refer Fig. 3.41, next page). Table 3.67 gives the unsaturation present in the films cured with different initiator concentration.

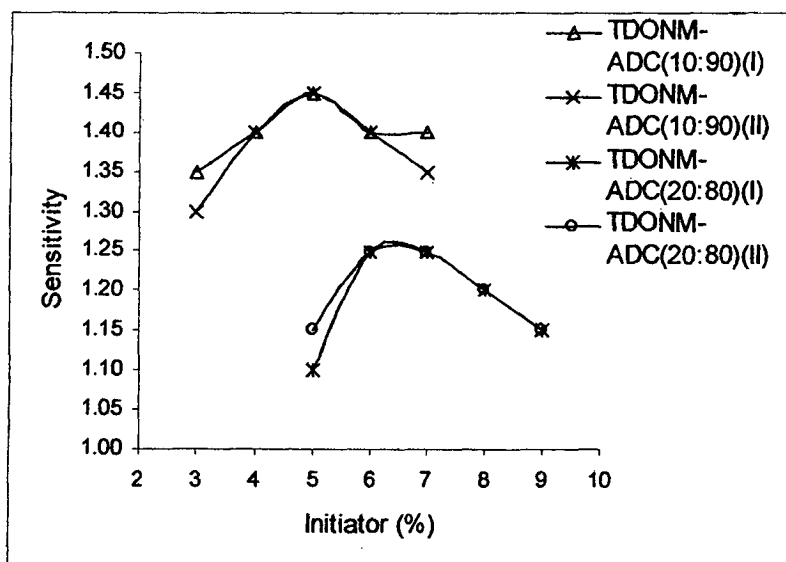


Fig. 3.40 Variation of the sensitivity of TDONM-ADC (10:90) and TDONM-ADC (20:80) films with the amount of initiator (I & II indicate batch no.)

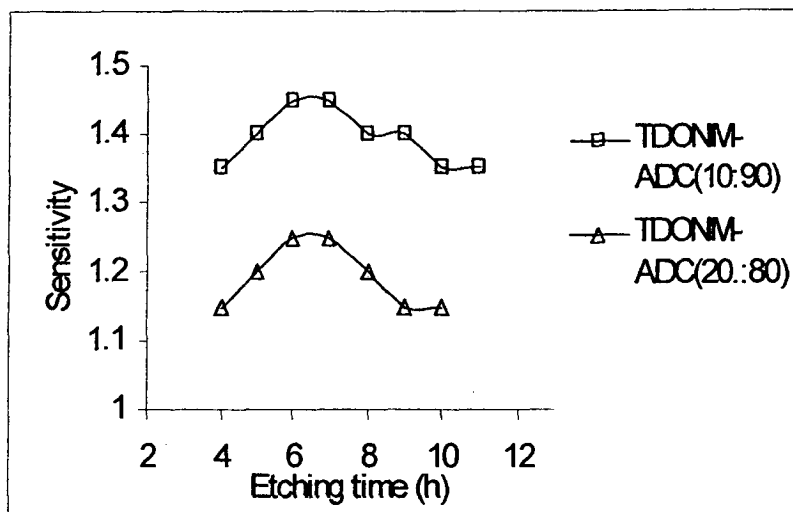


Fig. 3.41 Variation of sensitivity as a function of etching time

Sr. No.	Initiator Conc. (%)		Unsaturation (%)	
	I	II	I	II
1	3.0	5.0	10.25	11.25
2	4.0	6.0	8.54	9.45
3	5.0	7.0	6.25	7.58
4	6.0	8.0	4.50	5.45
5	7.0	9.0	3.89	3.50

Table 3.67 Percentage unsaturation in TDONM-ADC (10:90) (I) and TDONM-ADC (20:80) (II) films prepared with different initiator concentrations.

3.9. Uniformity of etching of the films:

The bulk polymerization leading to the three dimensional polymer network, like that of PADC, is usually non-uniform throughout the mass of the polymer. This is due to the variations in the microenvironment from point to point. This leads to the change in the observable properties of the polymer with respect to the depth from the surface. In order to compare the polymerization processes in the various plastic materials developed by us, the change in weight per unit area was studied as a function of etching time using their respective optimum etching conditions. The fission track diameter is also an important parameter that reflects the uniformity of etching in a plastic material. Both these parameters were studied and comparisons between both these methods have been done. The data for the different polymer materials have been presented in the form of figures. The studies for the films were carried upto its maximum observable sensitivity values.

3.9.1 PADC Plastic Track detector.

From the above data, it is noteworthy that the etching characteristics for the indigenously prepared PADC films show a similar linear trend as observed in case of PM PADC. Similar studies were also carried out for all the newly developed polymers and the results are given below. Fig. 3.42 gives the loss in weight per unit area for PADC films upon etching and Fig. 3.43 gives the fission fragment track diameters in PADC films upon etching with respect to time.(see next page)

i) Change in weight per unit area:

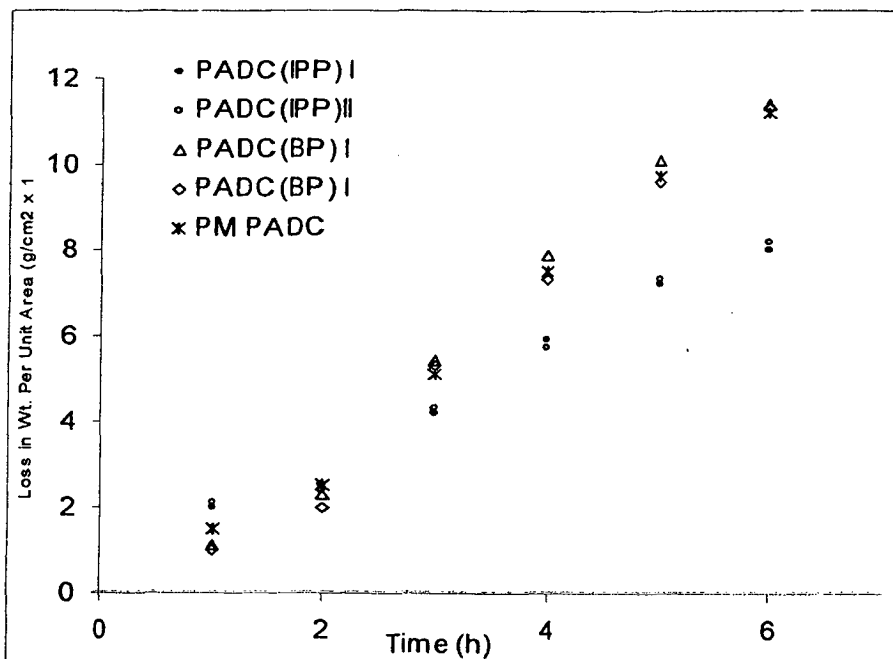


Fig. 3.42 Change in weight studies of PADC films.

ii) Fission fragment diameter method:

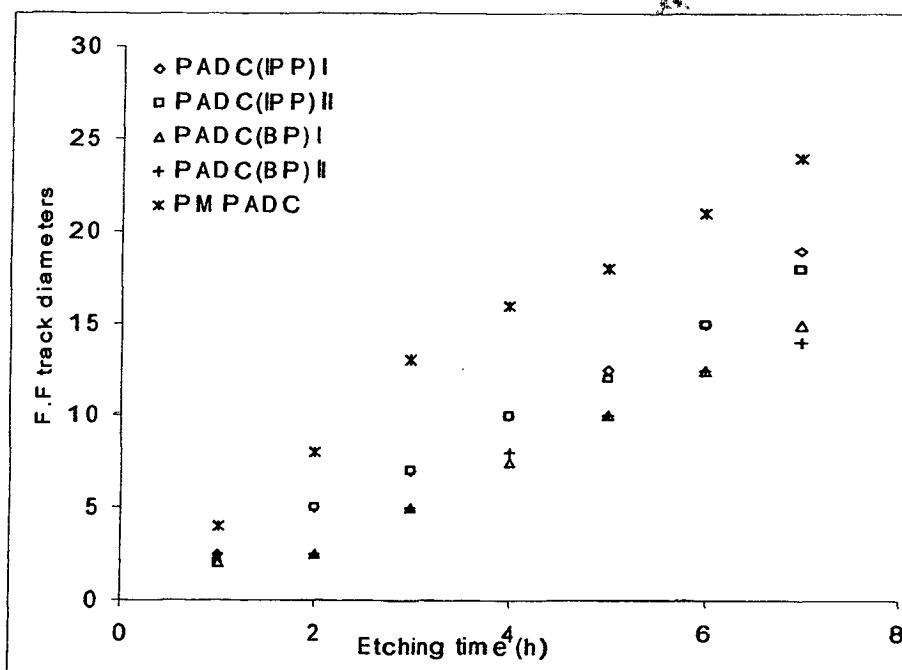


Fig. 3.43 Fission Fragment diameters in PADC films.

3.9.2 PNADAC and NADAC-ADC plastic Track Detectors.

Fig. 3.44 gives the loss in weight per unit area for PNADAC and NADAC-ADC films upon etching and Fig. 3.45 gives the fission fragment track diameters in PNADAC and NADAC-ADC films upon etching with respect to time. As expected the newly developed materials also show a linear response.

i) Change in weight per unit area:

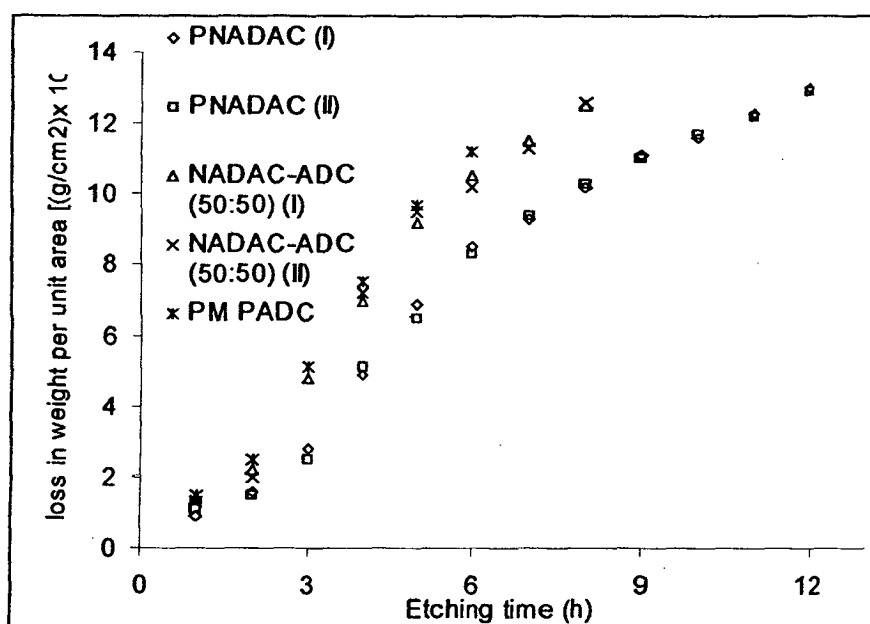


Fig. 3.44 Change in weight studies in PNADAC & NADAC-ADC films.

ii) Fission fragment diameter method:

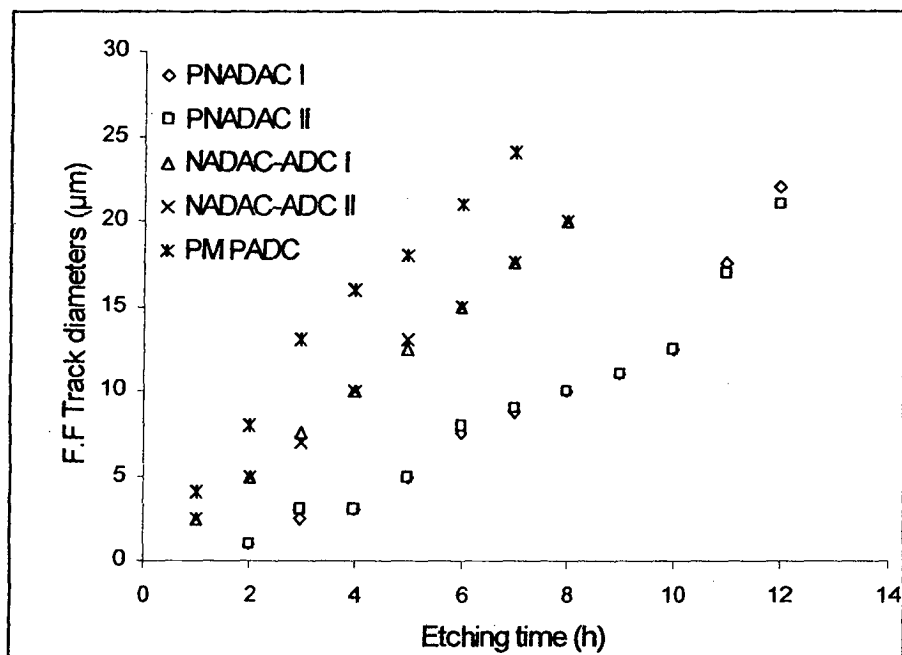


Fig. 3.45 Fission fragment diameters in PNADC & NADAC-ADC films.

3.9.3 ABNEC-ADC Nuclear Track detectors.

The ABNEC-ADC copolymers were also tested in a similar manner. Fig. 3.46 gives the loss in weight per unit area for ABNEC-ADC copolymer films upon etching and Fig. 3.47 gives the fission fragment track diameters in ABNEC-ADC copolymer films upon etching with respect to time. These track detectors are also found to show a linear response.

i) Change in weight per unit area:

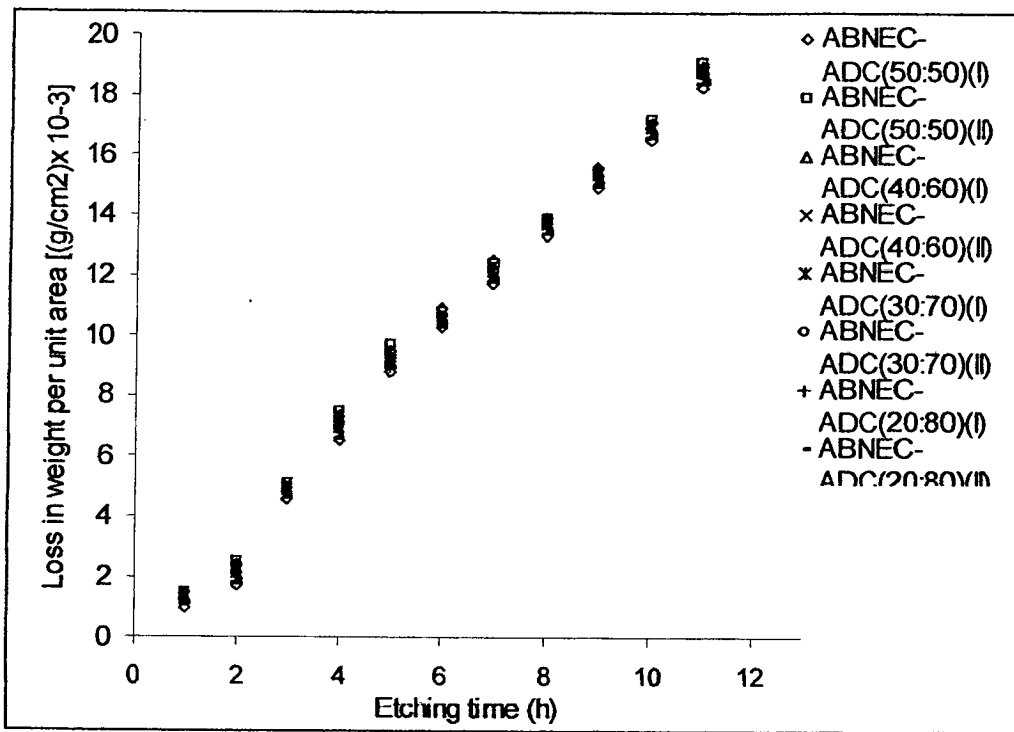


Fig. 3.46 Change in weight studies in ABNEC-ADC films

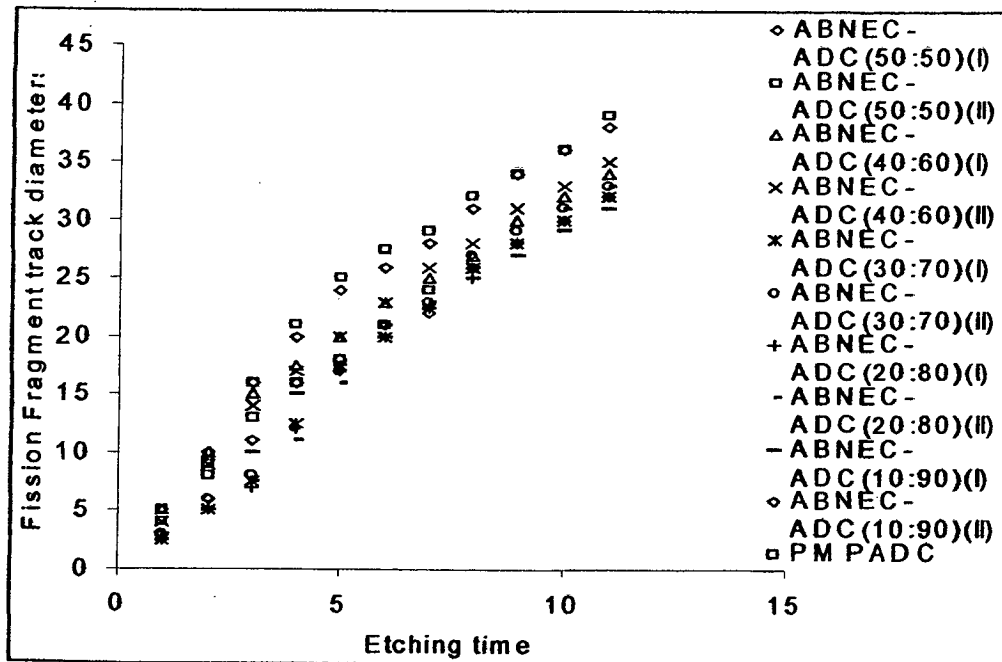


Fig. 3.47 Fission fragment diameters in ABNEC-ADC films

3.9.4 PTDONM and TDONM-ADC Nuclear Track Detectors:

i) Change in weight per unit area:

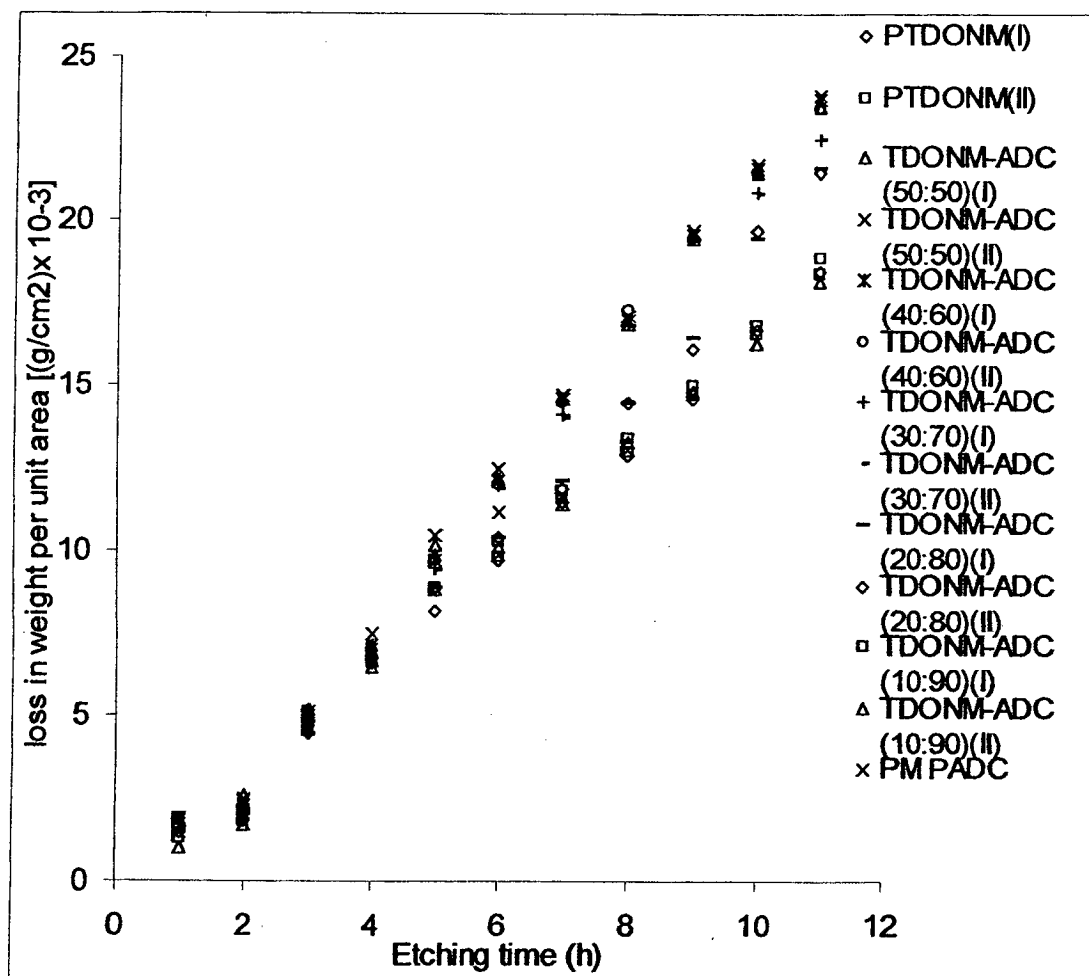


Fig. 3.48 Change in weight studies in TDONM films.

ii) Fission fragment diameter method:

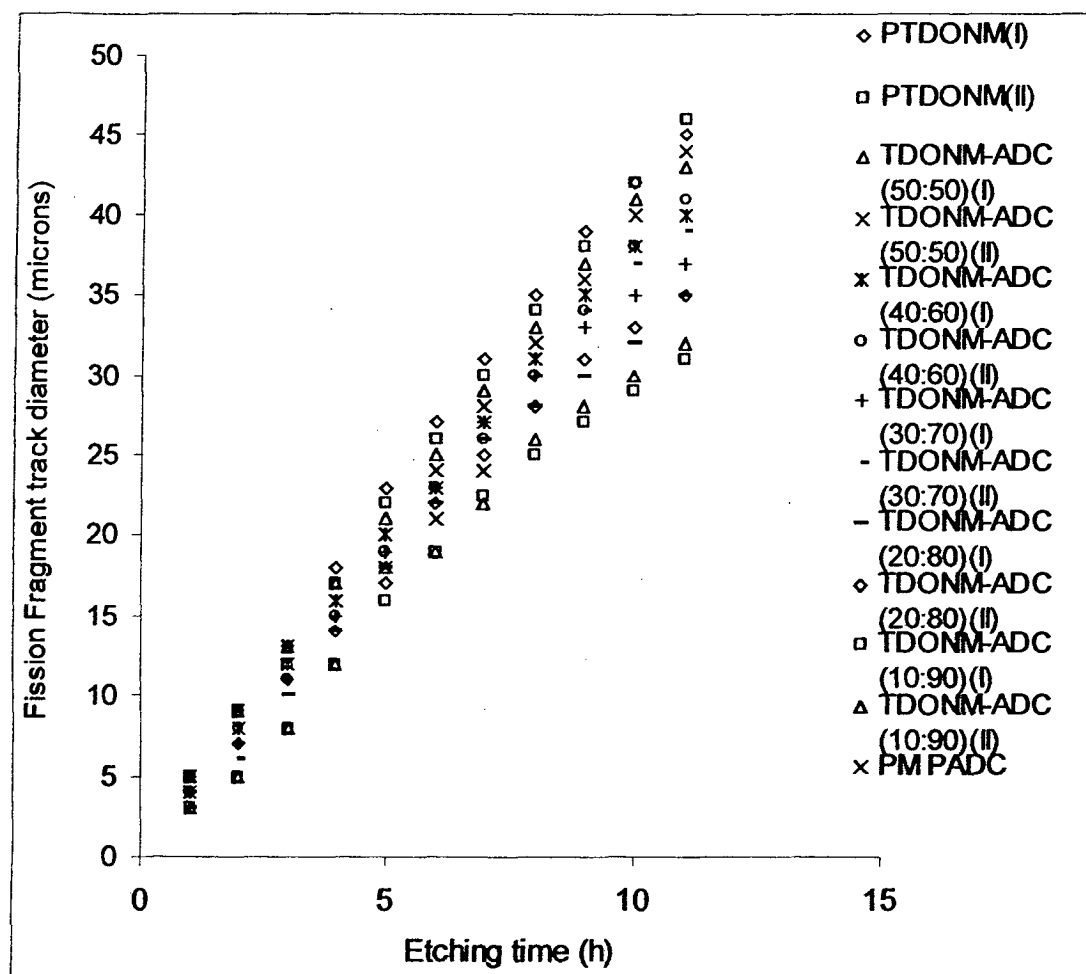


Fig. 3.49 Fission fragment diameters in TDONM films.

3.10. Alpha track detection efficiency of newly developed plastic nuclear track detectors.

In order to find the alpha track detection efficiency, it is important to know the optimum time, up to which the films need to be etched before counting the alpha tracks, hence the time at which the alpha track count would reach a saturation point is important.

3.10.1 Studies on variation of alpha track density with etching time.

In order to determine the optimum etching time for counting of alpha tracks for a particular plastic material, small pieces of the films of size 2 cm x 2 cm were exposed to 703703 dpm ^{239}Pu alpha particles at a distance of 2 cm from the source for 2 min. The pieces were then etched under its standard etching conditions. The tracks were counted after different etching time intervals using an optical microscope till a constant value was obtained for a particular material under study. The results are given in Fig. 3.50. It can be seen that the alpha track counting times vary considerably for the different materials. From the data obtained, the etching time at which the alpha tracks can be conveniently counted are given in Table 3.68.

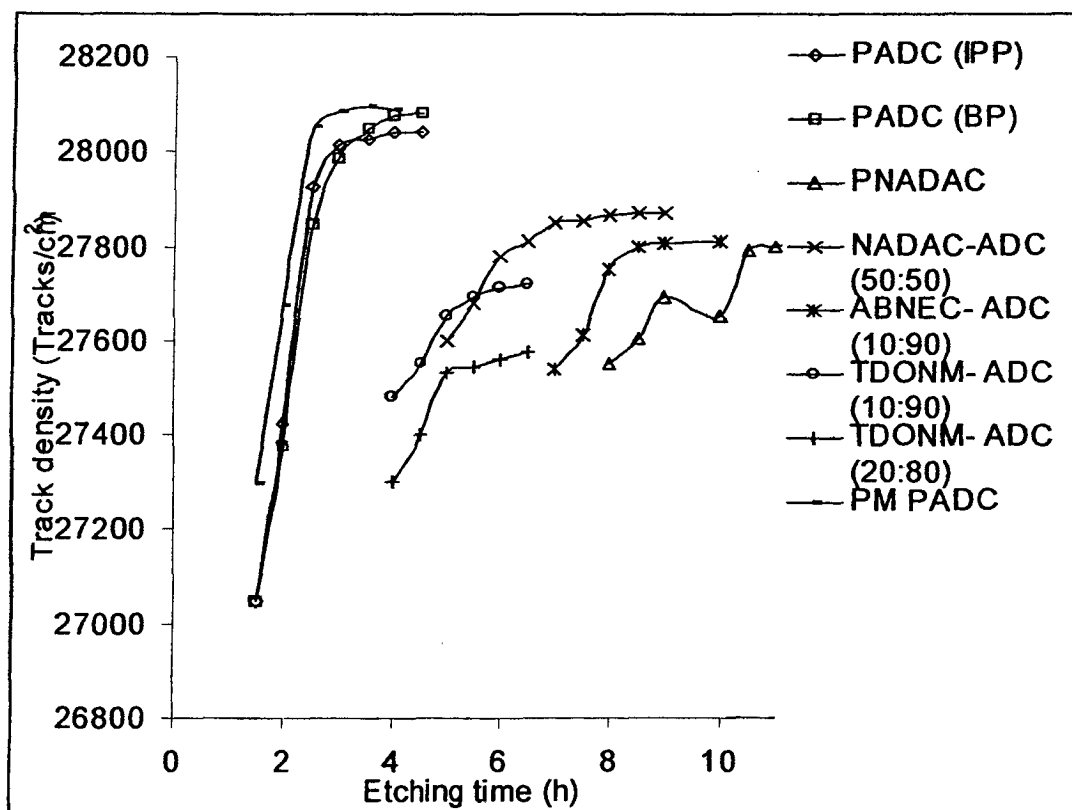


Fig.3.50 Alpha track density with respect to etching time for various track detectors.

Polymer Material	Etching time (h)
PADC(IPP)	3.0
PADC(BP)	3.5
PNADAC	10.5
NADAC-ADC (50:50)	7.0
ABNEC-ADC(10:90)	8.5
TDONM-ADC (10:90)	5.5
TDONM-ADC (20:80)	5.5
PM PADC	3.0

Table. 3.68. Optimum etching time for development of alpha tracks (exposure at 2 cm from source)

3.10.2 Determination of the background tracks.

Background tracks are due to the presence of natural radioactivity present in the environment. Background tracks due to presence of track like features in the detector material resulting from matrix faults in the material were also considered. These tracks are counted without exposing the films to any source but by etching under identical conditions. The background track densities found in the different materials (at the optimised time for respective detector) are given in table 3.69 (see next page).

A higher number of background tracks is seen in the indigenously developed track detectors. One of the probable reasons that can be attributed to higher background is the presence of fine dust particles in the monomer. Also the decomposition of the catalyst involves the evolution of gas micro-bubbles which may be trapped in the polymer matrix. It is also possible that micro air-bubbles are trapped in the liquid monomer film while filling the mold.

Material	Background tracks (per cm ²)
PADC(IPP)	250
PADC(BP)	240
PNADAC	300
NADAC-ADC	400
ABNEC-ADC (10:90)	210
TDONM-ADC (10:90)	240
TDONM-ADC (20:80)	240
PM PADC	90

Table 3.69 Background tracks observed in various polymers.

3.10.3 Alpha track detection efficiency.

The alpha track detection efficiency for the polymeric track detectors were determined as outlined in sec 2.1.3. The results are given in Table 3.70 (see next page)

Distance of Exposure (cm)	Time (min)	Tracks Expected (per cm ²)	Tracks observed (per cm ²)							
			PADC (IPP)	PADC (BP)	PNADAC	NADAC -ADC (50:50)	ABNEC -ADC (10:90)	TDONM -ADC (10:90)	TDONM -ADC (20:80)	PM PADC
1.0	0.5	28173	27789	27645	27789	27895	27700	27750	27625	27925
2.0	2.0	28173	27815	27745	27815	27860	27615	27720	27575	27890
2.5	2.0	18030	17630	17540	17580	17620	17620	17650	17600	17630

Table. 3.70 Alpha Tracks detected in various polymers.

Alpha particle track detection efficiency of the detectors are given in Table 3.71

Distance Exposure (cm)	Time (min)	Alpha particle track detection efficiency (%)							
		PADC (IPP)	PADC (BP)	PNADAC	NADAC -ADC (50:50)	ABNEC -ADC (10:90)	TDONM -ADC (10:90)	TDONM -ADC (20:80)	PM PADC
1.0	0.5	98.63	98.12	98.63	99.01	98.32	98.49	98.05	99.21
2.0	2.0	98.72	98.48	98.72	98.88	98.01	98.39	97.87	98.99
2.5	2.0	97.78	97.28	97.50	97.72	97.77	97.89	97.61	97.78

Table 3.71 Percentage efficiency of alpha track detection of various polymers

3.11. Correlation of sensitivities of plastic track detectors.

The alpha particle sensitivities of various plastic materials were compared with imported PADC (i.e. PM CR-39) under identical conditions of exposure. The results are given in Table 3.72.

Sr.No.	Plastic Material	Sensitivity
1	PM PADC (250 μ)	1.25
2	PM PADC (500 μ)	1.50
3	PADC (IPP)(500 \pm 10 μ)	1.35
4	PADC (BP)(500 \pm 10 μ)	1.20
5	PNADAC	1.35
6	NADAC-ADC (50:50)	1.80
7	ABNEC-ADC (10:90)	1.15
8	TDONM-ADC (10:90)	1.45
9	TDONM-ADC (20:80)	1.25

Table. 3.72 Alpha Sensitivity values in different track detectors

From the values obtained it can be seen that NADAC-ADC (50:50) copolymer is the most sensitive material that we have prepared. The copolymer is a mixture of a hexafunctional and tetrafunctional monomers, which probably results in the densest possible network. Also there is presence of two different radiation sensitive groups viz., Carbonate and Carbamate in higher quantities; this factor is also responsible to its high sensitivity value. The other polymers like PTDONM-ADC / PTDONM / ABNEC-ADC, inspite of having nitro and carbonate groups did not

show higher sensitivity. This may be due to the presence of free terminals in the polymer matrix in the form of nitro groups, there by leading to the formation of a less dense network & possibly even some decomposition of nitro groups in the polymer.

3.12. Measurement of alpha to fission branching ratios by sequential chemical etching of alpha and fission tracks in homo and copolymer films.

The sequential etching method for revelation of alpha and fission tracks in PADC materials have been carried out by Pandey *et al.*, (1993)¹³⁹. This method of revelation of alpha particle and fission fragment tracks can be used for studies of half lives, alpha to fission branching ratios and identification of radionuclides, using a single detector. The alpha particles and fission fragment tracks can be differentiated unambiguously if there is a significant difference in their size and appearance time in a given detector. The newly developed homo and copolymer materials fully meet the requirements for the sequential etching conditions due to their considerable differences in the track diameters as well as appearance time.

In order to find the alpha to fission ratio for ²⁵²Cf source the films were kept at a distance of 5 mm from the source in 2D geometry for 5 min. The results are shown in Table 3.73.
(see next page).

Detector	Fission tracks per mm ²	Alpha tracks per mm ²	α /F.F ratio geometry	
			2 π	4 π
PADC (IPP)	1.46x 10 ⁴	22.14 x 10 ⁴	15.25	30.50
PADC(BP)	1.46 x 10 ⁴	22.10 x 10 ⁴	15.20	30.40
PNADAC	1.48 x 10 ⁴	22.37 x 10 ⁴	15.11	30.22
NADAC-ADC	1.45 x 10 ⁴	22.35 x 10 ⁴	15.41	30.82
ABNEC-ADC (10:90)	1.44 x 10 ⁴	21.84 x 10 ⁴	15.15	30.30
TDONM-ADC (10:90)	1.45 x 10 ⁴	22.02 x 10 ⁴	15.20	30.40
TDONM-ADC (20:80)	1.46 x 10 ⁴	22.35 x 10 ⁴	15.30	30.60
PM PADC	1.46 x 10 ⁴	22.35 x 10 ⁴	15.30	30.60

Table 3.73. α /F.F branching ratio of ²⁵²Cf in different polymers.

It can be seen that the values obtained for newly developed nuclear track detectors compare well with that of PM PADC and can be used unambiguously for determination of α /F.F branching ratio.

4.0 CONCLUSIONS

In the present work, efforts were made to prepare PADC plastic nuclear track detector and to develop new monomers and polymers there of, and to study these materials for nuclear track detection. Various aspects of the studies carried out during this course of work has been presented below in a nutshell.

- 1) Three new monomers were designed and synthesized. Allyl chloroformate and isopropyl chloroformate were synthesized using BTC as a source of phosgene, which is a much safer alternative to phosgene gas.
- 2) Two new homopolymers and three copolymer materials were developed as Nuclear Track Detectors. The PADC material was prepared and used as a case study towards development of new materials.
- 3) A polymerization bath and a mold assembly was designed for preparing the plastic materials. A programmable external circulating bath (Julabo make) was used for external heating of the polymerization bath. Highly polished Optical Glass and Teflon were used to prepare the polymerization mold.
- 4) The kinetics of polymerization was studied by applying Dial's kinetic model for obtaining a constant rate polymerization cycle. Dial had proposed this model in order to achieve a constant rate of polymerization which would ensure no thermal runaways, leading to cracking or bad post etch surface characteristics of the films prepared. It was observed that kinetic model could not be applied for monomers which were thermally unstable under the polymerization conditions, or if the monomers had functional groups that would interact with the free radicals. But monomers like ADC, NADAC or their mixtures appear to follow this model. The studies carried out, thus proved that the model could be applied to a hexafunctional or a mixture of tetra and hexafunctional monomers.
- 5) The films obtained upon etching were found to have more background track like features compared to the PM PADC films this was observed for almost all the newly developed track

detectors. One of the reasons cited for these type of features is the uneven rate of polymerization, which should be taken care of by using the Dial's model for constant polymerization. It was observed that in spite of using the Dial's model for polymerization, these features could not be suppressed. This could be due to the presence of very fine dust particles in the monomer which are entrapped in the polymer matrix, which upon etching look like particle tracks. Similarly, the entrapment of gas bubbles, due to gasses like carbondioxide which are released during polymerization. Further efforts are required in this direction of reducing the background tracks observed in the indigenously developed detectors.

6) All the newly developed polymers were first studied for its track detection by exposing to electrodeposited radiation sources like ^{239}Pu and ^{252}Cf . Among the newly developed plastic materials PNADAC, NADAC-ADC, ABNEC-ADC (10:90), TDONM-ADC (10:90) & TDONM-ADC (20:80) could record the alpha particle auto radiograph whereas PTDONM could detect only low energy alpha particles. All the other polymeric materials developed could detect fission fragments.

7) In our efforts towards developing materials that would have greater sensitivity, it was observed that NADAC-ADC (50:50) copolymer showed the highest sensitivity value of 1.8 whereas PM PADC showed 1.25. The other materials compared well with that of PM PADC.

8) All the materials prepared, fullfill the requirements like lower etching time, optical clarity upon etching etc that are essential for polymeric track detector.

9) The alpha track detection efficiency and alpha to fission

fragment track ratio studies show that the newly developed films compare well with that of PM PADC films.

10) From our studies, we can conclude that the structure and sensitivity correlation for a nuclear track detector, is more dependent on the extent of cross-linking present besides the number of radiation sensitive groups available in the given polymer. Mere presence of radiation sensitive groups or certain linkages (e.g. $-\text{CH}_2-\text{CH}_2-\text{O}-\text{C}-$) present in the polymer may not make a polymer more sensitive to radiations as indicated in the literature .

5.0 References.

1. D.A Young, *Nature*, 1958, **182**, 375.
2. E. C. H. Silk and R. S. Barnes, *Philos. Mag.*, 1959, **4**, 970.
3. K. Becker, *Solid State Dosimetry*, CRC Press, Cleveland, 1973, Chapter 5.
4. R. L. Fliescher, P. B. Price and R. M. Walker, *Nuclear Tracks in Solids: Principles and Applications*, University of California Press, Berkeley, 1975.
5. M. Monnin, *Idea to Applications: Some Selected Nuclear Techniques in research Development*, IAEA Publication, 1978.
6. S. A. Durrani and R. K. Bull, *Solid state Nuclear Track Detection: Principles methods and Applications*, Pergamon Press, Oxford, 1985.
7. R. V. Griffith and L. Tommassino, *Dosimetry of Ionizing Radiations*, Academic Press, San Diego California, 1990, **Vol III**, Chapter 4.
8. A. M. Bhagwat, *Solid State Nuclear Track detection: Theory and Applications*, Indian Society of Radiation Physics, Kalpakkam Chapter, 1993.
9. W. Enge, *Radiat. Meas.*, 1995, **25(1-4)**, 11.
10. N. Yasuda, M. Yamamoto, k. Amemiya, H. Takahashi, A. kyan, K. Ogura, *Radiat. Meas.*, 1999, **31**, 203.
11. G. Guillott and F. Randlez, *J. Appl. Phys.*, 1981, **52(12)**, 7155.
12. G. Meesen and A. Poffiin, *Radiat. Meas.*, 2001, **34**, 161.
13. A. Barbu, A. Dunlop, D. Lesuer and R. S. Averbach, *Europhysics Letters*, 1991, **15**, 37.
14. D. A. Young, *Radiat. Meas.*, 1997, **27(4)**, 1997, 575.

15. R. L. Fliescher, P. B. Price, R. M. Walker, and E. L. Hubbard, *Phys. Rev.* 1967 a, **133**, 1443.
16. R. L. Fliescher, P. B. Price, R. M. Walker, and E. L. Hubbard, *Phys. Rev.* 1967 b, **156**, 353.
17. E. V. Benton, Charged particle tracks in polymers, No.4 USNRDL-TR-67-80, 1967.
18. H. G. Paretzke, *Radiat. Effects*, 1977, **34**, 3.
19. R. Katz and E. J. Kobetich, *Phys. Rev.*, 1968, **170**, 391.
20. M. Monin, *PNCF*, 1968, **68**, RI-9.
21. T. Portwood, D. L. Henshaw and J. Stezny, *Nucl. Tracks*, 1986, **12**, 109.
22. E. V. Benton, *Radiat. Effects*, 1970, **2**, 273.
23. A. Thompson, D. O'Sullivan, J. H. Jr. Adams and L. P. Beahm, *11th Int. Congr. On SSNTD*, Oxford: Pergamon, 1982, 171.
24. G. Somogyi, *11th Int. conf. on SSNTD*, Oxford: Pergamon, 1982, 103.
25. L. Tommassino, *Electrochemical Etching of Damaged Track Detectors by H. V. Pulse and Sinusoidal Waveform*, Internal Report- Lab. Dosimetria e Standardizzazione, CNEN Casaccia, Rome, 1970.
26. M. Monnin and G. Blanford, *Science N.Y.*, 1973, **181**, 743.
27. G. Somogyi, M. Toth-Szilzgyi, M. Monnin and J. Gourcy, *Nucl. Tracks*, 1979, **3**, 151.
28. S. A. R. Al-Naajjar, R. K. Bull and S. A. Duranni, *Nucl. Tracks*, 1979, **3**, 169.
29. G. M. Hassib, *Nucl. Instrum.Meth.*, 1975, **131**, 125.
30. W. G. Cross and L. Tommassino, *Health Physics*, 1968, **15**, 196.
31. L. Tommassino, N. Klien and P. Soloman, *Nucl. Tracks*

- Detection*, 1977, **1**, 63.
32. J. R. Harvey and A. R. Weeks, *Nucl. Tracks*, 1982, **6**, 201.
 33. R. H. Iyer and K. K. Dwivedi, *Radia. Meas.*, 2003, **36**, 62.
 34. Nadkarni V.S. and Samant S D, *Radiation Measurements*, 1997, **27(3)**, 505.
 35. Nadkarni V. S., and Samant S D., *Radiat. Meas.* 1996, **26(5)**, 657-661.
 36. S. Biswas, N. Durgaprasad, M. N. Vohra, *Sol. Phys.* 1983, **89**, 163.
 37. K. K. Dwivedi, G. Fiedler, *Radiat. Meas.*, 1988, **15**, 353.
 38. R. H. Iyer and N. K. Chaudhuri, *Radiat. Meas.*, 1997, **27**, 524.
 39. S. G. Marathe, V. K. Rao, S. M. Sahakundi, R. H. Iyer, *Inorg. Nucl. Chem.*, 1978, **40**, 1981.
 40. R. H Dewolfe and W. G. Young, *chapter in chemistry of alkenes*, Vol. 1, S. Patai, ed., Interscience, 1964.
 41. P. D. Bartlett and R. Altschul, *J. Am. Chem. Soc.*, 1945, **67**, 816.
 42. C. E. Schildknecht, *Polym. Eng. Sci.*, 1966, **6**, 240.
 43. P. D. Barlett and R. Altschul, *J. Am. Chem. Soc.*, 1945, **67**, 812.
 44. G. F. D'Alelio, U. S. P. 2,339,058.
 45. W. Sololina, *J. Russ. Phys. Chem. Soc.* 1896, **30**, 826.
 46. I. E. Muskat and F. Strain, U.S.P. 2,370,567/1945 (chem. Abstr., **39**, 4526⁶).
 47. W. R. Dial and C. Gould, U. S. P. 2,379,218/1945, (Chem. Abstr., **40**, 16964).
 48. B.G. Cartwright, E.K. Shirk, and P.B. Price, *Nucl. Instrm. Meth.*, 1978, **153**, 457.

49. *CR-39 Allyl diglycol carbonate monomer Bulletin 45A and casting and Material safety data sheet*, PPG industries, Inc., Pittsburgh, Pa., 1984.
50. Kitagaki, Tetsuro; Ogawa, Kinya; Taguchi, Kenichi; Muto, Hiroaki JP 1973-27699/1974 (Chem. Abstr., **83**,44000).
51. Kitagaki, Tetsuro; Ogawa, Kinya; Taguchi, Kenichi; Muto, Hiroaki JP 49011832/1974 (Chem. Abstr., **81**, 50268).
52. L. Velazquez, Perez Peraza Jorge, A. Gauia, Carlos, *Rev. Soc. Quim. Mex.*, 1991, **35(5)**, 215.
53. Emilian; Georgescu, Florentina; Dragan, Gabriel; Curcaneanu, Stefan; Georgescu, RO 106129/1989 (Chem. Abstr., **128**, 270975).
54. Toman, Jaromir; Zmolil, Premysl, CS 1987- 3881/19 (Chem. Abstr., **116**, 84363).
55. Toman, Jaromir; F. Ladislav, Z. Premysl, K. Josef CS 263910/1987. (Chem. Abstr. **113**, 58488).
56. C. Milos, P. Jiri, T. Jaromir, T. Libor CS 254619/1986 (Chem. Abstr. **111**, 25329).
57. B. Singh, J. K. Nigam, IN 159735/1983 (Chem. Abstr. **109**, 7098).
58. Pennwalt Corp. U.S.A (Chem. Abstr. **92**, 180682).
59. H. Yamana, T. Kunil, H. Nakai, JP 53012813/1978 (Chem. Abstr. **88**, 170749).
60. N. N. Alekseev, A. I. Borbulevich, N. F. Shtoda, G. S. Dedovets, SU 1,294,801/1987 Chem. Abstr. **107**, 6776).
61. Ugo, Romano EPO Appl.No. 0035304/1981 (Chem Abstr., **98**, 142969).
62. Ugo Romano GB 2 098 984/1981 (Chem Abstr., **96**, 69576).
63. M. Pellegrina, Y. Proux, EP 72325 (Chem. Abstr. **99**, 6486).

64. G. Tarle, Report PNL-SA-1982, 8200668, p. 74 (Chem. Abstr., **99**, 1836183p).
65. W. McGhee, D. Riley, *Journal of Organic Chemistry* 1995, **60 (19)**, 6205.
66. T. Shigemune, K. shikata, *Yuki Gosei kagaku Kyokaishi* 1985, **43(12)**, 1155.
67. G. Rokicki, PL 126725/1981 (Chem. Abstr., **102**, 166322).
68. Tokuyama Soda Co. Ltd., JP 56005442/1979 (Chem. Abstr., **96**, 103642).
69. Tokuyama Soda Co. Ltd., JP 19790628/1979 (Chem. Abstr., **96**, 103641).
70. Tokuyama Soda Co. Ltd., JP 19790630/1979 (Chem. Abstr., **96**, 68368).
71. K. Shikata, T. Shigemune, DE 2838701/1979 (Chem. Abstr., **90**, 186402).
72. G. Tarle, Report PNL-SA-1982, 8200668, p. 74 (Chem. Abstr., **99**, 1836183p).
73. S. J. Huang and J. F. Jhonson, Pac., Northwest lab., [Tech. Report], PNL-SA-1982, PNL-SA-707114, P.85 (Chem. Abstr., **99**, 183614q)
74. T. Portwood and J. Stezny, *Nucl. Tracks Radiat. Meas.*, 1984, **8**, 151.
75. L. Lembo, O. Civolani, L. Patrizii and G. Lodi, *Nucl. Tracks*, 1986, **12**, 633.
76. C. S. Yang, C. R. Davis, J. H. Groeger, S. J. Huang, J. F. Jhonson, D. E. Hadlock and M. A. Parkhurst, *Nucl. Tracks*, 1986, **12**, 547.
77. S. Ahmad, and J. Stejny, *Nucl. Tracks. Radiat. Meas.*, 1991, **19**, 11.

78. Tokuyama Soda Co. Ltd., JP 56015249/1981 (Chem. Abstr., **95**, 6498).
79. Tokuyama Soda Co. Ltd., JP 55059143/1980 (Chem. Abstr., **93**, 204082).
80. P. D. Bartlett and R. Altschul, *J. Am. Chem. Soc.*, 1945, **67**, 812.
81. C. E. Schildknecht, *Allyl compounds and their polymers*, Wiley-Interscience, NY, 1973, High Polymers Vol. XXVIII, Chapters. 1, 10.
82. G. R. Lucas and L. P. Hammett, *J. Am. Chem. Soc.*, 1942, **64**, 1928.
83. W. R. Dial, W. E. Bissinger, B. J. De Witt, and F. Strain, *Ind. Engg. Chem.*, 1955, **47**, 2447.
84. P. H. Fowler, V. M. Clapham, D. L. Henshaw, D. O'Sullivan and A. Thompson, *Proceedings of 10th International Conference on Solid State Nuclear Track Detectors*, Lyon, 1979, (Pub. 1980) p. 437.
85. D. L. Henshaw, N. Griffiths, O. A. L. Landen, S. P. Austin and A. A. Hopgood, *Proceedings of 11th International Conference on Solid State Nuclear Track Detectors*, Bristol, 1981, p. 137.
86. D. L. Henshaw, N. Griffiths, O. A. L. Landen and E. V. Benton, *Nucl. Instrm. and Meth.*, 1981, **180**, 65.
87. T. W. Turner, V. M. Clapham, A. P. Fews and D. L. Henshaw, *Proceedings of International Conference on Solid State Nuclear Track Detectors*, Bristol, 1981, p. 141.
88. T. Portwood, T. W. Turner, and A. P. Fews, *Nucl. Tracks Radiat. Meas.*, 1984, **8**, 155.
89. S. Szilagyí and G. Somogyi, *Nucl. Tracks Radiat. Meas.*,

- 1984, **8**, 171.
90. T. Portwood and J. Stejny, *Nucl. Tracks*, 1986, **12**, 113.
 91. J. Stejny and T. Portwood, *Nucl. Tracks*, 1976, **12**, 121.
 92. T. Portwood and J. Stejny . *Nucl. Tracks*, 1976, **12**, 117.
 93. V. S. Nikiforenko, Y. S. Zaitsev, V. V. Zaitsev, R. V. Kucher, N. I. Mikhailova, S. V. Muravchenko, V. A. *Doklady akademii Nauk SSSR* (1988), **300 (2)**, 400-3.
 94. E. Schnarr, E. K. Russell, *Journal of polymer Science*, 1980, **1893**, 913.
 95. R. I. Bellobono, M. Zeni, *Makromolekulare Chemie, Rapid Comm.* 1986, **7(11)**, 733.
 96. R. I. Bellobono, E. Selli, L. Righetto, P. Rafellini, L. Trevisan, *Makromolekulare Chemie*, 1989, 19098, 1945.
 97. M. D. McNeil, C. M. Hawley, M. Demeuse, Annual Technical Conference- Society of Plastics Engineers 1992, **92**, 2621.
 98. S. Ahmad and J. Stejny, *Nucl. Tracks. Radiat. Meas.*, 1991, **19**, 11.
 99. T. Portwood and J. Stejny, *Nucl. Tracks Radiat. Meas.*, 1984, **8**, 151.
 100. S. J. Huang, C. Davis, C. S. Vang, L. LeBarron, J. Feldman, J. H. Johnson, D. E. Hadlock and M. A. Parkhurst, *Radiat. Prot. Dosim.*, 1987, **20**, 37.
 101. S. Manzoor, H. A. Khan, Matiullah, M. Tufail, A. A. Qureshi, F. Ansari, R. Shoaib and L. Lembo, *Nucl. Tracks Radiat. Meas.*, 1988, **15**, 207.
 102. J. Stejny, J. Carrell and M. J. Palmer, *Radaition Meas.*, 2000, **32**, 299.
 103. K. Kinoshita and P. B. Price, *Rev. Sci. Instrum.*, 1980, **51**, 32.

104. G. Tarle, Repot PNL-SA-1982, 8200668, p. 74 (Chem Abstr., **99**, 183613p).
105. J. Stejny and T. Portwood, *Nucl. Tracks*, 1986, **12**, 59.
106. M. Fujii, R. Yokota and Y. Atarshi, *Nucl. Tracks Radiat. Meas.*, 1990, **17**, 19.
107. M. Fujii, and R. Yokota, *Nucl. Tracks Radia. Meas.*, 1988, **15**, 107.
108. K. Shikata and Y. Mizumoto, EP 136,653/1985; JP 180,609/1983. (Chem. Abstr., **102**, 227997).
109. Y. Mizumoto and K. Yomo, Jpn, Kokai. Tokkyo, Koho, JP 61,120,989/1986. (Chem. Abstr., **106**, 57594h).
110. K. Ogura, T. Hattori, M. Hirata, M. Asano, M. Yoshida, M. Tamada, H. Omichi, N. Nagaoka, H. Kubota and R. Katakai, *Radiation Meas.*, 1995, **25(1-4)**, 159.
111. K. Ogura, M. Asano, N. Yasuda and M. Yoshida, *Nucl. Instrum. Method. In Phys. Research B*, 2001, **185**, 222.
112. T. Tsuruta, *Radat. Meas.*, 1999, **31**, 99.
113. T. Tsuruta, *Radiat. Meas.*, 2000, **32**, 289.
114. G. Tarle, *Proceedings of International Cosmic Rays Conference*, Paris, 1981, 74.
115. T. Portwood and J. Stenjy, *Nucl. Tracks Radiat. Meas.*, 1984, **8**, 151.
116. P. B. Price and D. O'sullivan, *Proc. 11th Internat. Conf. on Solid State Nuclear Track Detectors*, Bristol, 1981, 929.
117. D. O'sullivan, A. Thompson, J. H. Adams, *Nucl. Tracks Radiat. Meas.*, 1984, **8**, 579.
118. De-Ling Pang, Lan-Di li and Bin Zhu, *Nucl. Tracks Radiat. Meas.*, 1993, **22**, 221.
119. M. Fujii, J. Nishimura and T. Kobayashi, *Nucl. Instrum.*

- Methods Phys. Res.*, 1984, **226**, 496.
120. T. Portwood, D. L. Henshaw and J. Stejny, *Nucl. Tracks*, 1986, **12**, 109.
 121. K. Ogura, T. Doke, H. Khinose, K. Kawahara, H. Tawara, S. Nakamura and S. Orito, *Nucl. Tracks Radiat. Meas.*, 1988, **15**, 315.
 122. L. Patrizii, *Nucl. Tracks Radiat. Meas.*, 1991, **19**, 641.
 123. I. A. Tahiri, Matiullah, M. S. Subhani, *Radiat. Meas.*, 2003.
 124. E. U. Khan., *Radiation Meas.*, 2002, **35**, 41.
 125. T. A. Gruhn, W. K. Li, E. V. Benton, R. M. Cassou and C. S. Jhonson, *Proceedings of 10th International Conference on Solid State Nuclear Track Detectors*, Lyon, 1979, 443.
 126. S. N. Husaini, *Radiat. Meas.*, 2002, **35**, 3.
 127. S. J. Huang and J. F. Jhonson, Pac. Northwest Lab., [Tech. Repot], PNL-SA-1982, PNL-SA-707114, P.85, (Chem.. Abstr., **99**, 183614q)
 128. J. Chavart and F. Spurny, *Nucl. Tracks Radiat. Meas.* 1988, **14**, 451.
 129. W. Enge, K. Grabisch, K. P. Bartholoma and R. Beaujean, proceedings of 10th International Conference on Nuclear Photography and Solid State Nuclear Track Detectors, Bucharest, 1992, 193.
 130. G. Somogyi and I. Hunyadi, *Nucl. Instrum. Meth.*, 1981, **190**, 443.
 131. S. A Amin and D. L. Henshaw, *Nucl. Instrum. Meth.*, 1981, **190**, 415.
 132. V. S. Nadkarni, S. G. Tilve and A. A. A. Mascarenhas, In dian Patent. Patent no. 196627, 1999.
 133. G. H.Schenk and M. Santiago, *Analytical Chemistry*, 1967,

- 39(14)**, 1795.
134. Bourgrignon, Jean, Sion, Marcel-Xavier, Morean and Micher, USP 4233245, 1980.
 135. F. Strain, W. E. Bissinger, W. R. Dial, H. Rudoff, B. J. DeWitt, H. C. Stevens and J. H. Langston, J. Am. Chem. Soc., 1950, **72**, 1254.
 136. K. Nozaki, *Ind. Engg. Chem. Anal. Ed.* 946, **18(9)**, 583.
 137. Vogel's textbook of Quantitative Inorganic analysis, 4th edition, 1978, 372.
 138. V. S. Nadkarni, Development of new solid state particle track detectors Ph. D. thesis, UDCT, Bombay, 1995.
 139. Pandey A. K., Sharma R. C., Kalsi P. C. and Iyer R. H., *Nucl. Instrum. and Meth. in Physics Research*, 1993, **B 82**, 151-155.

6.0. PUBLICATIONS.

1. A. Mascarenhas, S. G. Tilve, & V. S Nadkarni, Designing novel polymers for Solid state nuclear track detection: Novel homo and copolymers with allyl diglycol carbonate, from N-Allyloxycarbonyl diethanolamine-bis(allylcarbonate). *Designed Monomers and Polymers*, Vol. 8 (2), 177, 2005, VSP Publishers.
2. A. Mascarenhas, R. V. Kolekar, P. C. Kalsi, A Ramaswami, V. B. Joshi, S. G. Tilve and V. S. Nadkarni New Polymers for Solid State Nuclear Track Detection, *Radiation Measurements*, 41(1), 22, 2006.
3. V. S. Nadkarni, S. G. Tilve & A. Mascarenhas, Indian Process Patent no. 196627 entitled " An Improved Process for Preparation of carbonates.

Conference Presentations:

1. A. Mascarenhas, S. G. Tilve, & V. S. Nadkarni, Indigenous process for the preparation of ADC monomer and PADC nuclear track detector, National symposium on radiation and photochemistry, organised by IIT, Kanpur & ISRAPS during March 3-5, 2003.
2. A. Mascarenhas, S G Tilve & Nadkarni V.S. , A poster entitled "New Polymers for Nuclear track detection" Trombay Symposium on Radiation & Photochemistry, organised by BRNS, DAE & ISRAPS at BARC, Mumbai during January 8-12, 2004.
3. A. Mascarenhas, S. G. Tilve, & V. S. Nadkarni, Developing Polymers for Nuclear Track Detection, 13th National symposium on Solid state Nuclear Track Detection, Amritsar, November 2004. organised by Nuclear Track Society of India.
4. A. Mascarenhas, P C Kalsi, S G Tilve, A Ramaswami and V S

Nadkarni, Quantitative determination of Uranium in soil samples of Goa University campus area using Fission Track Method. 13th National symposium on Solid state Nuclear Track Detection, Amritsar, November 2004, organised by Nuclear Track Society of India.

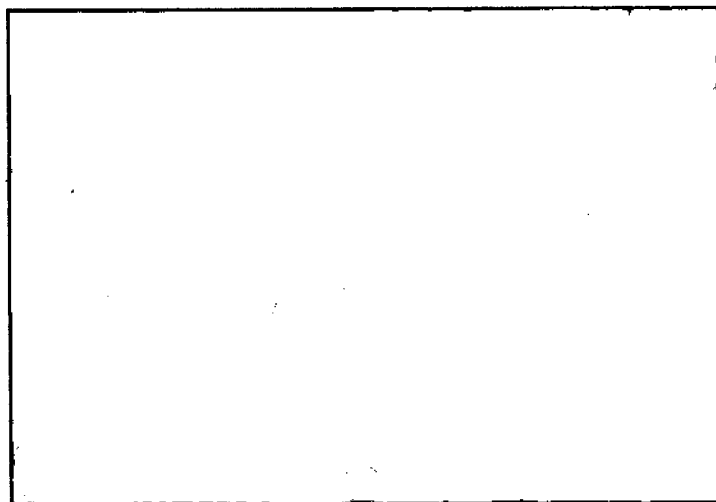
5. A. Mascarenhas, S. G. Tilve, & V. S. Nadkarni, Designing polymers for nuclear track detection, International conference on Polymers for Advanced Technologies, Thiruvananthapuram, 2004.
6. A. Mascarenhas, V. K. Mandrekar, S. G. Tilve & V. S. Nadkarni, Designing novel polymers for nuclear track detection, 14th National symposium on Solid state Nuclear Track Detection, Aligarh, 2005.
7. A. Mascarenhas, V. K. Mandrekar, S. G. Tilve & V. S. Nadkarni, Designing polymers for nuclear track detection, 4th National Symposium & Conference on Solid State Chemistry & Allied Areas, (ISCAS-2005).

Annexure I



Photomicrograph of ^{239}Pu alpha particle in PNADAC film

Magnification : 160 X. Exposure : 703703 dpm ^{239}Pu source
at 2.0 cm for 5 min. Etching : 6 N NaOH, 80 °C.

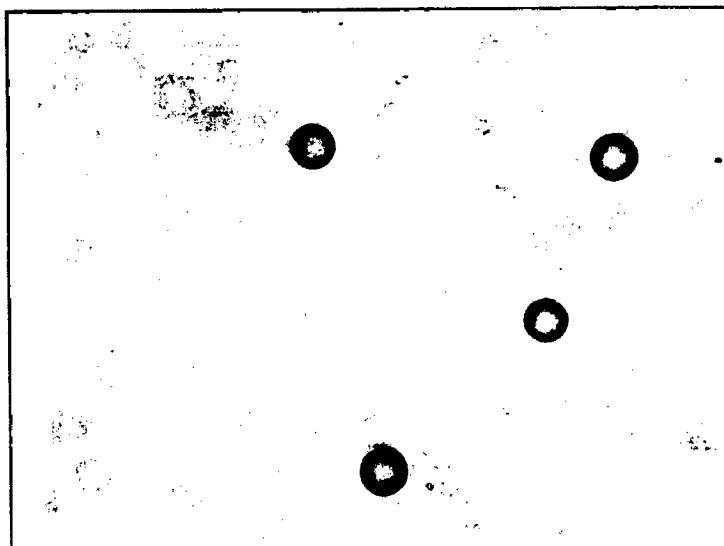


Photomicrograph of ^{252}Cf fission fragments & alpha particle in

NADAC - ADC (50 : 50) film. Magnification : 160 X. Exposure :
300 dpm ^{252}Cf in contact for 30 min. Etching : 6 N NaOH, 75 °C.



Photomicrograph of ^{239}Pu alpha particle in PADC film
Magnification : 80 X. Exposure : 703703 dpm ^{239}Pu source
at 2.0 cm for 2 min. Etching : 6 N NaOH, 70 °C.



Photomicrograph of ^{252}Cf fission fragments & alpha particle in
ABNEC - ADC (50 : 50) film. Magnification : 160 X. Exposure :
300 dpm ^{252}Cf in contact for 30 min. Etching : 6 N NaOH, 70 °C.